

Prospects for Enhancing Malaria Vaccine Efficacy by Combining Pre-erythrocytic Antigens

Thesis submitted for the degree of Doctor of Philosophy
Trinity Term 2017

Erwan Atcheson
St Edmund Hall

Word count: ~50,000

Abstract

Malaria causes almost half a million deaths each year. Existing interventions will almost certainly not be enough to tackle this enormous public health problem on their own. An effective vaccine is urgently needed. The leading malaria vaccine, RTS,S, confers suboptimal protective efficacy, and in addition targets only *Plasmodium falciparum* and not the other major species of human malaria, *P. vivax.* This thesis investigates the potential of combining pre-erythrocytic malaria vaccines as a means of enhancing protective efficacy. A novel mathematical model was developed which expresses probability of protection as a function of vaccine-induced humoural and cellular responses. The model predicts that combining partially effective vaccines should result in more than additive improvements in protective efficacy. This was supported by an experiment combining Rv21, a *P. vivax* circumsporozoite virus-like particle, with viral vectored *P. vivax* TRAP, the two leading pre-erythrocytic malaria vaccine antigens; this combination raised protective efficacy from 50% and 0%, respectively, to 100% sterile protection. It was also found that antigenic interference, a reduction in anti-CSP titres when Rv21 and PvTRAP are combined, occurred only in the presence of Matrix M adjuvant, and not when using alum, AddaVax or no adjuvant. With a view to creating a single-component multi-antigen vaccine, which would be more cost-effective than a multi-component vaccine, experiments were carried out to establish the virus-like particle Qβ as a platform capable of eliciting protective immunity via the display of short peptides derived from the CSP repeat region of both *P. vivax* and *P. falciparum*. For the first time, a tetramer peptide derived from the CSP repeat region of *P. vivax* VK210, AGDR, was shown capable of eliciting protective immunity alone. Finally, five novel linear B-cell epitopes were discovered, one from *P. falciparum* CSP, three from *P. vivax* TRAP and one from TRSP, each capable of conferring partial protection on mice. These epitopes were identified using novel screening methods, using sera from whole-protein vaccinated mice or by exploiting conservation within invasion protein sequences. Two of the protective epitopes, $(NANP)_6$ and (ADGN long) were combined and found to enhance protective efficacy as predicted by the mathematical model. Thus this thesis lays the groundwork for the development of a single-component multi-epitope malaria vaccine with enhanced protective efficacy.

Acknowledgements

Thanks must first go to my supervisor, Professor Arturo Reyes-Sandoval, for his scientific input, kind support and encouragement over the past four years. I also owe a large debt of gratitude to Professor Adrian Hill for his immeasurably valuable feedback and advice. It has been a real pleasure working and learning in the Jenner Institute.

All members of the Reyes group, past and present, deserve my very sincere thanks for their support, feedback, and development of a wonderful working environment. In no particular order, Joshua Blight, Cesar Lopez-Camacho, Elisangela Oliveira de Freitas, Fabiana Leoratti, Edu Alves, Nuriban Valero Pacheco, Lalo Montoya-Diaz, Marcos Moreli, Javier Ríos Valencia, Marina Giminez, Young Kim, Kate Harrison, Mark Tilley, Christin Reimer, Amar Lall and Heather West have all been excellent friends and colleagues. As indeed has the wider CCMP community, Aadil El-Turabi (with thanks to you and Ariane for the Qβ), Ariane Cruz Gomez, Martin Bachmann, Mona Mohsen, Gustavo Cabral de Miranda, Amy Flaxman, Pauline van Diemen, Elizabeth Allen, Claudia Lindemann, Ritu Mann-Nüttel, Elizaveta Elshina, Julia Whitehouse, Julia Branco, Yuko Yamaguchi, David Wyllie, and the Vector Core team, Ali Turner, Lou Rose, Marzena Wroblewska, Susan Morris, Becky Snaith, Neethi Gureddi, Rhys Hamon, and Jake Matthews, who should also be thanked for their hard work in preparing the viral vectored vaccines used in this thesis.

Sumi Biswas, Alex Fyfe, Sara Zakutanksy, Alex Spencer and Marta Ulaszewska have been of huge help in maintaining the Jenner Insectary and providing the mosquitoes crucial to my studies. Alex Spencer also provided much useful advice about mice. Anita Milicic, by maintaining the adjuvant bank, should be thanked for supplying the adjuvants used in this thesis. Chris Janse and Shahid Kahn have been great collaborators, and they, with Ahmed Salman, provided the transgenic malaria parasites without which the protective efficacy of my vaccines could not have been tested. Ahmed also helped with IFA. Thanks too should go to Lisbeth Soederberg and Rebecca Ashfield, and to Florian Brod and Julie Furze for reagents and assistance. I would also like to thank Heather Gray, Viv Clark, Stephen Laird, Douglas dos Santos Passos, Denise, Claudia, and all the staff at the FGF for the care and attention they gave to the 1,583 mice I used during these studies. And so I also acknowledge these mice. It is no small thing to ask of another species.

Jethro Tull, System of a Down, The Mamas and the Papas, Captain Beefheart and Ruins deserve credit for assisting with the analysis of the data.

Finally, I thank my family, David, Maman, Robbyn, Gwénaël, and Eleanor. Thank you for all your support, kindness and love over many, many years. I thank Oblomov el-Gato for his assistance during the write-up of the DPhil. I thank Cado for bringing me joy without bound. And I thank Sheila McCartan for her patience, love, and constant encouragement, for putting up with my excited jabber about mathematical models, and being a wonderful partner.

Considering the Snail

The snail pushes through a green
night, for the grass is heavy
with water and meets over
the bright path he makes, where rain
has darkened the earth's dark. He
moves in a wood of desire,

pale antlers barely stirring
as he hunts. I cannot tell
what power is at work, drenched there
with purpose, knowing nothing.
What is a snail's fury? All
I think is that if later

I parted the blades above
the tunnel and saw the thin
trail of broken white across
litter, I would never have
imagined the slow passion
to that deliberate progress.

- Thom Gunn

Table of Contents

Abstract **1**
Acknowledgements **3**
Table of Contents **5**
Table of Figures **11**
Table of Tables **13**
Chapter 1: **Introduction** **15**
1.1 The need for a malaria vaccine 15
1.2 The malaria life cycle 18
1.2.1 The pre-erythrocytic stage 19
1.2.2 The erythrocytic stage 20
1.2.3 The sexual and mosquito stage 21
1.3 Malaria pathogenesis 23
1.4 Naturally acquired immunity 26
1.5 Platforms for vaccine delivery 31
1.5.1 Whole pathogens 31
1.5.2 Proteins and polysaccharides 32
1.5.3 Virus-like particles 32
1.5.4 Viral vectored vaccines 33
1.5.6 DNA vaccines 34
1.6 Adjuvants 36
1.6.1 Alum 36
1.6.2 AddaVax and MF59 37
1.6.3 Matrix M 38
1.6.4 Genetic adjuvants 39
1.7 Whole sporozoite vaccines 41
1.7.1 Radiation-attenuated parasites 41
1.7.2 Live sporozoites under chloroquine prophylaxis 43
1.7.3 Genetically attenuated parasites 44
1.8 Circumsporozoite protein (CSP) 46
1.8.1 Nature and function of CSP 46
1.8.2 CSP vaccine history and mechanisms of protective efficacy 48
1.8.3 *P. vivax* CSP vaccine development 58
1.9 Thrombospondin-related adhesion protein (TRAP) 62
1.9.1 Function of TRAP 62
1.9.2 TRAP vaccines 63
1.10 Other pre-erythrocytic stage vaccines 67
1.11 Blood stage vaccines 69
1.12 Transmission-blocking vaccines 72
1.13 Combination malaria vaccines 75
1.14 Murine models of malaria 80
Chapter 2: Materials and Methods **83**
2.1 Immunology 83
2.1.1 Mouse PBMC IFNγ ELISpot 83
2.1.2 ELISAs: standard curve, affinity and subclass. 84
2.1.3 Vaccination 86
2.1.4 Vaccination combination simulations 86
2.1.5 Mouse strains used 87

2.1.6 Ethics statement ... 87
2.1.7 Hybridoma and monoclonal 2D3 PvTRAP antibody production ... 87
2.2 Parasitology ... 89
2.2.1 Infection of *Anopheles stephensi* mosquitoes with *P. berghei* ... 89
2.2.2 Dissection of mosquito salivary glands and challenge of mice with sporozoites ... 89
2.2.3 Thin blood smears and calculation of time to reach 1% blood stage parasitaemia ... 90
2.2.4 Cryopreservation of *P. berghei* infected red blood cells ... 90
2.2.5 Production of transgenic *P. berghei* parasites ... 91
2.2.6 Serial dilutions of infected red blood cells and sporozoites to determine blood-stage growth rate ... 93
2.3 Molecular biology, protein production and vaccine production ... 94
2.3.1 Design of proteins ... 94
2.3.2 Expression of proteins in HEK293 cells and purification ... 95
2.3.3 Expression of Hepatitis B surface antigen-based virus-like particles in *Pichia pastoris* and purification ... 96
2.3.4 Qβ virus-like particle production, purification and chemical coupling ... 98
2.3.5 $(NANP)_{60}$ design and manufacture ... 100
2.3.6 Chemical coupling to keyhole limpet hemocyanin ... 100
2.3.7 Viral vector design and production ... 101
2.3.8 E. coli transformations ... 102
2.3.9 SDS-PAGE ... 102
2.3.10 Western Blots ... 102
2.3.11 PvTRAP crystal structure visualisation ... 103
2.3.12 Calculation or prediction of peptide properties ... 103
2.3.13 Selection and identification of conserved amino acid sequences in *P. berghei* pre-erythrocytic invasion proteins ... 103
2.4 Statistical analysis ... 104
2.4.1 Statistical tests used ... 104
2.4.2 Non-linear curve fitting ... 105
2.4.3 Statistical definition of challenge outcomes ... 105
Chapter 3: **A mathematical model of the effects of combining pre-erythrocytic malaria vaccines ... 109**
Introduction ... 109
Results ... 116
3.1 Derivation of a probabilistic equation modeling pre-erythrocytic malaria vaccine efficacy ... 116
3.2 Time to 1% blood-stage parasitaemia as a function of antibody and CTL ... 119
3.3 Experimental estimates of g, p_b and p_c ... 123
3.3.1 Estimating g ... 123
3.3.2 Estimating p_b ... 129
3.3.3 Estimating p_c ... 131
3.4 Two experimental tests of the model using data from published literature ... 134
3.5 Simulations of vaccine combinations and implications for optimal vaccination strategies. ... 137

3.6 Implications for basic biology of *P. berghei* 141
Discussion 145
Chapter 4: Combining CSP virus-like particles with viral-vectored TRAP: immunogenicity and protective efficacy 151
Introduction 151
Results 154
4.1 The effects on immunogenicity of combining Ad-MVA PvTRAP with PvCSP virus-like particles, with various adjuvants. 154
4.1.1 Effect of vaccine combination on PvCSP-specific immunogenicity 155
4.1.2 Effect of vaccine combination on TRAP immunogenicity 158
4.1.3 Protective efficacy of super-optimal Rv21 ± Ad-MVA PvTRAP regimes 160
4.2 Suboptimal Rv21 and PvTRAP combination enhances protective efficacy 163
4.3 Effects on immunogenicity of genetic adjuvants with viral vectors encoding PvCSP and PvTRAP 165
4.4 Effects on immunogenicity and protective efficacy of intravenous administration of viral-vectored PvTRAP 167
4.5 Comparison of Rv21 and CSVS-like, two Hepatitis B surface antigen-based PvCSP virus-like particles 169
Discussion 172
Chapter 5: Towards a single component multi-epitope vaccine. Part 1: CSP repeat peptide vaccines 179
Introduction 179
Results 184
5.1 Immunogenicity and protective efficacy of short unit repeat CSP peptides from *P. falciparum* and *P. vivax* coupled to Qβ 184
5.2 CSP repeat region tetramers: homologous and sequential vaccination 188
5.2.1 Immunogenicity and protective efficacy of CSP repeat region tetramers 188
5.2.2 Sequential and tandem immunisation with native PvCSP and Qβ-$(AGDR)_3$ 192
5.3 Improving Qβ-NANP peptide vaccines 195
5.3.1 Effects on immunogenicity and protective efficacy of fusing a tetanus toxin $CD4^+$ T-cell epitope with $(NANP)_3$. 195
5.3.2 Increasing the number of unit repeats in Qβ-(NANP) vaccines 198
5.4 Attempts at a multi-species vaccine based on CSP repeat peptides 205
Discussion 213
Chapter 6: Towards a single component multi-epitope vaccine. Part 2: Alternatives to CSP repeat peptide vaccines 223
Introduction 223
Results 229
6.1 Non-repeat region CSP peptides as vaccines 229
6.2 High-throughput vaccine screening: from protein to neutralising linear B-cell epitope 239
6.3 High-throughput vaccine screening: exploiting conservation to identify neutralising linear B-cell epitopes 244
Discussion 248

Chapter 7: Discussion and Future Directions 259
7.1 Overview 259
7.2 A mathematical model of vaccine combination 261
7.3 Combining two *P. vivax* vaccines, Rv21 and viral-vectored TRAP 264
7.4 Qβ-peptide vaccines: virus-like particles displaying short peptide epitopes from the repeat region of CSP 265
7.5 The search for other neutralising linear B-cell epitopes 269
7.6 Final remarks 272
References 275

Table of Figures

Fig 1.2.1 Life cycle of malaria 18
Fig 1.4.1 Age stratification of malaria severity 26
Figure 1.9.1: Schematic structure of TRAP 63
Fig. 2.2.1 Phenotype of PvCSP-210/PvTRAP double transgenic *P. berghei*. 92
Figure 3.3.1 Estimates of blood-stage growth rate g from thin blood smears taken 24 hours apart. 124
Figure 3.3.2: Seeding blood-stage parasitaemia with infected red blood cells (iRBC) to obtain an estimate of blood-stage growth rate by non-linear curve fitting. 125
Figure 3.3.3 Varying *P. berghei* sporozoite inoculation to obtain an estimate of blood-stage growth rate by non-linear curve fitting. 127
Figure 3.3.4 Comparison of methods of calculating growth rate *g*. 129
Figure 3.3.5 Varying monoclonal antibody 3D11 dose to obtain estimates of probability of protection parameter p_b. 130
Figure 3.3.6 Estimating probability of protection parameter p_c by linear regression of SFU/million PBMC against time to 1% parasitaemia in two PvTRAP vaccination experiments 132
Figure 3.4.1 Synergy of neutralising antimalarial monoclonal antibody combination accurately predicted by the probabilistic mathematical model. 135
Figure 3.4.2 Accurate prediction of VSV-SUDV neutralising antibody combination 136
Figure 3.5.1 Simulation showing effects of adding a CTL-mediated vaccine to an antibody-mediated vaccine. 137
Figure 3.5.2 Simulation showing the average amount of each type of antibody required to achieve 80% protection as the number of antigen targets increases. 138
Figure 3.5.3 Simulation: a disparity in the potency of two monoclonal antibodies diminishes returns from their combination. 139
Figure 3.6.1 Histogram of time-to-1% values in naïve and vaccinated mice (BALB/c, 2207 parasite). 143
Fig. 4.1.1 Effects on PvCSP immunogenicity of adjuvants and viral-vectored TRAP on two PvCSP virus-like particles. 157
Fig. 4.1.2 Effects on viral-vectored PvTRAP immunogenicity following combination with PvCSP virus-like particles and/or adjuvants. 159
Fig 4.1.3. Protective efficacy of Rv21- and/or Ad-MVA PvTRAP-vaccinated mice 161
Fig. 4.2.1 Suboptimal Rv21 and PvTRAP combination enhances protective efficacy 164
Fig. 4.3.1 Effects on immunogenicity and protective efficacy of genetic adjuvants with viral-vectored PvCSP and PvTRAP 166
Fig. 4.4.1 Effects on immunogenicity and protective efficacy of intravenous administration of viral-vectored PvTRAP vaccine 168
Fig. 4.5.1 Comparison of Rv21 and CSVS-like, two Hepatitis B surface antigen-based virus-like particles 170
Fig. 5.1.1 Representative *P. falciparum* and *P. vivax* CSP sequences. 184
Fig. 5.1.2 Immunogenicity and protective efficacy of short unit repeat peptides from *P. falciparum* and *P. vivax* CSP coupled to Qβ VLPs. 185

Fig. 5.2.1 Immunogenicity and protective efficacy of CSP repeat region tetramers. **190**
Fig. 5.2.2 Sequential and tandem immunisation with native PvCSP-210 and Qβ-(AGDR)$_3$. **194**
Fig. 5.3.1 Effects on immunogenicity and protective efficacy of tetanus toxin CD4$^+$ T-cell epitope fusion with Qβ-(NANP)$_3$ **196**
Fig. 5.3.2 Effects on immunogenicity and protective efficacy of increasing the number of unit repeats in Qβ-(NANP) vaccines **199**
Fig. 5.3.3 Experimental validation of mathematical model of dose-titre relationship. **203**
Fig. 5.4.1 The effects of combining CSP repeat tetramers on immunogenicity and protective efficacy **208**
Fig. 5.4.2 Effects of combining natural CSP repeats on immunogenicity and protective efficacy **210**
Fig. 6.1.1 Serum responses to overlapping peptides representing the full length of PvCSP from PvCSP-vaccinated mice. **231**
Fig. 6.1.2 Non-repeat region CSP peptides as vaccines. **232**
Fig. 6.1.3 Effects on immunogenicity and protective efficacy of combining Qβ-(NANP)$_6$ and Qβ-(ADGN long) vaccines. **235**
Fig. 6.1.4 Immunodominance on a multi-epitope VLP **237**
Fig. 6.2.1 Identification of neutralising linear B-cell epitopes in *P. vivax* TRAP **240**
Fig. 6.2.2 2D3 PvTRAP monoclonal antibody specificity and neutralising potency. **242**
Fig. 6.3.1 Identification of neutralising linear B-cell epitopes by screening conserved peptides in *P. berghei*. **245**
Fig. 6.3.2 Effects on immunogenicity and protective efficacy of combining Qβ-(PLP1b) and Qβ-(TRSP) vaccines. **246**

Table of Tables

Table 2.1.1: Immunodominant PvTRAP peptides in mice. (Bauza et al. 2014) **84**
Table 2.2.1 Replacement transgenic *P. berghei* and accession numbers **93**
Table 2.3.1 Primary structures of proteins used in thesis **94**
Table 2.3.2 Primary structures of Hepatitis B surface antigen-based virus-like particles used in this thesis **96**
Table 2.3.3 Peptides coupled to Qβ in this thesis **99**
Table 2.3.4 Accession numbers of *Plasmodium* sporozoite surface-exposed invasion and migratory proteins used in alignments **104**
2.5 List of Materials **105**
Table 3.1.1 List of variables **118**
Table 3.2.1 List of variables **122**
Table 3.6.1: inferred or actual mean, lower and upper bounds for biological parameters of *P. berghei* infection in BALB/c mice **144**
Table 4.1.1 Vaccination regimes for each experiment in §4.1 ..... **155**
Table 4.2.1 Antigenic interference in malaria vaccine studies **174**
Table 5.1.1 Sequences of peptides coupled to Qβ in this section **185**
Table 5.2.1 Peptide sequences coupled to Qβ in this section **190**
Table 6.1.1 *P. berghei* proteins used for conservation-based screening of linear B-cell epitopes for protective efficacy **227**
Table 6.2.1 Protective efficacy of CSP Region I and II peptides used as vaccines in this chapter and in previous studies **249**

Chapter 1

Introduction

1.1 The need for a malaria vaccine

Malaria causes almost half a million deaths and 148-304 million clinical cases every year (1). A parasitic infection transmitted by mosquitoes, it is one of the leading causes of childhood mortality: children under five account for 70% of the deaths from malaria each year (1). Control measures such as long-lasting insecticide treated bednets and drug treatments have halved the incidence of malaria in just fifteen years (2). But with the rise of drug resistance, more frequent reports of insecticide resistance (1), and with the many remaining areas of high transmission likely to prove the most intractable to elimination programmes (3), an effective vaccine against malaria is more urgently needed than ever.

A disease prevalent in reptiles, birds and mammals (4), there are five species of malaria which infect humans: *Plasmodium falciparum*, *P. vivax, P. ovale* (which some consider composed of two separate species, *P. ovale curtisi* and *P. ovale wallikeri* (5, 6)), *P. malariae*, and the zoonotic *P. knowlesi* (7). *P. falciparum* causes almost 95% of cases, though outside of Africa *P. vivax* accounts for about 41% of cases (1). *P. vivax* is increasingly recognised as a major health burden in its own right (8), with all-cause mortality and morbidity much higher in individuals suffering the weekly to monthly relapse infections distinctive of this disease (9).

Once globally distributed, malaria is now chiefly confined to the tropics (10). *P. falciparum* is at its greatest intensity in sub-Saharan Africa

(1, 11). *P. vivax* is largely absent from most of sub-Saharan Africa but is widespread in South America and South-East Asia, where *P. falciparum* is often equally prevalent (12, 13). Malaria exists where mosquitoes of the *Anopheles* genus can transmit it; 41 out of the 465 known species of anopheline mosquito are considered significant vectors of the disease (14-16).

Malaria disproportionately affects the lowest-income people in the world, but it is also thought to contribute significantly to poverty (17), with estimates that malaria costs sub-Saharan Africa up to $12 billion in lost economic productivity every year in consequence of its enormous health burden (18).

An effective and affordable malaria vaccine would do much to alleviate these terrible problems (19-21). Vaccines and their distribution have been credited as one of the major achievements of public health (22), with one disease, smallpox, eradicated by a vaccine (23), and another, polio, close to being eradicated by another vaccine (24). Measles looks likely to be the next target (25). Malaria eradication is the stated goal of many in the global malaria community (26). This is unlikely to be achieved without new weapons to fight malaria with; an effective malaria vaccine would be one of the most powerful of those new interventions (3, 27). Indeed, the WHO, in the Malaria Technology Roadmap, have called for a malaria vaccine conferring 75% protective efficacy. The leading malaria vaccine, RTS,S is due to enter pilot distribution studies in sub-Saharan Africa next year (WHO press release, 24 April 2017). But with under 47% efficacy (28), it will be neither effective enough to eradicate malaria (27), and less cost-effective than the current leading malaria intervention, long-lasting insecticide-treated bednets (29). Nor does RTS,S have any efficacy against

P. vivax. This thesis is an attempt to further the development of a more effective malaria vaccine.

In this chapter, a basic introduction to malaria (the life cycle, pathogenesis, and natural immunity) is provided. There follows a general account of vaccine delivery platforms and adjuvants, and then a detailed account of malaria vaccines. This begins with whole sporozoite vaccines, followed by two sections on circumsporozoite protein (CSP) and thrombospondin related adhesion protein (TRAP) since these are the leading pre-erythrocytic subunit vaccines and form a focus of much of this thesis. This is followed by a briefer survey of other pre-erythrocytic, blood stage and transmission-blocking vaccines, as well as combination malaria vaccines. Finally the use of murine models for malaria vaccine development is evaluated.

1.2 The malaria life cycle

Figure 1.2.1 shows the life cycle of malaria. It divides into three stages, which are detailed below.

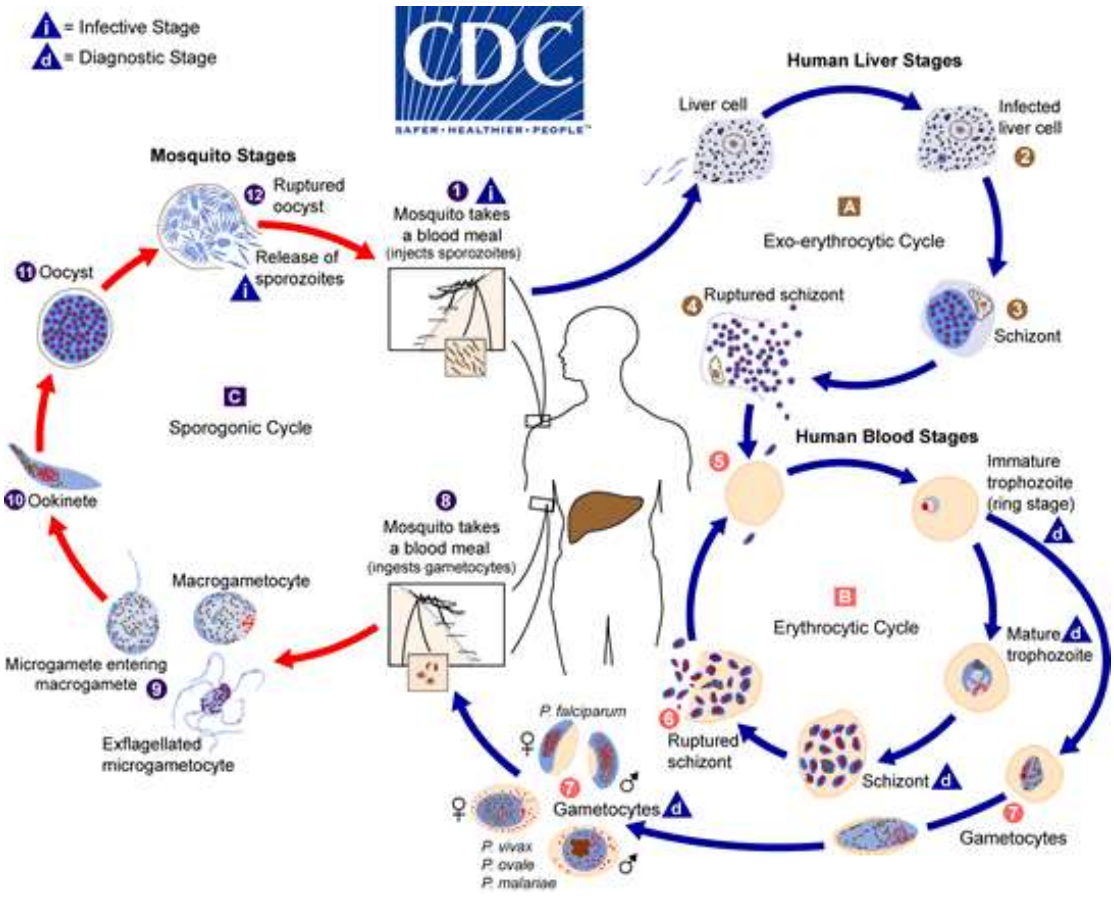


Fig 1.2.1 Life cycle of malaria

The life cycle of malaria divides into three stages: the **pre-erythrocytic** or liver stage, where sporozoites are injected into the blood by a mosquito, travel to the liver, invade hepatocytes, and replicate to form thousands of merozoites which seed the blood stage; the **erythrocytic** or blood stage, where cycles of invasion of red blood cells occur, with merozoites invading red blood cells, replicating, and bursting from red blood cells to infect fresh ones; at the blood stage, gametocytes or **sexual stages** form which, when a mosquito takes a blood meal, fuse to form a zygote and then a motile ookinete which invades the mosquito midgut to form an oocyst, where replication

of sporozoites occurs. These then migrate to the salivary glands preparatory to being delivered to another human host. (Figure from Centres for Disease Control and Prevention)

1.2.1 The pre-erythrocytic stage

Mosquitoes deposit a median 15-50 sporozoites in the skin per blood meal, or occasionally up to 500 (30-33). The sporozoites are not injected directly into capillaries, but rather into the surrounding dermis (34, 35). Over the ensuing several minutes to several hours, the motile sporozoites migrate into capillaries where they enter the circulation (33, 36). Once circulating, sporozoites arrest in the liver from as little as two (37) to 30 minutes (36, 38) later thanks to surface proteins such as CSP with an affinity for liver-expressed ligands (39, 40). The sporozoites penetrate the liver sinusoid endothelium, through or around resident Kupffer cells (41, 42), a liver-specific type of macrophage, and through or between endothelial cells (42). Sporozoites traverse several hepatocytes (43), which is thought to activate the sporozoite for invasion of a final host hepatocyte (44). Once inside a host liver cell, the parasite begins development into a schizont enclosed within a parasitophorous vacuole membrane (37, 43, 45). Development in the hepatocyte takes place over the course of two days in rodents, but longer in humans, with a development time of 5-6 days for *P. falciparum* and 8 days for *P. vivax* (46, 47). By the end of this period 1000 (*P. berghei* in laboratory mice) (48, 49) to 10,000 (*P. falciparum* in humans) (47) merozoites will have formed in each hepatocyte. In rodent malarias at least, these merozoites are not released directly into the blood, but rather packages of merozoites contained in host membrane bleb off to form merosomes which arrest in the narrow capillaries of the lung, and it is here that the merozoites are

released into the blood stream to initiate the erythrocytic stage of infection (50-53).

Some species of malaria, most notably *P. vivax* (54) but also (probably) *P. ovale* (55) and the primate malaria *P. cynomolgi* (56, 57), form dormant hypnozoites within hepatocytes instead of developing into a merozoite-producing schizont. These hypnozoites can be activated several weeks or even several years later, causing relapse infections after the primary infection has abated, with longer times to relapse associating with temperate areas, compared to tropical areas (58). Other malaria infections, including *P. falciparum* infection, or even bacterial infections such as *Salmonella enterica*, are thought able to trigger hypnozoite infection (59). These infections may be serving as a signal to the hypnozoite that conditions are favourable for transmission to mosquitoes.

1.2.2 The erythrocytic stage

Merozoites invade red blood cells to initiate the erythrocytic stage of infection. Repeated cycles of red blood cell invasion, replication and merozoite release occur (47). One or more merozoites invade a red blood cell (60); the parasite then forms a trophozoite, using haemoglobin and other cellular proteins as an energy source for development into a schizont (61), which forms 16-22 merozoites (in *P. falciparum*) (62) by nuclear division. Different species may have different preferences for their red blood cell host, with *P. vivax* (63-65) and *P. berghei* (66) having a preference for reticulocytes, but with *P. falciparum* merozoites less particular about the age of the red blood cell they invade (66, 67). This could account for higher levels of parasitaemia sometimes seen in *P. falciparum*-infected individuals compared to *P. vivax* infections (67, 68). With

some species of malaria sequestration of infected red blood cells can occur, notably in *P. falciparum* (47, 69), where at certain points in the erythrocytic cycle, synchrony (stages of red blood-cell infection occurring at the same time in the within-host population of infected red blood cells) (70) and sequestration collude to remove red blood-cells from the peripheral blood, making it possible to fail to detect infection using thin or thick blood smears (71, 72). This does not occur with *P. vivax* (71, 72) but does occur in certain circumstances during *P. berghei* infection (73).

Either immediately after the blood-stage infection is initiated (*P. vivax*) or after 10-40 days (*P. falciparum*) sexual stages, or gametocytes, are produced in a certain proportion of red blood cells instead of merozoites (47, 74). The gametocytes are male or female, and are acquired within red blood cells by mosquitoes taking a blood meal. This initiates the sexual or mosquito stage of infection.

1.2.3 The sexual and mosquito stage

Very soon after a mosquito ingests red blood cells harbouring gametocytes, the male forms begin exflagellating (75), with eight or more motile male microgametes forcibly escaping from the red blood cell, travelling to a female macrogamete and fusing to form a zygote (62, 76). The zygote develops into a motile ookinete which penetrates the midgut epithelium of the mosquito and lodges there to form an oocyst (47, 77). Over the course of about 10 days (77) each oocyst develops into thousands of sporozoites which migrate to the salivary glands, three weeks or so post-infection depending on the species (78),

preparatory to the mosquito taking a fresh blood-meal from a new host and initiating another round of the life cycle.

1.3 Malaria pathogenesis

A relatively small proportion of malaria cases – about 0.2% – result in death (1). However, because of the vast number of infections that occur each year, this still resulted in 429,000 deaths in 2015 (1). Malaria infection results in symptoms with a range of severity, from no symptoms (see §1.4 on natural immunity, below) to fevers and headaches, to severe malaria and death (71). Severe malaria proceeds from about 0.7% of infections, or about 1.4 million cases in 2015, and criteria set by the World Health Organisation include coma or cerebral malaria, respiratory distress, convulsions, severe anaemia, hypoglycaemia and acidosis, with all of these manifesting more strongly in children than in adults (71). As with direct mortality, severe malaria is a feature mainly of *P. falciparum*, with *P. vivax* associated with death from secondary causes due mainly to the severe anaemia resulting from frequent relapse infections (9). *P. vivax* also causes severe malaria, and at much lower parasite densities than *P. falciparum* (71). *P. ovale* species and *P. malariae* have lower mortality rates but *P. knowlesi* has been associated with a higher rate than *P. falciparum* malaria, although earlier treatment has since caused this to fall (79).

The causes of severe malaria are usually ascribed to either sequestration of red blood cells, metabolic factors, the host inflammatory response to the pathogen, or all three. *P. falciparum*-infected red blood cells are cytoadherent, permitting sequestration in the microvasculature, a property mediated in part by the PfEMP1 protein (80) encoded by the ~60-member *var* family (81), as well as by the *stevor* and *rif* gene families (82). Members of these families bind to various host receptors; for instance, ICAM-1 binding by a PfEMP1 variant is associated with cerebral malaria in consequence of ICAM-1 expression in the

brain microvasculature (83, 84). Other PfEMP1 variants associated with severe childhood malaria bind the endothelial protein C receptor, potentially interfering with anti-inflammatory effects mediated by protein C (85). Another variant of PfEMP1, VAR2CSA, is associated with increased susceptibility to malaria in pregnancy (86), as it binds to chondroitin sulphate A in the placenta (87). Rosetting – where infected red blood cells bind to uninfected red blood cells, forming clumps with the potential to block microvasculature (88, 89) – is a factor in cerebral (90) and severe malaria (91, 92). Rosetting is mediated by PfEMP1, RIFIN and STEVOR binding to CR1 (93), blood group A antigen and Glycophorin A (94), and Glycophorin C (95) on red blood cells, respectively. Sequestration and rosetting are thought to enable infected red blood cells, rendered detectably defective by parasite growth (96, 97), to avoid clearance by the spleen (98).

Sequestration, by reducing oxygen availability in affected organs, can lead to metabolic complications such as acidosis and hypoglycaemia which contribute to the morbidity and mortality of severe malaria (47, 98, 99). Oxygen deprivation leads to lactic acidosis, which in turn is associated with respiratory distress, one of the major manifestations of the severe form of the disease (100, 101). Hypoglycaemia can result from oxygen deprivation but also quinine treatment (99) and impaired gluconeogenesis (102), as well as the glucose demand from parasites (103, 104); it greatly increases the risk of mortality from severe malaria (105).

The other major cause of pathology in malaria infections is the host immune response. This can be initiated by malarial DNA bound to hemozoin activating TLR9 (106) which can also be activated by nucleosomes released from ruptured schizonts (107). GPI anchors activate TLR2 (108), while inflammasome

activation in macrophages is caused by heme (109). Lymphocytes also play a role in pathology: blood-brain barrier disruption by activated $CD8^+$ T-cells is implicated in cerebral malaria (110, 111). Pro-inflammatory cytokine production (TNF, IL-6) is stimulated by uric acid, a metabolic waste product released from infected red blood cells (112), and by vesicles (microparticles and exosomes) derived from infected red blood cells, which can activate macrophages via TLR4 (113). Activated monocytes produce TNF and reactive oxygen species in *P. vivax* infection (114), while cytokines like IFNγ, TNF and lymphotoxin-α are associated with cerebral malaria and have been shown to act synergistically to upregulate adhesion molecules in the brain, including ICAM-1, a ligand for PfEMP1 (115). TNF in malaria has also been shown to lead to dysfunctional red blood cell production and enhanced clearance, contributing to severe malarial anaemia (116). IL10, an anti-inflammatory cytokine which inhibits induction of TNF, is found at significantly lower levels in children with severe anaemia (117); in children with respiratory distress, both TNF and IL10 levels are significantly elevated but with a higher TNF:IL10 ratio indicating a strong overall proinflammatory milieu (118). These inflammatory responses can be protective in the majority of malaria cases, but excessive production in some individuals is a major contributor to the pathology of the disease (119, 120).

1.4 Naturally acquired immunity

In malaria endemic regions, the severity of malaria infection is age-stratified, with the number of individuals suffering severe malaria in steep decline after the first five years of life, and an increasing number of asymptomatic infections after 10 years (Fig. 1.4.1) (121). A mathematical model has suggested that as few as one or two malaria infections can protect against non-cerebral severe malaria (122) though more exposures are required for protection against cerebral malaria (123, 124); a more recent model suggests that both age and frequency of exposure are important factors (125).

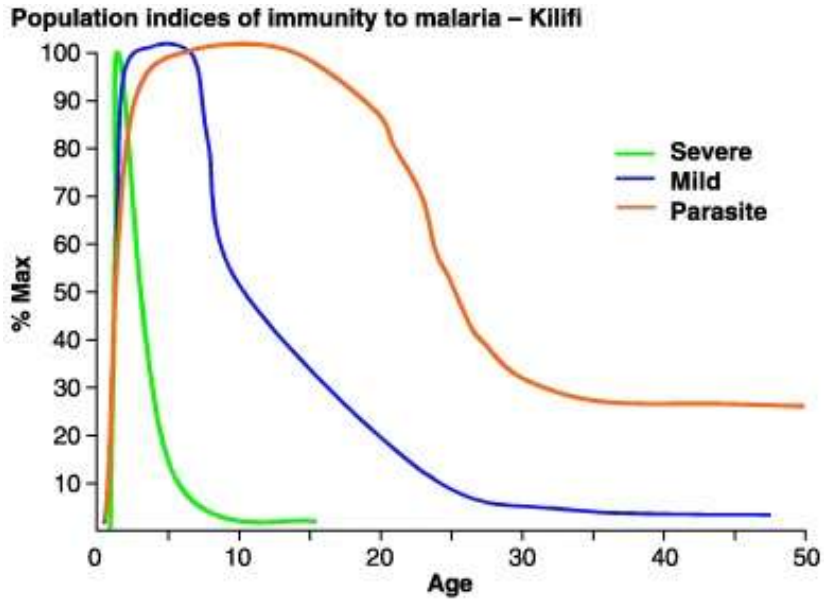


Fig 1.4.1 Age stratification of malaria severity

From (121)

The explanation for the waning severity of malaria episodes with time is the acquisition of natural immunity. Beginning at birth, studies have found cases of asymptomatic malaria possibly connected to the passive transfer of maternal anti-malarial antibodies across the placenta (126). In areas of high transmission

this initial resistance to clinical infection in infants appears to wane faster than in lower areas, leading some to question the effect (127), with some studies associating maternal antibody in the baby with protection, and others not, and some with enhanced risk of infection (128).

In any case, the role for acquired antibody- and cellular-mediated protection against malaria after infancy is more robust. Variant surface antigens expressed on infected red blood cells are able to mediate cytoadhesion. This contributes to pathogenesis. Naturally acquired antibodies against these variant surface antigens, and particularly against PfEMP1, are associated with a reduced risk of symptomatic malaria (129). Antigenic switching in PfEMP1 – the protein is coded by the *var* family of about 60 members – allows parasites to evade naturally acquired anti-PfEMP1 antibodies within the host (130) and could contribute to the length of time required to develop immunity to malaria in endemic areas.

Naturally acquired antibodies against merozoite invasion proteins also contribute to resistance to clinical or severe malaria, for instance against MSP1 (131), MSP3 (132), AMA1 (133), and GLURP (134). Many of these have been pursued as vaccine candidates, as indeed has PfEMP1, discussed below (§1.11). Interestingly, one merozoite invasion protein, PfRH5, elicits almost no antibody response in some Kenyan malaria-experienced individuals, and yet shows great promise as a blood-stage vaccine candidate (135). Since then naturally acquired antibodies to PfRH5, although less common than to other antigens, have been found in malaria-exposed individuals (136), but even so this suggests that naturally-acquired immunity may not necessarily be the best guide to choosing good subunit vaccine candidates. This is underlined by the fact that natural

immunity to malaria is never sterilising, but only controls the parasite or the pathology (137). Several studies have shown that that control is enhanced by breadth of response, i.e. a response to multiple antigens each of which is associated with some protection (132, 138).

Not only antibody responses, but naturally acquired cellular responses too associate with protection from malaria. Lymphocyte proliferation in response to MSP1 associates with protection from clinical malaria (131), with IFNγ responses in particular correlating with the time it takes to become parasitaemic in a Kenyan field study; but only as long as levels of anti-inflammatory IL-10 are low (139). In mice, adoptive transfer of $CD4^+$ T-cells specific for various blood-stage antigens is able to confer protection against *P. chabaudi* (140). Blood-stage infection with another rodent malaria species *P. berghei* induces $CD8^+$ T-cells (141), which, as discussed in the section on malaria pathogenesis above (§1.3), are associated with cerebral malaria (110, 111). In consequence of this occasionally detrimental aspect of lymphocyte responses to malaria infection, regulatory T-cells also play a role in determining whether a malaria infection becomes pathogenic or not (142).

As well as with the blood-stage, naturally acquired immunity exists for pre-erythrocytic antigens, for instance against PfCSP NANP repeats (143), TRAP and LSA1 (144), and STARP (145). These responses do not consistently associate with alleviation of clinical malaria, and it has been argued that they represent a marker of exposure rather than contributing to anti-parasite or anti-disease control (146). However, it has been found that high antibody responses against all three of the pre-erythrocytic antigens CSP, LSA-1 and TRAP in the same individual associates strongly with protection from malaria in Kenyan adults,

while such an association was not found for three blood-stage antigens (AMA-1, EBA-175 and MSP-1) (147), suggesting breadth of response at the pre-erythrocytic level is important in naturally acquired immunity. Cellular responses to pre-erythrocytic malaria antigens also play a role in naturally acquired immunity; indeed, the finding that HLA-B53 binding an LSA-1 peptide was associated with protection provided one of the first pieces of evidence that cytotoxic T-cells were helping protect humans against malaria (148).

P. vivax also generates naturally acquired immunity, and the evidence suggests that resistance to clinical malaria is generated more quickly for *P. vivax* than for *P. falciparum* (149). This may be due in part to *P. vivax* hypnozoites causing a series of relapses during a relatively short time scale (150), and resulting in a greater intensity of infection early on. Regarding the nature of the response, antibodies to blood-stage antigens appear to play an important role (151). Naturally acquired antibodies to Duffy binding protein (DBP) (152), a *P. vivax* merozoite surface protein essential for invasion (153) (with some exceptions (154)), are capable of inhibiting red blood cell binding (155). In naturally exposed groups, however, only a subset of individuals generate neutralising anti-DBP antibodies, which do correlate with protection, whereas total antibody responses to DBP do not associate with protection (156). Antibodies against PvMSP-1 have also been associated with protection (157), though not consistently (158), as well as an isotype-dependent association for PvMSP3 (159) and total IgG against the PvMSP9 N-terminus (160). Naturally acquired cellular immunity against *P. vivax* is also evident, with $CD4^+$ T-cells helping antibody production against PvTRAg (161) and PvMSP-1 (162). IFNγ- and IL-10-secreting $CD8^+$ responses against PvMSP8 (163) are also in evidence.

Whether these cellular responses associate with protection, or are pathological, is unknown.

Immunity against gametocytes can also be naturally acquired, with gametocyte prevalence in the blood decreasing amongst older (and hence more exposed) adults in Vietnam (164). Antibodies from individuals exposed to *P. vivax* (165) and *P. falciparum* (166) infection can reduce the infectivity of parasites to mosquitoes in a membrane feeding assay, as well as recognise gametocyte-harbouring red blood cells (167).

1.5 Platforms for vaccine delivery

1.5.1 Whole pathogens

The first vaccine was developed for smallpox. Inoculation or variolation, the introduction of the pustule matter from a smallpox sufferer into the skin of another, was practiced for centuries, and, if the patient survived, they became immune (168). Edward Jenner's breakthrough was to take folklore regarding the immunity of milkmaids to smallpox, and inoculate James Phipps, a local boy, with cowpox, a safer alternative. James Phipps then demonstrated immunity to a deliberate exposure of smallpox in the world's first clinical vaccine trial (169). Ethical review boards would have to wait several more centuries (170), but vaccination as a field of research and medicine was born.

Jenner's cowpox vaccine worked because the antibodies so generated were able to neutralise the related smallpox virus. The next vaccines to be developed were killed whole organism vaccines. Pasteur developed a rabies vaccine from dried rabbit nerve tissues, which saved the life of nine-year-old Joseph Meister (171). Several other killed whole organism vaccines soon followed (172, 173) including typhoid, cholera and plague (174). Serial passage of bovine tuberculosis on potatoes produced the BCG vaccine (175) which has now been delivered to more humans than any other vaccine (176).

Whole pathogen vaccines have led to some of the greatest achievements of modern medicine. Smallpox remains the only human pathogen to be eradicated, using live vaccinia viruses (23); similarly, polio has been reduced to a handful of cases mainly through use of whole attenuated polio viruses (24). Thanks to a live attenuated vaccine, measles may soon follow suit (25).

1.5.2 Proteins and polysaccharides

Toxins secreted by pathogens are often the causes of pathogenesis. Vaccines against diphtheria (177) and tetanus (178) toxins can be rendered non-toxic by formalin inactivation and heat; two researchers demonstrated their scientific commitment by self-administration of a lethal dose of the latter toxin, following vaccination. They survived (179, 180). Nor do proteins need to be toxoids to act as effective vaccines. To give just one example, many inactivated influenza vaccines are currently composed of hemagglutinin protein purified from egg-grown virus (174, 181). Polysaccharides are also able to elicit immune responses, which was exploited to produce pneumococcal (182) and meningitis (183) vaccines, amongst others. As only protein antigens can enlist T-cell help via peptides displayed on MHC class II, polysaccharides were later conjugated to proteins to elicit stronger and more durable antibody responses, particularly for administration to infants (184).

1.5.3 Virus-like particles

Some viral proteins, produced in expression systems like yeast or *E. coli*, will self-assemble to form virus-like particles (VLPs). The first such to be developed was the hepatitis B surface antigen VLP, expressed in *S. cerevisiae* (185). This was followed by human papilloma virus (186). VLPs are particularly effective at eliciting antibody responses, as the dense and ordered array of protein on their surface strongly activates B-cells, and their size is optimal for drainage to lymph nodes (187). Thus they are excellent platforms for eliciting antibody responses to heterologous proteins. RTS,S, the leading malaria vaccine, is a fusion of malarial PfCSP to hepatitis B surface antigen. Expressed in *S. cerevisiae* with

native hepatitis B surface antigen, it forms a highly immunogenic VLP (188). R21 (expressed in *P. pastoris* and consisting only of PfCSP-Hepatitis B surface antigen subunits) (189) or Rv21 (presenting PvCSP) (190) are further developments of the Hepatitis B surface antigen CSP VLP. Presentation of proteins or other moieties on virus-like particles is a burgeoning field, with new platforms in continuous development. These include plug-and-display systems based on the bacteriophage VLP AP205 (191). When this VLP subunit is fused to a SpyCatcher peptide moiety, and the antigen of interest is fused to a SpyTag moiety, spontaneous covalent bonds can form between them, thus facilitating straightforward decoration of the VLP with antigen. This has been used to present malarial transmission-blocking antigen Pfs25 and peptides from cancer-related proteins, and in both cases was able to elicit strong antibody responses after a single dose (191). Non-protein antigens have also been presented on VLPs, including nicotine chemically coupled to the Qβ bacteriophage (192).

1.5.4 Viral vectored vaccines

Since Hepatitis B surface antigen acted as the first VLP platform for presentation of a heterologous protein (193), it is appropriate that it in turn was the heterologous protein in the first viral vectored vaccine, delivered via a live vaccinia vector, and protective in chimpanzees (194). Another vaccinia virus, modified vaccinia strain Ankara (MVA), was originally developed as a smallpox vaccine but missed the opportunity to prove its efficacy before eradication of that disease (195). It has since seen extremely wide adoption as a vector for many pathogen-derived genes, from malaria (196), HIV (197), TB (198), the cancer-associated p53 gene (199), and influenza (200) amongst many others.

Adenoviruses, originally developed for gene therapy, have also since proven useful for vaccinologists (malaria (201), HIV (202), dengue (203) and others). Human adenoviruses, such as Ad5, although often immunogenic, can be rendered ineffective due to anti-vector immunity, because they derive from viruses circulating in the human population (204). This is why chimpanzee adenoviruses (205-207) and now gorilla adenoviruses (208) have been developed as alternatives. Other poxviruses (209-211) and alphaviruses (212, 213) have also served as viral vectors. Viral vectors are good at eliciting $CD8^+$ T-cell responses (214), particularly when used in prime-boost regimes with an adenovirus prime and vaccinia boost with an eight-week prime-boost interval (215, 216). But viral vectors are also potent inducers of antibody responses (217).

Exciting developments are taking place with cytomegalovirus (CMV) vectored vaccines. A rhesus CMV with particular gene deletions, encoding a simian immunodeficiency virus (SIV) antigen, protected 50% of macaques, with $CD8^+$ T-cells mediating protection (218). The immune response was found to be highly unusual: the $CD8^+$ T-cells were able to recognise MHC class II and responded to an extraordinary number of epitopes, potentially opening the way to new viral vectored vaccines recognising cryptic epitopes and of enhanced breadth, thus improving protective efficacy (219, 220).

1.5.5 DNA vaccines

DNA vaccines are simply plasmids encoding antigens injected into the skin or muscle. Pre-clinical studies have found them efficacious at generating antibodies (221) with protection mediated by $CD8^+$ T-cells (222), but this high

immunogenicity has not been replicated in humans (223, 224). It is not clear why DNA vaccines are less immunogenic in people, but strategies are being developed to improve efficacy. These include targeting the DNA to antigen presenting cells (225, 226); combining DNA vaccines with viral vectors (210, 227, 228) or proteins (229) in heterologous prime-boost regimes; delivering the DNA by methods like electroporation (230); or encoding cytokines and signalling molecules along with the gene of interest; IL-2, for instance (231). It is to be hoped these new strategies will help DNA vaccines meet their potential, for their simplicity and ease of manufacture makes them highly attractive delivery platforms.

1.6 Adjuvants

Vaccines formed of attenuated whole pathogens not only possess the antigens against which an adaptive immune response is trained, but a raft of innate-stimulating pathogen-associated molecular patterns such as bacterial cell wall components and viral DNA or RNA (232). Subunit vaccines, often consisting of just a single protein or polysaccharide, and produced to an increasingly pure standard, often lack these innate-stimulating components, and are typically less immunogenic and protective than whole organism vaccines (233). Hence adjuvants are often used with subunit vaccines to improve their immunogenicity. There are many adjuvants in development (234), though fewer licensed for human use (alum, MF59, AS03, AS04 and virosomes) (235). Here we will focus on those adjuvants used or discussed in this thesis.

1.6.1 Alum

Alum was the first adjuvant developed, used to augment immune responses to diphtheria toxoid (236). Its discovery was accidental, with the aluminium salt (potash) intended primarily to assist with precipitation of the toxoid; it was then found to improve antibody responses to the protein vaccine (237). Initially the improved titres were thought to derive from a depot effect, with slow release of the antigen perhaps stimulating secondary responses (238). However, it was later found that physically removing the 'depot' after vaccination made no difference to antibody responses (239), or lymphocyte responses (240). Instead, proposed mechanisms of alum adjuvanticity include NLRP3 inflammasome activation (241), strong binding and subsequent activation of dendritic cells

(242), the release of dendritic-cell-stimulating products like host DNA from cells killed by aluminium salts (243), or local uric acid production, a danger signal stimulatory to dendritic cells (244). Alum has been used very successfully with many licensed vaccines (245). Used with the leading malaria vaccine RTS,S, however, an alum adjuvant with monophosphoryl lipid A (MPL) (AS04) was much less immunogenic and protective than when an oil-in-water MPL and QS21 adjuvant (AS02) was used (246), following similar results when alum with RTS,S gave no protection, whereas alum with MPL and RTS,S gave 25% protection (188).

1.6.2 AddaVax and MF59

AddaVax, from InvivoGen, is a biosimilar to Novartis' (now GSK's) MF59 adjuvant. It is an oil-in-water adjuvant, composed of squalene oil with surfactants Tween 80 and Span 85 in water (247). Oil-in-water adjuvants have a long history, beginning with Freund's complete adjuvant, containing paraffin oil and mycobacteria, and later made incomplete by omission of the mycobacteria; it is used in veterinary vaccines (248). Freund's complete adjuvant causes severe pain and sometimes organ damage; it cannot be used in human vaccines (249). Freund's incomplete adjuvant was extensively tested with influenza vaccines (250), but has never been licensed for human use. MF59 in contrast has seen licensure, first with an influenza vaccine in Italy in 1997, and since then in other countries including the US; it was the second adjuvant after alum to achieve licensed status (247). MF59 acts to increase numbers of antigen-presenting cells trafficking to the injection site and then to lymph nodes (251), which may be mediated by an increase in ATP release from host cells at the site of injection

(252). MF59 increases germinal centre B-cell differentiation (253) and $CD4^+$ T-cell frequencies (254), enhancing the breadth, titre and affinity of antibodies (255).

In pre-clinical (murine) malaria vaccine studies, MF59 elicited lower antibody responses than montanide ISA720 (a water-in-oil adjuvant) and AS02, but higher titres than alum, when used with PvDBP. However, all three adjuvants outperformed MF59 in terms of eliciting antibodies with erythrocyte-binding blocking activity (256). Similarly, R21 formulated with AddaVax or MF59, although eliciting anti-CSP titres as high as that with Abisco-100 or Matrix M adjuvants, produced inferior T-cell responses, and there was a large difference in protective efficacy of the regimes in a challenge experiment (189). It has been argued, however, that murine immune responses to MF59 do not reflect those seen in clinical trials, particularly the Th2 skew in mice (247).

1.6.3 Matrix M

ISCOMs – immune stimulating complexes – were originally conceived as a means of enhancing antigen presentation to the immune system, by locking the antigen into cage-like particles (257) formed of cholesterol and saponins; these two compounds have high affinity for one another (258). It was later reported that the antigen needn't be incorporated into the ISCOM for it to have adjuvant effect (257). Different fractions of saponin, derived from the *Quillaja saponaria* tree, have different tolerability and immunogenicity profiles. By optimising the ratio of two such fractions, A and C, high immunogenicity and high tolerability was obtained and the Matrix M (or Abisco-100) adjuvant was developed (257). Early pre-clinical studies demonstrated high antibody and Th1 $CD4^+$ T-cell

frequencies, with a balanced Th1/Th2 profile (259), a response also found in clinical trials, where the potent antibody response with Matrix M allowed for dose sparing of a vaccine (260, 261). The mode of action, as with other adjuvants, is not fully understood, but Matrix M, in the absence of antigen, has been shown increase the recruitment of leukocytes to the spleen and to draining lymph nodes (262, 263). Its use with malaria vaccines has been promising: Matrix M induces more anti-PvDBPII antibodies with binding inhibition activity than with Montanide ISA720 adjuvant (264). In addition, as mentioned above (§1.6.2), Matrix M confers higher protective efficacy than AddaVax on mice vaccinated with R21 (189). The adjuvant used with the leading malaria vaccine, RTS,S/AS02, is itself a saponin-containing adjuvant, composed of QS21, a fraction of *Quillaja saponaria* extract, with MPL in an oil-in-water emulsion. As mentioned above, AS02 conferred much more robust protection against malaria challenge in a clinical trial than did alum/MPL (AS04) and the oil-in-water adjuvant alone (AS03) (246). AS01B, likewise containing MPL and QS21 but in a liposome rather than oil-in-water formulation, later outperformed AS02 in a separate clinical trial (265). Improved immunogenicity and protective efficacy was seen with AS01B, significantly so in terms of anti-CSP titres, but only marginally and not significantly in terms of protection against challenge. On this basis, AS01 became the preferred adjuvant for further clinical development of RTS,S (265).

1.6.4 Genetic adjuvants

Sequences that stimulate improved immune responses when genetically fused to the antigen of interest are called genetic adjuvants. One such is IMX313, a hybrid

version of the oligomerization domain from chicken complement-component 4 binding protein, which induces heptamer formation and enhances MSP1 titres in mice (266). The improvement likely derives from an enhanced ability to cross-link B-cell receptors, a property shared with virus-like particles (187). As well as enhancing antibody responses, IMX313 also adjuvants $CD4^+$ and $CD8^+$ T-cell responses when fused to the tuberculosis antigen 85A (267). However, this improvement did not translate to clinical trial of 85A fused to IMX313 (268). IMX313 has also been shown to improve the quality and quantity of antibodies to Pfs25 (269). It has served as the basis for a novel nanoparticle vaccine, fused to two different ligands, SpyCatcher and SnoopCatcher, which allows any two antigens fused to SpyTag and SnoopTag ligands to be easily coupled and efficiently displayed to the immune system (270).

A genetic adjuvant based on a completely different mechanism of action is the invariant chain (Ii), or CD74, which helps MHC class II assembly and trafficking to endosomes. When fused to a $CD4^+$ epitope, the C-terminal end of Ii, being trafficked to precisely the location of the MHC class II molecules, augmented T-cell responses (271, 272). The improvement in T-cell responses includes, unexpectedly given the association of Ii with MHC class II, $CD8^+$ T-cell responses (273, 274). It is not known how this $CD8^+$ T-cell adjuvant effect is mediated, but antigens fused to Ii show improved antigen presentation on MHC class I, and the presentation can occur independently of $CD4^+$ T-cell help (275). Since $CD8^+$ T-cells mediate TRAP-specific protection against malaria challenge, these findings were exploited by fusing Ii to ME–TRAP, delivered by viral vectors; Ii enhanced both $CD4^+$ and $CD8^+$ T-cell responses in mice and macaques (276).

1.7 Whole sporozoite vaccines

1.7.1 Radiation-attenuated parasites

Vaccination with whole parasites provided the first evidence that a vaccine against malaria was possible. Studies with birds and *P. gallinaceum* showed that formalin-treated sporozoites or those exposed to UV light and administered intravenously could protect the birds against sporozoite, but not erythrocytic, challenge (277). With the rodent malaria *P. berghei*, however, immunization with killed sporozoites wasn't successful, so a method of partial inactivation by treatment with radiation – radiation-attenuated sporozoites, or RAS – was developed and shown to confer protection on mice (278). It was shown that the RAS could invade liver cells, but not complete development in HepG2 cells (279). In 1973 the first volunteer was vaccinated with RAS from irradiated mosquitoes. He was protected against *P. falciparum* but not *P. vivax* infection (280). Several other volunteers were subsequently also entirely protected by this method (281, 282) and one person against both *P. vivax* and *P. falciparum* by vaccination with RAS from both species (283). High numbers of bites from irradiated mosquitoes were required: over 200-400 in order to be protected (282). RAS vaccination was safe, and protection seemed to last at least nine weeks, or 42 weeks if a booster vaccination was applied (284).

Vaccination by bites from hundreds of irradiated mosquitoes was not considered a practical strategy, so attention turned to subunit vaccines such as those based on CSP (285), discussed in §1.8 below. However, in 2002, a private company, Sanaria, was set up to commercially develop a RAS vaccine based on irradiated and dissected cryopreserved sporozoites (PfSPZ) (286). Injected subcutaneously or intradermally, PfSPZ were poorly immunogenic and only two

out of 44 volunteers were entirely protected against challenge; because of this, further work was carried out establishing in mice and non-human primates that intravenous injection was required to allow the parasites to reach the liver and partially develop in hepatocytes (287). Subsequently 100% protection was achieved using PfSPZ administered intravenously to human volunteers, when five doses of $1.35x10^5$ sporozoites were given (288). Many dose-escalation and dose-number studies (285) have led to clinical trials in malaria endemic areas, including a recent trial in Mali where 51% vaccine efficacy was obtained (289), a level comparable to RTS,S vaccines in field conditions in adults (290). Under field conditions, malaria vaccines must protect against heterologous challenge as well as against those strains homologous to the strain the vaccine is based on. Most PfSPZ trials used homologous challenges, so a recent study investigated its efficacy against heterologous challenge, finding that, if challenge occurred just nine weeks after final immunization, protection against homologous and heterologous malaria strains was equivalent, at 92% and 80% respectively. However, 24 weeks after final immunization, challenge with a heterologous strain was only 10% effective, while protection against the homologous strain remained high at 70% protection (291). With a homologous challenge, PfSPZ vaccination appears to remain protective against a repeat challenge for up to one year (292).

The mechanism of RAS-mediated protection is complex (293), but certainly involves antibodies, particularly against CSP, discovered from RAS studies (294, 295) and which the leading malaria vaccine, RTS,S, is based upon. When $CD8^+$ T-cells are depleted from RAS-vaccinated mice protection is lost (296, 297). Adoptive transfer of a RAS-elicited $CD4^+$ T-cell clone was also able to

protect mice, apparently through cytolytic activity (298); $CD4^+$ T-cell help is also vital for a good response to RAS vaccines (299). A recent PfSPZ trial associated antibody responses and $V\partial 2^+$ T-cells, but not other cellular responses, with protection from infection in humans (292).

P. vivax has not been entirely forgotten in RAS vaccine studies. In the first trial since two volunteers were vaccinated and protected against *P. vivax* using RAS of that species, a study using a median of 434 bites from irradiated *P. vivax*-infected mosquitoes resulted in 42% sterile protection in volunteers, similar to levels found using *P. falciparum* RAS with that schedule (300). Perhaps by chance, all the protected volunteers were women; though women are less susceptible to malaria than men (301)

1.7.2 Live sporozoites under chloroquine prophylaxis

RAS parasites arrest in the liver, unable to develop further than the trophozoite stage because of DNA damage from irradiation (279). Allowing the parasite to fully develop and then clearing the infection with chloroquine also provides complete protection from subsequent sporozoite challenge, as first demonstrated in mice in 1977 (302). However, instead of requiring 400-1000 bites to achieve high levels of protection, as with irradiated mosquitoes, 36-45 bites from non-irradiated mosquitoes with 13 weeks of chloroquine prophylaxis was sufficient to protect 100% of volunteers in a clinical trial (303) with 66% protection 28 months later (304). Blood-stage challenge of similarly vaccinated individuals resulted in no protection (305), suggesting that this regime protects via mechanisms targeting the liver stage. There is evidence for an association of cytotoxic $CD4^+$ and $CD8^+$ T-cells with sterile protection (306), though antibodies

from a sporozoite/chloroquine prophylaxis vaccine trial also found that antibodies raised by this regime could neutralise sporozoite gliding motility and *in vivo* infectivity (307).

Cryopreserved sporozoites combined with chloroquine prophylaxis (PfSPZ-CVac) can confer levels of 100% sterile protection on volunteers when the sporozoites are administered intravenously (308) but not intradermally (20% protection (309)). Most interestingly, the dose of sporozoites required for 100% protection is an order of magnitude less and required three shots, compared to the five shots required for cryopreserved PfSPZ delivered without chloroquine prophylaxis. This should markedly enhance the deliverability of this vaccine regime under field conditions. As with genetically attenuated parasites, discussed below, the reason for the apparently improved efficacy obtained by administering sporozoites under chloroquine chemoprophylaxis appears to be that a longer liver-stage development allows more antigens to be presented to the immune system, enhancing protection (310).

1.7.3 Genetically attenuated parasites

Liver-stage arrest of malaria parasites can be achieved by knock-out of crucial genes as well as by irradiation. Initial studies knocked out a single gene (*uis4* (311), *uis3* (312), or *p36p* (313)), which led to developmental arrest in the livers of mice and complete or almost complete protection against malaria challenge with *P. berghei.* A double-deletion *P. falciparum* parasite (*p52⁻/p36⁻*, (314)) became the first genetically attenuated parasite (GAP) to reach clinical trial, delivered to six volunteers by around 200 bites from infected mosquitoes (315). One volunteer developed blood-stage parasitaemia, demonstrating the principal

risk associated with GAP vaccines: breakthrough infections caused by incomplete attenuation (316). To avoid this problem a triple deletion *P. falciparum* GAP was produced (*p52⁻/p36⁻/sap1⁻* (317)). A trial using 10 volunteers resulted in no breakthrough infections after 150-200 bites from infected mosquitoes, a finding replicated with an analogous *P. yoelii* triple knockout, which conferred complete sterile protection on mice (318).

Another line of research has investigated the relative protective efficacy of late-arresting GAPs compared to early-arresting GAPs. As mentioned above, a longer liver-stage development may expose more antigens to the immune system. A study in mice compared an early-arresting GAP (*sap1⁻* (319)) and RAS vaccination with a late-arresting GAP (*fabb/f⁻* (320)), demonstrating that the late-arresting GAP conferred higher levels of sterile protection and significantly higher levels of $CD8^+$ T-cells (310).

1.8 Circumsporozoite protein (CSP)

1.8.1 Nature and function of CSP

The most studied malaria antigen is the circumsporozoite protein (CSP), first identified in 1980 for *P. berghei* (295, 321) and 1982 for *P. falciparum* and *P. vivax* (322). Present in oocysts (323-326) and on midgut (327) and salivary gland (295, 321) sporozoites, CSP plays a major role in exiting from oocysts (328), invading mosquito salivary glands (329, 330) and invading liver hepatocytes (295, 321, 331). It is the most abundant surface protein on sporozoites (332) which may be a factor contributing to its immunodominance (333). CSP has a molecular weight of 42 – 67 kDa in most malaria species (334) and is composed of three domains: an N-terminal domain, a long central repeat region, and a C-terminal domain where a GPI anchor attaches the protein to the sporozoite surface, as shown in Figure 1.8.1 (335-337).

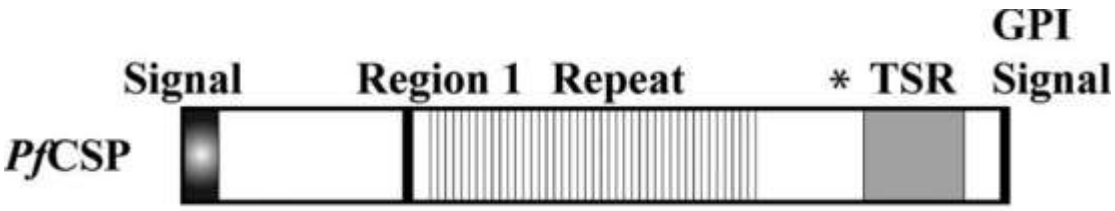


Figure 1.8.1: Schematic structure of circumsporozoite protein

Circumsporozoite protein can be divided into three domains, an N-terminal domain containing the conserved Region 1 KLKQP motif, a central region with repeats of 4-11 amino acids (depending on species) and a C-terminal domain with a conserved TSR domain and Region II motif. In addition there is a signal sequence at the N-terminal end of the protein, and a signal for a GPI anchor to the membrane at the C-terminal end. (Adapted from (338)).

During the pre-erythrocytic stage, at least two functions of CSP are important in facilitating invasion of liver hepatocytes. The first is motility,

permitting sporozoites deposited in the skin to migrate towards capillaries and move into the bloodstream (34) (35, 339). Motility is also crucial in traversing epithelium (43, 340). Anti-CSP antibodies have been shown to decrease or ablate sporozoite motility (35) which may contribute to the mechanism by which anti-CSP antibodies neutralise sporozoites (341).

The other important pre-erythrocytic function of CSP is adhesion to and invasion of hepatocytes (331). CSP binds heparan sulphate proteoglycans on the surface of hepatocytes (342, 343), a process in which both the N-terminal domain (39, 344) and C-terminal TSR region (343, 345) are implicated. The TSR region is apparently masked by the N-terminal domain until invasion begins, whereupon the N-terminal domain is cleaved and the TSR domain is revealed (346). HepG2-binding peptides are present in all three domains of CSP (347). Antibodies to the central repeat region (331) may neutralise sporozoites by interfering with the hepatocyte-binding properties of the central repeat region (347). Likewise, a plausible explanation for the neutralising activity of antibodies specific for the TSR domain (345, 348) and of antibodies interfering with proteolytic cleavage of the N-terminal domain (349) is that these antibodies interfere with the invasion of hepatocytes.

The contribution of CSP to infection does not cease once a sporozoite has successfully invaded a hepatocyte. Once the hepatocyte is infected CSP is exported through the parasitophorous vacuole membrane via PEXEL/VTM motifs in the N-terminal domain. Then, via a nuclear localization signal in the TSR domain, CSP is transferred to the nucleus using the same α3 (and to a lesser extent, α4) importins that translocate NFκB into the nucleus (350). This has been repeated using CSP in a colorectal cancer cell line (351). CSP outcompetes

NFκB importation leading to inhibition of expression of a large number of inflammatory genes, allowing enhanced growth of the intracellular parasite (350).

CSP also inhibits protein synthesis in hepatocytes and macrophages (352), probably by binding to ribosomal RNA (353). Whether this assists liver-stage development is unclear. Singh *et al.* (350) question whether CSP can have ribotoxic effects, given that CSP-transgenic mice (333) show no defects.

CSP is present in all malaria species and some regions show very high levels of conservation, chief of which are the N-terminal Region I (KLKQP) (335), present in all mammalian *Plasmodium* species but not the avian *P. gallinaceum* (336); and the C-terminal TSR domain containing Region II (PCSVTCGNG) (335), present in both avian and mammalian malarias (336). The central repeat region of CSP, though present in all species, varies considerably between them, always consisting of multiple repeats but consisting of NANP in *P. falciparum* (335), GDRADGQPA (354, 355), ANGAGNQPG, (356, 357) or the "vivax-like" APGANQ(E/G)GGAA (358) in *P. vivax*, NAAG in *P. malariae* (359), QGEGNPPAP or VPQGDPPAP in *P. ovale* (FLQU01000251.1, FLQV01001754.1, FLRD01000072.1, FLRE01000093.1) and GQPQAQGDGANA in *P. knowlesi* (360).

1.8.2 CSP vaccine history and mechanisms of protective efficacy

CSP has been a focus of malaria vaccine development since it was identified as a major immunogen following analysis of immune responses to RAS vaccination (322, 361) and since CSP-specific monoclonals proved protective in mice (295). Early attempts at a CSP subunit vaccine included short synthetic NANP peptides from the PfCSP repeat region coupled to carrier proteins (362), and 16 to 48

tandem repeats of PfCSP expressed in *E. coli* (363). In both cases sera from immunized mice were able to inhibit sporozoite invasion of HepG2 cells. The 32 tandem repeat PfCSP protein (FSV-1), absorbed to alum, was soon trialled in humans. It was well tolerated and conferred sterile protection on one volunteer (364). Similarly, the short $(NANP)_3$ peptide coupled to tetanus toxin conferred sterile protection on two volunteers in a separate phase I clinical trial (365). A direct comparison of tandem repeat-based peptides and proteins from PbCSP with RAS vaccination in mice demonstrated substantially lower protective efficacy of the peptide and protein CSP subunit vaccines, a result the authors argued was due to their failure to generate cellular immune responses (366). Adding the $NS1_{81}$ protein to FSV-1 provided T-cell help and, with the assistance of a different adjuvant, improved immunogenicity was obtained (367); but this did not enhance protective efficacy (368).

Another attempt to improve the immunogenicity and protective efficacy of the PfCSP subunit vaccine was made by fusing the CSP tandem repeat to the Hepatitis B surface antigen (R16HBsAg). This proved considerably more immunogenic in mice than a polypeptide of 32 NANP tandem repeats (193). The R16HBsAg vaccine was later tested in a phase I clinical trial and found to be safe and immunogenic (369). Meanwhile, evidence was accumulating for a role in protective immunity of CSP-specific T-cells. It was found that murine cytotoxic T-cells specific for an epitope in the C-terminal domain of PfCSP could lyse CSP-expressing fibroblasts (370). Likewise, adoptive transfer of cytotoxic T-cells specific for a C-terminal domain PbCSP epitope was able to protect naïve mice from challenge (371). Humans vaccinated with RAS were shown to generate cytotoxic T-cells against the same C-terminal domain epitope as did mice, and

could likewise lyse B-cells transfected with PfCSP (372). This led to inclusion of the C-terminal domain in the Hepatitis B surface antigen-based CSP vaccine. The first published report of this vaccine, RTS,S, was a clinical trial showing anti-CSP antibody responses, poor cellular responses, but protecting two out of six volunteers against malaria challenge (188).

RTS,S is now the world's leading malaria vaccine, having received a positive scientific opinion from the European Medical Agency in 2015; pilot programmes in Ghana, Kenya and Malawi will commence in 2018 to test the feasibility of large-scale delivery (WHO press release, 24 April 2017). But to get to this point, RTS,S has had to undergo several improvements in its formulation since the first clinical trial 20 years ago. These improvements have principally been to the adjuvant with which RTS,S is administered. In the first clinical trial, MPL with alum (AS04) generated higher levels of immunogenicity and protective efficacy than alum alone (188). The next trial tested RTS,S with one of three adjuvant formulations: AS04, AS03 (an oil-in-water emulsion) and AS02A (oil-in-water with MPL and QS21). RTS,S/AS04 and RTS,S/AS03 conferred sterile protection on 13% and 29% of volunteers respectively, whereas RTS,S/AS02A had an exceptionally high protective efficacy of 86%, despite similar anti-CSP titres in all groups (246). After 6 months, anti-CSP titres had declined by up to a half and protection had waned to 29% in the same AS02A group (373). The unusually high protective efficacy of RTS,S/AS02A in this trial may have been due to a fractional third dose having been administered for safety reasons instead of the intended full final dose; a follow-up study published recently repeated these findings with RTS,S/AS01, where a fractional third dose regime conferred significantly higher protection than the standard regime (87% versus

63% sterile protection respectively, p=0.04); this result could also be due to a delay in administering the third dose (374). While RTS,S/AS02A trials were on-going, including a field trial with children in Mozambique that showed 58% vaccine efficacy against severe malaria (375), preclinical studies identified an adjuvant formulation that provided enhanced immunogenicity and protective efficacy with RTS,S in rhesus macaques (376). The adjuvant was AS01B, consisting of MPL and QS21 in liposomes. It gave only marginally higher anti-CSP titres, but the cellular immunogenicity (by IFNγ ELISpot) was significantly higher (376). A head-to-head clinical trial in adults was subsequently organised and gave RTS,S/AS02A a vaccine efficacy of 32% compared to a vaccine efficacy with RTS,S/AS01B of 50%, with significantly higher anti-CSP titres and IFNγ ELISpot responses in RTS,S/AS01B (265). A phase IIb field trial in Kenya comparing the two adjuvants with RTS,S found that the superior immunogenicity of RTS,S/AS01B held, giving significantly better anti-CSP titres compared to RTS,S/AS02A, though no significant difference in protective efficacy on this occasion (377).

All this work led to the first Phase III trial of a malaria vaccine (or any parasite vaccine) in history, evaluating RTS,S/AS01 in children and infants in seven sub-Saharan African countries (378). All children and infants received three doses, at 0, 1 and 2 months from the start of the study. At 12 months, efficacy against clinical malaria in infants (6–12 weeks) was 31% (379) and in children (5–17 months) was 55% (380). By 18 months, efficacy had waned to 27% in infants and 46% in children (28). A forth dose was given at 20 months to some infants and children, and from then until the end of the study, vaccine efficacy was higher in the groups which received the forth dose, with efficacy in

children, compared to the control, of 26% and 11% respectively, and in infants, 24% and 8% respectively (381). Of note, a significant adverse event has been associated with RTS,S vaccination in these Phase III field studies: increased risk of meningitis (381). It has been suggested that the control vaccine, against rabies, could be conferring non-specific protection against meningitis, as the incidence of meningitis in RTS,S vaccinees is similar to background rates (382). Although representing a major milestone in malaria vaccine development, the efficacy from these Phase III studies falls far short of the WHO's stated goal of achieving a malaria vaccine providing 75% protective efficacy against clinical malaria (WHO Malaria Technology Roadmap, November 2013). This warrants continuing clinical and preclinical work on CSP and other malaria vaccines.

A higher-density variant of RTS,S, called R21, has been developed in the Jenner Institute (189). Expressed in *Pichia pastoris* rather than *Saccharomyces cerevisiae*, every monomer subunit in the R21 particle is a Hepatitis B surface antigen-PfCSP fusion protein. In contrast only one in four subunits in RTS,S present PfCSP, as that was the only way to stably produce the virus-like particle (188). R21 is highly immunogenic and protective in mice (189) and in on-going clinical trials (Adrian Hill, personal communication). Florian Brod (Jenner Institute) has performed experiments showing superior immunogenicity of R21 over RTS,S at low doses in murine experiments; in Chapter 5, this data is analysed and given an explanation using a novel mathematical model.

Several alternatives to the Hepatitis B surface antigen as a delivery platform for CSP have been and continue to be pursued. In particular, DNA and viral-vectored vaccines have been a major focus of investigation, as means of eliciting strong CSP-specific CD8+ T-cell responses. Such responses have been

shown to protect mice via adoptive transfer (371) and can be elicited in humans by RAS vaccination (372). A murine preclinical study of a PyCSP DNA vaccine demonstrated protection against challenge, which was dependent on CSP-specific antibodies, shown by serum transfer, and on $CD8^+$-specific T-cells, shown by depletion and subsequent abrogation of protection (383). A clinical trial of a PfCSP DNA vaccine demonstrated for the first time that $CD8^+$ T-cells could be elicited by a DNA vaccine in naïve human volunteers (384), but a follow-on trial in which a mixture of DNA vaccines encoding PfCSP and four other liver-stage antigens was used demonstrated no protective efficacy; CSP-specific $CD8^+$ T-cell responses were detected in under half of volunteers (224).

Viral vectors of CSP have a longer heritage. Vaccinia was used in 1984 to deliver PkCSP in a rabbit immunization experiment (385). Anti-CSP antibodies were generated, but it was not established that CSP-specific $CD8^+$ T-cells could be elicited as a result of vaccinia-vectored CSP vaccination until 1988 (370). Initial challenge experiments in mice using various viral vectors to deliver PyCSP demonstrated no protective efficacy (386) but protection using PyCSP-based viral vectors was later obtained using an influenza/vaccinia heterologous prime-boost regime in mice (387). A single shot of human adenovirus 5-vectored PyCSP was able to elicit higher CSP-specific $CD8^+$ T-cells than any previous vaccines and conferred substantial protection on mice (388) and quite soon an attenuated vaccinia virus, NYVAC-Pf7, provided the first test in humans of a viral-vectored malaria vaccine. NYVAC-Pf7 encodes seven malaria genes including PfCSP, but was poorly immunogenic and conferred much lower protective efficacy in comparison to other vaccines in trials at the time, particularly RTS,S (389). Similarly, later trials delivering PfCSP using either FP9 and MVA heterologous

prime-boost (390), adenovirus-5 homologous prime-boost (391) or chimpanzee adenovirus-63/MVA heterologous prime-boost (392) showed little or no protective efficacy, and although a later trial with DNA/Adenovirus-5 prime-boost of PfCSP with PfAMA1 showed 27% protective efficacy (393), this was associated with PfAMA1 cellular responses only (394). Of further interest, a replication-competent adenovirus displaying $(NANP)_5$ on its surface has been able to generate antibodies in mice capable of neutralising sporozoites in an *in vitro* invasion assay (395), but to a lesser extent in *Aotus nancymaae* monkeys (396). But perhaps the most novel recent use of a CSP-based viral vector is one that delivers a neutralising monoclonal antibody for expression in target cells: an adeno-associated viral vector encoding the PfCSP-specific murine monoclonal 2A10 was used to transduce mice and the mice were subsequently protected from challenge with PfCSP *P. berghei* transgenic parasites, by up to 70% (397).

In consequence of the early failures of CSP-based DNA and viral-vectored vaccines to confer sterile protection on volunteers, further investigations pursued combining these methods of delivery with each other, or with RTS,S. Preclinical work in mice (398) and macaques (399) delivering CSP with other antigens using heterologous DNA prime and vaccinia boost demonstrated this regime was protective. A later clinical trial showed no protective efficacy from a DNA-DNA-vaccinia-vectored PfCSP regime, in contrast to partial protective efficacy from the same regime encoding PfTRAP (400). A PfCSP-DNA/RTS,S sequential immunization regime was considered to have potential as volunteers vaccinated with PfCSP DNA followed by RTS,S had higher cytotoxic T-cell responses than RTS,S-only vaccinated volunteers (401) and the volunteers also had anti-CSP titres comparable to that of RTS,S alone (402). No challenge,

however, was undertaken to assess protective efficacy. Meanwhile, a clinical trial of RTS,S with viral-vectored PfCSP was underway, again with the motivation of combining an antibody and $CD4^+$ T-cell-inducing vaccine (RTS,S) with one that induced high $CD8^+$ T-cell responses, i.e. viral-vectored PfCSP. An RTS,S prime with a modified vaccinia virus Ankara (MVA) boost conferred partial protective efficacy of 33%, yielding lower than hoped for cellular responses (403). A study in macaques found that priming with adenovirus-35-vectored PfCSP and boosting with two shots of RTS,S ("ARR") produced better cellular responses and humoural responses equally good as either component alone (AA or RRR) (404). This led to a clinical trial testing the same regime (ARR) against RTS,S alone (RRR); in this case, although the ARR regime elicited superior cellular immunity, it produced a significantly worse humoural response, and there was no significant difference in protective efficacy (405).

Almost every type of vaccine vector has been used at some point to present CSP to the immune system. There isn't space here to give these other platforms a detailed treatment, so what follows is a brief list with a few highlights. So far we have seen that virus-like particles, viruses and DNA vaccines have been used to display CSP. Virus-like particles (VLPs) based on other than the Hepatitis B surface antigen have also been developed, including one based on the Hepatitis B core antigen. The latter was used to display central repeat B epitopes and a universal T-cell epitope from the C-terminal domain (406). In a phase I clinical trial this vaccine was poorly immunogenic, possibly as a result of using a suboptimal adjuvant, alum; the vaccine has not seen further development (406). Another VLP platform in development couples PfCSP to Qβ, a bacteriophage-derived VLP (407). With this platform higher titres against all

regions of the protein were obtained with Qβ-CSP than with soluble CSP, in both mice and macaques; it conferred 70% sterile protection on mice (407). Another VLP platform recently exploited for PfCSP presentation is the AP205 system, using SpyTag and SpyCatcher to covalently attach PfCSP to the VLP. In mice this generated significantly higher anti-CSP titres than the soluble protein (408). Two self-assembling peptide systems have also been used to generate anti-CSP vaccines. One, a self-assembling protein nanoparticle (SAPN) which couples an oligomerization domain to three $CD8^+$ T-cell epitopes and 4 – 6 NANP repeats protected mice against a PfCSP *P. berghei* transgenic parasite challenge (409, 410). The other self-assembling system fuses $(NANP)_3$ with the Q11 peptide which spontaneously forms nanofibres; these are immunogenic against $(NANP)_3$ in mice (411).

One CSP vaccine has sought to dispense with any platforms, consisting of a long synthetic peptide representing part of the C-terminal domain of CSP. This was shown to confer 60% sterile protection in mice against *P. berghei* (412), and has generated humoural and cellular responses in humans (413, 414), but has not protected any volunteers against challenge (415). Another minimal vaccine, $(NANP)_3$ coupled to tetanus toxoid, was mentioned earlier, and was able to protect one volunteer from malaria challenge; but it had poor seroconversion frequencies, from 53-71% (365).

Synthetic peptides representing the repeat region of CSP have also been used in the form of multiple antigenic peptides (MAPs), which are branched peptides based on a multiple lysine core (416). MAPs present 4, 8 or 16 peptides, which can be identical or different. The first MAP included $(NANP)_4$ and was able to generate antibodies which recognised native PfCSP (416). Soon T-cell epitopes

were included in MAPs and protective efficacies of 50-100% were achieved in mice against *P. berghei* (417) and *P. yoelii* challenge (418). In a clinical trial, a MAP presenting $(NANP)_3$ and a PfCSP $CD4^+$ epitope was able to generate antibodies reacting with live sporozoites, but this was restricted to certain HLA genotypes (419). Although no challenge was carried out, antibodies from these volunteers could neutralise PfCSP *P. berghei* transgenic parasites in an *in vitro* invasion assay (420). The HLA genotype limitation was overcome by inclusion of an apparently universal T-cell epitope from the C-terminal domain of PfCSP in a MAP-like vaccine synthesised by linking peptides to the lysine core via oxime bonds. This succeeded in obtaining 100% seroconversion in all volunteers (421).

Viruses are not the only pathogen-based vectors to be exploited as vaccine platforms: bacterial vectors have also been used to deliver CSP. The first and most studied bacterial vector was *Salmonella enterica*. Oral vaccination of mice with an avirulent strain encoding CSP was able to induce sterile immunity in about half of mice (422). It was safe when delivered to humans, but elicited poor humoural and cellular responses in most volunteers; $CD8^+$ T-cells from one volunteer displayed cytolytic activity, however (423). As intracellular bacteria, Salmonella should be well placed to stimulate $CD8^+$ T-cell-specific immunity; a strategy of exporting NANP repeats to the cell surface via MisL (424) and releasing it by cleavage (425) has shown it is possible to introduce proteins to the cytoplasm of host cells via bacterial vectors. NANP repeats are not $CD8^+$ T-cell epitopes, but another study exploiting the type III secretion system of Salmonella to deliver a PbCSP $CD8^+$ T-cell epitope was partially protective in mice (426). A similar export strategy was used in another study, this time with a heterologous boost of PfCSP DNA, which generated superior cellular responses

but inferior humoural responses to that of a homologous PfCSP DNA prime-boost regime (427). BCG has also been used as a vector for CSP, and induces CSP-specific antibodies and T-cell responses, but so far no challenge experiments have been carried out (428-431). An *E. coli* vectored PbCSP vaccine was able to protect against *P. berghei* challenge after subcutaneous immunization, with 50-75% sterile protection (432). Even parasites have been used as vectors for CSP: *Leishmania enriettii* transfected with PyCSP expressed the protein on its surface and mice immunized by intravenous administration of the transfected promastigotes enjoyed sterile protection of 14-25%, with anti-CSP antibodies and cytotoxic T-cell responses both generated (433). *Toxoplasma gondii* has also been used as a PyCSP vector, with 10% protection obtained in mice (434).

1.8.3 P. vivax CSP vaccine development

Although *P. vivax* vaccine development has a history almost as long as for *P. falciparum*, it has not since received the same level of attention (435). The first attempt at a PvCSP vaccine was a recombinant protein mainly consisting of the central repeat region expressed in yeast. Mice vaccinated with this protein in alum generated antibodies capable of neutralising sporozoites in an *in vitro* invasion inhibition assay (436). A challenge experiment in *Saimiri sciureus* monkeys using the same PvCSP construct (VIVAX-1), as well as a repeat-only construct ($NS1_{81}V20$), found that VIVAX-1 was as effective as RAS vaccination in conferring sterile protection (33%), with the repeat only vaccine slightly less effective (17%) (437). A clinical trial of a repeat-only $NS1_{81}V20$ vaccine saw poor seroconversion rates and no volunteers had sera showing any *in vitro* invasion inhibition efficacy (438). A paper published the following year offered an

explanation for the lack of efficacy of the repeat-based PvCSP vaccine in *Saimiri* monkeys: the vaccine was not eliciting anti-AGDR antibodies to a tetramer sequence within the nonamer unit repeat; whereas a protective monoclonal antibody did recognise it (439). People naturally exposed to vivax malaria mostly test positive for antibodies to the entire repeat region of PvCSP, but only 18% show antibodies to AGDR; this has also been found in volunteers vaccinated with $NS1_{81}V20$ (440). Mice vaccinated with AGDR, meanwhile, generated antibodies that could recognise AGDR and the native nonamer sequence (440), though no challenge has been carried out to test the protective efficacy of AGDR-based vaccines.

Multiple antigenic peptides, similar to those discussed above but presenting eight PvCSP B- and T-cell epitopes, have proven immunogenic in mice; the sera could recognise native sporozoites in immunofluorescence assays (441). Similar constructs, presenting two copies of the nonamer unit repeat of PvCSP and the P2 universal T-cell epitope from tetanus toxin protected 42% of *Saimiri boliviensis* monkeys against *P. vivax* challenge, though no unvaccinated control was used (442). Another *Saimiri* challenge experiment with the same MAP found an association between AGDR-specific titres and protection, as well as a correlation between such titres and peak parasitaemia (443).

A DNA vaccine encoding four vivax antigens including full-length PvCSP induced antibodies in mice which could recognise the native PvCSP protein but not the AGDR tetramer (444), which appears to be the only PvCSP DNA vaccine study performed to date. A baculovirus-vectored vaccine expressing both PvCSP and the sexual-stage antigen Pvs25 has conferred 43% sterile protection on mice challenged with PvCSP *P. berghei* transgenic sporozoites (445).

Three long synthetic peptides representing parts of the N-terminal, repeat region, and C-terminal domains of PvCSP have been used in several primate and clinical trials. An initial study in *Aotus* monkeys found that each of the three long synthetic peptides could generate antibodies and T-cell responses (446) and similar responses in humans (447). *In vitro* invasion inhibition potency of human antibodies and similar immunogenicity was shown in another clinical trial (448).

The leading *P. vivax* malaria vaccine candidate has been VMP001, developed at the Walter Reed Army Institute of Research. Expressed in *E. coli,* VMP001 consists of an almost full-length PvCSP sequence primarily based on a sequence cloned from an infected Korean individual, but possessing nine repeats of the VK210 sequence including variants of that type, and one unit repeat from the VK247 allelic form (449). VMP001 was able to generate antibodies specifically recognising the N-terminal domain, C-terminal domain, both VK210 and VK247 unit repeats, and the $(AGDR)_3$ peptide, and was able to agglutinate live *P. vivax* VK210 sporozoites (449, 450). It is immunogenic in macaques, including generation of $CD4^+$ T-cells, although anti-AGDR responses were only detected in half of the monkeys (451). VMP001-elicited antibodies generate some cross-species reactivity, recognising both *P. falciparum* and *P. vivax* in immunofluorescence assays; VMP001 can also reduce parasitaemia in *P. berghei*-challenged mice (452), possibly via conserved regions in the N- and C-terminal domains. VMP001 became the first *P. vivax* vaccine to be tested for efficacy in a clinical trial published in 2016 (453). The vaccine failed to induce sterile protection in any volunteer, though it did cause a significant delay in the onset of blood-stage parasitaemia, indicating that there was some vaccine effect. Though it generated antibodies to all three regions of PvCSP in all volunteers, there is no

report in that trial of anti-AGDR responses (453). The inability of the VMP001 vaccine to confer sterile protection in humans stands in contrast to the efficacy of VMP001 in *Aotus* monkeys, where some degree of sterile protection was observed (454), but again anti-AGDR responses were not examined.

The next generation PvCSP vaccine will almost certainly be a virus-like particle, given the enhanced immunogenicity associated with this platform. Our group has developed a Hepatitis B surface antigen-based PvCSP vaccine, Rv21, presenting a chimeric PvCSP containing nine VK210 unit repeats and ten VK247 unit repeats, as well as the C-terminal domain of the protein. This has proven highly protective in murine pre-clinical challenge studies against two separate PvCSP VK210 and VK247 *P. berghei* transgenic sporozoites, and is moving towards clinical trial (190). VMP001 has also been presented as a Hepatitis B surface antigen-based VLP, the CSV-S,S particle, which, like RTS,S, contains a mixture of VMP001-Hepatitis B surface antigen and non-fusion Hepatitis B surface antigen monomers. The antibody titres elicited by CSV-S,S were more durable than those of VMP001 in rhesus macaques, but perhaps of greater interest is the superior ability of CSV-S,S to generate anti-AGDR specific responses. 71% of CSV-S,S-vaccinated monkeys gave anti-AGDR responses but no anti-AGDR responses were detected in VMP001-vaccinated monkeys (455). Preliminary data comparing Rv21 with a CSV-S,S-like VLP is presented in Chapter 4.

1.9 Thrombospondin-related adhesion protein (TRAP)

1.9.1 Function of TRAP

TRAP was first identified as a target of monoclonal antibodies derived from PyRAS-vaccinated mice (456-458); it was then called Sporozoite Surface Protein 2, or SSP2. TRAP was soon identified in *P. falciparum* (459) and suggested to be the homologue of PySSP2 (460, 461). TRAP was found to localise to micronemes in the sporozoite (462) but is only released to the sporozoite surface after activation cues, likely to be from cellular contact (463). The protein saglin on salivary gland cells appears to be one binding partner for TRAP, allowing it to invade those organs (464). TRAP also binds to HepG2 cells, probably via the conserved Region II CSVTCG motif it shares with CSP (465) although another study suggests that basic residues downstream of this sequence are responsible for binding liver cells (466). Two adhesive domains in TRAP seem to be required for binding and invasion: an A-domain and a thrombospondin-like domain. Mutations in either of these decrease the infectivity of sporozoites to any cell type, and mutations in both ablate invasion entirely, without affecting gliding motility (467). A *TRAP*-knockout *P. berghei* parasite has added further evidence for the key role TRAP plays in salivary gland and mammalian liver invasion, also showing that it is required for gliding motility *in vitro* (468). Motility, important for the migration of sporozoites to salivary glands, and to dermal capillaries in the mammalian host, as well as through or around liver cells, is mediated by TRAP acting as a connection between the sporozoite surface and the cytoskeleton (469). TRAP binds aldolase and aldolase binds actin (470, 471). Actin in turn binds myosin and the entire complex drives forward motion by translocating to the sporozoite posterior, where TRAP is cleaved by rhomboid

and other proteases, freeing the machinery to bind more TRAP (472-474). Thus TRAP is a multifunctional protein involved in several stages of invasion and migration. A schematic structure of the protein is shown in Figure 1.9.1.

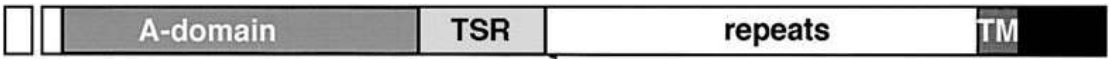


Figure 1.9.1: Schematic structure of TRAP

TRAP consists of two adhesive domains, an A-domain and a thrombospondin type-1 repeat (TSR) domain, followed by a disordered repeat region, a transmembrane domain, and a cytoplasmic tail that interacts with actin/myosin via aldolase. (Adapted from (467))

1.9.2 TRAP vaccines

Mice vaccinated with irradiated cells expressing PyTRAP, or SSP2, are protected from infection, but this is abrogated by $CD8^+$ T-cell depletion (475). That SSP2-specific $CD8^+$ T-cells mediate protection was later confirmed by adoptive transfer into mice, with one clone conferring complete sterile protection against *P. yoelii* challenge (476). It was also was shown that mouse-strain specific protection against *P. yoelii* could be obtained by adoptive transfer of SSP2-peptide specific $CD4^+$ T-cells (477). Humans vaccinated with RAS generate $CD8^+$ T-cells that respond to *P. falciparum* TRAP (478, 479).

These findings stimulated development of TRAP subunit vaccines designed to generate cellular immunity. An SSP2 (PyTRAP) DNA vaccine protected only one out of five strains of mice (480), but a DNA/MVA prime boost with PbTRAP conferred almost complete protection (88%) in BALB/c mice (196). A vaccine fusing PfTRAP with a multiple epitope string, ME-TRAP, underwent evaluation in series of small clinical trials to determine the optimum

dose, prime-boost interval, route, and number of shots combining DNA and MVA-vectored ME-TRAP. Giving several priming doses of DNA followed by MVA produced a clear delay in time to blood-stage patency, but no sterile protection (481); a field trial in Gambian adults of a DNA/MVA ME-TRAP regime likewise found low vaccine efficacy (10%) (482). The DNA-DNA-MVA ME-TRAP regime was later shown to confer greater protection in a clinical trial than the equivalent CSP regime, although sterile protection was still low (13%) (400). A trial comparing CSP and TRAP in an adenovirus-/MVA-vectored regime also found higher efficacy using TRAP (20% versus 33% sterile protection for CSP and TRAP respectively) (392). TRAP transcripts are detectable for longer in infected hepatocytes than those of CSP, potentially contributing to the greater efficacy of TRAP-based vaccines designed to elicit protective cytotoxic T-cell responses (483).

Heterologous prime-boost regimes using two different TRAP-encoding viral vectors began to be explored around this time, initially using the attenuated fowlpox FP9 and MVA. This regime conferred 40% sterile protection in one clinical trial, (484), with $CD8^+$ T-cells providing the source of IFNγ after FP9 priming, whereas the source of IFNγ after from DNA-priming came predominantly from $CD4^+$ T-cells (485). Pre-clinical work with adenoviral-vectored ME-TRAP showed greater protective efficacy than did MVA or FP9 (486). It was soon found that priming with adenoviral-vectored ME-TRAP and boosting with MVA conferred high and durable levels of protection in mice (216) dependent on $CD8^+$ effector/memory T-cells (487). To avoid anti-vector immunity associated with some human adenoviruses (204) and because of their unavailability for clinical trials (488) a chimpanzee adenovirus, ChAd63, was

used instead and found to be highly immunogenic using an eight-week prime-boost interval (206). A clinical trial in Oxford demonstrated sterile protection of 21% (489), and a field trial found that the $CD8^+$ T-cell frequencies induced in Kenyan volunteers actually higher than those from Oxford volunteers (490, 491). Partial protective efficacy of this regime was seen in Kenyan adults (67% reduced risk of infection) (492) but not in Senegalese adults (493). Field trials in children and infants from The Gambia and Burkina Faso show promisingly high cellular responses (494, 495).

P. vivax TRAP vaccines have seen less development. A long synthetic peptide representing part of the TSR domain did not show significant improvement over control vaccination in *Aotus* monkeys (496). However, a ChAd63/MVA regime using PvTRAP as an insert conferred 60% sterile protection on outbred CD1 mice, and partial protective efficacy in two other mouse strains, challenging using a PvTRAP *P. berghei* transgenic parasite (497). In the same study, $CD8^+$ T-cells were found to mediate protection, but passive transfer of anti-TRAP antibodies also protected mice from infection. Anti-TRAP sera has previously been found to inhibit gliding motility in *P. berghei* (498) and inhibit *P. falciparum* hepatocyte invasion *in vitro* (462), and sera from mice vaccinated with multiple antigen peptides based on PfTRAP B-cell epitopes also had *in vitro* cell-invasion inhibition potency (499). In contrast, antibodies raised by synthetic peptides representing PyTRAP epitopes failed to protect *in vivo* (463). A virus-like particle based on cucumber mosaic virus and displaying PvTRAP caused a significant delay in time to reach 1% blood-stage parasitaemia in a recent murine study with a PvTRAP *P. berghei* transgenic challenge, but no

sterile protection. Given the relatively low $CD8^+$ T-cell responses induced by the vaccine, antibody-mediated protection in that study is a possibility (500).

1.10 Other pre-erythrocytic stage vaccines

CSP and TRAP have been the focus of the vast majority of pre-erythrocytic vaccine development, but others are receiving increasing attention as it becomes clear that a single antigen target alone will not confer sufficient levels of protection (501). Screening serum and cellular responses after vaccination with radiation-attenuated sporozoites (502) and sporozoite inoculation under chemoprophylaxis (503) as well as transcriptomics studies (504) have generated a body of new potential antigens potentially associated with protection. The latter study (504) tested 21 DNA vaccines based on antigens identified by transcriptomics and found six providing protection in two separate rodent malaria models. Another study tested ten *P. falciparum* liver-expressed candidates in viral vectors against ten novel transgenic *P. berghei* parasites expressing the homologous *P. falciparum* gene. PfLSA1 and PfLSAP2 conferred $CD8^+$ T-cell-dependent protection on challenged mice (505). PfUIS3 and PfFalstatin, previously shown to protect against *P. yoelii* challenge using the orthologues in that species (506), also conferred significant but lower levels of protection. Another approach has used a phage display library to screen peptides with sporozoite inhibition properties (507). One was identified which apparently mimics a PbGAPDH epitope and which when conjugated to KLH confers protection on vaccinated mice. Natural anti-α-gal antibodies, generated by *E coli* in the gut, have been associated with protection in humans, and confer sterile protection on mice vaccinated with α-gal, suggesting that this glycan may be a novel pre-erythrocytic vaccine target as well (508). MAEBL, a sporozoite surface protein involved in salivary gland invasion though curiously not required for liver-stage infection (509) (but see (510)), and later identified as a vaccine

candidate from *P. falciparum*-vaccinated human serum (503), has been successfully used as a vaccine in mice against *P. yoelii* sporozoite challenge (511).

These methods of identifying antigens may lead to several new candidates going forward to clinical trial. Alternatives to CSP and TRAP have already advanced to that stage. CelTOS, important for invasion and cell-traversal in sporozoites (512), can apparently induce cross-species protection: recombinant PfCelTOS conferred protection against *P. berghei* challenge in mice (513). PvCelTOS provides protection against challenge with PvCelTOS *P. berghei* transgenic parasites, albeit at a modest level (514). PfCelTOS is currently undergoing Phase 1a studies (Clinical trial numbers NCT02174978 and NCT01540474). Recombinant PfLSA1 (liver stage antigen 1) conferred no protection on volunteers in a clinical trial (515), possibly because it failed to elicit the $CD8^+$ T-cell immunity shown to mediate protection in a pre-clinical study (505). Another clinical trial using recombinant LSA-3 has yet to be published (Clinical trial number NCT00509158).

1.11 Blood stage vaccines

Natural immunity to antigens of the pre-erythrocytic stage is weak and not thought to contribute greatly to protection; yet pre-erythrocytic vaccines are the most advanced in the field. Something of a reverse situation exists with blood-stage antigens, as none so far have shown the efficacy associated with RTS,S, despite a wide range of antigens tested. Nevertheless, the finding that transfer of IgG from naturally immune adults to children protected them from clinical malaria provided early proof of principle that if a blood-stage vaccine could recapitulate natural immunity, then much of the morbidity and mortality of malaria could be averted (516).

Sequestration is associated with pathology, so a PfEMP1 vaccine could prevent severe malaria by interfering with that protein's cytoadhesive properties. Aotus monkeys vaccinated with the CIDR1 region of PfEMP1, which mediates binding to endothelial CD36 (517), are protected from challenge with a homologous, but not heterologous, strain of parasite (518). Broader cross-strain antibodies can be generated in mice by using three different CIDR1s (519), and peptides against a conserved region have shown partial efficacy in Aotus monkeys (520). A major obstacle in developing a PfEMP1 vaccine is its vast diversity: it is coded for by a gene family of over 60 members (81). One PfEMP1 family member, VAR2CSA, mediates binding to chondroitin sulphate A on the placenta (87) and increases risk of malaria in pregnancy (86); a vaccine based upon it has reached phase I clinical trial and further studies will determine whether it can protect against pregnancy-associated malaria (521). Another candidate, P27A, part of an infected red blood cell surface antigen called Tex1,

has shown *in vitro* growth inhibitory activity (522) and has also gone to Phase I clinical trial (trial number NCT01949909).

Most other blood-stage vaccines have focused on merozoite surface antigens, hoping to generate antibodies capable of inhibiting merozoite invasion of red blood cells. MSP1, despite showing promise in Aotus challenge experiments (523, 524), has shown no protective efficacy in a field trial with Kenyan children (525). Another candidate, GMZ2, is a fusion of GLURP and MSP3 (526). MSP3 has shown some protective efficacy in a field trial in Burkina Faso (527, 528), and in a Phase I trial, antibodies from GLURP-vaccinated adults showed *in vitro* growth inhibitory activity against *P. falciparum*. Fused together as GMZ2, they show a combined vaccine efficacy of 27% against severe malaria in African children (529), lower than with RTS,S (380). A strain-specific field trial of AMA1 conferred strain-specific protection only (530) , while another based on two strains showed no efficacy, strain-specific or otherwise. To overcome any strain-specificity of protection due to polymorphism in the protein, a "diversity-covering" construct covering 97% of variability across strains was produced (531). In a macaque study, this vaccine produced antibodies with *in vitro* growth inhibition activity against three strains of *P. falciparum* (532). This candidate has reached clinical trial (trial number NCT02014727). Another candidate antigen, RH5, shows promise in part because of the low polymorphism associated with it (135). It demonstrates high *in vitro* growth inhibition activity against multiple strains of *P. falciparum* (135) and has conferred protective efficacy against heterologous challenge in *Aotus* monkeys. RH5 is in clinical trial, with viral vectors being used to deliver the antigen (trial number NCT02181088). SE36, based on SERA5, shows some efficacy in Aotus monkeys (533) and in Ugandan

adults (534), but has not been further pursued. Recombinant EBA0175 RII has proven immunogenic and antibodies have *in vitro* growth inhibition activity both from malaria-naïve (535) and malaria-exposed (536) volunteers.

Blood-stage vaccine development for *P. vivax* has focused on the merozoite-expressed Duffy binding protein (DBP) since, unlike *P. falciparum* which uses multiple mechanisms for invasion, DBP is (usually (154)) essential for *P. vivax* invasion and the widespread absence of its ligand on the red blood cells of sub-Saharan African people largely accounts the absence of *P. vivax* from that region (153). Antibodies raised in rabbits against region II of DBP inhibits *P. vivax* invasion of red blood cells *in vitro* (537) with a similar finding for the equivalent *P. knowlesi* antigen (538). A Phase Ia clinical trial using viral-vectored PvDBP region II has found it to be immunogenic and the generated antibodies have *in vitro* growth inhibition activity against several strains of *P. vivax* (539). Another *P. vivax* blood-stage vaccine, $PvMSP1_{19}$, is in pre-clinical development, generating antibodies, $CD4^+$ and $CD8^+$ T-cells in mice (540).

1.12 Transmission-blocking vaccines

When mosquitoes take a blood meal, they can take up circulating antibodies as well as malaria gametocytes. If those antibodies are against stages of malaria that develop in the mosquito, there is the potential for mosquito-stage development to be interrupted, and hence for further transmission of malaria via that mosquito to be blocked. Such vaccines would not prevent the vaccinee from experiencing clinical malaria, but it would, if effective, reduce overall incidence of malaria. There has been discussion concerning the ethical status of such an intervention; however, it is not without precedent, with primaquine, for instance, being delivered to people to destroy *P. falciparum* sexual stages, though this will confer no direct benefit to the patient (541).

Transmission-blocking, or sexual stage vaccines, target two separate stages: one, generating antibodies that can neutralise gametocytes before fertilisation; and the second, generating antibodies targeting the zygote and ookinete after fertilisation (542). Two gametocyte antigens have received the most attention: Pfs48/45 and Pfs230. Anti-Pfs48/45 antibodies have been found naturally acquired in malaria exposed individuals, and can reduce malaria transmission in membrane feeding assays (543). Nevertheless, Pfs48/45 vaccines have not yet advanced to clinical trial, in part because, like many sexual-stage antigens, the antigen contains a high number of cysteines and so is difficult to express as a correctly folded protein (544). Progress has been made on this front (545), however, and when a codon-optimised *E. coli* construct was administered to olive baboons the antibodies generated demonstrated 93% blocking activity in a membrane feeding assay (546). Coupling Pfs48/45 to a virus-like particle enhances the transmission-blocking ability (547). There is also

potential for a cross-species vaccine, as vaccination of mice with Pvs48/45 generates antibodies cross-reactive to Pfs48/45 (548). Pfs230, which exists as a complex with Pfs48/45 (549), is currently in clinical trial (trial number NCT02334462) and has shown transmission blocking activity when used to immunize mice (550) and rabbits (551).

Pfs25, expressed on ookinetes, is the leading transmission-blocking vaccine candidate, with several clinical trials completed or on-going (552). Knockout of *P. berghei* orthologue P25 and sister P28 proteins decreases mosquito midgut epithelium traversal (553). Immunization of mice with Pfs25 was found to generate transmission-blocking antibodies (554). A phase I clinical trial with the *P. vivax* orthologue Pvs25 also produced transmission blocking antibodies (555). Soon after, a trial testing Pfs25 and Pvs25 with Montanide ISA 51 adjuvant was halted due to unexpected reactogenicity (556). However, it has since undergone several more clinical trials, using alternatives to Montanide ISA 51. Most recently it has been conjugated to ExoProtein A, where transmission-blocking activity has once again demonstrated (557). This vaccine has undergone field trial in Mali (trial number NCT01867463). Other clinical trials deliver Pfs25 on a virus-like particle (trial number NCT02013687), or via viral vectors coupled to the genetic adjuvant IMX313 (trial number NCT02532049). IMX313, a moiety fused to Pfs25 which causes spontaneous nanoparticle formation, was previously found to enhance immunogenicity compared to Pfs25 alone (269), while adenoviral vectored Pfs25 constructs generated transmission-blocking antibodies in mice superior to that of Pfs25 in alum (558).

A third type of transmission blocking vaccine doesn't target the malaria parasite at all. Antibodies to AnAPN1, a mosquito midgut aminopeptidase,

inhibits *P. berghei* and *P. falciparum* development in mosquitoes (559), as well as *P. falciparum* and *P. vivax* under field conditions (560). The protective antibodies appear to recognise a single conserved linear B-cell epitope near the active site of the protein (560).

1.13 Combination malaria vaccines

Given that protective natural immunity is associated with breadth of response to multiple antigens, for pre-erythrocytic stages (147) as well as blood stages (132), it makes sense to try combining malaria subunit vaccines, either from the same stage or from different stages. CSP and TRAP were combined as vaccines almost as soon as they had been discovered, with transfected cells used as vectors. CSP and TRAP alone conferred partial protection on mice against *P. yoelii* sporozoites, but co-administration of both was completely protective (475). Later a group aimed to enhance protection by delivering CSP, TRAP, LSA1, MSP1, SERA, AMA1 and Pfs25 encoded in a single vaccinia vector, NYVAC-Pf7 (209). NYVAC-Pf7 generated good cellular responses in a clinical trial, but poor antibody responses, and only one volunteer out of 35 was completely protected (389). A DNA/canarypox virus prime-boost regime was developed using *Plasmodium knowlesi* CSP, TRAP, AMA1, and MSP1, and was partially protective in rhesus macaques (399, 561). The same regime, with *P. falciparum* antigens and with the addition of PfLSA1, was also immunogenic in rhesus macaques, and was the first combination malaria vaccine study to look for a decrease in CSP-specific responses in the combination group compared to a CSP-only group; no antigenic interference was found (562). Lower IFA titres using the same vaccine in mice were found with the 5-antigen cocktail compared to CSP alone, although the authors argue that this does not take into account the doses of CSP in each vaccine (563). A study in mice, using 4 separate plasmids encoding *P. falciparum* CSP, TRAP, CelTOS and LSA1, found only LSA1 and CelTOS titres diminished by antigenic interference (564).

Clinical trials focusing on combining pre-erythrocytic stage antigens have been carried out. One used a DNA vaccine delivering *P. falciparum* CSP, TRAP, EXP1, LSA1 and LSA3, and protected no volunteers (224), probably as a result of poor immunogenicity. At about the same time a combination of RTS,S and recombinant TRAP in AS02 was tested in malaria naïve adults (565). No protection was seen in RTS,S+TRAP or TRAP-only groups, possibly as a result of reduced anti-CSP titres in the RTS,S+TRAP group compared to the RTS,S-only group, and because TRAP delivered as a recombinant protein does not generate the high $CD8^+$ T-cell response that is required to mediate protection using this antigen (476). A model was proposed, using the murine model *P. berghei*, whereby antibodies against CSP could neutralise a proportion of sporozoites invading hepatocytes, thus reducing the liver-stage burden, enabling TRAP-specific cytotoxic T-cells to eliminate the remaining infection (566). This model was established using an adenovirus-prime, protein-boost CSP and viral-vectored TRAP combination strategy, which provided 100% protection in mice, compared to partial efficacy when either subunit vaccine alone was used. Depletion experiments and passive transfer of CSP-specific monoclonal antibodies supported the model (566). In that study, antigenic interference was only seen when viral-vectored CSP and viral vectored TRAP were combined, but not when exchanging the MVA boost for CSP for a protein-only boost. Similarly, no antigenic interference was seen when delivering RTS,S with viral-vectored ME-TRAP into separate limbs in a clinical trial with AS02, where very high levels of protection were seen, both in the combination group (82%) and in the RTS,S-only group (75%) (567). Because of the high protective efficacy, it could not be shown statistically that the combination was significantly more protective than

the single-subunit regime. Clinical trials combining R21 with ME-TRAP are on-going, and antigenic interference has been seen under conditions of co-administration (Adrian Hill, personal communication).

Aside from TRAP, the main companion antigens for CSP in combination studies have been AMA1 and MSP1. In rhesus macaques, RTS,S, MSP1 and AMA1 were given together, with AS02A as adjuvant. Anti-AMA1 titres were reduced in the presence of both RTS,S and MSP1, whether the vaccines were mixed or administered at separate sites (568). A clinical trial delivering *P. falciparum* CSP and AMA1 via DNA and adenovirus vectors achieved 27% sterile protection (393), associated with AMA1-specific effector memory $CD8^+$ T-cells and not CSP responses, although one case of protection despite low AMA1 and CSP responses was considered evidence that CSP was contributing something to the protective efficacy of the combination regime (394). In a screening experiment to test several novel liver-stage antigens, three *P. berghei* and two *P. yoelii* antigens were found to significantly improve protective efficacy, of which LISP1 and SLARP were common to both malaria species (504). Similarly, in another screening experiment, three *P. yoelii* liver stage candidates were found to be more protective when delivered in combination than in isolation (506). In a clinical trial, a polyprotein encoding six pre-erythrocytic antigens was delivered using viral vectors, but failed to show any protective efficacy against *P. falciparum* challenge, probably due to the low IFNγ responses elicited; competition between antigens was proposed as one mechanism which might explain the low responses (569). A mechanism of antigenic interference following combination of viral-vectored CSP and MSP1 was proposed in a study where their combination reduced $CD8^+$ responses to both antigens (570). The

reduction was seen in secondary responses, and *in vitro* experiments suggested that cells harbouring MVA vector encoding both antigens were more likely to be killed before they could stimulate secondary responses. Antigen competition on MHC class I was ruled out.

Blood-stage and sexual-stage antigen combinations also enhance the protective efficacy of vaccine candidates. Antibodies against *P. yoelii* MSP1 and MSP4/5 (571), PfRH5 with PfMSP1, PfAMA1, Pf38, PfEBA175, PfRH2 and PfRH4 (572), PfCyPRA and PfRH5 (573), and PfRH5, PfAARP, PfRH2, and PfEBA-175 with each other (574, 575) show enhanced growth inhibition activity in combination compared to those antibodies alone. Fusion proteins consisting of PfMSP3 and PfMSP1 (576) or PfMSP3, PfMSP1 and PfAARP (577) do not substantially enhance protection beyond that seen with MSP3 alone. A fusion of AMA1 and MSP1, meanwhile, has undergone clinical trial, and was found to be immunogenic, but the generated antibodies did not display substantial growth inhibitory activity (578). The sexual stage antigens Pys48/45 and Pys25, combined as co-injected DNA vaccines, interfere with each other, generating lower transmission blocking activity than Pys25 alone (579) but this was not seen with a similar combination of Pfs48/45 and Pfs25 DNA vaccines administered by electroporation in mice, where no decrease in antibody titres to either antigen occurred (580). The transmission-blocking activity of the combination and Pfs25 alone was too high to discriminate between them (580). A fusion of GLURP and Pfs48/45 is able to generate growth-inhibitory and transmission-blocking antibodies (581). In all, this demonstrates that if the conditions are optimised to avoid antigenic interference, a multi-antigen or

multi-stage malaria vaccine represents a promising strategy for enhancing protective efficacy.

1.14 Murine models of malaria

Human species of malaria do not naturally infect mice, but there are four species which can: *P. berghei, P. yoelii, P. chabaudi,* and *P. vinckei* (582). *P. berghei* is the species used in this thesis. Discovered in 1948 and naturally infecting tree rats (*Thamnomys surdaster*) (583), it was adapted for laboratory use with *Anopheles stephensi* mosquitoes (584) and mice (585), a process remaining largely unchanged today.

As well as playing a significant role in early malaria vaccine research (278, 294), *P. berghei* parasites now serve as means of testing *P. falciparum* and *P. vivax* vaccine candidates in mouse models against the homologous antigens. This is thanks to the development of transgenic *P. berghei* parasites, first achieved by plasmid-based transformation (586) and later by stable DNA integration into the genome of *P. berghei* (587). This has enabled creation of *P. berghei* parasites expressing *P. falciparum* or *P. vivax* genes, either in addition to the native *P. berghei* gene (PfAMA1 (588), and using the dispensable p230 locus (589)), or by creating hybrid *P. berghei* CSP with repeats from *P. falciparum* (590), or by complete replacement of the *P. berghei* gene with the homologous *P. falciparum* gene (e.g. PfCSP (189), PvCSP (190)). PfTRAP (591) and PvTRAP (497) replacement transgenic *P. berghei* parasites have been produced, as well as sexual stage antigen replacement parasites (Pfs25, (592); Pvs25 (593)). In all these cases the transgenic parasites have served to demonstrate that immune responses in mice against *P. falciparum* or *P. vivax* antigens can reduce or eliminate malaria infection, serving as a relatively inexpensive way to screen candidates before moving on to non-human primate studies or clinical trials. Transgenic parasites also serve to shed light on questions of basic biology (588,

591, 594), and fluorescently-labelled parasites have allowed visualisation of parasites, as well as quantification for *in vivo* and *in vitro* studies (595-597). Although some studies have shown an impact on mosquito or vertebrate infectivity from transgenic modification of *P. berghei* (590, 598), others have not (190, 497, 591).

It is questioned whether mice can serve as adequate models for human infection. The differences between the murine and human immune systems are well known, with mice displaying lower neutrophil counts in peripheral blood but more lymphocytes, CD4 present on human but not murine macrophages, and MHCII expression on T-cells in humans but not mice, amongst many other discrepancies (599). There are also differences in how protection is mediated against different species of malaria in mice, with perforin playing a role in memory $CD8^+$ T-cell-mediated protection against *P. yoelii* but not against *P. berghei* (600). Different strains of mice respond to different strains of *P. berghei* with different outcomes. C57BL/6 mice, for instance, develop cerebral malaria with *P. berghei* ANKA strain but not NK65 or K173 strains (601). It has also been found that differences in the neutralising potency of anti-CSP antibodies between two different CSP vaccines were not observable in mice but did emerge after trial in rhesus macaques (407). Nevertheless, all malaria vaccines showing protective efficacy in humans have also shown protective efficacy in mice, suggesting that even if some candidates do better in mice, the murine model is still an extremely practical way to down-select candidates for clinical trial (582). Progress with humanized mouse models, where human hepatocytes can form functional livers in mice, is providing a further tool for pre-clinical malaria research using mouse models (602). *P. vivax* hypnozoites have been found to develop in one such

model, opening the door to research on this difficult-to-study but extremely important feature of *P. vivax* infection (603). Another humanized mouse model was able to demonstrate reduced infection of *P. falciparum* following passive transfer of a PfCSP-specific neutralising monoclonal antibody, potentially allowing vaccine studies to proceed in humanized mice (604).

Chapter 2

Materials and Methods

2.1 Immunology

2.1.1 Mouse PBMC IFNγ ELISpot

IFNγ ELISpots were performed as previously described (605). MAIP ELISpot plates (Millipore) were coated with anti-mouse IFNγ (50 µL/well, 5 µg/mL, Mabtech) and stored overnight. 24 h later the coating antibody solution was removed and ELISpot plates were blocked using complete MEM media (100 µl per well, Sigma, 1 h, 37°C). PBMCs were obtained from blood via the tail vein of mice, with 5-6 drops collected in 200 µL 10 mM EDTA (Sigma) in sterile PBS (Sigma). Red blood cells were lysed by addition of 1 mL ACK lysis buffer (0.15 M NH_4Cl, 1 mM $KHCO_3$, 0.1 mM EDTA, pH 7.4, Sigma), followed by centrifugation (4000 rpm, 4 min, 20°C), removal of supernatant, and addition of 1 mL ACK and recentrifugation. The supernatant was removed and the pellet resuspended in 200 µL complete MEM (10% FBS, 4 mM L-glutamine, 5 mL/L penicillin/streptomycin, Sigma). Spleens from naïve mice were used as a source of antigen-presenting cells by homogenisation in PBS, filtration through a 70 µm cell strainer, centrifugation (1350 rpm, 5 min, 20°C), discarding of the supernatant, resuspension of the pellet in 5 mL ACK lysis buffer (< 5 min) and then repetition of the centrifugation. The splenocytes were resuspended in complete MEM to 10^7 cells/mL. Naïve splenocytes were added at 250,000 per well, one well without peptide and three with 5 µg/mL peptide per well for each mouse. The PvTRAP immunodominant peptides required for stimulation of

PvTRAP-specific $CD8^+$ T-cells were identified in (497) and are shown in Table 2.1.1 below.

Table 2.1.1: Immunodominant PvTRAP peptides in mice. (497)

Mouse strain	Peptide sequence
BALB/c	ITKVIPMLNGLINSLSLSRD
C57BL/6	LAVIGVGQGINHQFNRLIAG
C57BL/6	NHQFNRLIAGCRPREPNCKF

Isolated mouse PBMCs were counted (CASY counter) and added at three dilutions (1x, 0.33x, 0.11x) to splenocytes and peptides, then incubated for 18 h at 37°C. Plates were washed six times in PBS (Dynex plate washer) and biotinylated anti-mouse IFNγ added (Mabtech, 50 µL/well, 1 µg/mL in PBS), and incubated for 2 h RT. Plates were washed as before and streptavidin alkaline phosphatase added (Mabtech, 50 µL/well, 1 µg/mL in PBS) and incubated for 1 h RT. Plates were washed as before and colour development buffer added (BioRad, 50 µL/well). Plates were incubated (RT) until spots developed (5-15 min) then washed in water. Spots per well were enumerated using an AID ELISpot reader and AID software with background subtracted to give spot-forming units (sfu) per million PBMC.

2.1.2 ELISAs: standard curve, affinity and subclass.

Nunc Maxisorp 96-well plates (Sigma) were coated with antigen (50 µl, 1 µg/mL in PBS) and incubated overnight at RT. Plates were washed 6 times with PBS/0.05% Tween (PBS/T) (Sigma) and blocked for 1 h with 10% skimmed milk (Sigma) in PBS/T (100 µL/well). Microvette serum tubes (Sarstedt) were used to collect blood from tail veins of mice and serum obtained by centrifugation

(13,000 rpm, 10 min). Sera was typically diluted at 1:500 post-prime, 1:1000 post-second shot and 1:2000 post-third shot and applied to plates in triplicate after blocking (2 h RT incubation). Standard curves were prepared on each plate against antigen of interest by serial dilution of standard sera obtained from appropriately vaccinated mice by cardiac bleed. Plates were washed as before and goat anti-mouse whole IgG alkaline phosphatase conjugate (Sigma) applied (50 µl/well, 1:5000 in PBS/T, 1 h RT). Plates were washed as before and 1 mg/mL pNPP (Sigma) in diethanolamine buffer (Pierce) applied to the plates (100 µl/well) and allowed to develop with readings on a BioTech Microplate Reader taken at 14 minutes and 1 h at 405 nm. Titres were expressed as arbitrary ELISA units (EU) relative to a standard curve.

To determine the avidity index, a replicate ELISA was performed identical to and simultaneously with the standard curve ELISA, except that after 2 h incubation with diluted sera, 100 µL 7 M urea (Sigma) was applied to each well for 10 minutes (excluding the standard curve). Plates were then washed and the ELISA completed as before. The avidity index is the ratio of urea-treated to untreated ELISA units, as described in (606).

IgG subclass ELISAs (BioRad Mouse Typer Sub-Isotyping kit) were performed as for standard curve ELISAs with the following modifications. Following serum incubation anti-IgG1, anti-IgG2a, anti-IgG2b and anti-IgG3 were applied (50 µl per well, undiluted) and the standard curve incubated with anti-κ-chain IgG (1 h RT). Plates were washed as before and goat-anti-rabbit horseradish peroxidase conjugate applied (1:3000 dilution in PBS/T, 50 µL/well, 1 h RT, BioRad). Plates were washed as before and developed by application of

100 µL/well peroxidase substrate solution (BioRad). Reactions were stopped after 14 minutes by addition of 100 µL/well 2% oxalic acid (Sigma).

2.1.3 Vaccination

Vaccinations were performed by intramuscular injection using a 25G needle of 25 µL vaccine formulation each into the right and left hind leg muscles of isofluorane-anaesthetised mice. For intravenous administration (§4.4) 10^9 infectious units (iu) adenovirus in 50 µl PBS was injected into the tail vein using an insulin syringe (Fisher).

Adenovirus (simian adenoviral vector 63, ChAd63) vectors were typically given at 10^8 iu per dose, and modified vaccinia virus strain Ankara (MVA) at 10^7 plaque forming units per dose, with an 8 week prime boost interval, unless otherwise stated. Virus-like particles and protein vaccines were given at ranges from 1 to 20 µg, typically with two to three vaccinations administered at three week intervals unless otherwise stated.

Adjuvants, when used, were mixed with vaccines prior to administration. Alhydrogel alum (Brenntag Biosector) was used at 8.5 µL per dose in Tris buffer (Sigma), to which vaccines in Tris buffer were added and incubated for 1 h RT prior to vaccination. AddaVax (InvivoGen) was used at 25 µl/dose and Matrix M at 12 µg per dose except, where stated, at 5 µg/dose. Adjuvants were kindly provided by Dr. Anita Milicic from the Jenner Institute adjuvant bank.

2.1.4 Vaccination combination simulations

Equations described in Chapter 3 and in Chapter 5 were used to simulate variation in two variables, by specifying fixed parameter values and using

Microsoft Excel to calculate the dependent variable over a range of the independent variable. The results were plotted using GraphPad Prism (v 6, MacOS X).

2.1.5 Mouse strains used

6 week-old female BALB/c (H-2^d) mice and C57BL/6 (H-2^b) mice were used for vaccination experiments, with age-matched controls. TO outbred mice and BALB/c mice were used for parasite maintenance and mosquito feeds. All mice from Harlan/Envigo.

2.1.6 Ethics statement

All animals and procedures were used in accordance with the terms of the United Kingdom Home Office Animals Act Project License. The procedures were approved by the University of Oxford Animal Care and Ethical Review Committee (PPL 30/2889 and P9804B4F1).

2.1.7 Hybridoma and monoclonal 2D3 PvTRAP antibody production

Sp2/0ag14 cells were grown in DMEM with 10% FBS for two weeks, with 8-azaguanine (Sigma) added during the first week. One day prior to fusion macrophages were obtained from a naïve mouse and cultured in DMEM with HAT, HT and 10% FBS and penicillin/streptomycin. The following day the spleen from a mouse vaccinated with recombinant PvTRAP was removed, crushed in 5 mL PBS, passed through a 70 μm cell strainer, 10 mL PBS added, followed by centrifugation (1350 rpm for 5 min), resuspension of the cell pellet, treatment with 5 mL ACK for 5 min, then addition of 25 mL PBS and centrifugation as

before. The supernatant was discarded and cells resuspended in DMEM and counted using a haemocytometer. Sp2/0ag14 cells were gently mixed 1:10 with spleen cells (approx. $2x10^7$:$2x10^8$ cells) then centrifuged 10 min at 500 g RT. The supernatant was discarded and pellet loosened by flicking. 800 µl 50% PEG (MW 1500) at 37°C with 7.5% DMSO was added drop-by-drop over one minute in a water bath. 30 mL 37°C DMEM was then added drop by drop over 15 minutes followed by 10 min incubation. Cells were centrifuged for 5 min 500 g RT and the supernatant discarded. 48 mL DMEM/10% FBS/HAT/HT/pen./strep. was added and 500 µL/well applied to 24-well plates containing macrophages and incubated for 5 days (37°C, 5% CO_2), whereupon 500 µL of media was removed and replaced, with this process continuing until cells were growing and supernatant could be tested for the presence of PvTRAP-specific antibody by ELISA.

Wells testing positive for PvTRAP antibody by ELISA were selected for cloning by limiting dilution. Cells were resuspended in cloning medium DMEM/4 mM L-glutamine/20% FBS/10% Hybridoma Cloning Factor, counted and viability determined to be over 80%. Serial dilution of cells to 4, 2 and 1 cells/mL in cloning medium was performed, plated into 96-well plates and incubated at 37°C 8-10% CO_2 for 5-7 days. Wells containing cells were tested for monoclonal antibody by ELISA as before. One monoclonal antibody was obtained: 2D3.

2D3 and 3D11 monoclonals (3D11 is a PbCSP repeat region mAb, hybridoma obtained courtesy of Julie Furze) were obtained from hybridomas by propagation in DMEM/pen/strep/L-glutamine/20% ultra-low IgG FBS and incubated at 37°C 5% CO_2. The supernatant was removed and mAb purified

using a Pierce Protein G column, with mAb buffer exchanged into PBS using a 30 kDa MWCO Millipore centrifugal filter unit.

2.2 Parasitology

2.2.1 Infection of Anopheles stephensi *mosquitoes with* P. berghei

Cryopreserved mouse blood stocks of wild type or transgenic *P. berghei* from liquid nitrogen were defrosted and immediately administered to naïve BALB/c or TO mice by intraperitoneal injection (100 µL). Thin blood smears were taken daily and when gametocytes were observed mice were anaesthetised by intramuscular injection (Rompun/Ketaset) for mosquito feed. Mosquitoes starved for 2 h were allowed to feed for 10 – 15 m on anaesthetised infected mice. Blood was taken from mice to confirm exflaggelation of gametocytes by microscopy. After feeding, mosquitoes were returned to fructose/P-amino benzoic acid on cotton wool and maintained in the Jenner Institute insectary (19-21°C, 12 h light/dark cycle). One week after feeding a second feed was performed on an anaesthetised naive mouse to improve sporozoite yields. Mosquitoes were maintained for a total of 21 days prior to dissection of sporozoite-infected salivary glands. Thanks to Sara Zakutansky, Alex Fyfe, Sumi Biswas, Marta Ulaszewska and Alex Spencer for mosquito maintenance.

2.2.2 Dissection of mosquito salivary glands and challenge of mice with sporozoites

21 days after feeding on *P. berghei* infected mice, mosquitoes were sedated at 4°C for dissection. Salivary glands were dissected from mosquitoes under a microscope and removed by pipette into a glass tissue homogeniser containing

100 µL Schneider's insect media with 10% FBS. Sporozoites were liberated from salivary glands by gently homogenising three times and counted using a haemocytometer. Sporozoite concentration was typically adjusted to 10^4 sporozoites/mL for intravenous injection into the tail vein of mice of 100 µL (1000 sporozoites per dose, by insulin syringe) unless otherwise stated.

For sporozoites treated with monoclonal antibody prior to challenge, either 2D3 or 3D11 (see §2.1.7 above) was added to the required quantity of sporozoites at 190 µg/mL, incubated RT for 30 min and then injected at 1000 sporozoites/mouse as above.

2.2.3 Thin blood smears and calculation of time to reach 1% blood stage parasitaemia

Daily thin blood smears were prepared on glass slides from a drop of blood taken from the tail tip of challenged mice. Slides were fixed in methanol then stained in 5% Giemsa (Sigma) for 30 min and washed in water. 1000 red blood cells were counted for three to five consecutive days until the mouse reached 1% blood stage parasitaemia. Time to reach 1% blood stage parasitaemia was calculated by linear regression of $\log_{10}$ percentage parasitaemia against time post-challenge, as described in (487). Mice without parasites by day 15 were considered to have been conferred sterile protection against challenge.

2.2.4 Cryopreservation of P. berghei *infected red blood cells*

BALB/c mice with > 1% blood-stage parasitaemia were cardiac bled under isofluorane anaesthetic using a 25G needle and syringe with 2-3 µL heparin to prevent coagulation. Blood was immediately mixed 1:1 with 30% glycerol v/v in

PBS (Sigma), transferred to Nunc CryoTubes (Sigma), placed at -80°C in a Mr Frosty cryopreservation chamber for 24 h, then removed to liquid nitrogen.

2.2.5 Production of transgenic P. berghei *parasites*

Here the production of the double transgenic PvCSP-210/PvTRAP parasite is described in brief; it is given in more detail in Karolis Bauza's DPhil thesis (2012). The same method was used for all other transgene replacement parasites used in this thesis. The genes and accession numbers of the replacement genes are shown in Table 2.2.1. More detailed protocols can be found in (190, 260).

A PvTRAP construct described in (497) was used to electroporate PvCSP-210 transgenic *P. berghei* parasites; electroporations were performed by Chris Janse and Shahid Kahn. Positive selection with pyrimethamine, followed by negative selection with 5-fluorocytosine, resulted in selection of double replacement transgenic PvCSP-210/PvTRAP *P. berghei*.

Immunofluorescence assays with monoclonal anti-PvCSP-210 (MR4, 1:200 dilution) and a monoclonal anti-PvTRAP described below stained only the PvCSP-210/PvTRAP double transgenic and not wild type *P. berghei* sporozoites; similarly, anti-PbCSP 3D11 antibodies (1:1000) and serum from PbTRAP-vaccinated mice (1:50) stained only wild type and not PvCSP-210/PvTRAP transgenic *P. berghei* sporozoites (Fig. 2.2.1 A). The fitness of PvCSP-210/PvTRAP parasites was comparable to wild-type *P. berghei*, with no significant difference in oocysts per mosquito, sporozoites per mosquito (Fig. 2.2.1 B) or time to reach 1% blood-stage parasitaemia (Fig. 2.2.1 C).

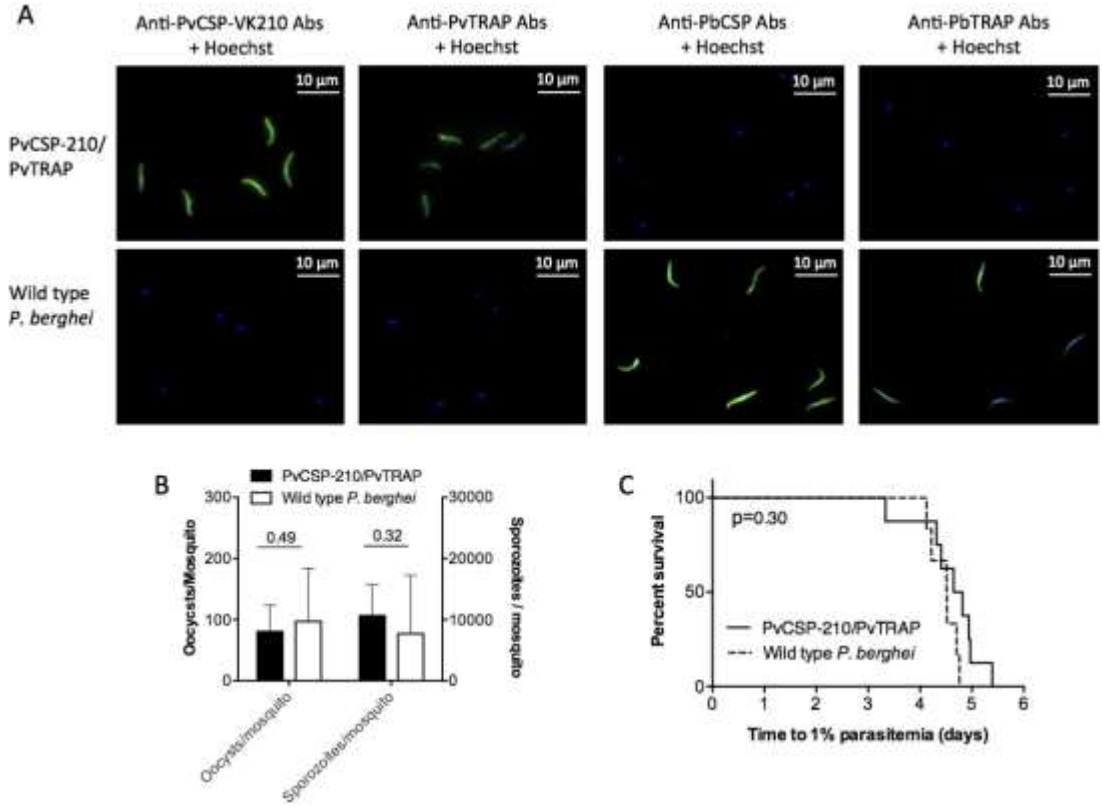


Fig. 2.2.1 Phenotype of PvCSP-210/PvTRAP double transgenic *P. berghei*

(A) PvCSP-210/PvTRAP or wild type *P. berghei* parasites were fixed and then stained in immunofluorescence assays with the indicated antibodies (green) and with nuclei-staining Hoechst-33342 (blue). Parasites were examined using a DMI-300B Leica fluorescence microscope. (Thanks to Ahmed Salman for IFA). (B) Mosquitoes infected with either parasite were dissected and oocysts per mosquito and sporozoites per mosquito determined over several experiments. Numbers represent t-tests between groups. (Thanks to Karolis Bauza for oocyst/mosquito data). (C) Naive mice were challenged by intravenous injection of 2000 sporozoites of either PvCSP-210/PvTRAP transgenic or wild type *P. berghei* and daily thin blood smears taken to determine time to reach 1% blood-stage parasitaemia by linear regression. P-value from log-rank test between groups.

Table 2.2.1 Replacement transgenic *P. berghei* and accession numbers

Parasite name	Transgene	Accession number
PvCSP-210	*PvCSP-210*	PVX_119355
PvCSP-247	*PvCSP-247*	Q7M3X0
Pv-CSP-210/PvTRAP	*PvCSP-210*	PVX_119355
	PvTRAP	XP_001614147.1
PfCSP	*PfCSP [3D7]*	Q7K740

2.2.6 Serial dilutions of infected red blood cells and sporozoites to determine blood-stage growth rate

Serial dilutions of infected red blood cells (iRBC) and sporozoites were performed for curve fitting to equations described in Chapter 3 (§3.3.1).

iRBC were obtained from unvaccinated donor BALB/c mice with > 1% blood-stage parasitaemia by cardiac bleed with a 25G needle and syringe containing 2-3 µl heparin. A thin blood smear was taken from this mouse for back-calculation of undiluted percent parasitaemia. Blood was immediately diluted 1:2 in a series of nine in PBS (Sigma) and 100 µl of each dilution injected intravenously into the tail vein of a BALB/c mouse. Calculation of the number of iRBC injected into each mouse was derived from donor mouse parasitaemia and on the assumption of 1.21×10^{10} RBC per 20 g BALB/c mouse (607).

Sporozoites from mosquito dissection (§2.2.2) were counted and serial diluted in Schneider's insect media to give, in one set of experiments, a series of 10000, 6667, 3333, 1667, 833 and 417 sporozoites per dose; and in another series of experiments, 16000, 8000, 4000, 1000, and 500 per dose. Thin blood smears and calculation of time to reach 1% blood-stage parasitaemia were determined as described in §2.2.3.

2.3 Molecular biology, protein production and vaccine production

2.3.1 Design of proteins

The primary structures of proteins used for ELISAs and vaccinations (coupled or uncoupled to virus-like particles) are shown in Table 2.3.1.

Table 2.3.1 Primary structures of proteins used in thesis

Name	Primary structure
PvCSP chimeric full (N-210-247-C)	THCGHNVDLSKAINLNGVNFNNVDASSLGAAHVGQSASRGRGLGENP DDEEGDAKKKKDGKKAEPKNPRENKLKQPGDRAAGQPAGDRAAGQP AGDRAAGQPAGDRAAGQPAGDRAAGQPAGDRADGQPAGDRADGQPA GDRADGQPAGDRADGQPAGNGAGGQAAANGAGNQPGANGAGGQAAA NGAGNQPGANGAGGQAAANGAGDQPGANGAGDQPGANGADDQPGA NGAGDQPGEDGAGNQPGANGAGDQPGGNGAGGQAAGGNAGGGQGQN NEGANAPNEKSVKEYLDKVRATVGTEWTPCSVTCGVGVRVRRRVNAA NKKPEDLTLNDLETDVCTMDK
PvCSP chimeric truncated (210-247-C)	GDRAAGQPAGDRAAGQPAGDRAAGQPAGDRAAGQPAGDRAAGQPAG DRADGQPAGDRADGQPAGDRADGQPAGDRADGQPAGNGAGGQAAAN GAGNQPGANGAGGQAAANGAGNQPGANGAGGQAAANGAGDQPGANG AGDQPGANGADDQPGANGAGDQPGEDGAGNQPGANGAGDQPGGNGA GGQAAGGNAGGGQGQNNEGANAPNEKSVKEYLDKVRATVGTEWTPC SVTCGVGVRVRRRVNAANKKPEDLTLNDLETDVCTMDK
PvCSP-210 (N210C)	THCGHNVDLSKAINLNGVNFNNVDASSLGAAHVGQSASRGRGLGENP DDEEGDAKKKKDGKKAEPKNPRENKLKQPGDRADGQPAGDRADGQP AGDRADGQPAGDRAAGQPAGDRADGQPAGDRADGQPAGDRADGQPA GDRADGQPAGDRAAGQPAGDRAAGQPAGDRADGQPAGDRAAGQPAG DRADGQPAGDRAAGQPAGDRADGQPAGDRAAGQPAGDRAAGQPAGD RAAGQPAGDRAAGQPAGNGAGGQAAGGNAGGGQGQNNEGANAPNEK SVKEYLDKVRATVGTEWTPCSVTCGVGVRVRRRVNAANKKPEDLTLN DLETDVCTMDK
PvCSP-247 (N247C)	THCGHNVDLSKAINLNGVGFNNVDASSLGAAHVGQSASRGRGLGENPD DEEGDAKKKKDGKKAEPKNPRENKLKQPEDGAGNQPGANGAGNQPG ANGAGNQPGANGAGDQPGANGAGNQPGANGAGDQPGANGAGNQPGA NGAGNQPGANGAGNQPGANGADDQPGANGAGNQPGANGAGNQPGA NGAGNQPGANGAGDQPGANGAGNQPGANGAGDQPGANGAGNQPGA NGAGNQPGANGAGNQPGANGAGNQPGANGAGGQAAGGNAANKKAG DAGAGQGQNNEGANATNEKSVKEYLDKVRATVGTEWTPCSVTCGVGV RVRRRVNAANKKPEDLTLNDLETDVCTMDK
PvTRAP	DEKVVDEVKYSEEVCNESVDLYLLVDGSGSIGYPNWITKVIPMLNGLIN SLSLSRDTINLYMNLFGNYTTELIRLGSGQSIDKRQALSKVTELRKTYTP YGTTNMTAALDEVQKHLNDRVNREKAIQLVILMTDGVPNSKYRALEV ANKLKQRNVSLAVIGVGQGINHQFNRLIAGCRPREPNCKFYSYADWNE AVALIKPFIAKVCTEVERVANCGPWDPWTACSVTCGRGTHSRSRPSLH EKCTTHMVSECEEGECPVEPEPLPVPAPLPTVPEDVNPRDTDDENENP NFNKGLDVPDEDDDEVPPANEGADGNPVEENVFPPADDSVPDESNVL PLPPAVPGGSSEEFPADVQNNPDSPEELPMEQEVPQDNNVNEPERSDS NGYGVNEKVIPNPLDNERDMANKNKTVHPGRKDSARDRYARPHGST HVNNNRANENSDIPNNPVPSDYEQPEDKAKKSSNNGYK

2.3.2 Expression of proteins in HEK293 cells and purification

Proteins were expressed as described in (608). pHLsec plasmids encoding the genes were transformed into *E. coli,* grown in 1 L LB broth (Fisher) and plasmids purified using a QIAGEN Maxiprep kit. HEK293 cells grown in roller bottles for 2-3 days (37°C) in Dulbecco's MEM (with non-essential amino acids and L-glutamine supplement, Sigma) were transfected using 0.5 mg plasmid DNA per roller bottle. The transfection cocktail was prepared by adding 80 µl chloroform per 1 mL plasmid, vortexing, centrifuging for 10 min (13,300 rpm), removing the DNA and adding to 50 mL serum free DMEM with 6 mL polyethylenimine (1 mg/mL), incubating for 10 m (RT) and then adding the transfection cocktail to cells in fresh DMEM/NEAA/L-glutamine. Transfected cells were incubated (37°C) for 4-5 d, and the supernatant containing the secreted proteins removed and centrifuged (3000 rpm, 10 min) and filtered (0.22 µm) to remove cell debris prior to purification.

His-tagged proteins were purified by nickel ion chromatography (Histrap 5 mL column, GE) using a 20 mM imidazole equilibration buffer and 500 mM imidazole elution buffer both with 0.5 M NaCl and 20 mM sodium phosphate (Sigma). Imidazole was added to the supernatant to 20 mM prior to column application. Gel filtration using a HiLoad 16/600 Superdex column (GE) was used after Histrap purification if required, with elution in PBS. Proteins were examined by SDS-PAGE and western blotting and stored at -20°C.

2.3.3 Expression of Hepatitis B surface antigen-based virus-like particles in Pichia pastoris and purification

Two virus-like particles were produced in *Pichia pastoris*: Rv21, a fusion of the truncated chimeric PvCSP (no N-terminal domain, nine 210 repeats and ten 247 repeats, and the C-terminal domain); and CSVS-like, including the N-terminal domain but possessing only one 247 unit repeat. Both PvCSP constructs were fused to Hepatitis B surface antigen at their C-termini, as shown in Table 2.3.2

Table 2.3.2 Primary structures of Hepatitis B surface antigen-based virus-like particles used in this thesis

Name	Primary structure
Rv21	MGDRAAGQPAGDRAAGQPAGDRAAGQPAGDRAAGQPAGDRAAGQPA GDRADGQPAGDRADGQPAGDRADGQPAGDRADGQPAGNGAGGQAAA NGAGNQPGANGAGGQAAANGAGNQPGANGAGGQAAANGAGDQPGA NGAGDQPGANGADDQPGANGAGDQPGEDGAGNQPGANGAGDQPGGN GAGGQAAGGNAGGGQGQNNEGANAPNEKSVKEYLDKVRATVGTEWT PCSVTCGVGVRVRRRVNAANKKPEDLTLNDLETDVCTMDKPVTNME NITSGFLGPLLVLQAGFFLLTRILTIPQSLDSWWTSLNFLGGSPVCLGQN SQSPTSNHSPTSCPPICPGYRWMCLRRFIIFLFILLLCLIFLLVLLDYQGM LPVCPLIPGSTTTNTGPCKTCTTPAQGNSMFPSCCCTKPTDGNCTCIPIP SSWAFAKYLWEWASVRFSWLSLLVPFVQWFVGLSPTVWLSAIWMM WYWGPSLYSIVSPFIPLLPIFFCLWVYIEPEA
CSVS-like	MTHCGHNVDLSKAINLNGVNFNNVDASSLGAAHVGQSASRGRGLGEN PDDEEGDAKKKKDGKKAEPKNPRENKLKQPGDRADGQAAGNGAGGQ PAGDRAAGQPAGDRAAGQPAGDGAAGQPAGDRADGQPAGDRADGQP AGDRAAGQAAGNGAGGQAAANGAGNQPGGGNAANKKAEDAGGNAGG NAGGQGQNNEGANAPNEKSVKEYLDKVRATVGTEWTPCSVTCGVGVR VRRRVNAANKKPEDLTLNDLETDVCTPGPVTNMENITSGFLGPLLVLQ AGFFLLTRILTIPQSLDSWWTSLNFLGGSPVCLGQNSQSPTSNHSPTSCP PICPGYRWMCLRRFIIFLFILLLCLIFLLVLLDYQGMLPVCPLIPGSTTTN TGPCKTCTTPAQGNSMFPSCCCTKPTDGNCTCIPIPSSWAFAKYLWEW ASVRFSWLSLLVPFVQWFVGLSPTVWLSAIWMMWYWGPSLYSIVSPFI PLLPIFFCLWVYIEPEA

The genetic sequences were codon optimised for expression in yeast (GeneArt, InVitrogen), cloned into pPink-HC (InVitrogen) and amplified in *E. coli.* Plasmids were purified using a QIAGEN Maxiprep kit and used to electroporate four strains of *P. pastoris* (knock-out *ade2, ade2-pep4, ade2-prb1,* or *ade2-pep4-*

prb1). White colonies were selected using PAD plates (InVitrogen). Protein expression was induced as described in the PichiaPink Expression System Manual (InVitrogen, Publication number MAN0000717). In brief, after kinetics analysis, single colonies of transformed *P. pastoris* strains 3 and 4 were used to inoculate 25 mL BMGY media (1% w/v yeast extract, 2% w/v peptone, 0.1 M potassium phosphate buffer, 1.34% yeast nitrogen base, $4x10^{-5}$ % biotin, 1% glycerol), grown shaking at 28°C (250 rpm) for 2-3 days, then grown to 1 L. Cells were harvested and resuspended in BMMY (containing 0.5% methanol instead of glycerol) for induction of expression. Media was supplemented to 0.5% methanol every 24 h for 4-5 days, then cells harvested (1500 g, 5 min, RT).

Cell pellets were lysed using 10 mL lysis buffer (0.1% Triton, 1 mM EDTA, 1 mM $MgCl_2$, 10 mM Tris, pH 7.8) with 1 g glass beads, a protease inhibitor tablet, and 1 μL Benzonase (Sigma), with 10 rounds of 1 min vortex/1 min on ice. The lysed cells were then incubated for 10 min RT, followed by 1500 g centrifugation for 5 min. The supernatant was further centrifuged for 20 min at 14000 g (RT) for clarification prior to purification.

Purification was performed by C-tag affinity chromatography (Life Technologies) against the EPEA C-tag added at the C-terminal of Rv21 and CSVS-like, with elution using PBS equilibration buffer and 20 mM Tris/2 M $MgCl_2$ elution buffer, followed by gel filtration (HiPrep 16/60 Sephacryl S-500, GE) with PBS elution, when required. Eluted fractions were checked for protein using SDS-PAGE and western blots.

2.3.4 Qβ virus-like particle production, purification and chemical coupling

Qβ-transformed *E. coli* from glycerol stock was grown to 1 mL in LB/carbenicillin, then transferred to 1 L M9 media (with 2 mL $MgSO_4$, 5 mL 40% glucose, 50 mL casamino acid, 500 µL vitamin B1, and 100 mg/mL carbenicillin) and incubated at 37°C 250 rpm for 18 h. Cells were pelleted (4500 rpm, 25 min, 4°C) and the supernatant discarded. The pellet was resuspended in PBS, centrifuged again (20 min, 14,000 g), and supernatant discarded. The pellet was lysed using lysis buffer (20 mM $NaPO_4$ pH 7.5, 0.1% triton x-100, 5 mM EDTA, 100 U/g cells Benzonase, 10 µL/g cells Lysonase, 10 µL/ml protease inhibitor), and freeze/thawing the pellet in dry ice twice. Lysed cells were sonicated for 1 min (15 s on/30 s off, 30% intensity), centrifuged at 14,000 g for 25 min, and the supernatant collected and filtered. Fractogel purification was carried out using 20 mM $NaPO_4$ pH 7.2 buffer with either 150 mM or 1 M NaCl, followed by size exclusion chromatography.

Coupling Qβ to full-length chimeric PvCSP (Table 2.3.1) was performed by derivatising Qβ with reactive groups using succinimidyl-6-[(β-maleimidopropionamido)hexanoate] (SMPH) at 10X molar excess SMPH (1 h, 250 rpm RT), followed by three 1 m 100 kDa spin filtrations with PBS (Amicon 0.5 mL) to remove free SMPH. Free sulfhydryl groups were generated on chimeric PvCSP by reacting with SATA followed by deactylisation, to allow coupling to derivatised Qβ particles. Peptides were synthesised with free cysteines rendering SATA derivation unnecessary. Peptides or SATA-treated PvCSP were then incubated with SMPH-derivatised Qβ for 3 h (250 rpm, RT) and Qβ-VLPs stored at -20°C.

Some Qβ-peptide vaccines were produced which display multiple peptides on their surface ("Triple-VLP," Multi-VLP," and "Charged 210qpag Double VLP," Chapters 5 and 6). Chemical coupling of peptides in these cases was performed by adding all the desired peptides to SMPH-derivatised Qβ simultaneously, with 3 h incubation as before.

A list of peptides coupled to Qβ and used as Qβ-peptide VLPs in this thesis is given in Table 2.3.3. All peptides were synthesised by ThinkPeptides.

Table 2.3.3 Peptides coupled to Qβ in this thesis

Name	Sequence*
$(AGDR)_2$	**CGG**AGDRAGDR
$(NANP)_2$	**CGG**NANPNANP
$(AGDR)_2(NANP)_2$	**CGG**AGDRAGDRNANPNANP
$(AGDR)_3$	**CGG**AGDRAGDRAGDR
$(NANP)_3$	**CGG**NANPNANPNANP
$(AGNG)_3$	**CGG**AGNGAGNGAGNG
$(NANP)_3$-$(AGDR)_3$	**CGG**NANPNANPNANPGGAGDRAGDRAGDR
$(AGDR)_3$-$(NANP)_3$	**CGG**AGDRAGDRAGDRGGNANPNANPNANP
210qpag	**CGG**AGDRADGQPAGDRADGQPAG
210agdr	**CGG**DRADGQPAGDRADGQPAGDR
SVTCG	SVTCGVGVRVRRRVNAANKK**GGC**
LGEN	LGENPDDEEGDAKKKKDGK**GGC**
(vivax) KLKQP	**CGG**KAEPKNPRENKLKQP
ttNANP	**CGG**QYIKANSKFIGITENANPNANPNANP
tt	**CGG**QYIKANSKFIGITE
247gang	**CGG**AGNQPGANGAGNQPGANG
$(GANG)_3$	**CGG**GANGGANGGANG
$(AEDG)_3$	**CGG**AEDGAEDGAEDG
$(NADG)_3$	**CGG**NADGNADGNADG
$(NANP)_1$	**CGG**NANP
$(GGGG)_2(NANP)_1$	**CGG**GGGGGGGGNANP
$(NANP)_2$	**CGG**NANPNANP
$(NANP)_6$	**CGG**NANPNANPNANPNANPNANPNANP
Esp short	**CGG**EDNEKLRKPKH
Esp long	**CGG**DDGNNEDNEKLRKPKHKKLKQPADGN
ADGN long	ADGNPDPNANPNVDP**GGC**
$(NVDP)_6$	**CGG**NVDPNVDPNVDPNVDPNVDPNVDP
PBLP	**CG**GEHNDILVNDDGSYH
SSP3	CGNGYRLMEGYNIQYD
SIAP1	**CG**GLKYLSRRKNGTTHP
Maebl a	**CGG**KNHANDIKNEKEYDM
Maebl b	CVILGTHEQER
RON4	CDKILSEMFKILTE
Falstatin	**CG**GKYYIVYSYYRPF

P113	**CGG**SDIKDMIEDRYNE
PLP1 a	**CG**GDSECTPDVYEQKK
PLP1 b	CGGNPIKDVTKEENL
RON3 b	NNLFEKNLGTG**GC**
TRSP	DIGIKIRARVSSN**GGC**
A08	**CGG**ELIRLGSGQSIDKRQALSKV
B10	CTEVERVANAGPWDPWTAASVT
C07	**CGG**DEDDDEVPPANEGADGNPVEEN
C11	**CGG**PAVPGGSSEEFPADVQNNPD
D03	**CGG**ERSDSNGYGVNEKVIPNPLD
D05	**CGG**NERDMANKNKTVHPGRKDS
D09	**CGG**NSDIPNNPVPSDYEQPEDKAKK
210qpag charged	**CG**KKKAGDRADGQPAGDRADGQPAG

* **CGG** sequence in bold is linker with free cysteine added to enable chemical coupling. In some cases natural cysteines were used.

2.3.5 $(NANP)_{60}$ design and manufacture

A DNA construct coding for 60 copies of (NANP) was synthesised and codon optimised for expression in *E. coli* by GeneArt. The construct was cloned into plasmid pRSET (InVitrogen) downstream of a His-tag sequence and enterokinase cleavage site. The plasmid was used to transform *E. coli* BL21(DE3)pLysS and carbenicillin used to select for transformants, with chloramphenicol used to maintain the pLysS plasmid. Colonies were picked, used to inoculate 3 mL cultures (LB, 50 μg/mL carbenicillin, 35 μg/mL chloramphenicol) and grown overnight (37°C, 250 rpm), then scaled to 1 L. Once culture reached OD600=0.5 IPTG was added to a concentration of 1 mM, and grown for 24 h. Cells were harvested by centrifugation and lysed by sonication. The supernatant was filtered and applied to a Histrap HP column for purification by affinity chromatography as in §2.3.2. Coupling of purified $(NANP)_{60}$ to Qβ proceeded as described in §2.3.4, and to keyhole limpet hemocyanin as described in §2.3.6.

2.3.6 Chemical coupling to keyhole limpet hemocyanin

Peptides and proteins were coupled to keyhole limpet hemocyanin (KLH, Life Technologies) by crosslinking with EDC (Fisher) following the manual from Thermo Scientific (MAN0011256_EDC_UG). In brief, 2 mg KLH in 0.1 M MES pH 5 buffer was added to the peptide or protein to be coupled with 50 µL EDC (10 mg/mL) and incubated RT for 2 h, then desalted using an Amicon 0.5 mL 100 kDa spin filter into PBS to remove excess EDC and peptide. In one case, in an attempt to produce a branched or linear polypeptide, the peptide was pre-treated with EDC for 2 h (RT) prior to conjugation to KLH.

2.3.7 Viral vector design and production

ChAd63-PvTRAP and MVA-PvTRAP were prepared by Karolis Bauza and the Jenner Institute Vector Core team as described in (17). CS-IMX313-, Tc24-IMX313-, TRAP-Ii-, and TRAP-Ii-IMX313-containing viral vectors were prepared by Amar Lall and the Jenner Institute Vector Core team.

In brief, the antigens of interest were cloned into adenoviral or MVA entry plasmids, followed by a second cloning step integrating the antigen of interest into a destination vector in the case of adenoviral vectors. The plasmids were linearised to permit transfection of host cells. Linearised adenoviral destination vectors were used to transfect 293TREx cells permissive for replication-incompetent adenoviruses, and recombinant adenovirus purified using a caesium chloride gradient. Linearised MVA shuttle vectors were used to transfect chick embryo fibroblasts co-transfected with an MVA shuttle vector expressing GFP, allowing exchange of antigen and GFP. GFP-expressing cells were selected by MoFlo cell sorting (D. Worth, Jenner Flow Sorting Facility) and used to infect

further chick embryo fibroblasts. Adenoviral titres are given in infectious units (iu) and MVA titres in plaque-forming units (pfu).

2.3.8 E. coli *transformations*

DHα one-shot cells (Thermo Fisher) were thawed on ice and 50 µL added to 1 – 10 µL (1 – 10 ng) DNA plasmid and mixed gently. The transformation mix was incubated on ice for 30 minutes then heat shocked for 45 s at 42°C in a water bath. The transformation mix was returned to ice for 3 minutes, then 950 µL of SOC media added and incubated for 1 h 37°C at 225 rpm. 20 – 200 µL of transformation was plated on carbenicillin selective agar plates and incubated overnight, whereupon 3 – 5 colonies were picked and grown in LB/Carbenicillin.

2.3.9 SDS-PAGE

Protein samples for analysis by SDS-PAGE were incubated 1:1 with 2x Laemmli buffer (BioRad) and 2-Mercapatoethanol (Gibco) for 5 m at 95°C before loading on an any-kD stain-free gel. Gels were run at 150 V for 5 min and thereafter 200V until completion, then imaged using a ChemiDoc XRS imaging system (BioRad). Precision plus protein ladders (BioRad) were used to determine sample molecular weights, with analysis performed using BioRad Image Lab software.

2.3.10 Western Blots

Following SDS-PAGE analysis gels were transferred to nitrocellulose membranes (BioRad) using the TransBlot Turbo transfer system (BioRad), blocked in skim milk solution (Sigma) for 1 h, washed three times in PBS/T (5 min per wash) then incubated with primary antibodies (anti-PvCSP-210, 1:4000; anti-PvCSP-

247, 1:40,000; MR4/BEI) for 1 h, washed as before, incubated with goat anti-mouse HRP conjugated secondary antibody (BioRad, 1:300), washed as before and developed using a WesternC Chemiluminescence kit (BioRad) with visualisation using a ChemiDoc XRS imaging system (BioRad).

2.3.11 PvTRAP crystal structure visualisation

The PvTRAP crystal structure (4HQO) was visualised and coloured using PyMol.

2.3.12 Calculation or prediction of peptide properties

Length, net charge, aliphatic index, instability index and hydrophobicity were calculated or predicted using the CAMP.R3 feature calculator (http://www.camp3.bicnirrh.res.in/featcalc). Molecular weight and theoretical pI were calculated using the ExPasy ProtParam tool (web.expasy.org/protparam).

2.3.13 Selection and identification of conserved amino acid sequences in P. berghei *pre-erythrocytic invasion proteins*

A list of surface-exposed sporozoite proteins involved in invasion and migration (609) was used as the starting point for identifying conserved regions of *Plasmodium* invasion proteins for design of peptides to act as vaccine candidates. Homologues of selected proteins were identified by protein BLAST using PlasmoDB (plasmodb.org), Uniprot and NCBI. Alignments to identify conserved regions were performed using Clustal Omega (www.ebi.ac.uk/Tools/msa/clustalo/) and transmembrane domains predicted using TMHMM Server 2.0 (www.cbs.dtu.dk/services/TMHMM/) to identify likely

extracellular regions of proteins. Conserved regions of these proteins were identified visually and used as the basis for choosing 16-20 amino acid sequences for synthesis. Table 2.3.4 gives the accession numbers for each protein used in each alignment.

Table 2.3.4 Accession numbers of *Plasmodium* sporozoite surface-exposed invasion and migratory proteins used in alignments

	TRSP	PBLP	SSP3	SIAP1	MAEBL	RON4	Falstatin	P113	PLP1/ SPECT2	RON3
Pb*	A1X5V6-1	A0A113RBV9								
Pb ANKA	A0A077X8K3	PBANKA_071220	PBANKA_1425200	PBANKA_1006200	PBANKA_0901300.2	PBANKA_0932000	PBANKA_0813000	PBANKA_1022500	PBANKA_1006300	PBANKA_1464900
Pch	A0A077TLB8		PCHAS_1427000	PCHAS_1007100	PCHAS_0702500	PCHAS_0912300	PCHAS_0813300	PCHAS_1023300	PCHAS_1007200	PCHAS_1467100
Pcy				PCYB_031630	PCYB_095300	PCYB_092210		PCYB_133650		
Pf 3D7	Q8I2A0	PF3D7_0818600	PF3D7_0812300	PF3D7_0408600	PF3D7_1147800.2	PF3D7_1116000	PF3D7_0911900	PF3D7_1420700	PF3D7_0408700	PF3D7_1252100
Pf IT		PFIT_082150 0	PFIT_081520 0	PFIT_040720 0	PFIT_1148400.1	PFIT_111680 0	PFIT_091210 0	PFIT_142170 0	PFIT_040730 0	PFIT_125230 0
Pg	A0A151LWY9	PGSY75_0818600								
Pk		PKH_051320	PKNH_1428300	PKNH_0306600	PKNH_0945700	PKNH_0913700	PKNH_0709900	PKNH_1337300	PKNH_0306700	PKNH_1472100
Pr	A0A060RRJ1		PRCDC_0811700	PRCDC_0406000	PRCDC_1146100.1		PRCDC_0910000	PRCDC_1420000	PRCDC_0406100	PRCDC_1251500
Pv		PVX_089485	PVX_123155	PVX_000815	PVX_092975	PVX_091434	PVX_099035	PVX_085445	PVX_000810	PVX_101485
Py					AF031886.2					
Py 17X			PY17X_1427200	PY17X_1007600	PY17X_0902700.1	PY17X_0934000	PY17X_0816300	PY17X_1024400	PY17X_1007700	PY17X_1467600
Py 17XNL				PY00455	PY05977					
Py YM			PYYM_1429000	PYYM_1007600	PYYM_0902200.1	PYYM_0933400	PYYM_0816000	PYYM_1024100	PYYM_1007700	PYYM_1469000

* Key: Py, *Plasmodium yoelii*; Pf IT, *P. falciparum* IT; Pr, *Plasmodium reichenowi*; Pv *P. vivax*; Pcy *P. cynomolgi*; Pk *P. knowlesi*; Pb *P. berghei*; Py 17XNL, 17X, YM, *P. yoelli* 17XNL, 17X, YM; Pch *P. chabaudi*; Pf 3D7 *P. falciparum* 3D7; Pg *P. gaboni;* Pb ANKA *P. berghei ANKA*

2.4 Statistical analysis

2.4.1 Statistical tests used

GraphPad Prism (MacOS v6) and Microsoft Excel were used for all statistical analyses performed. Student's t-test and ANOVA with Bonferroni's multiple

comparisons test were used on parametric data comparing two or more groups respectively.

2.4.2 Non-linear curve fitting

The non-linear curve-fitting function in GraphPad Prism was used to fit specified equations to data.

2.4.3 Statistical definition of challenge outcomes

The three sporozoite challenge outcomes used in this thesis are defined as follows. Sterile protection, or "protection," represents a case where a mouse has no detectable blood-stage parasitaemia by fifteen days post-infection. A mouse is classified as "delayed" if the time to reach 1% blood stage parasitaemia in that mouse is greater than the mean time to reach 1% blood-stage parasitaemia of naïve or control mice in that experiment plus 2 standard deviations. A mouse is "not delayed" if the time to reach 1% blood-stage parasitaemia is less than 2 standard deviations above the mean of naïve or control mice.

2.5 List of Materials

Reagent	Company	Cat. No.
0.22 μm filters		
2 x Laemmli sample buffer	BioRad	610737
2-Mercaptoethanol	Gibco	BRL 31350-010
25 G needle	Fisher	10753785
70 μm cell strainer		
8-azaguanine	Sigma	A5284
AddaVax	InvivoGen	
Alhydrogel	Brenntag Biosector	

Amicon 0.5 mL 100 kDa spin filter	Millipore	UFC510024
Anti-mouse IFN-γ mAb AN18	Mabtech	3321-3-1000
Anti-mouse-IFN-γ mAbR4-6A2, biotinylated	Mabtech	3321-6-1000
anti-PvCSP-210/anti-PvCSP-247	MR4	MRA-1028K
Benzonase	Sigma	E8263
C-tag column	Life Technologies	491307001
Carbenicillin		
Casamino acid		
Chloramphenicol		
Chloroform		
Desalting column		
DH5α T1R Max Efficiency 1 SHOT	Thermo Fisher	12297-016
diethanolamine buffer	Pierce	34064
DMSO	Sigma	D2650
Dulbecco's MEM - HIG	Sigma	D6546
Dulbecco's PBS	Sigma	D8537
EDC cross-linking reagent	Fisher	11851335
ELIspot colour development kit (BioRad AP Conjugate sub kit)	BioRad	170-6432
Fetal Bovine Serum	Sigma	F9665
Giemsa stain	Sigma	GS1L
Glass beads	Sigma	G8772
Glass slides		
Glucose		
Glycerol	Sigma	G5516
Goat anti-mouse whole IgG alkaline phosphatase conjugate	Sigma	A-3562
Goat anti-rabbit horseradish peroxidase conjugate	BioRad	172-1064
Heparin		
HiLoad 16/600 Superdex	GE	28989335
HiPrep 16/60 Sephacryl S-500	GE	28935606
Histrap HP 5 mL column	GE	17-5248-02
HT	Life Technologies	11067-030
Hybridoma Cloning Factor	Fisher	IG50-0615
Imidazole	Sigma	I2399
Imject mcKLH (in MES Buffer)-2 mg	Life Technologies	77653
Immun-Star WesternC Chemiluminescence Kit	BioRad	170-5070
IPTG		
L-Glutamine	Sigma	G-7513
L-glutamine solution	Sigma	G7513
LB broth	Fisher	12821670
Lysonase		
MAIP Elispot Plates	Millipore	MAIPS4510
Matrix M	Isconova	

Maxisorp 96-well plates (NUNC)	Sigma	442404
MEM Non-essential amino acids	Sigma	M7145
MES		
MgSO4		
Microvette serum tubes	Sarstedt	16.44
Mini-PROTEAN TGX Stain Free Gels, Any kD, 12-well	BioRad	4568125
Mouse Typer Sub-Isotyping kit	BioRad	172-2055
Mr Frosty cryopreservation chamber		
Na_2EDTA	Sigma	ED2SS
NaPO4		
Nunc cryotubes	Sigma	V7384
Oxalic acid	Sigma	75688
Penicillin-Streptomycin	Sigma	P-0781
Peroxidase substrate solution	BioRad	
PichiaPink Media Kit	InVitrogen	A11156
PichiaPink Vector Kit	InVitrogen	A11152
Plastipack 1ml luer syringe	BD	300013
pNPP tablets	Sigma	N-2765
Precision Plus Protein Unstained Standards, 1 ml	BioRad	1610363
Precision Plus Protein WesternC Pack	BioRad	1610385
Protease inhibitor cocktail	Sigma	P8215
Qiagen maxiprep kit	Qiagen	12163
Roller bottles		
SATA		
Schneider's media		
Skim milk powder	Sigma	70166
SMPH	Pierce	0022363
Sodium chloride	Sigma	
Sodium phosphate	Sigma	
Streptavidin Alkaline Phosphatase	Mabtech	3310-10
Surgical blades	VWR	SWAN3002
Trans-Blot Turbo Mini Nitrocellulose Transfer Packs	BioRad	1704158
TRIS buffer	Sigma	T5912-1L
Triton X-100		
Trizma-HCl	Sigma	T-2569
Tween-20		
urea	Sigma	U5378
Vitamin B1		
X200 Micro Fine Insulin syringe 0.5mL 29G	Fisher	13161931

Chapter 3

A mathematical model of the effects of combining pre-erythrocytic malaria vaccines

Introduction

In this chapter, a novel mathematical model is derived, expressing the probability of sterile protection as a function of antibody and cytotoxic T-cell frequencies. An extension of this model expressing time to reach 1% blood stage parasitaemia in terms of the same variables is also developed. The goal of this work is to establish a framework in which combination vaccine experiments can be evaluated and interpreted, as well as establish the theoretical basis upon which combination vaccines might be expected to enhance efficacy. Models also often shed light on hidden biological processes, and so this model may turn out to be of use in that regard. Perhaps most importantly, these models will help inform decisions on the optimal vaccination strategies to pursue. Increasingly, immunologists and vaccinologists recognise the desirability of developing mathematical models as an aid in obtaining a mechanistic understanding of biological processes and so contributing to our progress in obtaining practical goals (610).

Another reason for developing a pre-clinical, murine model of malaria vaccine combination is to bridge the gap between pre-clinical and clinical trials of vaccines. This would facilitate translation of the findings from pre-clinical to clinical trials. Three models of human malaria vaccine combination have been developed for clinical or field conditions, by Saul *et al.,* (611, 612), White *et al.,*

(613, 614), and Walker *et al.,* (615). As explained below, there are important differences between typical controlled human malaria infection and field studies and pre-clinical murine experiments which make desirable the development of a specifically murine model. A summary of the three human malaria models follows, together with an explanation of the aim of the murine model.

White *et al.* (613, 614) follow Saul *et al.* (611, 612) in developing a model based on the assumption that the dose-response relationship between adaptive immune responses and the probability of a sporozoite surviving those can be modeled using a Hill function. White *et al.* consider an alternative, which is that the relationship can be modeled using an exponential dose-response relationship. Here we'll consider the exposition in (613) as it lucidly explicates both models.

For the Hill function and exponential models, the parameters of interest are x_{ij}, the antibody titre to a specific antigen in a given individual; r_{ij}, the probability that a sporozoite survives the immune response x_{ij}; and β_j, the antibody titre which reduces the probability of sporozoite infection by half. If we assume that a Hill-function captures the relationship between x_{ij} and r_{ij} then the model is

$$r_{ij} = {1}\Big/{1 + (\frac{x_{ij}}{\beta_j})^{\alpha}}$$

where α is the shape parameter. If the dose-response relationship is assumed to be exponential, on the other hand, then the relationship is

$$r_{ij} = e^{-x_{ij}\log(2)/\beta_j}$$

From this core, White *et al.* and Saul *et al.* expand the two models to include the variation in numbers of sporozoites inoculated per bite, assuming

that the distribution is geometric, and also include the variation in antibody responses, assuming that the distribution is lognormal; variation in biting rates is also incorporated if field conditions are considered. In (613) the exponential and Hill-function models are compared using clinical trial data. The exponential curve is found to fit best. In contrast, in (614) the Hill-function model is found to fit that antibody data better. Thus at present it is not possible to say which model better fits the data.

Walker *et al.* (615) present a third model, explicitly designed to capture the effects on protective efficacy of CSP-specific antibodies and TRAP-specific cytotoxic T-cells. Here four equations are assumed to capture the dynamic effects of adaptive immunity on infection:

$$\frac{\mathrm{d}H}{\mathrm{d}t} = -\alpha_2 H$$

$$\frac{\mathrm{d}M}{\mathrm{d}t} = \gamma M$$

$$H_0 = (1 - \alpha_1) f S_0$$

$$M_T = r H_T$$

where H is the number of infected hepatocytes at time t; α_2 the vaccine-induced rate of removal of infected hepatocytes; M the number of merozoites at time t; γ the blood-stage growth rate; H_0 the initial number of infected hepatocytes at the beginning of the liver-stage of the life-cycle; α_1 the vaccine-induced modifier of sporozoite invasion probability; f the proportion of sporozoites that successfully invade hepatocytes; S_0 the number of sporozoites inoculated; M_T the number of

merozoites seeding the blood stage of infection; and r the number of successful merozoites released per infected hepatocyte H_T after the liver-stage incubation period T.

As with White *et al.* and Saul *et al.*, Walker *et al.* expand the basic model to adapt it to controlled human malaria infections (CHMI), where variation in the number of sporozoites injected per mosquito requires modeling using a negative binomial distribution. As with the other models, that of Walker *et al.* is found to fit real CHMI data well, and predicts that a combination of CSP and TRAP vaccines will enhance protective efficacy.

As will be seen, the model developed in this chapter closely follows the work of White *et al.*, Saul *et al.* and Walker *et al.,* but adapted to murine systems and deriving the equations from more fundamental biological assumptions. The probabilistic interpretation of sporozoite infectivity is owed to (616). The principal differences between human and murine challenge experiments are that in CHMI and field trials there is great variation in the number of sporozoites inoculated, whereas in the pre-clinical murine experiments used to screen vaccines in this thesis, fixed and known quantities of sporozoites are injected intravenously. In contrast, the infectivity of sporozoites appears to vary markedly between murine challenge experiments, whereas it is not known if this is the case in CHMI or field trials of human malaria vaccines. The model presented below adapts the three models above by simplifying the sporozoite-inocula component of the models, to make it more usable for murine studies, while at the same time taking into account the wide variation in sporozoite infectivity between murine challenge experiments.

The second major difference between the model presented in this chapter and the models of White *et al.*, Saul *et al.* and Walker *et al.* is an attempt to derive a relationship between the level of adaptive immune components (antibodies and cytotoxic T-cells) and sporozoite survival from very simple probabilistic assumptions. The models of White *et al.* and Saul *et al.* do not derive a dose-response relationship, rather they assume one, modeling it either as Hill function or as an exponential function. Walker *et al*. do not attempt to model the relationship, but they model the combination of vaccines of known protective efficacy only. It is the aim of this chapter to present a model which helps bridge the gap between pre-clinical and clinical malaria vaccine studies, as well as presenting a novel method of modeling the combination of vaccines which puts it on a firmer theoretical footing.

Another goal of this chapter is to derive a function expressing time to reach 1% blood stage parasitaemia, one of the main metrics of vaccine efficacy used in this thesis, as a function of antibody and cytotoxic T-cell frequencies. As well as conferring complete sterile protection, pre-erythrocytic vaccines can also reduce the number of merozoites seeding the blood stage of infection by reducing the number of infected hepatocytes (617). This can result in a delay in time to patency, positivity by qPCR, or, as in this thesis, time to reach 1% blood-stage parasitaemia (487).

To achieve an expression containing this metric of pre-erythrocytic vaccine efficacy, a simple model of blood-stage malaria growth is used. There are many available models, ranging from very simple exponential growth models (615, 618) to those modified to take account of sequestration or periodicity (619, 620), erythrocyte kinetics (621), blood-stage immunity (621-623), as a

discontinuous process (624), as a discrete-time process (625, 626), as a sine-wave function (617, 620), or as a normal cumulative density function (627). To develop the model presented in this chapter, the most simple exponential growth model was chosen. This was motivated by considerations of tractability, with simpler models being easier to apply to experimental interpretation. It was also motivated by the fact that the metric of challenge outcome used in this thesis, time-to-1%, is based on the simple exponential growth model, and hence is the most appropriate growth model to incorporate into a vaccine combination mathematical model which uses time-to-1% as a metric of vaccine effect. But above all the use of the simpler exponential growth model is justified by the finding in (618) that it is as accurate in predicting parasitaemia levels in controlled human malaria infection studies as more complex models such as the sine-wave and normal cumulative density function models which account for phenomena such as sequestration and periodicity.

Application of the mathematical expressions derived below to the rodent malaria model used in this thesis require an estimate of the blood stage growth rate between 0% and 1%. This is obtained using three different methods, blood smears, and non-linear curve fitting to sporozoite- and infected red blood cell-titration data. The results are found to be in close agreement with each other, and the obtained growth rate value, of 3.5 infected red blood cells per infected red blood cell per day, is used to derive values for other unknown parameters in the equations, allowing simulations of vaccine combinations and optimal vaccination strategies. Finally, the model is tested against available published data and found to agree closely with it.

In short, a theoretical basis for the enhancement of efficacy obtained with vaccine combination regimes is derived from simple biological assumptions. Variables such as the blood-stage growth rate in the murine malaria model are estimated within in the context of the model, and used to generate simulations informing optimal strategies for the combination of pre-erythrocytic malaria vaccines.

Results

3.1 Derivation of a probabilistic equation modeling pre-erythrocytic malaria vaccine efficacy

Here I derive an equation representing the protective effects of antibody and cytotoxic T-cell (CTL)-eliciting vaccines from minimal probabilistic assumptions. For ease of exposition, equations are numbered and the symbolic representations highlighted in bold immediately following or preceding their definition. Also see Table 3.1.1 for a complete list of definitions of symbols used in this section.

The assumptions are:

i) a unit of monoclonal antibody or CTL has a fixed probability ($\boldsymbol{p_b}$ or $\boldsymbol{p_c}$ respectively) of preventing successful infection by a given sporozoite. "Successful infection" denotes the event where a given sporozoite invades a hepatocyte and fully develops to initiate blood-stage infection.

ii) the probabilities p_b and p_c are independent.

iii) the probability $\boldsymbol{p_Z}$, that a given sporozoite successfully infects, is independent.

The aim is to derive an expression linking the probability of sterile protection $\boldsymbol{p_S}$ with the number of units of antibody $\boldsymbol{b}$, CTL $\boldsymbol{C}$, number of sporozoites $\boldsymbol{Z}$ and unit probabilities of preventing successful invasion p_b and p_c.

To achieve sterile protection, each sporozoite must fail to initiate blood stage infection. The probability that a given sporozoite fails to infect is $(1-p_Z)$, and hence the probability p_S that all sporozoites fail to infect is

(1) $p_S = (1 - p_Z)^Z$

The probability that a given sporozoite infects is a function of its natural infectivity ***i*** and the probability that the antibodies and CTL in the system all fail to prevent infection. Here I interpret natural infectivity probabilistically: in the absence of antibodies or CTL, a given sporozoite has a probability ***i*** of successful infection. In the absence of antibodies or CTL, $p_Z = i$.

The probability p_Z that a given sporozoite will successfully infect in the presence of antibodies and CTL is the product of the probability that each unit of antibody and each unit of CTL fails to prevent infection, and the natural infectivity. The probability that every unit b of antibody fails to prevent a given sporozoite infecting is $(1-p_b)^b$ and likewise the probability that every unit C of CTL fails to prevent a given sporozoite infecting is $(1-p_c)^C$. Hence the probability that all units of antibody and CTL fail, and that a given sporozoite infects, is

(2) $p_Z = i * (1 - p_b)^b * (1 - p_C)^C$

From **(1)** and **(2)** we get

(3) $p_S = (1 - (i * (1 - p_b)^b * (1 - p_C)^C))^Z$

Table 3.1.1 List of variables

p_S	probability of sterile protection
i	natural infectivity of sporozoites
p_b	probability that a unit of antibody prevents successful infection
b	quantity of antibody
p_C	probability that a unit of CTL prevents successful infection
C	quantity of CTL
Z	number of sporozoites in challenge

3.2 Time to 1% blood-stage parasitaemia as a function of antibody and CTL

As well as conferring sterile protection, effective pre-erythrocytic vaccines cause a delay in time to patency by decreasing the number of merozoites initiating the blood stage of infection. Here I derive equations linking the time taken to reach a given level of blood-stage infection with the quantity of antibodies and CTL. To this end I have assumed a simple model of growth: at time ***t*** from the beginning of blood-stage infection, the number of infected red blood cells (**iRBC**) is given by

(4) $iRBC = M * (g^t)$

where ***M*** is the number of infected red blood cells seeding the blood stage infection at time t=0 and ***g*** is the growth rate, which is the average number of infected red blood cells generated from each infected red blood cell.

In this thesis the metric by which challenge outcome is assessed is ***T***, time taken post-infection to reach 1% blood-stage parasitaemia; hereafter truncated to "time-to-1%". Since t in **(4)** refers to time after the beginning of the blood-stage infection, and T refers to time taken to reach 1% iRBC after sporozoites are injected into a mouse, to substitute T into **(4)** we need to take into account the time for pre-erythrocytic development, t_1. If the number of red blood cells (RBC) in the system is ***B***, then iRBC = 1% = $B/100$ when $t = T - t_1$. Then from **(4)** we get:

(5) $M = \frac{B}{100 * g^{T-t_1}}$

The number of iRBC initiating blood-stage infection, *M,* is the product of the number of infected hepatocytes contributing to the blood stage, ***L***, and the average number of iRBC each infected hepatocyte contributes, ***R***: *M = L*R.* Therefore

(6) $L = \frac{B}{100 * R * g^{T - t_1}}$

The number of successfully infected hepatocytes, *L,* is in turn the product of the probability that a given sporozoite infects, p_Z, and the number of sporozoites injected, *Z*: $L = p_Z * Z$. If in a given experiment $\boldsymbol{L_N}$ represents the average number of infected hepatocytes in naive mice and $T = \boldsymbol{T_N}$, and $\boldsymbol{L_V}$ represents the number of infected hepatocytes in the vaccinated mouse with $T = \boldsymbol{T_V}$, then from **(2)** we obtain

(7) $L_N = Z * i$

(8) $L_V = Z * i * (1 - p_b)^b * (1 - p_C)^C$

and from **(6)** we obtain

(9) $L_N = \frac{B}{100 * R * g^{Tn - t_1}}$

(10) $L_V = \frac{B}{100 * R * g^{Tv - t_1}}$

Therefore

$$\textbf{(11)}\ \frac{L_V}{L_N} = (1-p_b)^b * (1-p_c)^C = \left(\frac{B}{100*R*g^{Tv-t1}}\right) \Big/ \left(\frac{B}{100*R*g^{Tn-t1}}\right)$$

If we assume that B and R are identical in vaccinated and unvaccinated mice, then

$$\textbf{(12)}\ (1-p_b)^b * (1-p_c)^C = g^{Tn-Tv}$$

By taking the logarithm of **(12)** we obtain T_V as a function of quantity of antibody and CTL in the system:

$$\textbf{(13)}\ T_V = -\frac{\log(1-p_b)}{\log g} * b - \frac{\log(1-p_c)}{\log g} * C + T_N$$

If vaccine effects are mediated exclusively by antibody or CTL, that is if b or C = 0, we obtain the following linear equations:

$$\textbf{(14)}\ T_V = -\frac{\log(1-p_b)}{\log g} * b + T_N$$

$$\textbf{(15)}\ T_V = -\frac{\log(1-p_c)}{\log g} * C + T_N$$

Table 3.2.1 List of variables

M	Number of iRBC initiating blood-stage infection
B	Number of RBC in mouse
R	Number of iRBC produced per infected hepatocyte
L	Number of successfully infected hepatocytes
L_V	Number of successfully infected hepatocytes in vaccinated mouse
L_N	Number of successfully infected hepatocytes in naive mouse
T	Time to 1% blood-stage parasitaemia
T_V	Time to 1% blood-stage parasitaemia in vaccinated mice
T_N	Time to 1% blood-stage parasitaemia in naive mice
g	growth rate of blood stage parasite

3.3 Experimental estimates of g, p_b and p_c

3.3.1 Estimating g

The growth rate g of blood-stage parasitaemia may not be constant over the entire course of infection, and may not be constant between the initial blood-stage infection ($t = 0$) and 1% blood-stage parasitaemia ($t = T$). However, for the purposes of the model described in this chapter, it is important only that the effective growth rate g averaged between $t = 0$ and $t = T$ is invariant between mice, vaccinated or otherwise.

Evidence that pre-erythrocytic vaccines do not affect blood-stage growth rate comes from parasitaemia counts of thin blood smears taken 24 hours apart, either side of time-to-1% (Fig. 3.3.1). This demonstrates that the average growth rate, defined as the ratio of % parasitaemia of one day to the previous, is not significantly different when using different transgenic *P. berghei* sporozoites (Fig. 3.3.1 A), between BALB/c and C57BL/6 mice (Fig 3.3.1 B), or between vaccinated and naive BALB/c mice (Fig 3.3.1 C). These data together give a value of g=3.26 ± 0.07.

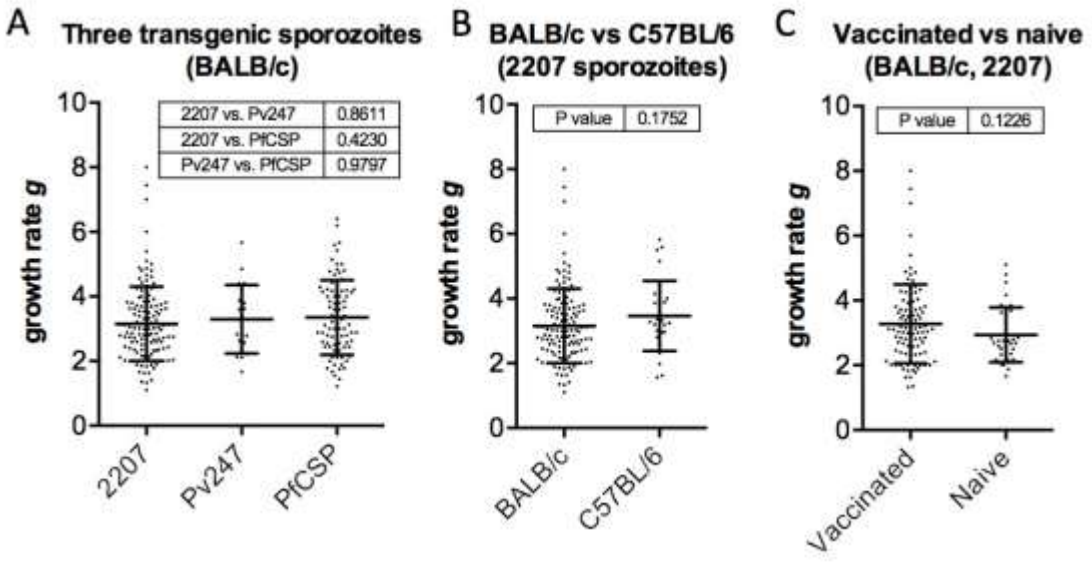


Figure 3.3.1 Estimates of blood-stage growth rate g from thin blood smears taken 24 hours apart.

Thin blood smears (n=273) were taken one day either side of 1% blood-stage parasitaemia for (A) three different transgenic *P. berghei*; (B) two strains of mouse using PvCSP-210/PvTRAP transgenic *P. berghei* ("2207" parasites); and (C) vaccinated and unvaccinated BALB/c mice using PvCSP-210/PvTRAP transgenic *P. berghei*. Growth rate g was calculated by dividing parasitaemia on the day after reaching 1% infected red blood cells by that of the previous day. Shown in tables in each graph are p-values for comparison of groups by (A) ANOVA with Tukey's multiple comparisons test and (B, C) t-test. No significant differences between groups were found. The data together give a value for $g = 3.26 \pm 0.07$ (SEM).

An estimate of g from blood smears around time T will not necessarily give us an accurate value: as stated above, g may not be constant between $t = 0$ and $t = T$. It is also difficult to determine whether the high levels of variation in g seen in Fig. 3.3.1 are real or a result of experimental error. An alternative approach is to artificially seed the blood-stage infection with a dilution series of iRBC (M) and curve fit a modified form of equation **(5)** to a plot of M against $T+0.5$. ($t_1 = 0.5$ d as the population of iRBC from a donor mice will be in various

stages of the 24 h replicative cycle; if the distribution is balanced, the mean will be 0.5 d).

(5) $M = \frac{B}{100 * g^{T+0.5}}$

Fig 3.3.2 shows the results of four independent experiments. Fitting the curves with the question of whether g was shared between each data set or not returned the conclusion that g was shared with a p-value of 0.57. The subsequent global value of g is 3.50 ± 0.12. Curve-fitting gives much lower variance in g than the blood-smear method of Fig. 3.3.1, suggesting that that variance is indeed due to experimental error.

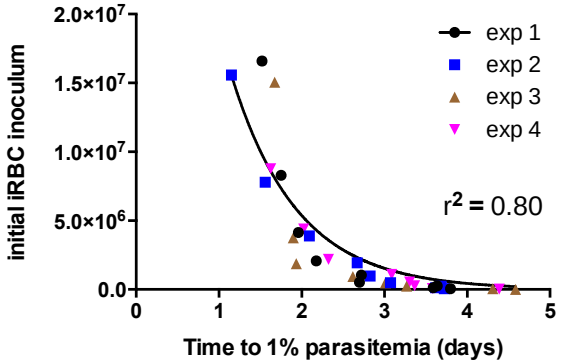


Figure 3.3.2: Seeding blood-stage parasitaemia with infected red blood cells (iRBC) to obtain an estimate of blood-stage growth rate by non-linear curve fitting.

Dilution series of PvCSP-210/PvTRAP transgenic *P. berghei* iRBC were intravenously injected into 6-8 week old BALB/c mice and time to 1% blood stage parasitaemia inferred by linear regression from daily thin blood smears (n=34). Curve-fitting to the equation $M = \frac{B}{100 * g^{T+0.5}}$ was performed using Prism to obtain a value for the growth rate g where M is the number of iRBC injected, T time-to-1% in the challenged mouse, and B the average number of RBC in a 22 g BALB/c mouse. A value of g = 3.50 ± 0.12 was obtained. Best fit values are given ± SEM.

Curve-fitting to equation **(5)**, though producing a relatively precise value of g, may still not be accurate. The merozoites from the mice used as the source of the iRBC in the above experiments were obtained when blood-stage parasitaemia was 1% or higher; conceivably merozoites at this stage could have phenotypic differences from those emerging from the liver in a natural infection, and those phenotypic differences could affect g. A method which ought to perfectly recapitulate natural infection and give an accurate value of g is curve fitting to the following equation derived from **(6)** and **(7)**:

$$\textbf{(16)}\ Z = \frac{B}{100*R*i*g^{T-t_1}}$$

Although R and i are unknowns and i at least will vary between experiments, g can be determined independently of R and i as can be more easily seen in a linear version of **(6)** where a plot of T against $\log(Z)$ will have slope $-1/\log(g)$:

$$\textbf{(17)}\ T = \frac{-1}{\log g} * \log Z + (t_1 + {\log \frac{B}{100*R*i}}/{\log g})$$

As well as **(6)** there is a second equation linking Z to T to which non-linear curve fitting could be applied. Under the model here presented, there will be a time T_{max} representing the longest possible time to 1% parasitaemia, occurring when just one infected hepatocyte seeds the blood-stage infection. In a procedure analogous to the derivation of **(11)** and **(12)** above, the ratio of $L_N/(L=1)$ gives

(18) $Z = \frac{g^{Tmax-Tn}}{i}$

If estimating g is the objective it makes no difference which equation is used for curve-fitting.

Challenging mice with a dilution series of sporozoites and measuring the subsequent values of T thus permits a potentially more accurate method of estimating g. Figure 3.3.3 shows two experiments using this method, the first using data from Karolis Bauza (DPhil 2012) with wild-type *Plasmodium berghei,* and the second with my own data using the double transgenic 2207 Pv210/PvTRAP parasite used in Fig. 3.3.2.

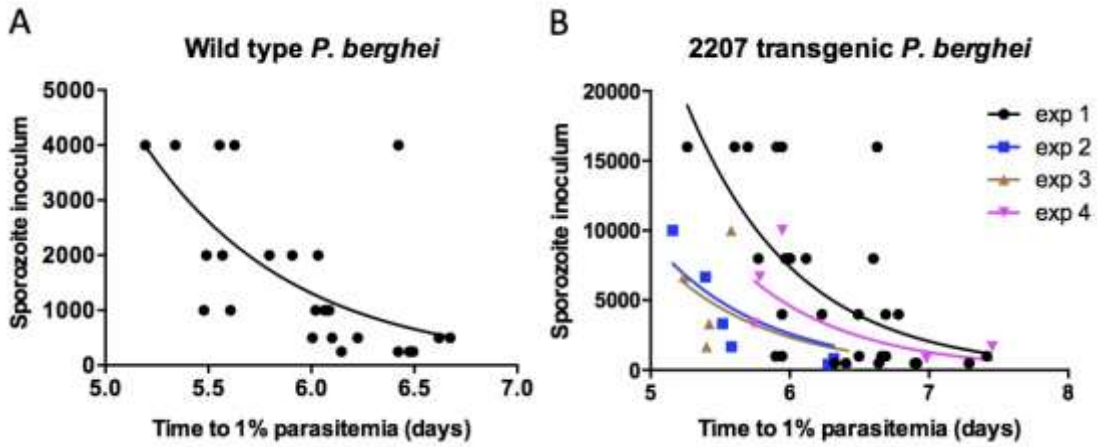


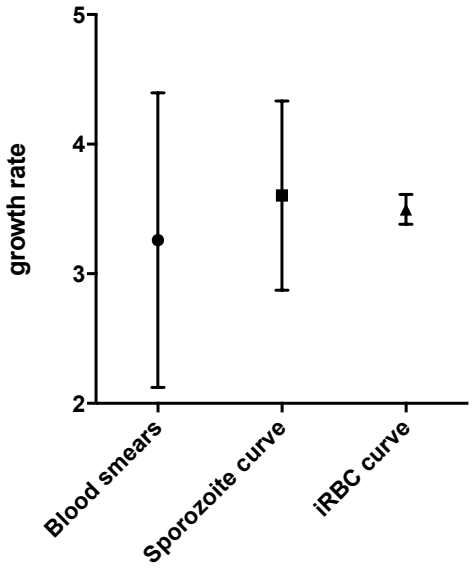
Figure 3.3.3 Varying *P. berghei* sporozoite inoculation to obtain an estimate of blood-stage growth rate by non-linear curve fitting.

Dilution series of wild-type (A) or PvCSP-210/PvTRAP transgenic (B) *P. berghei* were intravenously injected into 6-8 week old BALB/c mice and time to 1% blood stage parasitaemia was inferred by linear regression from daily thin blood smears. Curve-fitting to the equation $Z = \frac{g^{Tmax-Tn}}{i}$ was performed using Prism to obtain a value for the growth rate g where Z is the number of sporozoites injected, T_{max} maximum time-to-1%, T_N time-to-1% in a challenged mouse,

and *i* the infectivity of sporozoites. A value of $g = 4.0 \pm 1.5$ was obtained from (A, n=24) and $g = 3.6 \pm 0.9$ from (B, n=46). Best fit values given ± SEM.

Curve-fitting was successful using both wild-type and transgenic *P. berghei* and gave values of $g = 4.0 \pm 1.5$ and $g = 3.6 \pm 0.9$. Instructed to test whether *g* was shared between all five data sets (one wild type *P. berghei* and four from 2207 transgenic *P. berghei*) Prism best fits the data on the assumption that *g* is shared (p=0.86). The combined value for *g* is 3.6 ± 0.73.

A comparison of all three methods of calculating *g,* using thin blood smears, curve-fitting to varied iRBC inocula, and curve-fitting to varied sporozoite inocula, is shown in Fig. 3.3.4. The values for *g* obtained from varying sporozoite and iRBC inocula are in close agreement and not significantly different from each other. The value for *g* from thin blood smears is significantly lower than that from varying sporozoite inocula, suggesting that by the time 1% parasitaemia is reached, growth may be slowing slightly, possibly as reticulocytes, the preferred blood cell type for invading merozoites, become scarcer. Since the *g* values obtained from sporozoite- and iRBC-curves are in close agreement with each other, and that of the iRBC curve is relatively precise, the value from the latter curve-fitting of $g = 3.5 \pm 0.1$ is used for the remainder of this thesis.



Tukey's multiple comparisons test	Adjusted P Value
Blood smears vs. Sporozoite curve	0.0325
Blood smears vs. iRBC curve	0.4079
Sporozoite curve vs. iRBC curve	0.8702

	Blood smears	Sporozoite curve	iRBC curve
Mean	3.260	3.604	3.497

Figure 3.3.4 Comparison of methods of calculating growth rate *g*.

Values for g were obtained using thin blood smears (n=273), curve fitting to a dilution series of intravenously injected sporozoites (n=70), and to a dilution series of intravenously injected infected red blood cells (iRBC) (n=34). Comparison of methods was performed using ANOVA with Tukey's multiple comparisons test. P-values are shown in the table, together with mean values for g by each method.

3.3.2 Estimating p_b

p_b can be estimated by varying the quantity of antibody in a system and challenging with a fixed dose of sporozoites. If monoclonal or polyclonal antibody are injected we can be certain all vaccine effects are due to antibody alone; that is, CTL C=0 and from **(3)**:

(19) $p_S = (1 - (i * (1 - p_b)^b))^Z$

and from **(13)**:

(14) $T_V = -\frac{\log(1-p_b)}{\log g} * b + T_N$

These two equations allow two independent methods for estimating p_b. The first method requires injecting groups of mice with varying quantities of antibody and curve-fitting **(18)** to a plot of percent protection against quantity of antibody b injected. The second method exploits time-to-1% (T) data from the same experiment: a plot of T_V against b will give a straight line of slope $(\log(1-p_b))/(-\log(g))$ as shown in **(14)**. By using the value of g estimated in section 3.3.1 above, we can obtain another estimate of p_b.

The following estimate of p_b is based on data from Karolis Bauza (DPhil thesis 2012) using the *P. berghei* CSP-specific monoclonal 3D11 and wild-type *P. berghei* challenge. Figure 3.3.5 shows estimates of p_b using curve-fitting to **(18)** (Fig. 3.3.5 A) and linear regression to **(14)** (Fig 3.3.5 B).

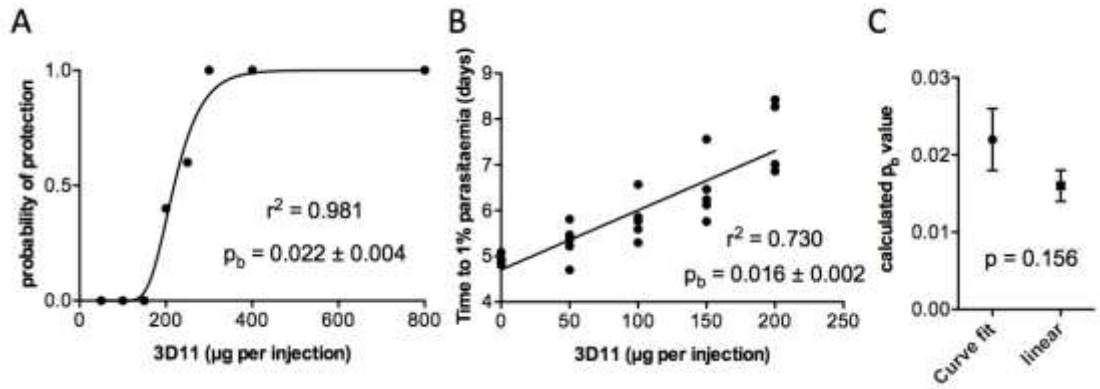


Figure 3.3.5 Varying monoclonal antibody 3D11 dose to obtain estimates of probability of protection parameter p_b.

Mice were injected on each of three consecutive days with varying quantities of the *P. berghei* sporozoite-neutralising monoclonal antibody 3D11 prior to intravenous challenge with 2000 wild-type *P. berghei* sporozoites (n=5-6 per group). (A) A value for the probability of protection parameter p_b was obtained by non-linear curve fitting to $p_S = (1 - (i * (1 - p_b)^b))^Z$, where p_S is

the probability of sterile protection, b the quantity of 3D11 mAb injected, and Z the number of sporozoites used to challenge the mice. (B) An alternative value for p_b was obtained by linear regression of a plot of [3D11] versus time to reach 1% blood-stage parasitaemia (obtained by linear regression using daily thin blood smears); p_b was calculated from the slope using the equation $T_V = -\frac{\log(1-p_b)}{\log g} * b + T_N$. (C) Comparison of p_b values obtained from (A) and (B), using t-test. Values shown ± SEM. Data from Karolis Bauza DPhil thesis.

The two methods give precise estimates of p_b and in good agreement with one another (p=0.16 by t-test, Fig. 3.3.5 C). Since curve-fitting to **(18)** does not rely on a value for g it is taken to be more reliable and hence the estimate p_b = 0.022 ± 0.004 is used for simulations in the sections below.

3.3.3 Estimating p_c

As with p_b two independent methods can be used to estimate p_c : if only CTL are present in the system, b = 0 and so curve-fitting can be performed against this equation derived from **(3)**:

(20) $p_S = (1 - (i * (1 - p_C)^C))^Z$

p_c can also be derived from the linear equation

(15) $T_V = -\frac{\log(1-p_c)}{\log g} * C + T_N$

with a value for g. The only way to ensure CTL are the sole mediators of efficacy is by adoptive transfer of CTL; but even this method would give an inaccurate

value due to the high rate of cell death associated with this method. Vaccination with viral-vectored TRAP is usually thought to be mediated chiefly or exclusively by TRAP-specific CTL. On this assumption, **(15)** can be used with time to 1% parasitaemia from TRAP vaccination experiments. But see Chapter 6 for evidence that antibodies against TRAP also mediate protection.

Figure 3.3.6 shows data from two independent experiments by myself and by Karolis Bauza using viral-vectored vivax TRAP vaccination and challenge using the double transgenic Pv210/PvTRAP parasite.

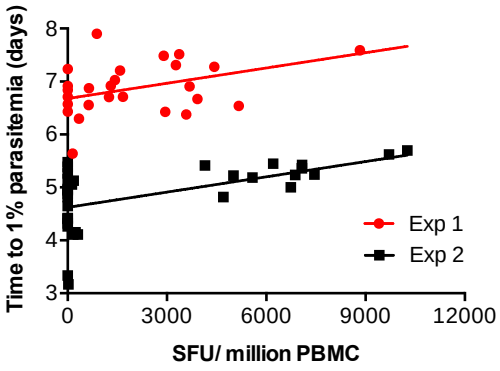


Figure 3.3.6 Estimating probability of protection parameter p_c by linear regression of SFU/million PBMC against time to 1% parasitaemia in two PvTRAP vaccination experiments.

Two sets of female BALB/c mice (n=26, 34) were vaccinated with *P. vivax* TRAP delivered using viral vectors (adenovirus prime and MVA boost, 8 weeks apart). ELISpots were performed using PBMCs obtained from mice 2 weeks following boost immunization. Mice were challenged one week post-boost with either 5000 (experiment 1, red circles) or 2000 (experiment 2, black squares) PvCSP/PvTRAP transgenic *P.* berghei sporozoites. Time to reach 1% blood-stage parasitaemia was obtained by linear regression using daily thin blood smears. Linear regression using Prism and analysis of the slopes returns a pooled slope value of 9.62E-05 ± 2.17E-05, with the probability of the slopes being different of p=0.63. From the equation $T_V = -\frac{\log(1-p_c)}{\log g} * C + T_N$ where T_V = time-to-1% in vaccinated mice, g = blood stage growth rate, C = SFU/million

PBMC, T_N = time-to-1% in naïve mice, and p_C = probability of protection by a unit of C, and using a value of g = 3.5 ± 0.1, a value of p_C = 1.21E-04 ± 2.72E-05 is obtained. Values shown ± SEM. Data in experiment 2 (black squares) comes from Karolis Bauza's DPhil thesis.

The two experiments give identical slopes by analysis in Prism (p=0.63 that there is a difference in the slopes) and from the pooled slope a value of p_c = 1.21E-04 ± 2.72E-05 is obtained, assuming a value of g = 3.5.

3.4 Two experimental tests of the model using data from published literature

In this section it is shown that the model presented in this chapter is consistent with the outcome of two experiments published in existing literature. These are cases where two neutralising monoclonal antibodies are tested in isolation and in combination. In both cases, the mathematical model, suitably adapted, predicts outcomes very close to those obtained.

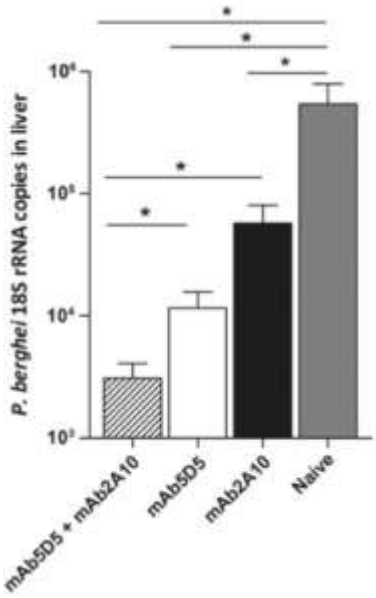
In the first paper (349) two neutralising antimalarial antibodies are combined, one specific for the central repeat region of *P. falciparum* CSP, and the other for a CSP N-terminal domain-specific epitope. Figure 3.4.1 shows these effects of combining these two monoclonal antibodies on 18S rRNA copies of *P. falciparum* CSP-replacement *P. berghei* in mice following challenge. To apply the model to this data further adaptation is required as shown below.

It is assumed that the number of rRNA copies of *P. berghei* is linearly proportional to the number of infected hepatocytes. In that case, equation **(11)** can be adapted thus:

$$\mathbf{(21)}\ \frac{\boldsymbol{L_V}}{\boldsymbol{L_N}} = \frac{\boldsymbol{rRNA_V}}{\boldsymbol{rRNA_N}} = (1 - p_{b1})^{b1} * (1 - p_{b2})^{b2}$$

Comparing the rRNA values in mice treated with one monoclonal ($rRNA_V$) to that of naive mice ($rRNA_N$) provides estimates of p_b for each individual monoclonal, shown in the table in Figure 3.4.1. A prediction of their combination can then be obtained using the same equation by treating the rRNA copy number in mice receiving both monoclonals as the unknown, and all the other variables

as known. The actual and predicted values of rRNA copy number are in close agreement, giving validation to the model.



mAb	rRNA copies	µg mAb	pb
naïve	5.43E+05	-	-
mAb5D5	1.14E+04	25	0.1432
mAb2A10	5.71E+04	100	0.0223

both mAbs	rRNA copes	error
predicted	1.20E+03	3.52E+02
actual	3.08E+03	9.83E+02

Figure 3.4.1 Synergy of neutralising antimalarial monoclonal antibody combination accurately predicted by the probabilistic mathematical model.

Two *P. falciparum* CSP-specific monoclonal antibodies were intravenously injected into C57BL/6 mice (n=5) individually or in combination (mAb5D5: 25 µg; mAb2A10: 100 µg) and challenged with 10,000 PfCSP-replacement *P. berghei* sporozoites. *P. berghei* rRNA copy numbers in each mouse liver were obtained 42 hours later by RT-qPCR. The probability of protection parameter p_b for each antibody and prediction of their combination of was obtained using the equation $\frac{rRNA_V}{rRNA_N} = (1 - p_{b1})^{b1} * (1 - p_{b2})^{b2}$ where $rRNA_V$ and $rRNA_N$ are the rRNA copy numbers in mAb-treated and naïve mice respectively, and b_1 and b_2 the quantity of each of the two antibodies. Errors are given as ± SEM. Data from (349).

The second paper (628) demonstrates increased neutralisation when two monoclonals are combined against a recombinant vesicular-stomatitis virus with Sudan virus glycoprotein (VSV-SUDV) (Fig. 3.4.2 A). Curve-fitting equation **(19)**

to each mAb (m8C4 and FVM09) allows estimates of p_b for each mAb to be obtained. These are then used to obtain a prediction of the neutralisation effected by the combination of both mAbs, shown in Fig. 3.4.2 B. As can be seen, there is again close agreement between the actual and predicted values.

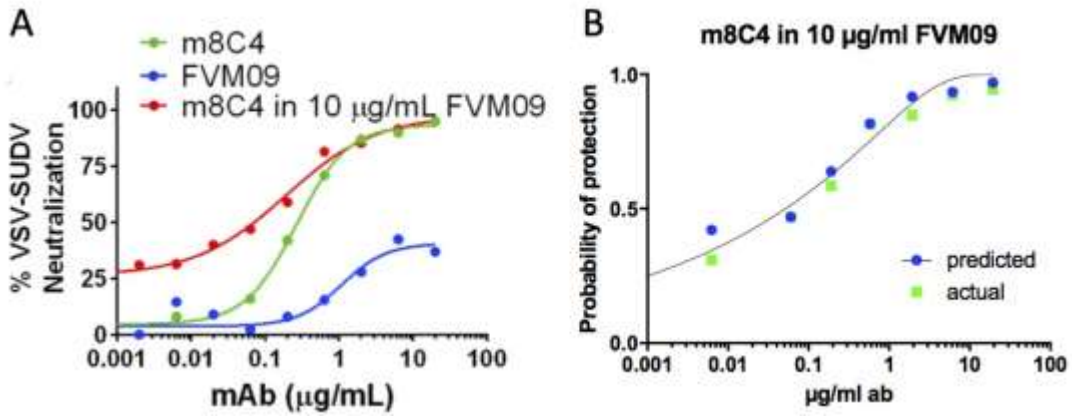


Figure 3.4.2 Accurate prediction of VSV-SUDV neutralising antibody combination.

VSV-SUDV-GP-Luc viruses were incubated with either of two neutralising antibodies m8C4 and FVM09 at various concentrations, and neutralisation measured as a function of luminescence compared to untreated virus. A combination of m8C4 titrated with a fixed concentration of FVM09 (10 µg/ml) was also performed. (A) shows the author's actual results. (B) shows actual and predicted results by curve fitting the original single-antibody curves to the equation $p_S = (1 - ((1 - p_b)^b))^Z$ to obtain values for the probability of protection parameter p_b for each antibody, which then allowed prediction of the combination of both antibodies. p_S is neutralisation; b quantity of monoclonal antibody; and Z is the effective dose of infectious virus. Data from (628).

3.5 Simulations of vaccine combinations and implications for optimal vaccination strategies.

Using the values of g, p_b and p_c obtained in section 3.3 above, we can simulate combinations of CSP and TRAP–containing vaccines. These are the two leading pre-erythrocytic vaccine candidates. If CSP efficacy were chiefly mediated by antibodies, and TRAP efficacy by CTL, combining a TRAP vaccine to a CSP vaccine would be expected to enhance protective efficacy as shown in Figure 3.5.1 below:

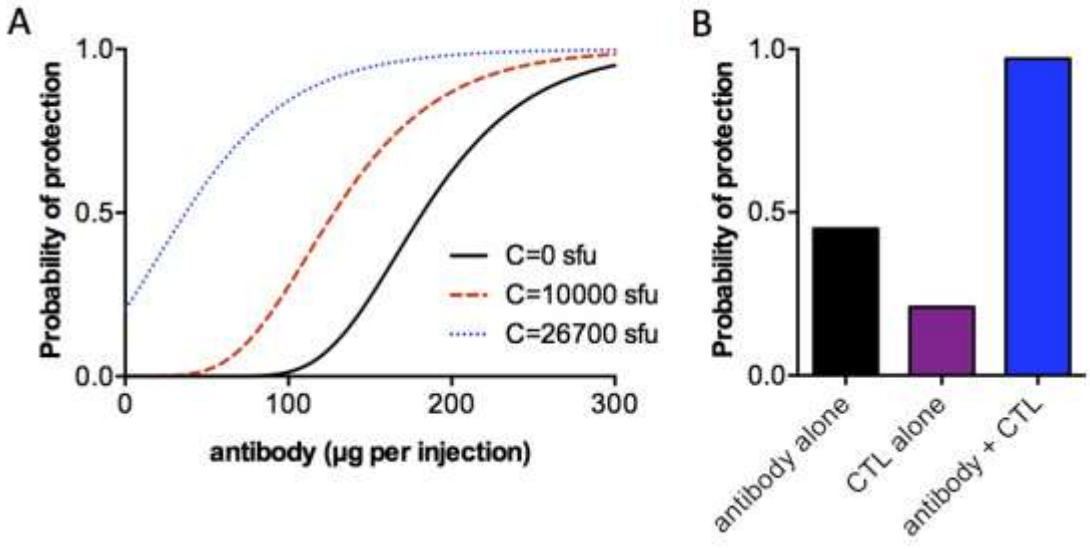


Figure 3.5.1 Simulation showing effects of adding a CTL-mediated vaccine to an antibody-mediated vaccine.

Simulations were performed using the equation $p_S = (1 - (i * (1 - p_b)^b * (1 - p_C)^C))^Z$ where p_S is the probability of sterile protection, i the natural infectivity of sporozoites, p_b and p_C the probability of protection parameters with antibodies b and cytotoxic T-cells C respectively. Using experimentally-derived values of p_b = 0.022 and p_C = 1.21E-04, (A) shows a simulation of the effect of increasing antibody concentration with various fixed concentrations of cytotoxic T-cells. (B) shows that combining an antibody-inducing vaccine of 45% efficacy with a CTL-inducing vaccine of 21% efficacy is predicted to give a protective efficacy of 97%.

Figure 3.5.1B shows that the combination of TRAP and CSP should have a more than additive effect, raising protective efficacy from 21% and 45% for TRAP and CSP to over 97%. Likewise two antibody- or two CTL-inducing vaccines together should have more than additive effects if the model presented here is sound. The combination of vivax TRAP and vivax CSP vaccines is explored in practice in Chapter 4.

The effects of combining antibody-inducing vaccines is investigated in the simulation shown in Figure 3.5.2. With each additional antibody of unique epitope specificity the quantity of each antibody type required to achieve 80% protection is reduced. If the value p_b of each antibody of unique epitope specificity is the same, then the sum of antibody required to achieve a certain level of protection is a constant. Since achieving moderate levels of antibody against each of a wide range of epitope targets is likely to be easier than achieving high levels of antibody against just a single target, the former is an attractive vaccine strategy. This thesis contributes to the development of such a vaccine in Chapters 5 and 6.

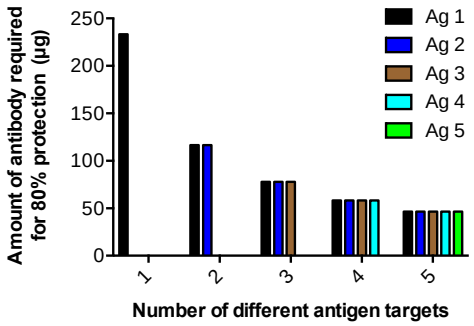


Figure 3.5.2 Simulation showing the average amount of each type of antibody required to achieve 80% protection as the number of antigen targets increases.

The equation $p_S = (1 - (i * (1 - p_b)^{n*b}))^Z$ is used to simulate the effects of combining neutralising antibodies (quantity, (µg), b) of different epitope specificity, assuming each has equal potency (probability of protection parameter p_b identical for all antibodies, using

experimentally derived value for 3D11 mAb of p_b = 0.022), where p_S is the probability of sterile protection, i the natural infectivity of sporozoites, n the number of antibodies of different epitope specificity, and Z the number of sporozoites, using Z = 1000 and i = 0.04. Shown is the quantity of each type of one to five antibodies required to obtain 80% sterile protection.

The previous section (§3.4) suggested that the p_b values of neutralising monoclonal antibodies can be almost an order of magnitude different from one another. Figure 3.5.3 demonstrates that in a conventional challenge experiment with sterile protection as the primary metric of vaccine efficacy, adding mAb2A10 to mAb5D5 would have virtually no measurable impact, with the CSP N-terminal specific mAb5D5 contributing almost all the overall protective efficacy.

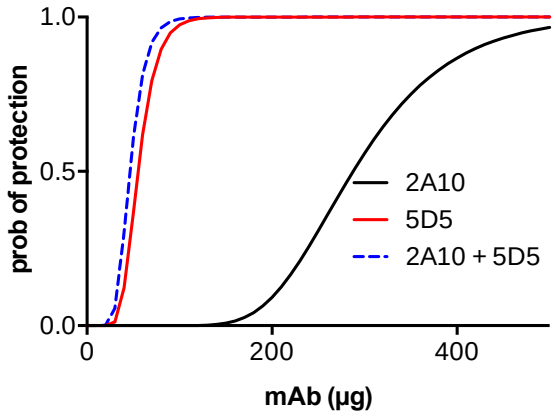


Figure 3.5.3 Simulation: a disparity in the potency of two monoclonal antibodies diminishes returns from their combination.

The equation $p_S = (1 - (i * (1 - p_{b1})^{b1} * (1 - p_{b2})^{b2}))^Z$ is used to simulate the effects of combining two antibodies of widely different potency (probability of protection parameters p_{b1} and p_{b2}, using experimentally derived values for *P. falciparum* CSP-specific monoclonal antibodies 2A10 (b_1; p_{b1} = 0.022) and 5D5 (b_2; p_{b2} = 0.143), where p_S is the probability of sterile protection, i

the natural infectivity of sporozoites, and Z the number of sporozoites, using $Z = 1000$ and $i = 0.04$.

This illustrates another important implication of the mathematical model: vaccine combination strategies will only noticeably result in enhancement of protection if the p_b values of the elicited antibodies are comparable. If one antibody type has a much higher p_b than another, then little or no enhancement of protective efficacy will be achieved by combining them. Ultimately the question of which vaccines to combine will be determined by considerations of cost-effectiveness. In this thesis I am mainly concerned to discover and optimise protection-enhancing combinations of pre-erythrocytic malaria vaccines.

3.6 Implications for basic biology of *P. berghei*

If the equations derived in this chapter accurately describe the dynamics of malaria infection, then they can be used to infer bounds on unknown parameters, namely R (the number of iRBC deriving from each infected hepatocyte), and T_{max} (the maximum time-to-1%, which occurs when only one hepatocyte is successfully infected). In addition, although it varies from experiment to experiment, i (the natural infectivity of sporozoites) can be estimated for the typical experiment, with an average time-to-1% in naïve mice of 6.7 d (T_N = 6.7 d) in experiments where 1000 sporozoites are inoculated (Z = 1000). Because these are average values over many experiments, it is assumed any experimental errors in these values are negligible, and that there is no systematic error. Another parameter, the time it takes parasites to develop in the liver before seeding the blood stage, t_1, is taken from existing literature to be 2.1 d (629). The growth rate g is taken to vary between 3.4 and 3.6 based on data presented in §3.3.1. B, the number of red blood cells in a 22 g BALB/c mouse, is taken from the literature to be 1.23E+10 (607).

On this basis, a minimum value for T_{max} can be obtained from the equation

$$\textbf{(22)}\ T_{max} = t_1 + {\log\left(\frac{B}{(100*R)}\right)}\Big/{\log g}$$

derived from equation **(9)** using L_N = 1 when $T_N = T_{max}$. Using the bounds of $g \leq$ 3.6 and $R \leq$ 1000 (48) places a minimum bound of $T_{max} \geq$ 11.2 d.

A maximum bound on T_{max} is placed by i, the infectivity. The probability that a given sporozoite infects cannot be greater than 1. Using the equation

(23) $T_{max} = T_N + {\log(i * Z)}/{\log g}$

derived from equation **(18)**, using $i \geq 1$ and the lower bound of $g \geq 3.4$ gives a upper bound of $T_{max} \leq 12.3$ d.

R is also bounded by $i \leq 1$. From the equation

(24) $R = \frac{B}{(100 * i * Z * (g^{Tn - t1}))}$

derived from equation **(16)**, and using the upper bound of $g = 3.6$, a lower bound of $R \geq 340$ is obtained.

Finally, a minimum infectivity i for the typical experiment is obtained using the upper bound $R \leq 1000$, using the equation

(25) $i = \frac{B}{(100 * R * Z * (g^{Tn - t1}))}$

likewise derived from **(16)**. This gives a lower bound on infectivity $i \geq 34\%$.

It is difficult to experimentally confirm *in vivo* values for R and i. On the other hand, data is available from the challenge experiments performed in this thesis against which to compare the predicted value of T_{max}. Figure 3.6.1 is a histogram showing the frequency of values of time-to-1% in naïve and vaccinated mice.

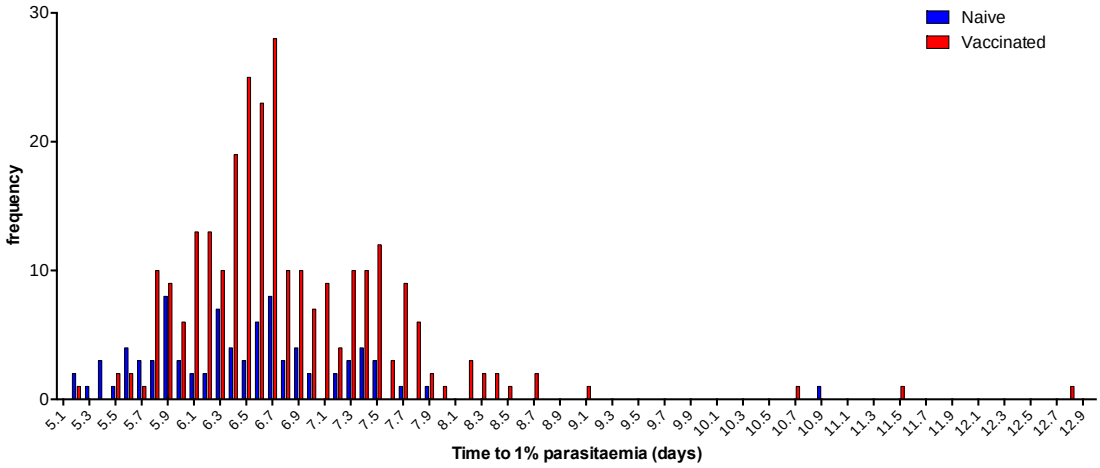


Figure 3.6.1 Histogram of time-to-1% values in naïve and vaccinated mice (BALB/c, 2207 parasite).

Daily blood smears of naïve (n=84, blue bars) and vaccinated (n=269, red bars) mice challenged with varying quantities of sporozoites were used to calculate time to reach 1% blood-stage parasitaemia by linear regression analysis. Shown is the frequency of mice reaching 1% blood stage parasitaemia at each time period (0.1 d intervals) between 5 days and 13 days post-infection.

Two vaccinated mice reach 1% parasitaemia at T = 11.5 and 12.8 d; and one naïve mouse at T = 10.9 d. Given experimental error and some natural variation in R, this data is at least consistent with the value for T_{max} predicted by the above bounding estimates.

Table 3.6.1 summarises the bounds placed on all variables described in this section.

Table 3.6.1: Inferred or actual mean, lower and upper bounds for biological parameters of *P. berghei* infection in BALB/c mice

	lower	mean	upper
t_1		2.1 d	
T_N		6.7 d	
Z		1000 spz	
B		1.23E+10 RBC	
g	3.4	3.5	3.6
T_{max}	11.2		12.3
R	340		1000
i	0.34		1

Discussion

In this chapter a mathematical model of vaccine combination has been derived from simple probabilistic assumptions. It is designed to be of particular use in analysing and interpreting murine pre-erythrocytic malaria vaccine challenge experiments, of which the outcomes for assessment are sterile protection and time to reach 1% blood-stage parasitaemia. The latter is a metric commonly used in laboratories including those at the Jenner Institute (487).

The model was found to fit pre-clinical data well enough to allow estimates of the fundamental parameters p_b and p_c (probabilities that a unit of antibody or cytotoxic T-cells, respectively, prevent successful infection by a given sporozoite) (§3.3.2 and §3.3.3). This in turn allowed simulation of the effect of combining vaccines (§3.5, Fig. 3.5.1). It was predicted that a CSP-like vaccine conferring 45% efficacy and a TRAP-like vaccine conferring 21% efficacy would, assuming no antigenic interference, confer a combined protective efficacy of 97%. This is in very close agreement with another CHMI model (615) which, using the same baseline vaccine parameters, predicted the combination to give an efficacy of 97.5%. In contrast, a Hill-function based model (612) is predicted to give an enhancement from 50% for one antibody-inducing vaccine to only 75% with the addition of an equally efficacious and immunogenic vaccine, with a similar result in (613). The discrepancy between models in the expected increase in efficacy with combinations of vaccines is unlikely to be due to differences in the core dose-response relationship assumed or derived, but rather in the inclusion by Saul *et al.* and White *et al.* of a component in the models accounting for the distribution of antibody responses to vaccination in a population. Including this probably makes the simulations of Saul *et al.* and White *et al.* more

reliable, and hence represents a limitation in the model presented in this chapter. Further work expanding the model to capture variation in antibody levels across a population will help complete the model and securely bridge the gap between pre-clinical and clinical malaria vaccine studies.

All models, however, are in agreement that combining pre-erythrocytic malaria vaccines would markedly enhance protective efficacy (see Fig. 3.5.2, §3.5), and therefore vaccine combination represents an attractive strategy for improving on the low protective efficacy currently seen with the leading malaria vaccine candidate RTS,S/AS01 (379, 380). However, Saul (611) cautions that combining vaccines will only result in enhanced efficacy if they individually have comparable efficacy, a finding repeated in §3.5 (Fig. 3.5.3) using the model presented in this chapter.

A formal comparison between the model presented in this chapter and those presented by White *et al.* (613, 614) and Saul *et al.* (611, 612) (summarised in the introduction to this chapter) reveals that the model in this chapter is not mathematically equivalent to the Hill function- or exponential-based models, and hence is novel. To recapitulate, the two models are:

$$r_{ij} = {}^{1}\Big/_{1 + (\frac{x_{ij}}{\beta_j})^{\alpha}}$$

and

$$r_{ij} = e^{-x_{ij}\log(2)/\beta_j}$$

where x_{ij} is the antibody titre to a specific antigen in a given individual, r_{ij} is the probability that a sporozoite survives the immune response x_{ij}, β_j is the antibody titre which reduces the probability of sporozoite infection by half, and α is the shape parameter of the Hill function. r_{ij} is equivalent to $(1\text{-}p_b)^b$ in terms of this

chapter's model, where b is the antibody titre and so $b = x_{ij}$. When $b = \beta_j$, $r_{ij} = ½ = (1-p_b)^{Bj}$. Hence $(1-p_b) = (½)^{1/Bj}$ and so on the basis of my model, in the terms used by White *et al.,*

$$r_{ij} = (\frac{1}{2})^{x_{ij}/\beta_j}$$

Further work is needed to show whether this probabilistically-derived alternative to the Hill-function and exponential dose-response relationships better fits available data. It does at least possess at least one advantage over the other models, in that it is derived from explicit propositions which can in principle be altered to generate other biologically-grounded models. Hence the approach taken in this chapter to generate a mathematical model of vaccine combination should, with further work, enable basic assumptions about the immunology behind the model to be experimentally tested.

Some experimental data has recently been published which could shed light on the reliability of one of the foundations on which the model is based, from Spencer *et al.* (630). In that study the authors control the number of CSP-specific $CD8^+$ T-cells by adoptive transfer, and the number of sporozoites used to challenge mice by intravenous injection. Thus they are able to alter the effector to target (E:T) ratio *in vivo* at will. The authors show that mice challenged with the same E:T ratio, but greater numbers of both $CD8^+$ T-cells and sporozoites, recruited more liver-resident $CD8^+$ T-cells into division and were better protected against challenge. This contradicts the independence assumption made in §3.1 that the probability p_C that a unit of cytotoxic T-cells has a fixed probability of preventing successful infection; instead, p_C may be a function of the number of sporozoites inoculated. This would have the consequence of the

model underestimating the efficacy of $CD8^+$ T-cell vaccines at high challenge doses. Whether the finding that high sporozoite doses are relatively easier to protect against will be relevant to CHMI and field conditions, where smaller sporozoite inocula are the norm, remains to be seen.

The value for the growth rate, *g,* obtained in this chapter (§3.3.1) should be reliable within the context of the model, since it is derived by curve fitting to that model. However, it will not necessarily agree with other calculated values. Published values for the blood stage growth rate vary widely, from 8.5 – 10.4 (631), 10 (632), 6.5 – 7.5 (633), 4.7 – 6.2 (634) to 4.2 (635). Thus my estimate, 3.5, is at the lower range of the spectrum. There could be various reasons for this. Blood stage growth rate appears to decrease with increasing parasite density (631); sequestration has also been proposed to affect calculations of values for the blood stage growth rate (635). In *P. falciparum* it has been shown that the parasite multiplication rate *in vitro* varies between strains of parasite (636), so it is possible that it may vary between clones of *P. berghei* also, although in this chapter no difference between three transgenic clones and wild-type *P. berghei* was found (§3.3.1).

The value for *g* used in this thesis is the correct one to use in the context of the model, but inaccuracy in that value would affect estimates of the values of other biological parameters derived in §3.6. Sequestration, the most likely reason for a discrepancy between my value and other published values of *g*, would cause the values for *R* (the number of iRBC deriving from each infected hepatocyte) and T_{max} (the maximum time-to-1%, which occurs when only one hepatocyte is successfully infected) to be underestimated. Thus these values are presented in this chapter primarily to demonstrate in principle that such

unknown values can be obtained the model I have presented. Nevertheless, there is reason to believe that the values estimated for *R,* T_{max} and *i* (the infectivity of sporozoites in naïve mice) are of approximately the correct magnitude. In the all the experiments I have performed during this thesis, the maximum time to 1% parasitaemia values have been quite close to that of the predicted value for T_{max}, 11 – 12 days (Fig 3.5.3). Furthermore, a high value for *g* is incompatible with high infectivity, and a low infectivity is incompatible with, for instance, a dose of 150 sporozoites per mouse giving 100% infection in 18 mice, as was the case in an experiment presented in §4.5 below, so the low value of *g* and the high value of *i* I give are at least consistent with my own experimental results. Published data on sporozoite infectivity to mouse livers *in vivo* has traditionally put the value quite low: 0.02% for BALB/c and 8.2% for C57BL/6 mice (637), and 3.8% for A/J mice (638). These estimates were later criticised for making inaccurate assumptions about the size and shape of infected hepatocytes, and a revised infectivity of 1% – 1.6% for C57BL/6 mice was calculated (639). All these estimates for infectivity are much lower, however, than my own minimum bound on infectivity of 34% in BALB/c mice. Two things may explain this. The first is that the above estimates assume a random distribution of infected hepatocytes through the liver, whereas sporozoites tend to infect hepatocytes around portal venules (640, 641). Secondly, improved salivary gland dissection techniques, particularly the use of Schneider's media lacking activating bicarbonates which increase sporozoite death (642), may have resulted in greater infectivity of sporozoites than obtained historically. Indeed, a paper cited above from 1994 obtains blood-stage infections in 0/5 and 2/5 BALB/c mice injected with 500 and 5000 sporozoites respectively (637). As mentioned above, in one

experiment 18/18 BALB/c mice were infected with 150 sporozoites, and in all my thesis over 300 naïve BALB/c mice have been injected with 1000 sporozoites per dose; all but one have developed blood-stage parasitaemia in consequence. Thus the infectivity of 34% I derive may be plausible, but how accurate it is remains to be seen, given the caveats outlined above.

In summary, a novel mathematical model based on simple probabilistic assumptions has been developed in this chapter. It expresses either probability of sterile protection, or time to reach 1% blood-stage parasitaemia, as a function of antibody or cytotoxic T cell frequencies, and is validated by application to previously published data. The model represents a theoretical advance on previous work which does not derive a dose-response relationship from basic biological assumptions. Moreover, it demonstrates that malaria vaccine combinations should, if antigenic interference can be avoided, markedly enhance efficacy compared to either component alone. The rest of this thesis attempts to turn theory into practice.

Chapter 4

Combining CSP virus-like particles with viral-vectored TRAP: immunogenicity and protective efficacy

Introduction

The need for a *P. vivax* vaccine is pressing, with over 8 million cases in 2015 (1). The leading malaria vaccine, RTS,S, is designed to protect only against *P. falciparum* (188). The leading *P. vivax* vaccine, VMP001, shows little protective efficacy against controlled human malaria infection (453). The disease is difficult to treat, because of relapse infections from dormant liver-stage hypnozoites (54, 58), and because the only available drug to remove hypnozoites, primaquine, causes haemolysis in individuals with glucose-6-phosphate dehydrogenase deficiency, a common condition (643). An effective pre-erythrocytic vaccine against *P. vivax* would have the potential to prevent the morbidity and mortality associated with blood-stage infection, interrupt transmission, and prevent hypnozoite formation. This chapter investigates two methods of improving existing *P. vivax* pre-erythrocytic vaccines: firstly, by combining them, and secondly with adjuvants, including genetic adjuvants.

Rv21, a virus-like particle based on the Hepatitis B surface antigen and displaying a hybrid PvCSP on its surface, has been developed in this lab. Rv21 confers high levels of sterile protection against challenges either with PvCSP-VK210 or PvCSP-VK247 replacement *P. berghei* transgenic parasites (190). Viral vectored PvTRAP has likewise shown good efficacy against PvTRAP replacement *P. berghei* challenge, though not to the same high level as Rv21 (497). These two

proteins, PvCSP and PvTRAP, are the leading *P. vivax* pre-erythrocytic antigens. The theoretical model presented in Chapter Three predicts that combining these vaccines, in the absence of antigenic interference, should result in a very sizeable improvement in protective efficacy over either vaccine alone. Given that similar combinations of PbCSP and PbTRAP (475, 566) and PfCSP and PbTRAP (189) in mice have produced this expected improvement, the same could be anticipated with *P. vivax* CSP and TRAP. That is, as long as there is no antigenic interference. One clinical trial has found antigenic interference between PfCSP and PfTRAP resulting in poor protective efficacy (565), so this could also happen with the equivalent *P. vivax* antigens. For this reason, and because adjuvants were previously either unused or not compared to others with PvTRAP (497) and Rv21 (190), various adjuvants are tested with the combination Rv21 and PvTRAP vaccines, to see if and when antigenic interference might occur. Genetic adjuvants, also previously untested with PvCSP or PvTRAP antigens, are investigated.

In this chapter, antigenic interference is found to occur with Matrix M but not AddaVax or alum adjuvants, with both Rv21 and Qβ-PvCSP when combined with viral-vectored PvTRAP; further more, the same patterns of antigenic interference occurs in two different strains of mouse. AddaVax, Matrix M and Alum appear to be equally potent adjuvants of anti-CSP titres with PvCSP virus-like particles, but the only adjuvant to have any noticeable effect on PvTRAP-specific immunogenicity is Matrix M, and then only with C57BL/6 mice and not BALB/c mice. An initial very high challenge demonstrates that Rv21 can confer very high efficacy compared to little or none from PvTRAP, so the vaccines are titred such that each provides sub-optimal protection alone; 100% protection is

obtained when both are combined, supporting the prediction of Chapter Three. Two genetic adjuvants, IMX313 (266) with PvCSP, and the invariant chain (Ii) (271, 272) with PvTRAP, show improvements in anti-PvCSP titres and PvTRAP-specific $CD8^+$ T-cells respectively. Intravenous boosting with viral vectors, shown to enhance protective efficacy with other pre-erythrocytic antigens in the Jenner (Adrian Hill, personal communication) is here not found to improve protection. Finally, some initial results from a study comparing Rv21 with a CSVS-like (455) VLP suggest that Rv21 may produce a higher quality and quantity of anti-CSP antibody response.

This is the first time an enhancement of protective efficacy with PvCSP and PvTRAP is demonstrated, and the first study to show that antigenic interference can be avoided by using a different adjuvant. In addition, the challenge experiments use a novel double-transgenic *P. berghei* parasite, with PvTRAP and PvCSP-VK210 replacing the endogenous sequences without affecting infectivity of the sporozoite.

Results

4.1 The effects on immunogenicity of combining Ad-MVA PvTRAP with PvCSP virus-like particles, with various adjuvants.

Two virus-like particles (VLPs) were used as carriers for a chimeric PvCSP containing nonamer repeat motifs from both the two major allelic variants VK210 and VK247 (see Chapter 2 for more details). Rv21 is a fusion protein delivered as a hepatitis B surface antigen-based (VLP). Qβ-CSP is a VLP derived from the Qβ bacteriophage to which chimeric CSP is chemically coupled.

PvTRAP was delivered using adenovirus and MVA in a prime-boost regime, previously shown to be optimal for generating high levels of TRAP-specific cytotoxic T-cells.

Adjuvants have the potential to enhance or alter immunogenicity, so three different adjuvants were used in combination with PvCSP and/or PvTRAP, in two different mouse strains, as shown in Table 4.1.1

Table 4.1.1 Vaccination regimes for each experiment in §4.1

	Prime			Boost			Prime-boost
Experiment	CSP-VLP (μg)	Ad-TRAP (iu)	Adjuvant	CSP-VLP (μg)	MVA-TRAP (pfu)	Adjuvant (μL)	interval (weeks)
BALB/c, Rv21 ± Ad-M TRAP							
Rv21 + Ad-M TRAP	1.5	$1x10^8$	-	1.5	$1x10^7$	-	8
Rv21	1.5	-	-	1.5	-	-	8
Ad-M TRAP	-	$1x10^8$	-	-	$1x10^7$	-	8
Rv21 + Ad-M TRAP + Add	1.5	$1x10^8$	Addavax, 25 μL	1.5	$1x10^7$	Addavax, 25 μL	8
Rv21 + Add	1.5	-	Addavax, 25 μL	1.5	-	Addavax, 25 μL	8
Ad-M TRAP + Add	-	$1x10^8$	Addavax, 25 μL	-	$1x10^7$	Addavax, 25 μL	8
Rv21 + Ad-M TRAP + MM	1.5	$1x10^8$	Matrix M, 12 μg	1.5	$1x10^7$	Matrix M, 12 μg	8
Rv21 + MM	1.5	-	Matrix M, 12 μg	1.5	-	Matrix M, 12 μg	8
Ad-M TRAP + MM	-	$1x10^8$	Matrix M, 12 μg	-	$1x10^7$	Matrix M, 12 μg	8
C57BL/6, Rv21 ± Ad-M TRAP low dose							
Rv21 + Ad-M TRAP	0.5	$0.6x10^8$	-	0.5	$0.6x10^7$	-	1
Rv21	0.5	-	-	0.5	-	-	1
Ad-M TRAP	-	$0.6x10^8$	-	-	$0.6x10^7$	-	1
Rv21 + Ad-M TRAP + MM	0.5	$0.6x10^8$	Matrix M, 12 μg	0.5	$0.6x10^7$	Matrix M, 12 μg	1
Rv21 + MM	0.5	-	Matrix M, 12 μg	0.5	-	Matrix M, 12 μg	1
Ad-M TRAP + MM	-	$0.6x10^8$	Matrix M, 12 μg	-	$0.6x10^7$	Matrix M, 12 μg	1
C57BL/6, Rv21 ± Ad-M TRAP high dose							
Rv21 + Ad-M TRAP	5	$1x10^8$	-	5	$1x10^7$	-	1
Rv21	5	-	-	5	-	-	1
Ad-M TRAP	-	$1x10^8$	-	-	$1x10^7$	-	1
Rv21 + Ad-M TRAP + MM	5	$1x10^8$	Matrix M, 12 μg	5	$1x10^7$	Matrix M, 12 μg	1
Rv21 + MM	5	-	Matrix M, 12 μg	5	-	Matrix M, 12 μg	1
Ad-M TRAP + MM	-	$1x10^8$	Matrix M, 12 μg	-	$1x10^7$	Matrix M, 12 μg	1
BALB/c, Qβ-CSP ± Ad-M TRAP							
Rv21 + Ad-M TRAP	8	$1x10^8$	-	8	$1x10^7$	-	8
Rv21	8	-	-	8	-	-	8
Ad-M TRAP	-	$1x10^8$	-	-	$1x10^7$	-	8
Rv21 + Ad-M TRAP + Add	8	$1x10^8$	Addavax, 25 μL	8	$1x10^7$	Addavax, 25 μL	8
Rv21 + Add	8	-	Addavax, 25 μL	8	-	Addavax, 25 μL	8
Ad-M TRAP + Add	-	$1x10^8$	Addavax, 25 μL	-	$1x10^7$	Addavax, 25 μL	8
Rv21 + Ad-M TRAP + MM	8	$1x10^8$	Matrix M, 12 μg	8	$1x10^7$	Matrix M, 12 μg	8
Rv21 + MM	8	-	Matrix M, 12 μg	8	-	Matrix M, 12 μg	8
Ad-M TRAP + MM	-	$1x10^8$	Matrix M, 12 μg	-	$1x10^7$	Matrix M, 12 μg	8

4.1.1 Effect of vaccine combination on PvCSP-specific immunogenicity

Viral-vectored TRAP has an adjuvant effect on anti-CSP titres. This is found with both C57BL/6 and BALB/c mice, and using both Rv21 and Qβ-CSP, and for both allelic variants of PvCSP, VK210 and VK247 (Fig. 4.1.1 A, F). The adjuvant effect of PvTRAP-encoding viral vectors occurs when using Addavax or Alum as an adjuvant, but not when using Matrix M. When Matrix M is used, a diminution of the anti-PvCSP titre when PvTRAP viral vectors are co-administered is seen relative to that elicited by Rv21 or Qβ-CSP used alone (and indeed, when PvCSP

soluble protein is used alone or with PvTRAP viral vectors) (Fig. 4.1.1 A, F). The adjuvanting properties of PvTRAP viral vectors on PvCSP VLPs is seen after adenoviral priming as well as after MVA boosting (though to a lesser extent with Addavax than with no adjuvant); similarly, antigenic interference from PvTRAP viral vectors with Matrix M is seen both after adenoviral prime and after MVA boost (Fig. 4.1.1 C, D). Long term kinetic profiles up to 280 days after Rv21 priming in BALB/c mice reveals that adjuvant effect on anti-PvCSP titres from PvTRAP viral vectors is maintained long-term (Fig. 4.1.1 C) When adjuvants are used, however, any differences in anti-PvCSP titre from PvTRAP viral vectors, whether positive or negative, diminish and disappear by day 180 (Fig. 4.1.1 C). Titres are maintained to a high level in Rv21-vaccinated BALB/c mice up to day 280 post-priming, falling by less than an order of magnitude from peak values (Fig. 4.1.1 C).

Viral-vectored PvTRAP has no discernable effect on affinity of anti-PvCSP-210 antibodies as measured (avidity index, Fig. 4.1.1 B). IgG subclass profiles are broadly similar between groups of Rv21-vaccinated mice (Fig. 4.1.1 E). However, viral vectors have a noticeable influence on IgG2a/IgG1 ratios, with the addition of viral-vectored TRAP skewing the ratio in favour of IgG2a (Fig. 4.1.1 E).

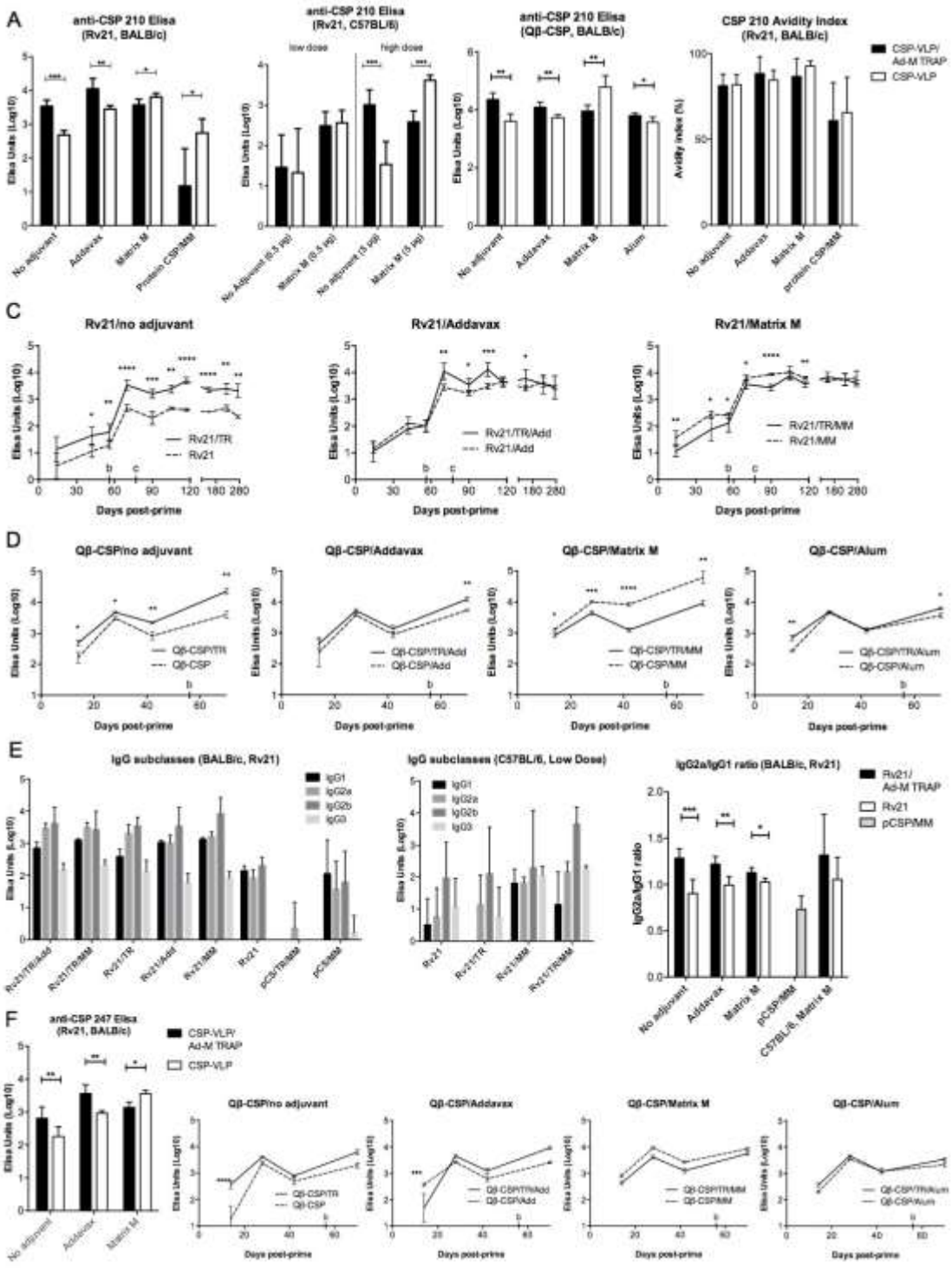


Fig. 4.1.1 Effects on PvCSP immunogenicity of adjuvants and viral-vectored TRAP on two PvCSP virus-like particles.

A hepatitis-B surface antigen-based VLP (Rv21) and a Qβ VLP both presenting *P. vivax* CSP, or protein CSP unconjugated to a VLP, were used to vaccinate two strains of mouse by intramuscular injection: BALB/c mice (n=6 per group, 2 shots, 8 week prime-boost interval; Rv21: 1.5 μg per dose; Qβ-CSP 8 μg per dose) or C57BL/6 mice (Rv21, n=6 per group, 2 shots, 1

week prime-boost interval; “Low Dose”: 0.5 μg per shot; “High Dose”: 5 μg per shot). CSP-VLPs were mixed and simultaneously co-injected with viral-vectored adenovirus-prime, MVA-boost *P. vivax* TRAP, and/or the adjuvants Addavax, Matrix M, or alum (alhydrogel). (A) anti-PvCSP-210 ELISAs. (B) PvCSP-210 avidity index, obtained as a ratio of 7M urea-treated to untreated ELISA units. (C) PvCSP-210 antibody kinetics in Rv21/BALB/c mice. (D) PvCSP-210 antibody kinetics in Qβ-CSP/BALB/c mice. (E) PvCSP-210 IgG subclasses and IgG2a/IgG1 ratio. (F) anti-PvCSP-247 ELISAs and antibody kinetics. “b” and “c” on kinetics graphs represent boost and challenge time-points respectively. ELISAs performed using standard curves. All ELISAs from sera collected two weeks post-boost unless otherwise stated. Means are shown ± SD. Statistical analysis: ANOVA with Tukey’s multiple comparisons post-test. * $p<0.05$; ** $p<0.01$; *** $p<0.001$; **** $p<0.0001$. Thanks to Eduardo Montoya for C57BL/6 “High Dose” data.

4.1.2 Effect of vaccine combination on TRAP immunogenicity

Rv21 sometimes appears to act as a T-cell adjuvant when co-administered with viral-vectored PvTRAP. TRAP-specific $CD8^+$ T-cell responses, as measured by ELISpot, are significantly higher with Rv21 than without it in the presence of Matrix M (BALB/c, $p<0.01$; C57BL/6 “High Dose,” $p<0.01$) and without adjuvant (C57BL/6 high dose, $p<0.01$). The effect is not seen when using Addavax. Protein CSP also appears to adjuvant TRAP-specific $CD8^+$ T-cell responses when combined with Matrix M (BALB/c, $p<0.01$).

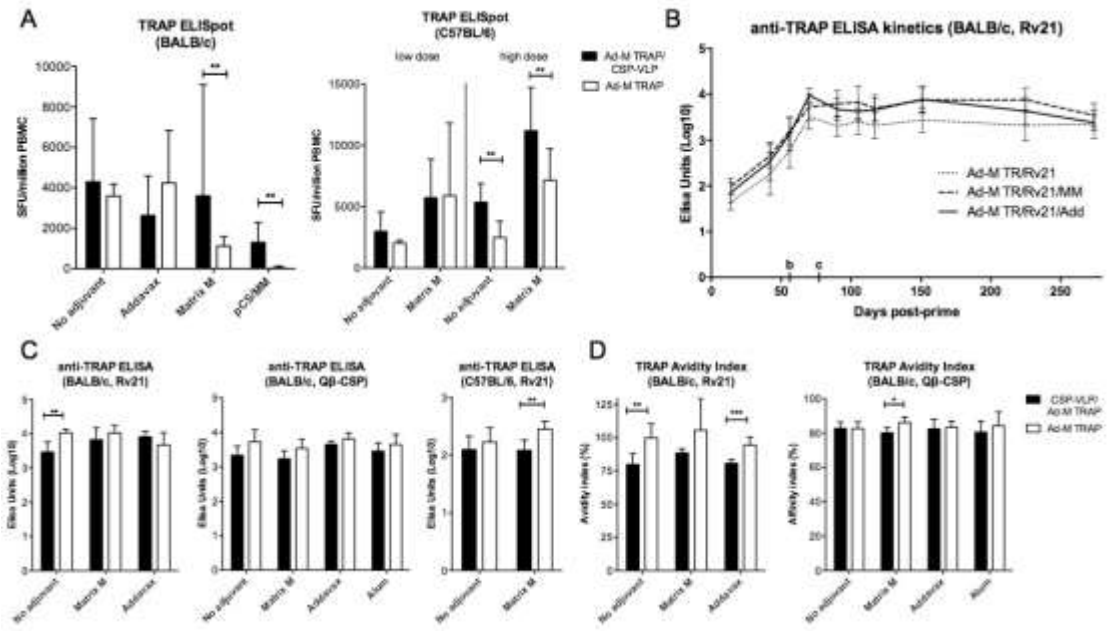


Fig. 4.1.2 Effects on viral-vectored PvTRAP immunogenicity following combination with PvCSP virus-like particles and/or adjuvants.

Viral-vectored PvTRAP (adenovirus (Ad) prime, MVA boost) was administered intramuscularly to BALB/c mice (n=6 per group; 10^8 infectious units Ad, 10^7 plaque-forming units MVA, 8 week prime-boost interval) or C57BL/6 mice (n=6 per group; "High Dose": as for BALB/c; "Low Dose": 0.6x high dose; 1 week prime-boost interval). PvTRAP vectors were administered alone or in combination with PvCSP virus-like particles (Rv21, Qβ-CSP) or PvCSP recombinant protein ("pCS"), and/or with adjuvants Addavax, Matrix M, or alum (alhydrogel). (A) PvTRAP-specific T-cell responses by ELISpot using mouse-strain specific $CD8^+$ T-cell epitopes. (B) anti-PvTRAP ELISA kinetics in PvTRAP + Rv21 groups. (C) anti-PvTRAP ELISA responses two weeks post-boost. (D) anti-PvTRAP antibody avidity index, obtained as a ratio of 7M urea-treated to untreated ELISA units. "b" and "c" on kinetics graphs represent boost and challenge time-points respectively. ELISAs performed using standard curves. Means are shown ± SD. Statistical analysis: ANOVA with Tukey's multiple comparisons post-test. * $p<0.05$; ** $p<0.01$. Thanks to Eduardo Montoya for C57BL/6 "High Dose" data.

As with PvCSP responses, PvTRAP antibody titres are maintained at a high level for up to 280 days post-boost (Fig. 4.1.2 B), with a 5- to 10-fold

reduction in titres from peak. Addition of either Rv21 or Qβ-CSP appears to diminish anti-TRAP titres and affinity, although this effect is only occasionally statistically significant (titres: BALB/c, Rv21 without adjuvant, and C57BL/6, Rv21 with Matrix M, $p<0.01$ in both cases; avidity index: BALB/c, Rv21, without adjuvant $p<0.01$, with Addavax $p<0.001$, and BALB/c with Qβ-CSP and Matrix M, $p<0.05$) (Fig. 4.1.2 C, D).

4.1.3 Protective efficacy of super-optimal Rv21 ± Ad-MVA PvTRAP regimes

Rv21- and PvTRAP-vaccinated mice were challenged to assess protective efficacy (Fig. 4.1.3). Only Rv21-vaccinated groups, whether with or without co-administration of PvTRAP, showed convincing evidence of protective efficacy, with 100% sterile protection being achieved in most cases regardless of mouse strain (Fig. 4.1.3 A, C; low doses of Rv21 (0.5 μg) in C57BL/6 mice showed a delay in time-to-1% only, no sterile protection: Fig. 4.1.3 B).

There is a trend for improved protective efficacy when combining PvTRAP with Rv21; but it cannot be inferred that this is due to PvTRAP-specific immunity assisting Rv21-elicited immunity, for three reasons. First, PvTRAP viral vectors adjuvant anti-PvCSP titres, and so the apparent increase in protective efficacy seen with Rv21+TRAP may be mediated solely by an increased quantity of PvCSP-specific antibodies. Secondly, in many cases the Rv21-only regime conferred very high levels of protection, up to 100%, making an improvement in efficacy with PvTRAP co-administration hard to detect. Thirdly, PvTRAP-only vaccination conferred barely any protection against challenge, most likely because the strength of the challenge was too high (a high challenge dose was chosen because Rv21 had previously shown very high levels

of protective efficacy). An ideal test of whether combining Rv21 and PvTRAP improved efficacy would come from an experiment where the adjuvant effects of viral vectors were controlled for, where Rv21 dose was reduced to give suboptimal protection, and where the challenge dose was reduced to allow PvTRAP-specific immune responses an opportunity of contributing to protection. This experiment was performed and described in the next section.

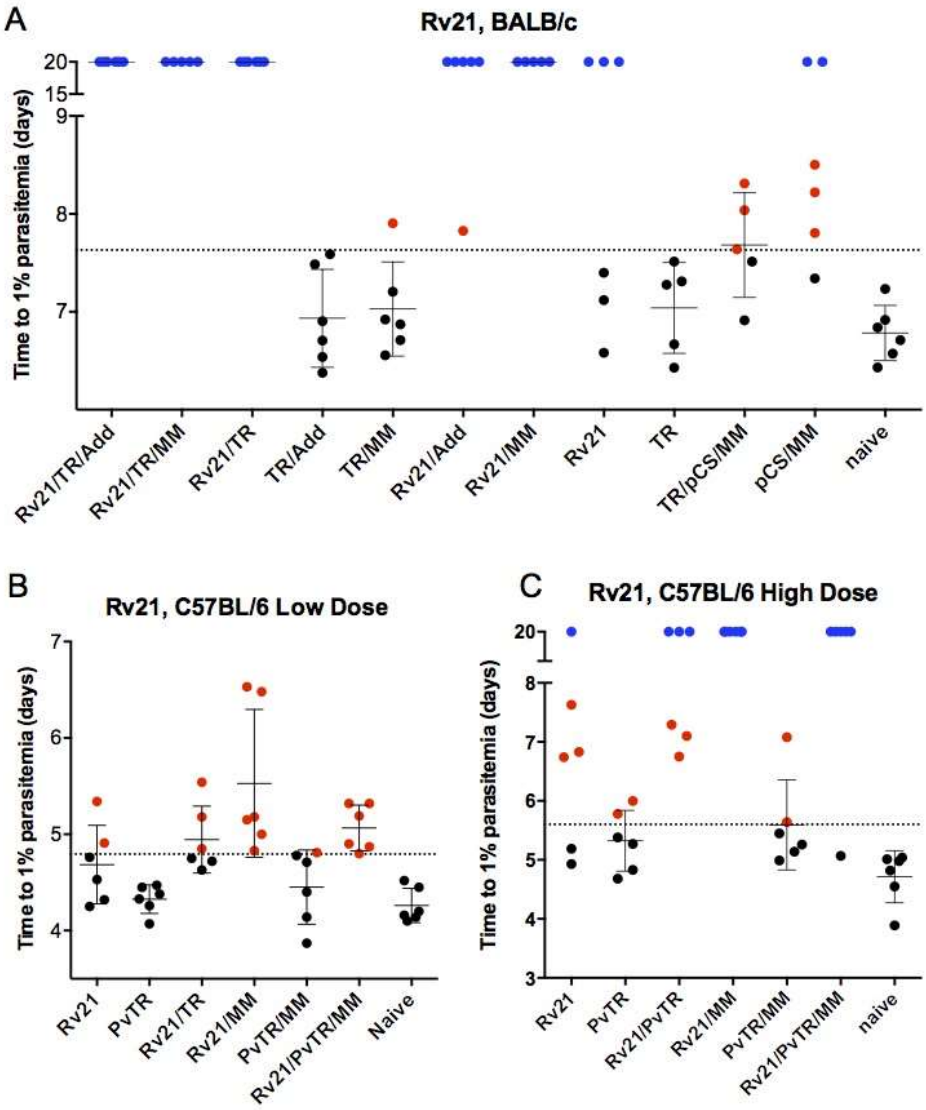


Fig 4.1.3. Protective efficacy of Rv21- and/or Ad-MVA PvTRAP-vaccinated mice

BALB/c (A) or C57BL/6 (B, C) mice (n=6 per group) were vaccinated by intramuscular injection with Rv21 with or without co-administration of Ad-MVA PvTRAP and/or adjuvants Addavax or

Matrix M. Three weeks post-boost mice were challenged by intravenous injection of PvCSP-210/PvTRAP transgenic parasites using (A) 5000 sporozoites or (B) 3500 sporozoites and 5000 sporozoites for “Low Dose” and “High Dose” groups respectively. Time to reach 1% parasitaemia was calculated by linear regression from daily thin blood smears. Shown are means ± SD. Lines represent two standard deviations above the mean time-to-1% in naïve mice; mice with time-to-1% above this value are classed as ‘delayed’ and coloured red. Mice without blood-stage parasitaemia by day 15 are coloured blue and classed as cases of sterile protection. Thanks to Eduardo Montoya for C57BL/6 “High Dose” data.

4.2 Suboptimal Rv21 and PvTRAP combination enhances protective efficacy

As described in the previous section, the ideal experimental test of whether combining Rv21 and PvTRAP enhances protective efficacy is to contrive a state where single- and double-component vaccine regimes both elicit identical PvCSP- and PvTRAP-specific immune responses, and where both single-component vaccine regimes confer partial but not total protection.

To achieve this, BALB/c mice were vaccinated as detailed in Fig. 4.2.1 A. Because Rv21 was sometimes found to adjuvant PvTRAP-specific $CD8^+$ T-cell responses (Fig. 4.1.2), in order to compensate for this a *P. falciparum* CSP VLP, R21, was combined with the viral-vectored TRAP regime, and equivalent TRAP-specific titres were obtained between TRAP- and Rv21/TRAP-vaccinated groups (Fig. 4.2.1 B, C). Similarly, since PvTRAP viral vectors were previously found to boost Rv21-elicited anti-PvCSP titres (Fig. 4.1.1), viral vectors encoding a *Trypanosoma cruzi* antigen were co-administered with Rv21 to control for this adjuvanting effect. Anti-PvCSP titres were successfully made equivalent between Rv21- and Rv21/TRAP-vaccinated groups (Fig. 4.2.1 B). Thus any improvement in protective efficacy could only be attributed to both PvCSP- and PvTRAP-specific immunity acting together.

Challenge with PvCSP/PvTRAP transgenic *P. berghei* sporozoites saw the single-component vaccine regimes confer partial protection: 50% sterile protection in the case of Rv21-vaccinated mice, and a delay in time-to-1% in the case of TRAP-vaccinated mice. Combining Rv21 and TRAP enhanced sterile protection to 100% (Fig. 4.2.1 D).

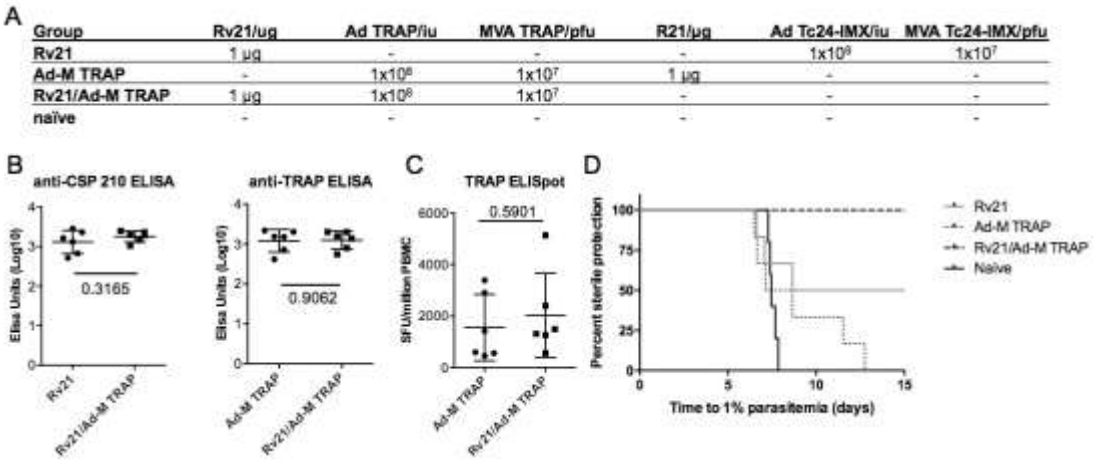


Fig. 4.2.1 Suboptimal Rv21 and PvTRAP combination enhances protective efficacy.

BALB/c mice (n=6 per group) were vaccinated with Rv21 and/or adenovirus-prime MVA-boost viral vectored PvTRAP as shown in the table (A), with a one week prime-boost interval. (B) ELISAs demonstrating equivalent PvCSP- or PvTRAP-specific antibody titres between Rv21- or PvTRAP- and Rv21/PvTRAP-vaccinated groups (by standard curve ELISA). (C) PvTRAP-specific ELISpot using $CD8^+$ TRAP peptide stimulation demonstrating equivalent $CD8^+$ T-cell response between PvTRAP- and Rv21/PvTRAP-vaccinated groups. (D) Mice were challenged 3 weeks post-boost by intravenous injection of 1000 PvCSP/PvTRAP transgenic *P. berghei* sporozoites. Daily thin blood smears were used to determine time to reach 1% blood-stage parasitaemia by linear regression. Mice reaching 15 days without blood-stage parasitaemia were considered to have sterile protection. P-values are shown from unpaired t-tests. Means are given ± SD. Controls used in vaccination: R21 is a hepatitis B surface antigen based virus-like particle presenting *P. falciparum* CSP. Tc24-IMX, a *Trypanosoma cruzi* antigen, was used as control viral vector vaccinations.

4.3 Effects on immunogenicity of genetic adjuvants with viral vectors encoding PvCSP and PvTRAP

The genetic adjuvants IMX and the invariant chain (Ii) have been shown to adjuvant antibody and $CD8^+$ T-cells respectively with various antigens. To examine their potential with PvCSP and PvTRAP viral vectors encoding these antigens with or without IMX and/or Ii were produced and used to vaccinate mice as shown in Fig. 4.3.1.

Adenoviral-vectored PvCSP-IMX showed significantly higher anti-PvCSP titres compared to Ad-PvCSP at every time point post-prime, with up to an order of magnitude difference between the vaccines (Fig 4.3.1 A). The titres between the groups drew closer over time and by 2 weeks post-boost with MVA there was no significant difference between them. A challenge with PvCSP/PvTRAP transgenic *P. berghei* sporozoites gave no evidence of protective efficacy by any group, consistent with the relatively low anti-PvCSP titres generated by these viral vectors (Fig. 4.3.1 A).

Both IMX ($p=0.028$) and IMX-Ii ($p=0.0025$) fused to PvTRAP augmented PvTRAP-specific ELISpot responses compared to PvTRAP alone, post-boost with MVA. In contrast, after prime with adenoviral vectors encoding these antigens, Ad-PvTRAP-IMX-Ii gave significantly higher ELISpot responses than Ad-PvTRAP-Ii ($p=0.021$), and there was no significant difference between Ad-PvTRAP-Ii and Ad-PvTRAP ($p>0.9999$).

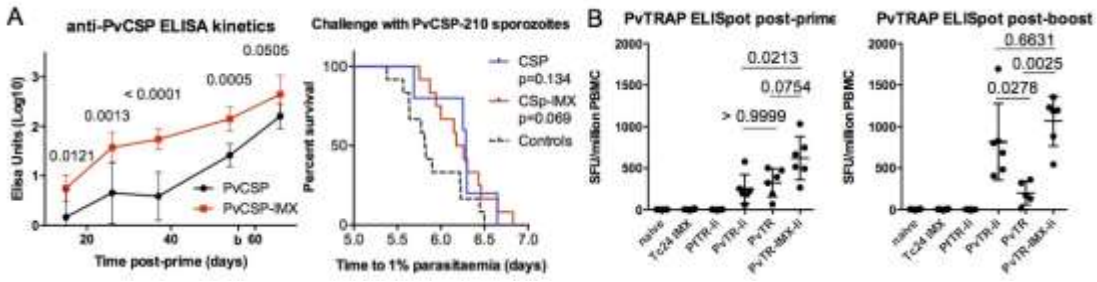


Fig. 4.3.1 Effects on immunogenicity and protective efficacy of genetic adjuvants with viral-vectored PvCSP and PvTRAP

(A) C57BL/6 mice (n=6 to 12 per group) were vaccinated by intramuscular injection of viral-vectored PvCSP or PvCSP-IMX; the heptamer-forming IMX moiety was genetically fused to PvCSP (adenovirus prime with an MVA boost eight weeks post-prime, indicated by 'b' on the ELISA graph). Control groups included naïve animals (unvaccinated) and vaccinated with viral-vectored *Trypanosoma cruzi* antigen Tc24 fused to IMX. Sera was taken every two weeks and standard curve ELISAs performed to determine PvCSP-210-specific antibody responses. Numbers above each time point represent t-tests between groups at that time point. A challenge was performed by intravenous injection of 1000 PvCSP/PvTRAP transgenic *P. berghei* sporozoites three weeks post-boost and time to 1% blood-stage parasitaemia determined by linear regression from thin blood smears taken daily. p-values are from log-rank tests compared to control. (B) C57BL/6 mice (n=6 per group) were vaccinated as in (A) but with viral-vectored PvTRAP or PvTRAP-Ii with the invariant chain (Ii) genetically fused to PvTRAP (PvTR-Ii), or both Ii and IMX fused to PvTRAP (PvTR-IMX-Ii). Control groups using vectors encoding Tc24-IMX or PfTRAP-Ii were included. IFNγ ELISpots were performed on PBMCs freshly isolated from blood taken two weeks post-vaccination, using a $CD8^+$ PvTRAP peptide for stimulation. Numbers represent p-values between groups from ANOVA with Bonferroni's multiple comparisons test.

4.4 Effects on immunogenicity and protective efficacy of intravenous administration of viral-vectored PvTRAP

Intramuscular vaccination followed by intravenous vaccination of *P. falciparum* liver-stage antigens has been shown to enhance protective efficacy. The mechanism appears to be a 'pulling' effect, whereby intravenous boosting with adenovirus, which localizes to the liver, draws circulating $CD8^+$ cells to that location, increasing the probability that they will locate and destroy infected hepatocytes.

These findings were not replicated with *P. vivax* TRAP, in the two experiments shown in Fig. 4.4.1. The immunogenicity, by PvTRAP-specific ELISpot, of adenovirus intramuscular (i.m.) prime, adenovirus intravenous (i.v.) boost is not significantly higher than the conventional adenovirus/MVA i.m. prime boost regime, nor higher than an adenovirus i.m homologous prime boost regime (Fig. 4.3.1 A). This was expected, given that the ELISpot was performed using circulating PBMCs, whereas the intravenous boost is intended to increase $CD8^+$ T-cell presence specifically in the liver; this was not examined. A challenge experiment, however, revealed no significant difference between i.m. and i.v. adenovirus-boosted groups, although the mouse with the highest ELISpot SFU was completely protected from infection, in the i.v. boost group (Fig. 4.4.1 A)

The second experiment (Fig. 4.4.1 B) was intended to increase the quantity of circulating PvTRAP-specific $CD8^+$ T-cells before 'pulling' with intravenous adenovirus PvTRAP administration. Again, intravenous boosting showed no significant improvement in ELISpot responses, as expected. However, once again intravenous 'pulling' showed no improvement in protective efficacy;

in fact, it had significantly lower protective efficacy than an intramuscular adenovirus PvTRAP third vaccination (Fig. 4.4.1 B).

A

group	prime (d0) (10^8 iu)	boost (d14)
Ad-TR i.m.	i.m Ad-TR	i.m. Ad-TR (10^8 iu)
Ad-TR i.v.	i.m Ad-TR	i.v. Ad-TR (10^8 iu)
MVA-TR i.m.	i.m Ad-TR	i.m. MVA-TR (10^7 pfu)
Ad-Tc24-IMX i.v.	i.m Ad-TR	i.v. Ad-Tc24-IMX (10^8 iu)
naive	-	-

B

group	prime (d0) 10^8 iu	boost (d7) 10^7 pfu	iv (d21) 10^8 iu
im im im	i.m Ad-TR	i.m. MVA-TR	i.m. Ad-TR
im im iv	i.m Ad-TR	i.m. MVA-TR	i.v. Ad-TR
im im iv Tc	i.m Ad-TR	i.m. MVA-TR	i.v. Ad-Tc24-IMX
iv im	i.v Ad-TR	i.m. MVA-TR	-
iv im iv	i.v Ad-TR	i.m. MVA-TR	i.v Ad-TR
naive	-	-	-

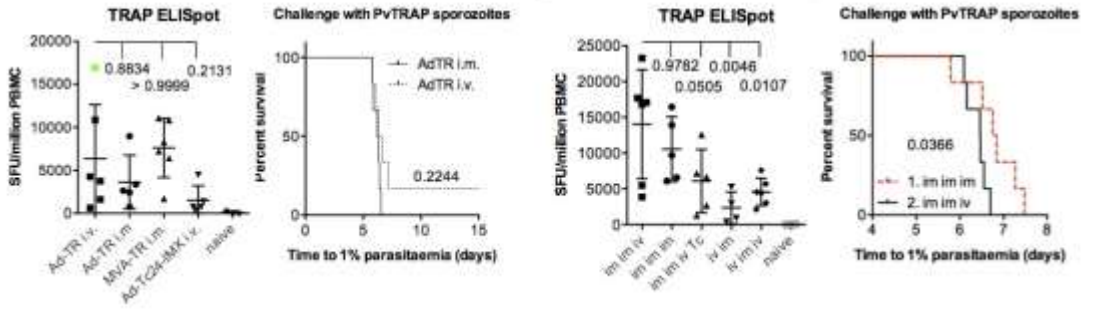


Fig. 4.4.1 Effects on immunogenicity and protective efficacy of intravenous administration of viral-vectored PvTRAP vaccine

BALB/c mice (n=6 per group) were vaccinated according to the protocols shown in tables (A) and (B). Also included in the tables are the times post-prime of each vaccination, the route (i.m: intramuscular; i.v: intravenous) and the vaccine (Ad-TR: adenovirus-PvTRAP; MVA-TR, MVA-PvTRAP; Ad-Tc24IMX, Adenovirus Tc24IMX, a *Trypanosoma cruzi* antigen used as control). PvTRAP-specific IFNγ ELISpots were performed using PBMCs from blood taken one week before challenge using a PvTRAP $CD8^+$ immunodominant epitope for stimulation. Numbers represent p-values from ANOVA with Bonferroni's multiple comparisons test between the indicated groups. Mice were challenged by intravenous injection (A) two weeks post-boost and (B) on day 32 post-prime with 1000 transgenic PvCSP/PvTRAP *P. berghei* sporozoites. Daily thin blood smears were taken to determine time to reach 1% blood-stage parasitaemia by linear regression. Numbers on survival curves represent p-values from log-rank tests between the indicated groups.

4.5 Comparison of Rv21 and CSVS-like, two Hepatitis B surface antigen-based PvCSP virus-like particles

Two Hepatitis B surface antigen-based PvCSP virus-like particles have been developed: Rv21, in our group, and CSVS-S, based on the VMP001 construct developed by the Walter Reed Army Institute of Research. CSVS-S is expressed in *S. cerevisiae* in a 1:4 ratio with non-fusion Hepatitis B surface antigen. Here a CSVS-like construct, expressed in *P. pastoris* and containing purely PvCSP-construct-Hepatitis B surface antigen subunits was produced for comparison to Rv21. The primary sequences of the PvCSP proteins fused to the Hepatitis B surface antigen subunits are shown in Fig. 4.5.1 A. Both have C-terminal domains and nine VK210 repeat units. Rv21 includes ten VK247 repeat units, and CSVS-like only one; finally, Rv21 lacks the N-terminal domain, whereas CSVS-like includes it.

An experiment in BALB/c mice revealed differences in immunogenicity (Fig. 4.5.1 B). Interestingly, although both VLPs generated similar titres and avidity indices against a peptide containing two VK210 repeats ("210qpag", Fig. 4.5.1 C), Rv21 generated a small but significant increase in titres compared to CSVS against two forms of native PvCSP-210, with (N210C, $p=0.0032$) or without (210C, $p=0.0052$) the N-terminal domain. This difference was more pronounced in the relative avidity indices of the two VLPs: about double the avidity index for Rv21 compared to CSVS-like for both N210C ($p=0.0001$) and 210C ($p=0.0022$).

PvCSP-247-specific immunogenicity, measured using the "247gang" peptide containing two repeats from PvCSP-247 (Fig. 4.5.1 C), was weak, with detectable titres in only five Rv21-vaccinated mice and one CSVS-like-vaccinated mouse.

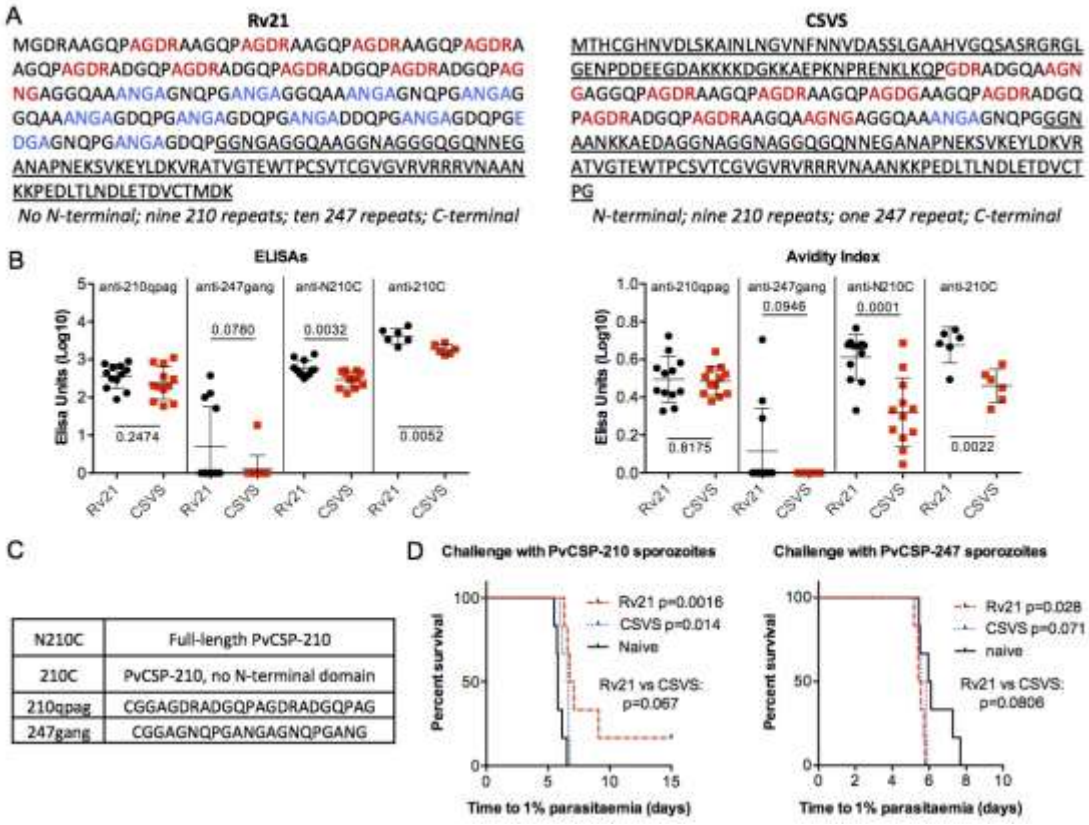


Fig. 4.5.1 Comparison of Rv21 and CSVS-like, two Hepatitis B surface antigen-based virus-like particles

DNA sequences encoding the polypeptides shown in (A) were genetically fused to Hepatitis B surface antigen and expressed in *Pichia pastoris*. The PvCSP-based polypeptides differ in N-terminal domain (excluded in Rv21, present in CSVS-like) and in number of PvCSP-210 (red) and PvCSP-247 (blue) repeat units as shown. Virus-like particles were purified and used to vaccinate BALB/c mice (n=12 per group, two vaccinations of 1.5 µg per shot 2 weeks apart). (B) Sera was taken from mice ten days post-boost and used in standard curve ELISAs and avidity index calculated by the ratio of ELISA units of sera treated with 7 M urea to untreated sera. Numbers represent t-tests between groups. (C) Antigens used in ELISAs in (B). (D) Two weeks post-boost mice were challenged by intravenous injection of either 750 PvCSP-210/PvTRAP or 150 PvCSP-247 transgenic *P. berghei* sporozoites. Thin blood smears taken daily were used to estimate time to reach 1% blood-stage parasitaemia by linear regression. P-values from log-rank tests compared to naïve except where indicated.

Both CSVS-like and Rv21 conferred significant protection on vaccinated mice when challenged with PvCSP-210/PvTRAP transgenic *P. berghei* sporozoites (fig. 4.5.1 D; p-values compared to naïve: Rv21, p=0.0016; CSVS-like, p=0.014). Rv21 conferred sterile protection on one mouse and there was a greater delay in that group compared to CSVS-like, but the difference between the two VLPs was not statistically significant (p=0.067). A challenge with PvCSP-247 transgenic *P. berghei* sporozoites showed no evidence of efficacy by either vaccine, consistent with the poor anti-247 immunogenicity seen with this short (17 day) prime-boost regime.

Discussion

In this chapter, the combination of Rv21 and viral-vectored PvTRAP was shown to enhance protective efficacy compared to either subunit vaccine alone, but Rv21 administered optimally is much more protective than viral-vectored PvTRAP. Antigenic interference, affecting anti-PvCSP titres, only occurs when using Matrix M as an adjuvant, and not with AddaVax, alum or no adjuvant. Viral vectored PvTRAP shifts the IgG2a/IgG1 ratio of anti-PvCSP antibodies towards an IgG2a response, but adjuvants, particularly Matrix M, rebalance the ratio. Antibody responses elicited by Rv21 or PvTRAP are both very durable. Genetic adjuvants also significantly enhance PvCSP and PvTRAP immunogenicity, but intravenous boosting with viral-vectored PvTRAP was not found to enhance protective efficacy. Finally, Rv21 appears to generate a better quality and quantity of anti-CSP response than the CSVS-like vaccine.

Thus, for the first time, a combination of *P. vivax* antigens is shown to be a viable strategy for enhancing protective efficacy (§4.2, Fig 4.2.1). Given the low protective efficacy seen with the leading *P. vivax* VMP001 vaccine (453), as well as with the *P. falciparum*-specific RTS,S (380), this finding and others (189, 475, 566) makes a strong case for pursuing antigen combination as a strategy for developing next generation malaria vaccines. The greatest obstacle to combination strategies is antigenic interference between the vaccine components, which by reducing one or more parts of the immune response, can ablate any enhancement to be gained from combining individual vaccines (565, 566, 569, 570). Here for the first time antigenic interference is shown to be adjuvant-dependent (§4.1, Fig. 4.1.1), and hence in cases where it occurs,

different formulations, with different adjuvants, should be trialed as a means of avoiding it.

A survey of malaria vaccine combination studies does not shed any light on which conditions promote antigenic interference (see Table 4.2). Saponin-based adjuvants sometimes are (265, 568) and sometimes aren't (567, 644) associated with it. Mixing and co-injecting the vaccines into one site sometimes does (570) and sometimes doesn't (580) result in antigenic interference, and the same goes for delivery of the component vaccines into separate sites (antigenic interference in some cases, (579), but not in others (567)). This represents one of the limitations of the current study: there are no clear rules yet discernable for when antigenic interference will occur, so findings from this study may not hold with different antigens, different delivery platforms, or in different species; in each case, the optimal regime must be determined empirically, which is not, in general, the most efficient approach. Since antigenic interference represents the major obstacle to successful vaccine combination, and since, as this thesis argues, the best approach for enhancing subunit vaccine efficacy lies in combining multiple antigens, it would be extremely valuable for the field to carry out a systematic study into the mechanisms and conditions of antigenic interference. Some work on this has been done, with enhanced killing of double viral vector-harbouring cells blamed for reduction in $CD8^+$ T-cells (570), IL-10 release associated with one viral vaccine repressing responses to another (645) and competition for $CD4^+$ T-cell help and between B-cells for antigen suggested as a reason for interference when epitopes are physically connected (646); but more can be done. What is clear is that, when there is no antigenic interference, and

when a challenge is performed, combining malaria antigens results in enhancement of protection (see Table 4.2.1).

Table 4.2.1 Antigenic interference in malaria vaccine studies

Model	Antigens and platform	Delivery	Adjuvant	Antigenic interference	Ref	enhancement of protection
mice	PfRESA fusion to influenza antigens	mixed	ISCOM (with saponin)	none found	(644)	n/a
mice	Ad-MVA PyCSP and PyMSP1	mixed	none	PyMSP1 abs and CD8+ T-cells for both	(570)	n/a
mice	PyMSP1 and PyMSP4/5 proteins	mixed	CFA or IFA	increased PyMSP1 titres	(571)	enhancement
mice	PfCSP, PfTRAP, PfLSA1, PfAMA1, PfMSP1 separate DNA plasmids	mixed	Vaxfectin (cationic lipid)	yes: lower CSP cellular and IFA tires. May not be comparable, 1/5th dose of CSP in combination group.	(563)	n/a
rhesus	RTS,S; AMA1, MSP1 proteins	mixed or separate	AS02A	AMA1 titres; AMA1 cellular response only with MSP1, RTS,S 'restores' responses; no difference with separate injections	(568)	n/a
rhesus	PfCSP, PfTRAP, PfLSA1, PfAMA1, PfMSP1 separate DNA plasmids; boosted with poxvirus encoding all five (including CSP-only primed animals)	mixed	PBS or CRL1005 (polymer/ cationic surfactant)	none found	(562)	n/a
mice	CSP LSA1 TRAP CelTOS, DNA plasmids, electroporation	mixed?	none	LSA1 and CelTOS reduced titres; CSP lower IFNγ	(564)	n/a

mice	LSA3, STARP, Exp1, Pfs16, TRAP, LSA1 (DNA prime, MVA boost)	fusion protein	none	none found	(647)	n/a
mice	Pfs48/45, Pfs25, DNA plasmid (electroporation)	mixed	none	none found	(580)	not determinable
human	RTS,S, Ad-MVA ME-TRAP	separate sites	AS01B	none found	(567)	enhancement, but not statistically significant
mice	Py25, Py48/45	separate sites	none	lower antibody responses for both antigens	(579)	reduction
mice	PbCSP, PbTRAP (viral vectored both, versus Ad-MVA PbTRAP + Ad-protein PbCSP	mixed or separate sites	none, except Matrix M with protein CSP	lower antibody and cellular responses for both antigens with viral vectors. Lower CSP titres with Ad-P CSP/Ad-M TRAP only with mixture group, not with separate sites.	(566)	enhancement
human	RTS,S, PfTRAP protein	mixed	AS02	Lower antibody titres for PfCSP	(565)	no enhancement
rats/ rabbit	PfRH5, PfF2, PfAARP, PfRH2 proteins	mixed	CFA/IFA	none found	(575)	enhancement

It has not, to my knowledge, previously been shown that viral vectors will shift the IgG2a/IgG1 ratio of antibodies against a separate antigen towards the IgG2a isotype, as has occurred in this study (Fig. 4.1.1). The result is not a surprise, given that IFNγ, production of which is stimulated by immune recognition of viral infection (648), enhances IgG2a production and suppresses IgG1 production (649, 650). Similarly, the propensity of Matrix M (259) and AddaVax (or MF59) (252) to give a 'balanced' Th1/Th2 profile is consistent with the reduction in shift of the IgG2a/IgG1 ratio when these adjuvants are combined with viral-vectored PvTRAP and Rv21. The significance of this is that

opsonization of sporozoites (651), a process mediated by particular IgG subclasses, has been associated with protection following vaccination with RTS,S (652). However, in all the studies performed in this thesis, no consistent association of protection with any given IgG isotype was found (data not shown); indeed a recent study found opsonic activity associated with lack of protection in RTS,S-vaccinated volunteers (653). A straightforward experiment could be conducted to determine the relative contribution of each IgG subclass to protection, however: a neutralising monoclonal antibody, like the PbCSP-specific 3D11, could through cloning be used to generate a panel of monoclonal antibodies identical in all but their Fc regions, and passively transferred to mice prior to challenge, allowing any difference in protective efficacy to be determined.

Genetic adjuvants with viral-vectored vaccines have previously been shown to enhance antibody responses (with IMX313, (266, 269)) and cellular responses (with IMX313, (267), and with the invariant chain, (271-274, 276)). This is the first time these genetic adjuvants have been used with *P. vivax* antigens, and it is gratifying that they enhance immunogenicity with PvCSP and PvTRAP (§4.3, Fig. 4.3.1), as found with other antigens, as this offers another avenue for improving on existing *P. vivax* vaccines. This is also the first time that both Ii and IMX313 have been combined with any single antigen, and this led to the greatest enhancement of titres after a single immunisation, but lacking a control PvTRAP-IMX313 group, it is not possible to infer that there is an additive or synergistic effect from combining genetic adjuvants; a further study comparing PvTRAP-IMX313-Ii with both PvTRAP-Ii and PvTRAP-IMX313 will need to be carried out.

Priming with adenoviral-vectored malaria liver stage antigens, followed by boosting by intravenous administration of the same antigen (either adenoviral- or MVA-vectored) has been shown by Anita Gola (personal communication) and others in the Jenner to 'pull' circulating antigen-specific $CD8^+$ T-cells generated by the prime vaccination to the liver, increasing the likelihood that they find and destroy sporozoite-infected hepatocytes. This works for OVA, PfLSA1, PfLSAP2, and PfTRAP, but not, in my hands, PvTRAP (§4.4, Fig. 4.4.1). It is not clear why there is a discrepancy, but it is possible that greater protection, and hence the ability to see a difference with an intravenous Ad-PvTRAP boost, would have come about in the experiment shown in Fig. 4.4.1 A if protection were not so difficult to achieve using this model, using BALB/c mice and the double transgenic PvTRAP/PvCSP *P. berghei* parasite. Very few instances of sterile protection have been achieved with this double transgenic parasite and PvTRAP vaccination (see results in this chapter and in Chapter 6), in contrast to challenges with a single transgenic (497). It is possible that there is less expression or secretion of PvTRAP in infected hepatocytes with the double transgenic, thus affecting MHC class I presentation of PvTRAP peptides and decreasing the likelihood of TRAP-specific $CD8^+$ T-cells finding and destroying infected hepatocytes; this could be tested by performing IFA on infected hepatocytes, compared to wild-type or single PvTRAP transgenics. It is also possible that the duration between intravenous 'pull' and challenge is too short in my experiments; in cases where enhanced protection has been seen, three to eight weeks pass before challenge, whereas in my experiments challenge occurred two weeks after the boost. Intravenous administration of high doses of viral vectors has now proven safe in human volunteers at the Jenner, allowing

the protective efficacy of this vaccine strategy to proceed to Phase I/II clinical trials (Adrian Hill, personal communication).

Rv21 appears more immunogenic than the CSVS-like (455) VLP in a head-to-head challenge (§4.5, Fig. 4.5.1). This is consistent with data shown later in this thesis, where a PvCSP construct lacking the N-terminal domain (like Rv21) confers much greater protection on mice than one including the N-terminal domain (which the CSVS-like VLP also includes) (see Chapter 5). Nevertheless, the inconsistency between the anti-210 peptide and anti-full length CSP responses between Rv21 and CSVS-like, where no significant difference and a highly significant difference in titres are seen, respectively, suggests the need for further experiments to verify this.

In summary: combining antigens, using adjuvants, and using genetic adjuvants all provide means of enhancing the protective efficacy of *P. vivax* vaccines. The combination of Rv21 and PvTRAP enhances protection, as predicted in Chapter Three. This opens the door to strategies using this or other antigen combinations as a means of enhancing *P. vivax* vaccine efficacy. The greatest obstacle to enhanced protective efficacy by antigen combination, antigenic interference, is shown to be avoidable by changing the adjuvant with which the combination vaccine is administered.

Chapter 5

Towards a single component multi-epitope vaccine

Part 1: CSP repeat peptide vaccines

Introduction

In Chapter 4 we saw that enhanced protection could come from combining PvCSP and PvTRAP vaccines, a result that supports previous findings with PbCSP and PbTRAP (475, 566) and PfCSP and PbTRAP (189), as well as with other malaria vaccine combinations (571, 575). The next generation malaria vaccine must be more effective, but of equal concern is enhanced *cost*-effectiveness. As things stand, the leading malaria vaccine RTS,S is projected to be less cost-effective than insecticide-treated bednets (29). A vaccine with multiple components is likely to be substantially more expensive to manufacture and distribute than a single component vaccine (654), and although ultimately cost-effectiveness is, of course, a function of both cost and efficacy, if a single component vaccine displaying multiple antigens could maintain the enhancement of efficacy seen with both vaccines, it would likely be highly cost-effective. This chapter sets the groundwork for developing a multi-antigen, single-component vaccine by providing proof of concept that short peptides from the CSP repeat region can be displayed on a Qβ virus-like particle and generate protective immunity in mice. Co-display of such short peptides from *P. vivax* and *P. falciparum* is attempted; but immunodominance by one of the peptides, the main potential obstacle to a single component combination vaccine, is also seen. Chapter 6 focuses on screening for other linear peptides to include with CSP

repeat-based peptides, and together these two chapters build the groundwork for a single-component multi-antigen vaccine, including one with cross-species efficacy.

Short peptides vaccines based on the PfCSP repeat tetramer NANP have a long history of development: an $(NANP)_3$ peptide coupled to tetanus toxin was one of the first subunit malaria vaccines tested in a clinical trial, and although it only protected two volunteers (365), this and another trial with a greater number of NANP repeats (364) demonstrated that a protective subunit vaccine based on PfCSP was possible. The concept of using these short peptides was taken forward with multiple antigenic peptides, or MAPs, branched peptides based on a multiple lysine core. MAPs can present 4-16 peptides, either identical to one another or different (416). After some preclinical development (417, 418), clinical trials using an $(NANP)_3$-presenting MAP (419) or MAP-like polyoxime (421) generated antibodies in volunteers that were capable of reacting with live sporozoites (419) and neutralising PfCSP *P. berghei* transgenic sporozoites in an *in vitro* invasion assay (420). Virosomes have been used to deliver $(NPNA)_5$ in clinical trials, generating antibodies capable of recognising sporozoites in an immunofluorescence assay (655, 656). BCG has also been used as a vector, presenting short NANP repeats and demonstrating immunogenicity in mice (657). Similarly NANP repeats have been presented on the surface of an adenovirus vector, eliciting antibodies with *in vitro* invasion capability (395). More recently self-assembling nanoparticle (SAPN, (409, 410)) or nanofibre (411) platforms presenting three to six copies of the NANP unit repeat have been tested in mice and either shown protection against a PfCSP *P. berghei* transgenic parasite challenge, or *in vitro* invasion inhibition of generated antibodies. *P. vivax*

CSP unit repeats have also been displayed as MAPs (441) and shown evidence of protective efficacy in *Saimiri boliviensis* monkeys (442, 443). In this chapter, however, given the potent ability of virus-like particles to generate high levels of antibodies (187), it was decided to present short peptides on a virus-like particle (Qβ), and test them for protective efficacy.

With *P. vivax* CSP vaccines, unlike with *P. falciparum* CSP, protection is associated with a sub-region, AGDR, within the unit nonamer repeat GDRADGQPA (439, 443). A short peptide vaccine based on AGDR has been tested in mice, and elicits antibodies, (440) but it has never before been tested for protective efficacy; here, this is done using a PvCSP-VK210 transgenic *P. berghei* parasite in mice. Again, unlike *P. falciparum,* there is considerable allelic variation in *P. vivax* CSP unit repeats (357), so the other major allelic variant PvCSP VK247 repeat nonamer ANGAGNQPG (356) is also here tested for protective efficacy as a Qβ-peptide vaccine. An attempt is made at identifying tetramers within the PvCSP-247 unit repeat equivalent to AGDR capable of inducing protective immunity as tetramer repeats. Alternative PfCSP repeat tetramers to NANP are also tested for protective efficacy, apparently for the first time.

In this chapter, a novel homologous prime-boost strategy is also tested to determine if priming with native PvCSP and boosting with Qβ-$(AGDR)_3$ enhances protection, by focusing the immune response against the protective AGDR epitope, as has previously been attempted with, for instance, HIV epitopes (658). Full and truncated forms of PvCSP are compared for protective efficacy, previously investigated for *P. falciparum* CSP using a transgenic PfCSP parasite (658), but never for PvCSP.

Good antibody responses usually require $CD4^+$ T-cell help (232). The potential low immunogenicity of peptides is sometimes counteracted by coupling them to carrier proteins with T-cell helper epitopes (for example, (365)). A pre-clinical study using MAPs examined the effects on immunogenicity of including the P2 or P30 universal $CD4^+$ T-cell epitopes (659). They found that including P2 on a *P. berghei* CSP unit repeat MAP improved titres 100-fold, and P30 with a *P. falciparum* NANP MAP saw a ten-fold improvement in titres. In this chapter, fusion peptides of NANP and P2 are used to determine whether this is a good strategy for enhancing the immunogenicity of the Qβ-$(NANP)_6$ platform. The effect on immunogenicity of increasing the number of NANP repeats is also investigated.

Finally, a cross-species vaccine is produced, combining *P. vivax* and *P. falciparum* CSP repeat peptides on a single Qβ VLP and tested for protective efficacy. Only one vaccine combining these B-cell epitopes has been constructed to date, to our knowledge, and never tested for protective efficacy (660).

In this chapter it is shown that short peptides representing CSP-derived unit repeats from *P. falciparum* and *P. vivax,* displayed on separate Qβ VLPs, are immunogenic and protective, in some cases conferring as much as 100% sterile protection on mice challenged with transgenic *P. berghei* sporozoites. It is also shown for the first time that vaccination with an AGDR-repeat peptide can confer protective immunity, and that heterologous boosting of native PvCSP-primed mice with this Qβ-$(AGDR)_3$ VLP can enhance protective efficacy. Full-length PvCSP, although as immunogenic as a truncated form missing the N-terminal domain, confers far lower protective efficacy than the latter. The universal $CD4^+$ T-cell epitope P2 enhances the affinity of elicited anti-NANP antibodies, and high

affinity is shown to associate with protection. Increasing the number of NANP unit repeats also increased immunogenicity and protective efficacy; a novel mathematical model predicts this will be a saturating relationship. Finally, a single-component cross-species malaria vaccine displaying both *P. falciparum* and *P. vivax* CSP unit repeat epitopes is tested, but the NANP epitope is found to be immunodominant, signaling that further optimization will be required before a cross-species vaccine based on these epitopes can become a reality.

In all, this chapter provides proof of concept that short peptide vaccines displayed on Qβ can be highly immunogenic and protective. It paves the way for investigation of other short linear B-cell epitopes using the Qβ platform, and lays the groundwork for development of a single-component multi-epitope VLP, expected, from the work in Chapters 3 and 4, to markedly enhance protective efficacy.

Results

5.1 Immunogenicity and protective efficacy of short unit repeat CSP peptides from *P. falciparum* and *P. vivax* coupled to Qβ

The central repeat regions of both *P. falciparum* and *P. vivax* CSP are known targets of neutralising antibodies. Consequently, this region was considered a good place to start in the search for small linear B-cell epitopes that could be coupled to Qβ virus-like particles in an attempt to make a single component multi-epitope malaria vaccine.

The primary structures of representative *P. falciparum* and *P. vivax* CSP are shown in Fig. 5.1.1, with the central repeat regions and variations within those regions highlighted. Peptides consisting of two (or in the case of NANP, two and three) of these unit repeats were synthesized as shown in Table 5.1.1. The peptides were coupled to Qβ and used to immunize BALB/c mice as shown in Fig. 5.1.2.

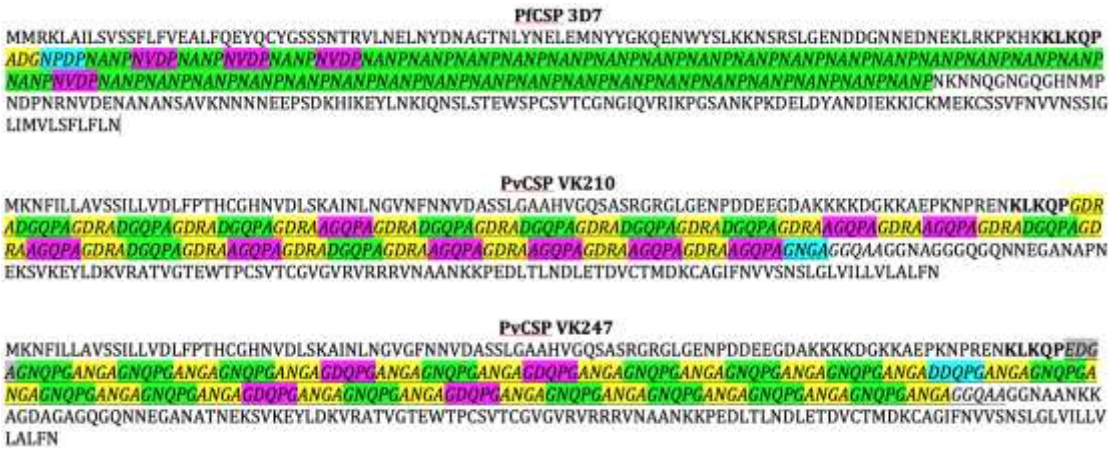


Fig. 5.1.1 Representative *P. falciparum* and *P. vivax* CSP sequences.

CSP is divided into three domains: N-terminal, central repeat region, and C-terminal. The composition and variation of the central repeat regions are highlighted in colour.

Table 5.1.1 Sequences of peptides coupled to Qβ in this section

$(NANP)_2$	CGGNANPNANP
$(NANP)_3$	CGGNANPNANPNANP
210agdr	CGGDRADGQPAGDRADGQPAGDR
210qpag	CGGAGDRADGQPAGDRADGQPAG
247gang	CGGAGNQPGANGAGNQPGANG

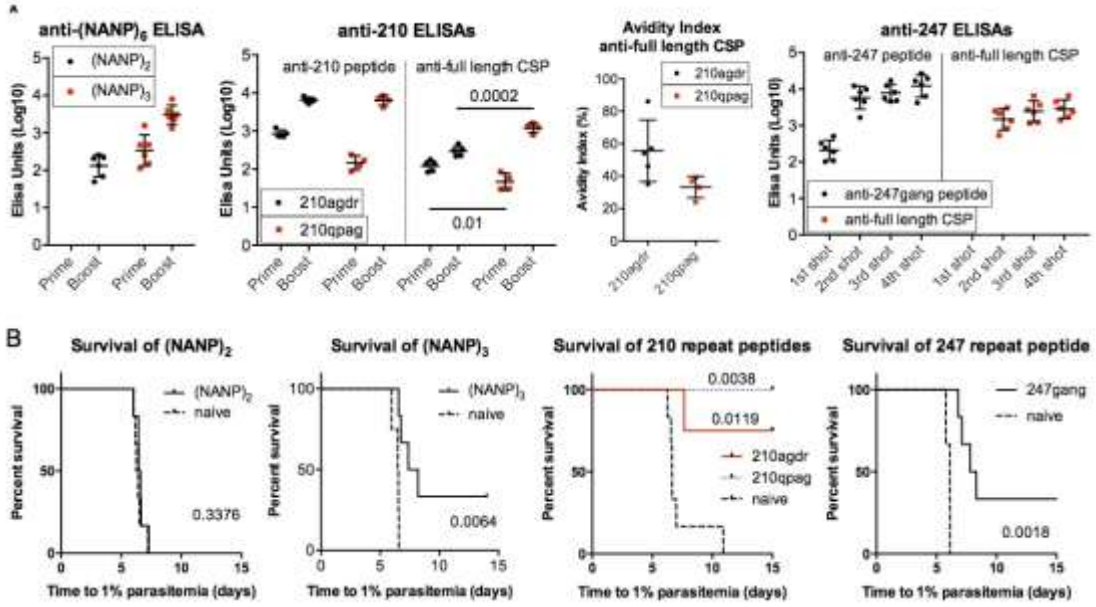


Fig. 5.1.2 Immunogenicity and protective efficacy of short unit repeat peptides from *P. falciparum* and *P. vivax* CSP coupled to Qβ VLPs.

BALB/c mice (n=6) per group were vaccinated by intramuscular injection with peptides chemically coupled to Qβ virus-like particle and delivered with Matrix M adjuvant. Each peptide consists of two unit repeats of the central repeat region of *P. vivax* CSP VK210 ("210agdr" and "210qpag", 3 μg per dose), or VK247 ("247gang", 3 μg per dose), or *P. falciparum* CSP ("$(NANP)_2$", 8 μg per dose) or three unit repeats in the case of "$(NANP)_3$" (20 μg per dose). A three week prime-boost interval was used except in the case of $(NANP)_2$ where a one week interval was used. (A) Standard curve ELISAs were performed to determine the antibody response against peptides and against full-length CSP. The avidity index, the ratio of 7M urea-treated versus untreated ELISAs, was obtained for VK210 peptide vaccines. Means are shown ± SD. Numbers represent p-values from t-tests between indicated groups. (B) Mice were challenged by intravenous injection of 1000 sporozoites; in the case of $(NANP)_2$- and $(NANP)_3$-vaccinated mice, PfCSP-replacement *P. berghei* sporozoites were used. For 210agdr and 210qpag, PvCSP-

210/PvTRAP *P. berghei* sporozoites were used, and for 247gang a PvCSP-247 replacement *P. berghei* parasite was used. Time to reach 1% blood-stage parasitaemia was calculated by linear regression from daily thin blood smears. P-values from Log-rank tests in comparison to naïves are shown.

The Qβ-peptide vaccines were highly immunogenic, generating high titre antibodies that recognized short peptides representing the repeat sequences against which they were vaccinated, as well (in the case of *P. vivax* CSP repeat-based vaccines Qβ-210qpag, Qβ-210agdr and Qβ-247gang) the native protein (Fig. 5.1.2 A). All of the vaccines except Qβ-$(NANP)_2$ conferred sterile protection on mice challenged with *P. berghei* sporozoites with their endogenous CSP replaced by the appropriate *P. falciparum, P. vivax* VK210 or VK247 CSP (Fig. 5.1.2 B).

Interestingly, two variants of the *P. vivax* VK210 repeat peptide, 210agdr and 210qpag, differed in their immunogenicity. These peptides vary only in the exact order of amino acids, not the composition (see Table 5.1.1); yet Qβ-210qpag elicits significantly higher antibody titres after boosting against native CSP VK210 than does Qβ-210agdr ($p=0.021$, Fig. 5.1.2 A), even though after prime Qβ-210qpag induced significantly lower titres than 210agdr ($p=0.01$). There is also a difference in avidity for native CSP VK210, with Qβ-210agdr eliciting antibodies with a higher avidity index than Qβ-210qpag, though this is not significant (Fig 5.1.2 A). Together this suggests that slight differences in peptide amino acid order could alter the conformation and/or the immunogenicity of the antibodies elicited. Since both VK210-based vaccines

conferred high levels of protection, it is not possible to draw conclusions as to which might be superior (Fig 5.1.2 B).

5.2 CSP repeat region tetramers: homologous and sequential vaccination

5.2.1 Immunogenicity and protective efficacy of CSP repeat region tetramers

The *P. vivax* CSP VK210 central region is composed of varying numbers of a nonamer unit repeat, (A/D)GQPAGDRA (Fig. 5.1.1). It has previously been found that only repeat-specific antibodies that recognise the AGDR sequence underlined within this nonamer can neutralize *P. vivax* VK210 sporozoites. Here, the protective efficacy of Qβ-peptide vaccines presenting two or three copies of this AGDR tetramer, Qβ-$(AGDR)_2$ and Qβ-$(AGDR)_3$, were investigated, using BALB/c mice. The vaccines produced modest antibody titres in an ELISA against native full length PvCSP-210 and good anti-$(AGDR)_3$ titres, and the Qβ-$(AGDR)_3$ vaccine was able to confer a significant though modest protective effect compared to naïve mice when challenged with 1000 PvCSP/PvTRAP transgenic *P. berghei* sporozoites (Fig. 5.2.1). Qβ-$(AGDR)_2$ did not confer any measurable degree of protection.

I hypothesize two possible mechanisms of action, which are not mutually exclusive:

1) Antibodies interfere with central repeat-region function, but only if they bind to AGDR.

2) AGDR-specific antibodies interfere with function or cleavage of the KLKQP-containing region 1, necessary for invasion.

Hypothesis 2 derives from the observation that in PvCSP-210, the four amino acids immediately following the highly conserved KLKQP site are GDRA (Fig 5.1.1), a motif present twice in the peptide coupled to the Qβ-$(AGDR)_3$ vaccine: CGGAGDRAGDRAGDR.

Tetramers based on the CSP repeat region from the other major strain of *P. vivax,* VK247, and from *P. falciparum* 3D7, were designed and trialed to see if they could confer protective efficacy similar to that of Qβ-$(AGDR)_3$. Three types of tetramer were designed: first, based on the four amino acids immediately following the KLKQP motif; secondly, for PvCSP-247, by analogy with the position of AGDR within the PvCSP-210 nonamer repeat; or thirdly by identifying minor tetramer variants within PfCSP or PvCSP-210.

For PvCSP-247, the tetramer following the KLKQP sequence is EDGA, so a Qβ-$(AEDG)_3$ vaccine was produced. The predominant nonamer repeat in PvCSP-247 is (GNQPGANGA); GANG (underlined) was judged to occupy a position analogous to that of AGDR within the PvCSP-210 nonamer repeat. Hence a Qβ-$(GANG)_3$ vaccine was also produced.

In *P. falciparum* CSP the predominant unit repeat, NANP, is a natural tetramer (see Fig. 5.1.1), and §5.1 above reports on the protective efficacy of Qβ-peptide vaccines based on this repeat. The tetramer following the KLKQP motif in PfCSP is different, however: ADGN, so the virus-like particle Qβ-$(NADG)_3$ was produced (Fig 5.2.1).

PvCSP-210 and PfCSP possess minor variants of the repeat unit. In PfCSP this is NVDP, so Qβ-$(NVDP)_6$ was constructed for testing. In PvCSP-210 there is a minor variant tetramer AGNG, occupying a position that AGDR normally occupies; thus Qβ-$(AGNG)_3$ was produced (Fig 5.2.1).

Table 5.2.1 Peptide sequences coupled to Qβ in this section

$(AGDR)_2$	CGGAGDRAGDR
$(AGDR)_3$	CGGAGDRAGDRAGDR
$(AGNG)_3$	CGGAGNGAGNGAGNG
$(GANG)_3$	CGGGANGGANGGANG
$(AEDG)_3$	CGGAEDGAEDGAEDG
$(NADG)_3$	CGGNADGNADGNADG
$(NVDP)_6$	CGGNVDPNVDPNVDPNVDPNVDPNVDP

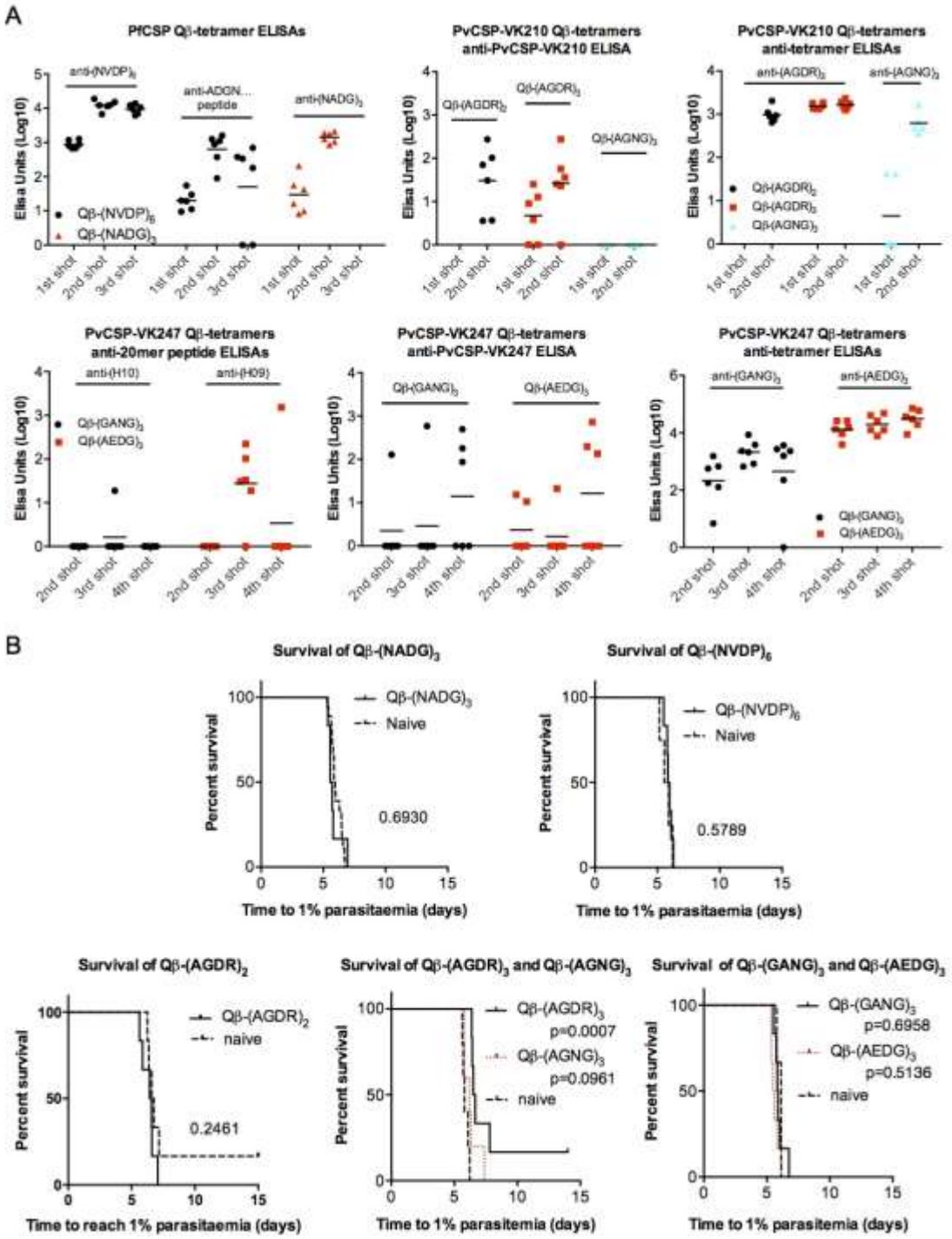


Fig. 5.2.1 Immunogenicity and protective efficacy of CSP repeat region tetramers.

BALB/c mice (n=4-6 per group) were vaccinated by intramuscular injection with peptides consisting of 2, 3 or 6 copies of tetramers derived from *P. falciparum* CSP or *P. vivax* CSP VK210 or VK247, chemically coupled to Qβ virus-like particle and delivered with Matrix M adjuvant. Mice were given two to four shots with a three week interval between shots. A dose of 3 μg Qβ-peptide per shot was used except with $(AGDR)_2$ (8 μg per shot) and $(AGDR)_3$ and $(AGNG)_3$ (20 μg per shot). (A) Immunogenicity in ELISAs from plasma taken two weeks post-vaccination. ELISAs performed against indicated peptides or proteins. ADGN… peptide from *P. falciparum* CSP: ADGNPDPNANPNVDP. From *P. vivax* CSP VK247: H09: GPEDGAGNQPGANGAGNQPG. H10: GANGAGNQPGANGAGNQPGA. (B) Mice were challenged three weeks after the final immunization by intravenous injection of 1000 transgenic *P. berghei* sporozoites: PfCSP-replacement sporozoites in the case of Qβ-$(NADG)_3$ and Qβ-$(NVDP)_6$; PvCSP-210/PvTRAP in the case of Qβ-$(AGDR)_2$, Qβ-$(AGDR)_3$, and Qβ-$(AGNG)_3$; and PvCSP-247 in the case of Qβ-$(GANG)_3$ and Qβ-$(AEDG)_3$. Time to reach 1% blood-stage parasitaemia was calculated by linear regression using daily thin blood smears. P-values from Log-rank tests in comparison to naïves are shown.

Unlike Qβ-$(AGDR)_3$, none of these other tetramer-based vaccines conferred any sterile protection upon mice (Fig. 5.2.1 B). All the vaccines were highly immunogenic when sera was tested in ELISAs against the peptides with which the mice had been vaccinated (Fig. 5.2.1 A). However, Qβ-$(AGNG)_3$ produced no detectable response against native PvCSP-210. The PvCSP-247 based vaccines Qβ-$(GANG)_3$, and Qβ-$(AEDG)_3$ failed to elicit detectable antibody responses in half (or more) of mice, to either native PvCSP-247 or to short 20 amino-acid peptides (“H09” and “H10”) containing the tetramers within the native PvCSP-247 sequences (Fig. 5.2.1 A). The PfCSP-based Qβ-$(NVDP)_6$ gave a more promising ELISA response to a native 20 amino acid peptide containing NVDP within its sequence, but did not provide any discernible protective efficacy (Fig 5.2.1).

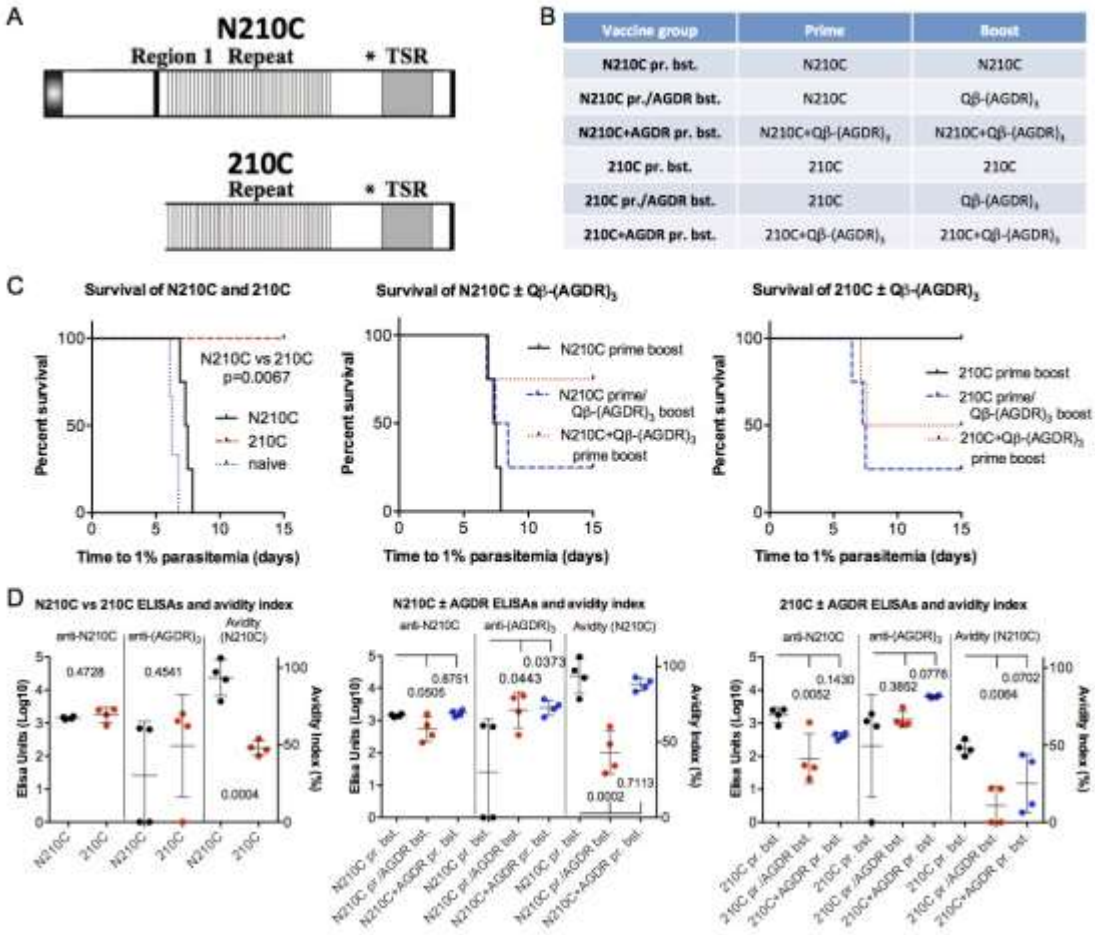
5.2.2 Sequential and tandem immunisation with native PvCSP and Qβ-(AGDR)$_3$

Since PvCSP-210 repeat region-specific antibodies apparently must recognise the AGDR tetramer within the nonamer unit repeat (Fig. 5.1.1), I investigated whether tandem or sequential immunization of the native PvCSP with Qβ-(AGDR)$_3$ might enhance protective efficacy, by at once raising antibodies against the native structure and promoting an AGDR-focused response. Mice were vaccinated with either full-length PvCSP containing the N-terminal, repeat region and C-terminal domains, ("N210C") or with a truncated form of PvCSP containing only the repeat region and C-terminal domain ("210C"; see schematic, Fig. 5.2.2 A). As well as homologous prime-boost with either form of PvCSP, groups of mice were either given tandem or sequential doses of Qβ-(AGDR)$_3$ as detailed in Fig. 5.2.2 B.

Challenge of mice with 1000 PvCSP-210/PvTRAP transgenic *P. berghei* sporozoites revealed a large difference in the protective efficacy conferred by full-length (N210C) versus truncated (210C) forms of PvCSP. 210C gave 100% protection, but N210C gave no protection ($p=0.0067$, Fig. 5.2.2 C). There was no detectable difference in antibody titres to full length CSP or the (AGDR)$_3$ peptide between these two forms of PvCSP, but there was a highly significant difference ($p=0.0004$) in the affinity of the elicited antibodies to N210C, with those mice vaccinated with 210C showing much lower affinity to the full length form of PvCSP (Fig. 5.2.2 D). It may be that there is a conformational difference between N210C and 210C, and that only antibodies recognizing the truncated (210C) form are neutralising.

Tandem or sequential vaccination with Qβ-$(AGDR)_3$ had quite different effects depending on whether used in conjunction with N210C or 210C. Adding Qβ-$(AGDR)_3$ to N210C enhanced protective efficacy, particularly in the N210C+ Qβ-$(AGDR)_3$ homologous prime-boost regime (Fig. 5.2.2 C). The most significant effect of adding Qβ-$(AGDR)_3$ to N210C is in increasing AGDR-specific titres ($p= 0.044$ and 0.037 for N210C prime/Qβ-$(AGDR)_3$ boost and N210C+Qβ-$(AGDR)_3$ homologous prime-boost respectively) (Fig. 5.2.2 D) suggesting that focusing the immune response on this tetramer may be the cause of the improvement in protective efficacy.

In contrast to the outcome from combining N210C with Qβ-$(AGDR)_3$, combining 210C with Qβ-$(AGDR)_3$ reduced protective efficacy in comparison to the 210C homologous prime-boost regime (Fig. 5.2.2 C). In 210C-based regimes, Qβ-$(AGDR)_3$, despite improving anti-$(AGDR)_3$ titres somewhat, resulted in a reduction of anti-N210C titres and avidity (Fig. 5.2.2 D). It is not clear why anti-PvCSP and anti-AGDR antibodies can be maintained at high titres with N210C/Qβ-$(AGDR)_3$ regimes but not with the 210C/Qβ-$(AGDR)_3$ regimes. It is still possible that, were a strategy based on 210C and Qβ-$(AGDR)_3$ developed capable of eliciting optimal antibodies against both of these antigens, protective efficacy compared to the 210C homologous prime-boost regime could be enhanced.



Vaccine group	Prime	Boost
N210C pr. bst.	N210C	N210C
N210C pr./AGDR bst.	N210C	Qβ-(AGDR)$_3$
N210C+AGDR pr. bst.	N210C+Qβ-(AGDR)$_3$	N210C+Qβ-(AGDR)$_3$
210C pr. bst.	210C	210C
210C pr./AGDR bst.	210C	Qβ-(AGDR)$_3$
210C+AGDR pr. bst.	210C+Qβ-(AGDR)$_3$	210C+Qβ-(AGDR)$_3$

Fig. 5.2.2 Sequential and tandem immunisation with native PvCSP-210 and Qβ-(AGDR)$_3$. BALB/c mice (n=4 per group) were immunized with full length ("N210C") or truncated ("210C) versions of PvCSP-210, as depicted schematically in (A) (adapted from (338)). Some mice also received Qβ-(AGDR)$_3$ in addition to either PvCSP-210 construct, or as a boost instead of the PvCSP-210, as shown in the table (B). Mice received 3 µg of each immunogen per shot with Matrix M adjuvant, using a prime-boost regime with interval 3 weeks. 3 weeks after boosting, mice were challenged by intravenous injection of 1000 transgenic PvCSP/PvTRAP transgenic *P. berghei* sporozoites (C). P-value from comparison of N210C to 210C by log-rank test. (D) 2 weeks post-boost, serum was collected for mice for evaluation of immune responses by standard curve ELISA. Serum responses were tested against N210C and (AGDR)$_3$ and avidity index determined by taking the ratio of ELISA units from serum treated or untreated with 7M urea. Numbers represent P-values from t-tests (2 groups) or ANOVA with Tukey's multiple comparison post-test (3 groups).

5.3 Improving Qβ-NANP peptide vaccines

5.3.1 Effects on immunogenicity and protective efficacy of fusing a tetanus toxin CD4⁺ T-cell epitope with $(NANP)_3$.

Antibody responses can sometimes be improved by including a $CD4^+$ T-cell epitope to stimulate T-cell help. To see if this strategy would improve the immunogenicity of short peptides presented on Qβ, the universal T-cell epitope P2 from tetanus toxin (tt) was fused to $(NANP)_3$ and BALB/c mice vaccinated as detailed in Fig. 5.3.1 A.

No improvement in anti-$(NANP)_6$ titre was obtained by fusing tt to $(NANP)_3$, (Fig. 5.3.1 B), with a slight but not statistically significant improvement in protective efficacy (Fig. 5.3.1 C). An improvement in the affinity of anti-$(NANP)_6$ antibodies was seen with the Qβ-tt-$(NANP)_3$ group, however (Fig. 5.3.1 B; $p=0.0029$). This may have practical consequences, as a separate and larger experiment shows that when anti-$(NANP)_6$ titres are equal, differences in challenge outcome strongly associate with differences in antibody affinity (Fig. 5.3.1 E).

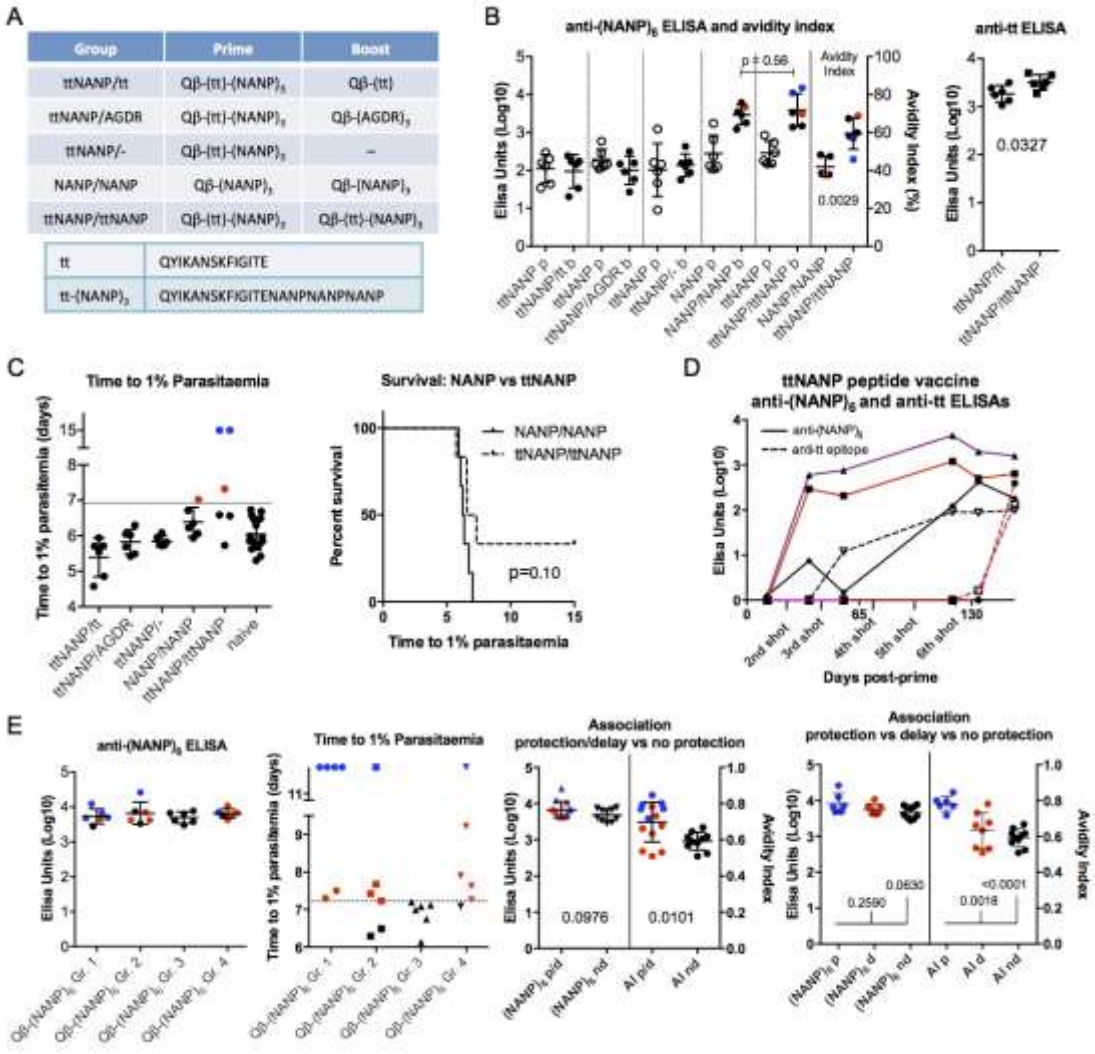


Fig. 5.3.1 Effects on immunogenicity and protective efficacy of tetanus toxin CD4⁺ T-cell epitope fusion with Qβ-(NANP)$_3$.

Qβ VLPs were chemically coupled with tetanus toxin P2 epitope (tt) or tt fused to (NANP)$_3$ and BALB/c mice (n=6 per group) were vaccinated according to the regime shown in (A). Mice were vaccinated by intramuscular injection (using 1 μg per dose, two shots, three week prime-boost interval, and with Matrix M adjuvant). (B) Serum was collected from mice two weeks post-prime and post-boost and standard curve ELISAs performed against (NANP)$_6$ and tt. The avidity index was calculated by taking the ratio of anti-(NANP)$_6$ titres with and without treatment of sera with 7 M urea. T-tests were performed to determine differences between selected groups. (C) Mice were challenged with 1000 PfCSP transgenic *P. berghei* sporozoites three weeks post-boost. Daily thin blood smears were used to determine time to reach 1% blood-stage parasitaemia by linear regression. In (B) and (C) mice with sterile protection are coloured blue, and those with a delay

in time to reach 1% blood-stage parasitaemia coloured red, where "delay" is defined as time-to-1% greater than the mean of naïve challenged mice plus two standard deviations. P-value from log-rank test. (D) In a separate experiment, three BALB/c mice were vaccinated with tt-$(NANP)_3$ peptide in Matrix M (8.4 μg per dose). Standard curve ELISAs against $(NANP)_6$ and tt were performed on sera two weeks post-shot. (E) In a third experiment, BALB/c mice (n=6 per group) were vaccinated with Qβ-$(NANP)_6$ and ELISAs and challenge performed as in (B) and (C). Associations with protection were obtained by dividing mice into two or three groups following challenge: protected or delayed (p/d) versus no delay (nd), or protection (p) versus delay (d) versus no delay (nd). Numbers represent p-values t-tests (comparing two groups) or ANOVA with Tukey's multiple post-test (comparing three groups).

Interestingly, anti-tt antibodies were also detected by ELISA in mice primed with Qβ-tt-$(NANP)_3$, with anti-tt titres significantly higher (p=0.03) in mice boosted with Qβ-tt-$(NANP)_3$ compared to those boosted with Qβ-tt (Fig 5.3.1 B).

A separate experiment was performed with four mice vaccinated using tt-$(NANP)_3$ peptide alone, that is not coupled to a virus-like particle, in Matrix M. Antibody responses were detectable both against $(NANP)_6$ and tt (Fig. 5.3.1 D). Remarkably, the peak anti-$(NANP)_6$ titres in three of the four mice were comparable with those of mice vaccinated with Qβ-$(NANP)_3$, at over 1000 ELISA units. However, seroconversion was less consistent than that with Qβ-$(NANP)_3$, with one mouse showing no detectable responses even after 6 shots.

The experiment outlined in Fig 5.3.1 A was also designed to test the hypothesis that anti-$(NANP)_6$ responses could be boosted by priming with Qβ-tt-$(NANP)_3$ and boosting with Qβ-tt. This hypothesis derives from the possibility that memory $CD4^+$-T-cells, restimulated by a $CD4^+$ t-cell epitope, can help

stimulate memory B-cells in the absence of the B-cell epitope. Fig. 5.3.1 B shows no evidence of such a boosting effect, suggesting that, under the conditions of this experiment at least, the hypothesis is not true.

5.3.2 Increasing the number of unit repeats in Qβ-(NANP) vaccines

Peptides consisting of 1, 2, 3 or 6 NANP repeats were synthesized and coupled to Qβ to see if increasing the number of NANP repeats would increase the immunogenicity of Qβ-(NANP) vaccines. ELISAs performed on sera from BALB/c mice vaccinated with these Qβ-$(NANP)_n$ vaccines demonstrated an apparently linear relationship between titre and number of NANP repeats (Fig. 5.3.2 A), at least for the first two shots (first shot, r^2=0.986, p=0.007; second shot, r^2=0.992, p=0.0039). The relation still existed, though more loosely, after a third vaccination (r^2=0.890, p=0.0028) but a failure to boost titres in most mice after a fourth shot seems to have terminated the relationship (r^2=0.815, p=0.097). Excluding the non-boosting forth shot, the relationship between number of shots and titre also appears to be linear for Qβ-$(NANP)_2$ (r^2=0.394, p=0.005), Qβ-$(NANP)_3$ (r^2=0.916, p<0.0001) and Qβ-$(NANP)_6$ (r^2=0.643, p<0.0001), though the linearity of this relationship is perhaps only convincing for Qβ-$(NANP)_3$. The avidity index was also highest for mice vaccinated with Qβ-$(NANP)_6$, and higher titres and affinity translated into increasing protection with increasing numbers of NANP repeats (Fig 5.3.2 A).

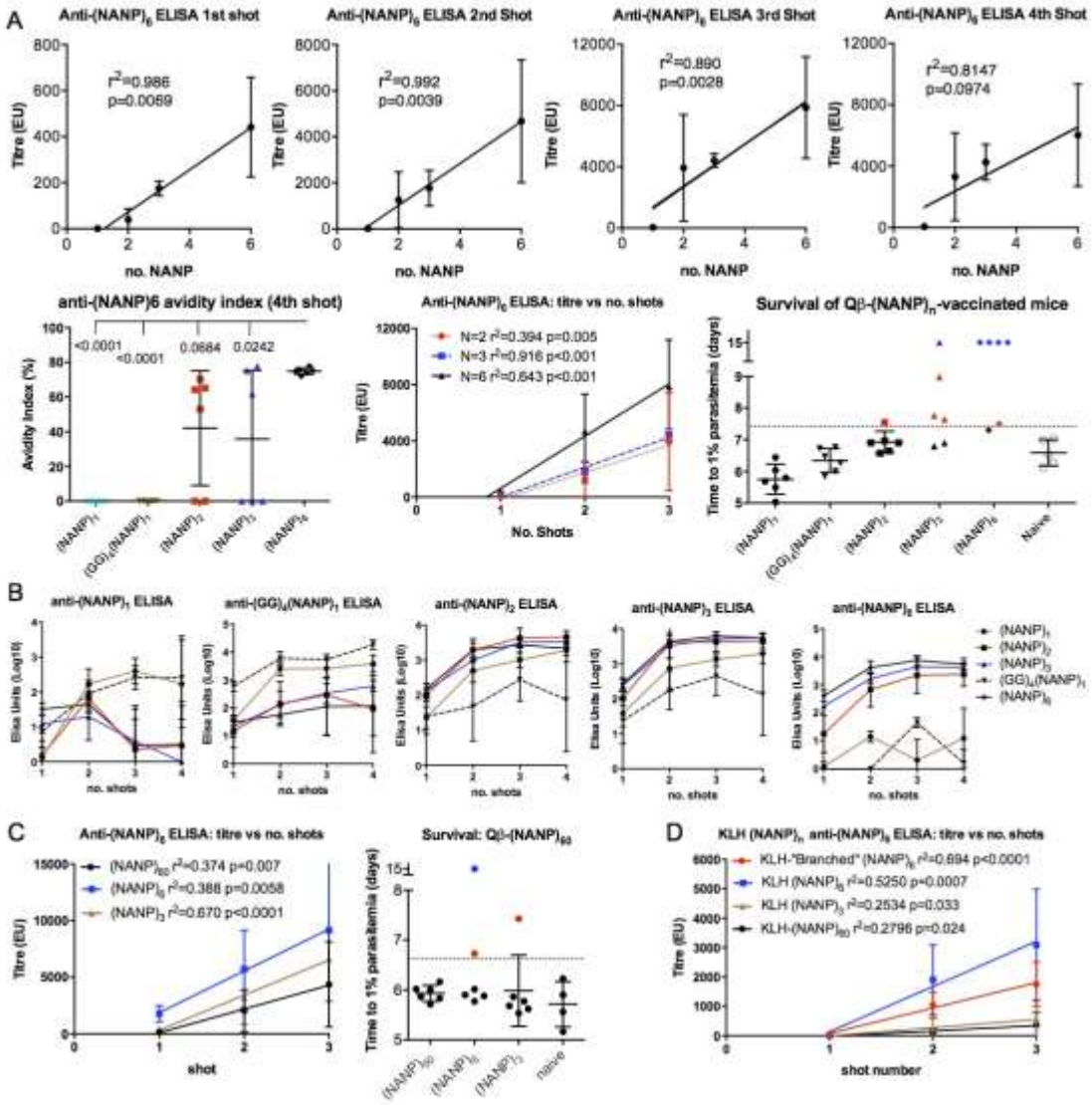


Fig. 5.3.2 Effects on immunogenicity and protective efficacy of increasing the number of unit repeats in Qβ-(NANP) vaccines

Qβ-$(NANP)_n$ VLPs were constructed by synthesizing peptides with varying numbers of (NANP) unit repeats (n=1,2,3,6) and $(GG)_4(NANP)_1$ and chemically coupling them to Qβ. (A) These VLPs were used to vaccinate BALB/c mice (n=6 per group) by intramuscular injection of 3 μg doses in Matrix M adjuvant, with four shots given at three week intervals. Serum was taken two weeks after each shot and used in standard curve ELISAs against $(NANP)_6$. r^2 and p-values from linear regressions are shown. Avidity indices two weeks post-fourth shot was obtained from the ratio of titres using sera treated or untreated with 7 M urea; shown are p-values from ANOVA with Tukey's multiple post-test in comparison to Qβ-$(NANP)_6$-vaccinated mice. Three weeks after the fourth vaccination mice were challenged by intravenous injection of 1000 PfCSP transgenic *P.*

berghei sporozoites. Thin blood smears were taken daily to determine time to reach 1% blood-stage parasitaemia by linear regression. In challenge data, points coloured blue represent sterile protection, and points coloured red represent a delay in time-to1%, defined as time-to-1% greater than average naïve time-to-1% plus 2 standard deviations, with the boundary represented by a dotted line. (B) Serum from mice in (A) were also used to determine antibody titres specific for each variable number of (NANP) repeats, two weeks post shot as before. (C) A construct containing 60 (NANP) repeats was expressed in *E. coli*, purified and chemically coupled to Qβ for comparison to Qβ-$(NANP)_6$ and Qβ-$(NANP)_3$. Vaccinations, ELISAs and challenge were performed as for (A). (D) The $(NANP)_{60}$ polypeptide was chemically coupled to keyhole limpet hemocyanin (KLH), as were $(NANP)_6$ and $(NANP)_3$. For "branched" $(NANP)_6$ the peptide was pretreated for 2 h with carbodiimide before coupling to KLH, in an attempt to induce multimerisation of the peptide. BALB/c mice (n=6 per group) were vaccinated with 10 μg per dose of KLH-peptide at three-week intervals. Standard curve ELISAs against $(NANP)_6$ were performed on sera taken two weeks post-shot. r^2 and p-values from linear regressions are shown. For all graphs, mean ± standard deviation is shown.

Qβ-$(NANP)_1$- and Qβ-$(GG)_4(NANP)_1$-vaccinated mice, though generating no or low responses against $(NANP)_6$ in ELISAs, did generate high titres against $(NANP)_1$ and $(GG)_4(NANP)_1$ peptides as ELISA coating antigens; indeed, they generated higher titres against those peptides than any Qβ-$(NANP)_n$ with two or more NANP repeats (Fig 5.3.2 B). Similarly, Qβ-$(NANP)_2$-vaccination generated the highest titres in an $(NANP)_2$ ELISA (Fig 5.3.2 B). In $(NANP)_3$ ELISAs Qβ-$(NANP)_6$ mice began to produce the highest titres, as with $(NANP)_6$ ELISAs, suggesting that $(NANP)_n$ peptides of one or two repeats have a different conformation from that of three or more (Fig 5.3.2 B).

An attempt was made to see if $(NANP)_{60}$ coupled to Qβ or keyhole limpet hemocyanin (KLH) would give substantially higher titres, and whether the

linearity of the relationship would continue. Both Qβ-$(NANP)_{60}$ and KLH-$(NANP)_{60}$ elicited lower titres than the comparable Qβ- or KLH- coupled $(NANP)_6$ or $(NANP)_3$ vaccines respectively (Fig 5.3.2 C and D). Chemical coupling of the $(NANP)_{60}$ construct may have been less efficient than that with the short peptides; if so this would explain the failure of this construct to generate high anti-$(NANP)_6$ titres. An attempt to multimerize $(NANP)_6$ by 2 h incubation with carbodiimide prior to KLH conjugation produced a vaccine ("KLH-branched $(NANP)_6$") that likewise elicited lower titres than KLH-$(NANP)_6$. Long peptides may couple less efficiently to carriers. A challenge of Qβ-$(NANP)_{60}$ mice with PfCSP transgenic *P. berghei* sporozoites confirmed that the anti-$(NANP)_6$ titres generated by it were insufficient to confer protection (Fig 5.3.2 C).

Theoretically, the relationship between the number of NANP repeats and anti-$(NANP)_6$ titre is not expected to remain linear indefinitely. The point at which the relationship saturates is yet to be experimentally determined, but the mathematical model developed below suggests that it will saturate at some point. This model is partially validated (see Fig. 5.3.3).

The model, relating titre to dose, $\boldsymbol{V}$, number of unit repeats, $\boldsymbol{N}$, and density of peptides, $\boldsymbol{\partial}$, on each VLP, derives from the following assumptions:

1. There is a fixed and finite quantity of epitope-specific B-cells in a naïve mouse, equal to $\boldsymbol{B_{max}}$.
2. The net quantity of antibodies $\boldsymbol{R}$ secreted by a given activated epitope-specific B-cell $\boldsymbol{B_A}$ and descendent B-cells resulting from its proliferation will be a constant: $R = f * B_A$, where $\boldsymbol{f}$ is a function describing the number of B-cells

generated by proliferation of the original activated B-cell B_A and the number of antibodies released by each.

3. The probability that a given epitope on a given VLP binds and activates a B-cell after a VLP/B-cell encounter, $\boldsymbol{p_n}$, is independent of ∂, V, and N.

4. The probability $\boldsymbol{p_a}$ that a given B-cell is activated is independent of the activation status of any other B-cells.

If ∂, V and N are given, then the number of activated B-cells B_A is:

(1) $B_A = B_{max} * p_a$

Since $R = f * B_A$, the maximum number of antibodies released $\boldsymbol{R_{max}} = f*B_{max}$. Therefore:

(2) $R = R_{max} * p_a$

Failure to activate a B-cell, $p_{\text{-}a}$, occurs when each unit epitope on each VLP which encounters a B-cell fails to trigger activation. A given unit epitope on a VLP has a probability p_n of activating the B-cell, and probability $p_{\text{-}n} = 1 - p_n$ of failing to activate the B-cell. On a given VLP there are $\partial*N$ unit epitopes; the probability that they all fail to activate the B-cell is $(1\text{-}p_n)^{\partial*N}$. If p_V is the probability that a VLP encounters a B-cell, then on average a B-cell will have p_V*V encounters. Thus the probability that each unit epitope on each VLP which encounters a B-cell fails to activate it is $p_{\text{-}a} = (1\text{-}p_n)^{\partial*N*pV*V}$. If the dose V is expressed in arbitrary units (e.g. μg or ng) then p_V can for practical purposes be set equal to one. Thus

(3) $p_a = 1 - p_{-a} = 1 - (1 - p_n)^{\partial * N * V}$

and from (2) and (3)

(4) $R = R_{max} * (1 - (1 - p_n)^{\partial * N * V})$

Antibody responses in this thesis are given as titres, in arbitrary ELISA units derived from standard curves. Titre represents the greatest dilution giving a positive response in an ELISA. If we set aside differences in affinity, the amount of antibody giving a positive response 2 or 3 standard deviations above background in any given ELISA will be a constant quantity. Thus the quantity of antibody in the undiluted original will be directly proportional to the titre, so titre ought to represent a good proxy to antibody quantity, in µg or any other unit of measure. Fig. 5.3.3 A supports this.

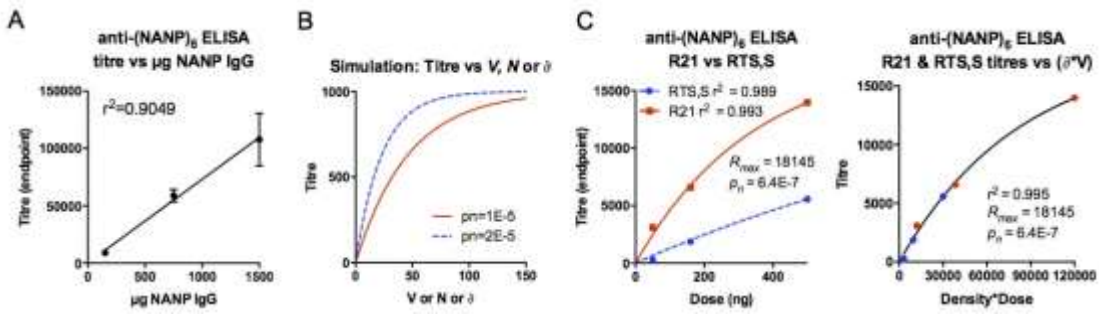


Fig. 5.3.3 Experimental validation of mathematical model of dose-titre relationship.

(A) IgG purified from mice vaccinated with PfCSP-based R21 VLP was injected intravenously into BALB/c mice (n=8 per group) and serum taken for endpoint ELISA five hours later. r^2 value from linear regression. Data from Kat Collins' DPhil thesis. (B) Simulation of dose (V) or number of unit epitopes per surface peptide (N) or density of peptide per VLP (∂) versus titre using $R =$

$R_{max} * (1 - (1 - p_n)^{\partial * N * V})$ where R is titre, R_{max} is maximum titre, and p_n is the probability that a given epitope on a VLP encountering a B-cell activates that B-cell. (C) BALB/c mice (n=10 per group) were vaccinated with R21 and RTS,S, hepatitis B surface antigen-based PfCSP vaccines. R21 has 4 times the density of PfCSP as RTS,S. Three different doses of each vaccine were administered by intramuscular injection and endpoint ELISAs performed on sera taken post-vaccination. Curve-fitting the equation in (B) (using Prism) to R21- and RTS,S-elicited titres generated the graphs shown in (C), and the hypothesis that R21 and RTS,S have different p_n was rejected (p=0.783). Also shown in (C) is the titre against (dose * density) which the model predicts ought to form a single curve of improved r^2. R21 and RTS,S data kindly provided by Florian Brod.

A simulation using equation (4) graphically shows the predicted relation between titre and dose, number of unit epitopes per peptide, or density of peptides on a VLP (Fig. 5.3.3 B). The simulation suggests that the relation will only be linear at small scales, and should in fact be saturating. Florian Brod has performed an experiment using small doses of R21 and RTS,S VLPs. These are hepatitis B surface antigen-based VLPs displaying PfCSP with 19 NANP repeats. R21 displays four times the density of PfCSP that RTS,S displays. The model predicts that p_n will be shared between curves fit to the titres using equation (4). This is the case: asked whether the different or shared p_n fits the data best, Prism returns a shared p_n (p=0.783) (Fig. 5.3.3 C). This is visually demonstrated by plotting titre against $\partial * V$, which gives, as expected, a single curve with high r^2=0.995 (Fig. 5.3.3 C).

5.4 Attempts at a multi-species vaccine based on CSP repeat peptides

The leading malaria vaccine, RTS,S, displays a single antigen (CSP) from a single species of malaria (*P. falciparum*). As many *P. vivax* as *P. falciparum* cases occur each year, and between them *P. falciparum* and *P. vivax* account for 98% of all cases of malaria globally, so a vaccine protecting against both species is desirable. Previously in this chapter (§5.1 and §5.2) short peptides derived from the repeat region of CSP of both *P. vivax* and *P. falciparum* have shown protective efficacy when coupled to Qβ. In the present section the effects on immunogenicity and protective efficacy of combining those short peptide vaccines are investigated.

Figure 5.4.1 shows the effect of combining the AGDR tetramer from the PvCSP-210 repeat region with the NANP tetramer from PfCSP. Fusion peptides with both epitopes, mixing of separate VLPs, and co-display of both epitopes on a single VLP were used as the three methods of delivery.

The effects on immunogenicity of using fusion peptides differ depending on whether the NANP epitope is proximal to or distal from the Qβ VLP core. In most cases, titres against $(AGDR)_3$ or $(NANP)_6$ decrease to some extent as a result of presenting both on a single peptide, although the decrease is often statistically non-significant. When AGDR is proximal to the Qβ core, as in Qβ-$(AGDR)_2(NANP)_2$ and Qβ-$(AGDR)_3(NANP)_3$, (Fig. 5.4.1 A and C), there is a small and non-significant decrease in anti-$(AGDR)_3$ titres, but in the case of Qβ-$(AGDR)_2(NANP)_2$ there is a significant decrease in anti-PvCSP-210 titres ($p=0.0029$, with over an order of magnitude difference in titres). The effects on anti-$(AGDR)_3$ are similar if the $(AGDR)_3$ epitope is distal from the Qβ core, as in Qβ-$(NANP)_3(AGDR)_3$ (Fig 5.4.1 B and C), with a small but significant decrease in

anti-$(AGDR)_3$ seen in one experiment (Fig. 5.4.1 C, p= 0.03) and a small but non-significant increase in anti-$(AGDR)_3$ titres in another experiment (Fig. 5.4.1 C). In contrast, there is no difference in the anti-PvCSP-210 titres elicited by Qβ-$(NANP)_3(AGDR)_3$ and Qβ-$(AGDR)_3$ (Fig. 5.4.1 B), compared to the large decrease in anti-PvCSP-210 titres seen when Qβ-$(AGDR)_2(NANP)_2$ is used.

The abrogation of anti-$(NANP)_6$ titres when $(NANP)_3$ is proximal to the Qβ core is more marked. With Qβ-$(NANP)_3(AGDR)_3$, in both experiments there is an order of magnitude decrease in anti-$(NANP)_6$ titres (Fig. 5.4.1 B, p=0.001; C, p=0.002); whereas when $(NANP)_3$ is distal from the Qβ core (Qβ-$(AGDR)_3$-$(NANP)_3$), there is no effect on anti-$(NANP)_6$ titres (Fig. 5.4.1 C). When Qβ-$(AGDR)_2(NANP)_2$ is used there is a small but significant decrease in anti-$(NANP)_6$ titres (Fig. 5.4.1 A, p=0.03).

Mixing and co-injection of separate Qβ-$(AGDR)_3$ and Qβ-$(NANP)_3$ VLPs has no discernable effect on anti-$(AGDR)_3$ or anti-$(NANP)_6$ titres compared to injection of the respective single-component VLPs alone (Fig. 5.4.1 C). A single-component Qβ(AGDR)(NANP)(mix) VLP was produced by simultaneously coupling separate $(AGDR)_3$ and $(NANP)_3$ peptides to Qβ. This resulted in a particle slightly less immunogenic against $(AGDR)_3$ (a two- to three-fold decrease in anti-$(AGDR)_3$ titre, p=0.047) but it was as immunogenic against $(NANP)_6$ as the single-component, single-epitope particles (Fig. 5.4.1 C).

Challenge experiments gave outcomes consistent with immunogenicity, with Qβ-$(AGDR)_2$ and Qβ- $(NANP)_2$ showing no efficacy, nor Qβ-$(AGDR)_2(NANP)_2$ with a simultaneous challenge of PvCSP-210/PvTRAP and PfCSP *P. berghei* transgenic sporozoites (Fig. 5.4.1 A). Qβ-$(AGDR)_3$ and Qβ-$(NANP)_3$ conferred

partial protective efficacy, but a challenge using both PvCSP-210/PvTRAP and PfCSP *P. berghei* simultaneously on Qβ-$(NANP)_3(AGDR)_3$-vaccinated mice resulted in no discernable protective efficacy, probably because of the poor anti-$(NANP)_3$ titres elicited using this fusion peptide construct (Fig. 5.4.1 B). In the third experiment (Fig. 5.4.1 C) all mice were challenged with PfCSP transgenic *P. berghei* sporozoites, but efficacy was modest, with only a delay in time to reach 1% blood-stage parasitaemia seen in three mice, and no sterile protection, and only Qβ-$(NANP)_3$-vaccinated mice showing a significant difference in time-to-1% compared to Qβ-$(AGDR)_3$-vaccinated control mice ($p= 0.0085$, ANOVA with Bonferroni's multiple comparisons test).

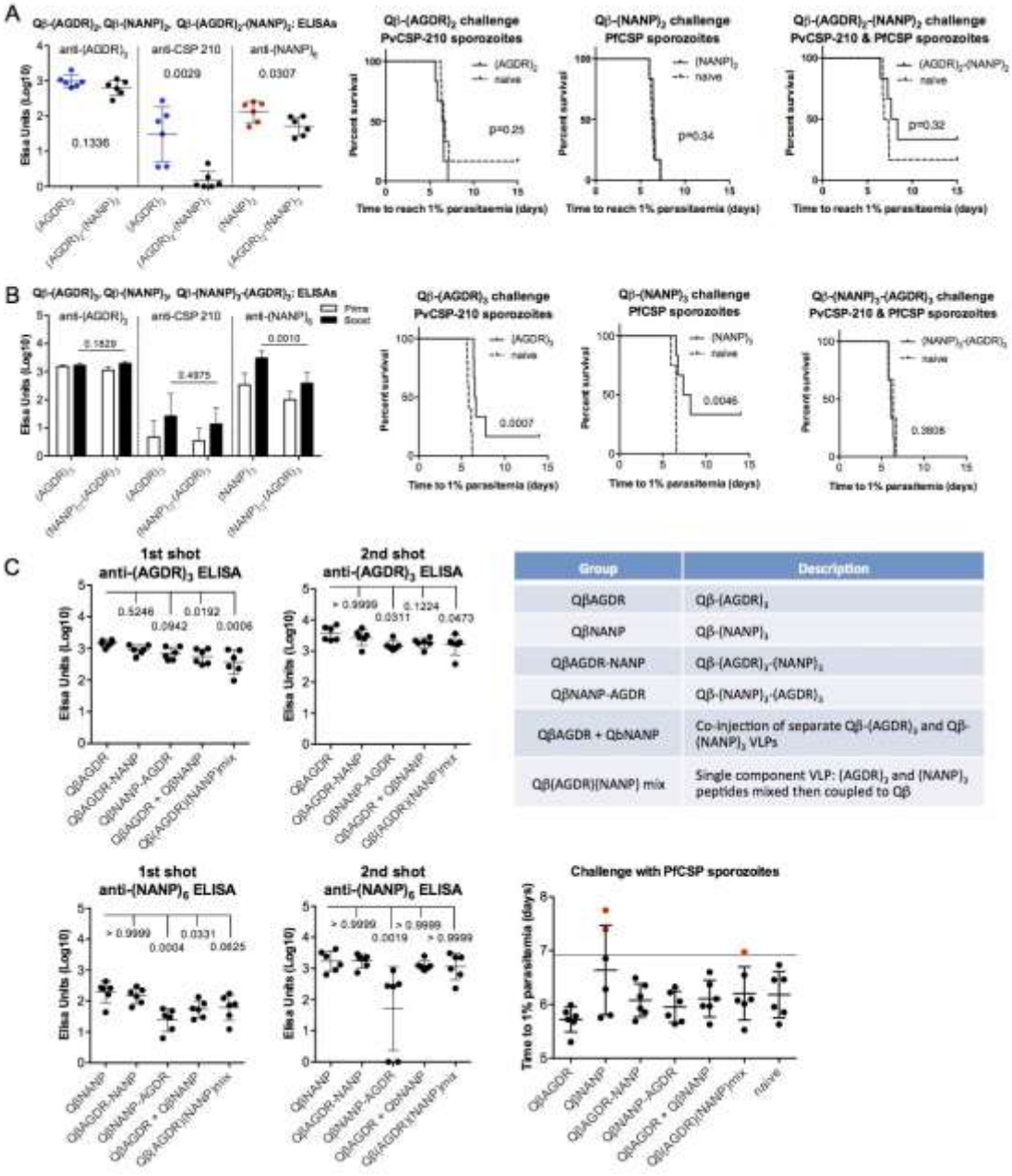


Fig. 5.4.1 The effects of combining CSP repeat tetramers on immunogenicity and protective efficacy

BALB/c mice (n=6 per group) were vaccinated by intramuscular injection of Qβ-peptide vaccines displaying varying numbers and combinations of the *P. vivax* CSP repeat region-derived tetramer AGDR or the *P. falciparum* CSP repeat region tetramer NANP. Matrix M adjuvant was used. Serum for standard curve ELISAs was taken two weeks post-shot. Mice were challenged by intravenous injection of 1000 sporozoites of either PvCSP/PvTRAP or PfCSP transgenic *P. berghei;* challenge was performed three weeks after the second vaccination. Time to reach 1% blood-stage parasitaemia was calculated by linear regression from thin blood smears taken daily. Numbers

on graphs represent p-values for t-tests (when comparing two groups) or ANOVA with Bonferroni's multiple comparisons test (when comparing three or more groups). P-values on survival curves from log-rank tests. (A) $(AGDR)_2$, $(NANP)_2$ or the fusion protein $(AGDR)_2(NANP)_2$ were used as peptides on Qβ vaccines. Two shots at 8 μg per dose were given 1 week apart. (B) $(AGDR)_3$, $(NANP)_3$ or the fusion protein $(NANP)_3(AGDR)_3$ were used as peptides on Qβ vaccines. Two shots of 20 μg per dose were used with a three-week prime-boost interval. (C) Mice were vaccinated with peptides as shown in the table, using 3 μg per dose with a 3 week prime-boost interval.

In §5.1 peptides with two of the natural nonamer unit repeats from PvCSP-210 and PvCSP-247 were shown to confer protection on mice against challenge; and in §5.3.2 protective efficacy was also obtained using $(NANP)_6$ displayed on Qβ. Here I describe a study using a single-component VLP presenting all three peptides on a single Qβ particle by chemically coupling the three peptides simultaneously (called the "Triple VLP", Fig. 5.4.2).

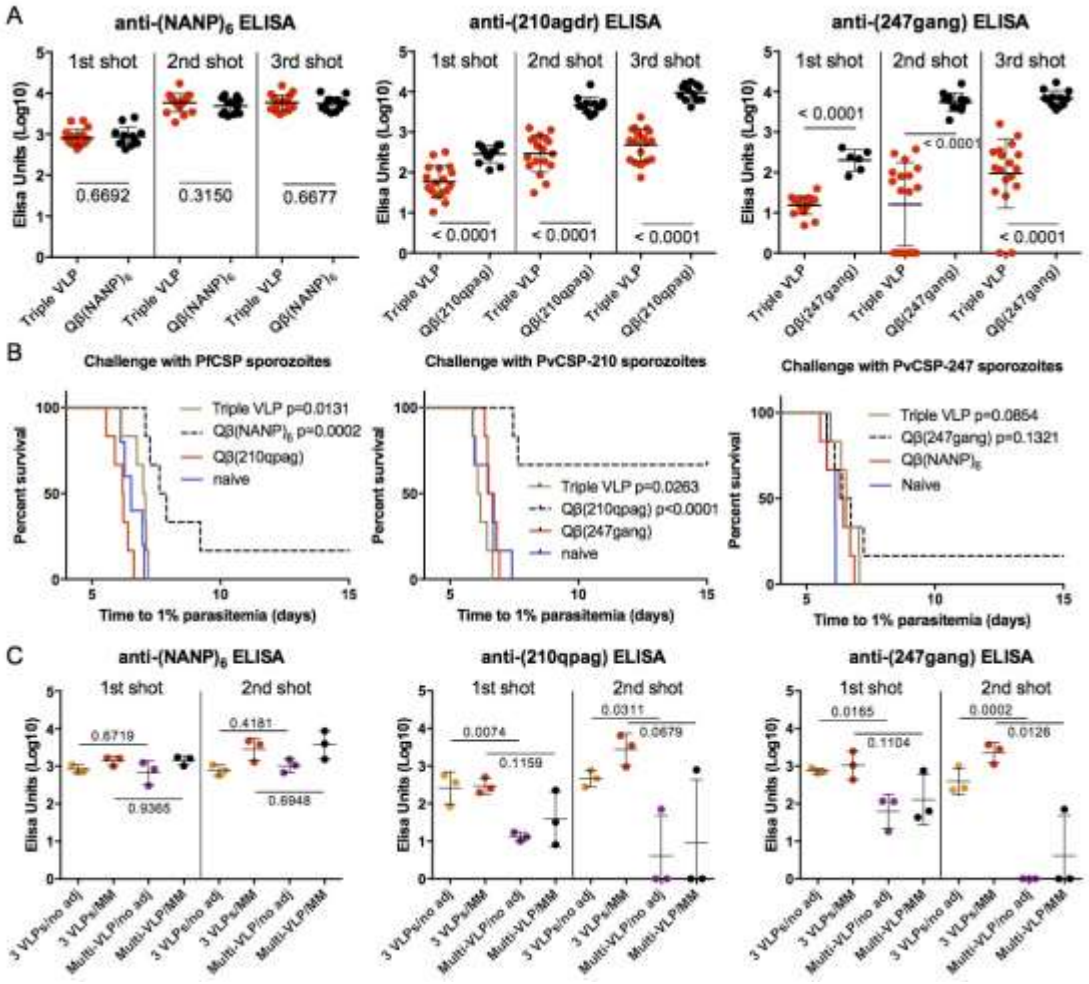


Fig. 5.4.2 Effects of combining natural CSP repeats on immunogenicity and protective efficacy

BALB/c mice were vaccinated by intramuscular injection of Qβ-peptide vaccines presenting two to six copies of CSP unit repeats from PfCSP, PvCSP-210 or PvCSP-247 or combinations of these. (A) Standard curve ELISAs using serum from mice two weeks post-vaccination (3 μg per dose, 3 week prime-boost interval). $(NANP)_6$, (AGDRADGQPAGDRADGQPAG) ("210qpag", based on PvCSP-210 repeat region) or (AGNQPGANGAGNQPGANG) ("247gang" based on PvCSP-247 repeat region), or all three simultaneously coupled to form a single-component vaccine, ("Triple VLP"). Matrix M adjuvant was used; n=12 to 18 per group. (B) Mice from (A) were challenged three weeks after the final vaccination with 1000 transgenic *P. berghei* sporozoites expressing either PfCSP, PvCSP-210 or PvCSP-247 as indicated. Thin blood smears were taken daily to determine time to reach 1% parasitaemia (by linear regression). P-values from log-rank test against naive and control-vaccinated mice are shown. (C) Mice (n=3 per group) were vaccinated

with a mixture of 1.5 μg of each of the three single-component VLPs described in (B), or with a single-component "Multi-VLP" presenting eight antigens including those described in (B). A three-week prime-boost interval was used with or without Matrix M. Serum was taken two weeks post-vaccination for standard curve ELISAs. Numbers on graphs represent the p-values from t-tests between indicated groups.

Fig. 5.4.2 A shows that, while anti-$(NANP)_6$ titres are unaffected by presentation on the Triple VLP, anti-210agdr and anti-247gang titres are very adversely affected, abrogated by an order of magnitude or more ($p<0.0001$) compared to the respective single-epitope vaccine. Both the Triple VLP and Qβ-$(NANP)_6$ showed evidence of protective efficacy against PfCSP *P. berghei* challenge ($p=0.01$ and 0.0002 respectively), though Qβ-$(NANP)_6$ was significantly more protective than the Triple VLP ($p=0.0036$). In contrast, although Qβ-(210qpag) conferred significant protection against PvCSP-210 challenge ($p<0.0001$), the Triple VLP conferred no protection, reflecting the abrogation in anti-(210qpag) titres. Neither the Triple VLP nor Qβ-(247gang) showed statistically significant protective efficacy in this experiment (Fig. 5.4.2 B), though Qβ-(247gang) did confer sterile protection on one mouse.

In Chapter 4 antigenic interference when combining Rv21 with viral-vectored PvTRAP was only seen in the presence of Matrix M and not other adjuvants. Since all the experiments described in this chapter used Matrix M as an adjuvant, a further experiment was conducted to determine its potential involvement in the immunodominance exhibited by $(NANP)_6$. Fig. 5.4.2 C shows that the same pattern of immunodominance seen with the Triple VLP is seen with a "Multi-VLP" presenting the same three peptides and five others

(described in §6.1 below), and that the addition of Matrix M adjuvant makes no difference.

Discussion

In this chapter short peptides derived from CSP repeat regions of *P. falciparum* and *P. vivax,* coupled to Qβ, were shown to be highly immunogenic and protective against transgenic *P. berghei* challenge. This lays the groundwork for the development of a single-component malaria vaccine consisting of linear B-cell epitopes displayed on a virus-like particle.

Short peptides representing 2-3 unit repeats from PfCSP or PvCSP VK210 and PvCSP VK247 can induce about 40% sterile protection, or in the case of two canonical repeats from PvCSP-VK210, 100% protection (§5.1). An $(AGDR)_3$ peptide coupled to Qβ, based on a tetramer epitope within the PvCSP-210 nonamer unit repeat, induced partial protective immunity, the first time this has been demonstrated (§5.2.1). Qβ-$(AGDR)_3$ was also able to enhance protective efficacy when used to boost mice primed with full length PvCSP (§5.2.2). Proximity of the GDRA motif to KLKQP, and interference of antibodies with the function of that conserved region, was hypothesized to explain the high levels of protection seen with the PvCSP-VK210 nonamer and AGDR-based Qβ-peptide vaccines. Alternative CSP repeat tetramers from PvCSP-VK247 and PfCSP were also tested using the Qβ-peptide platform, but none were found to confer any protection on mice against challenge (§5.2.1). In experiments investigating ways to optimise the immunogenicity and protective efficacy of short peptide VLP vaccines, the universal T-cell epitope from tetanus toxin, P2, was fused to $(NANP)_3$ and found to enhance the affinity of anti-NANP antibodies (§5.3.1). A separate experiment demonstrated the importance of affinity in determining the outcome of challenge, which strongly associates with protection when anti-NANP titres do not (§5.3.1). Increasing the number of NANP repeats per peptide

also improves immunogenicity (§5.3.2), and a positive linear relation between the number of repeats and the anti-$(NANP)_6$ titre was found (§5.3.2). A novel mathematical model, partially validated, predicted a saturating relationship, but the number of NANP repeats at which this begins to occur could not be inferred. Finally, attempts were made at cross-species vaccines presenting *P. falciparum* and *P. vivax* CSP repeat epitopes. Fusion peptides presenting AGDR and NANP repeats were found to suffer from immune interference and could not protect against challenge with two PvCSP-VK210 and PfCSP replacement *P. berghei* transgenic sporozoites. A Qβ VLP displaying PvCSP-VK210 and PvCSP-VK247 nonamer repeat peptides and $(NANP)_6$ saw strong immunodominance by $(NANP)_6$, demonstrating that this will be the main hurdle towards producing a cross-species vaccine.

These findings are consistent with previous studies where partial protective efficacy was obtained using short CSP-repeat peptides as vaccines. $(NANP)_3$ coupled to tetanus toxin has protected two human volunteers against *P. falciparum* challenge (365), and a multiple antigen construct displaying two copies of the canonical PvCSP-VK210 sequence has conferred sterile protection on up to 42% of *Saimiri boliviensis* monkeys, though unvaccinated control groups were not used, thus not permitting full infectivity of the *P. vivax* sporozoites to be confirmed (442, 443). To my knowledge, protective efficacy using a short peptide vaccine based on the PvCSP-VK247 canonical unit repeat has not previously been shown in any animal model before now; a multiple-antigen construct including this epitope has previously been produced, and although (weakly) immunogenic in mice, the antibodies so generated did not recognise PvCSP-VK247 *P. vivax* sporozoites in an immunofluorescence assay (660). In this

chapter, however, it has been shown that the PvCSP-247 repeat epitope, as a short peptide displayed on Qβ, was highly immunogenic and protected mice against challenge with PvCSP-247 transgenic *P. berghei* sporozoites (§5.1).

The AGDR epitope within the canonical PvCSP-VK210 nonamer unit repeat has received some attention from the vivax malaria vaccine community since a paper showed that *Saimiri* monkeys vaccinated with a recombinant PvCSP protein did not generate antibodies against this tetramer, and were not protected; but that a monoclonal specifically recognising AGDR was protective (439). Responses to the AGDR tetramer were later associated with protection in *Saimiri* monkeys using a multiple antigen construct to deliver the nonamer epitope (443). The only pre-erythrocytic vivax vaccine to be tested by controlled human malaria infection, VMP001 (453), does not confer any sterile protection and generally fails to generate a detectable anti-AGDR response, while virus-like particle (455) or nanoparticle (661) display of VMP001 can, although in the former case 100% seroconversion was not obtained. Thus the protective efficacy seen here for the first time with Qβ-$(AGDR)_3$-vaccinated mice, and the enhancement in protective efficacy it provides when used to boost full-length PvCSP-primed mice, is encouraging, validating AGDR-peptide based vaccination as a strategy for improving the protective efficacy of PvCSP-VK210-based vaccines. AGDR-peptide vaccination has been used before, with *Aotus* monkeys and BALB/c mice vaccinated with $(AGDR)_6$ coupled to keyhole limpet hemocyanin (440). Although mouse sera recognised the native PvCSP sequence and *P. vivax* sporozoites by immunofluorescence, that from *Aotus* monkeys did not. Thus it remains to be seen whether and how an AGDR-peptide based

vaccination regime, alone or in heterologous prime-boost to 'focus' the immune response to this protective epitope, would enhance protection in humans.

No equivalent tetramer within the canonical PvCSP-VK247 nonamer unit repeat sequence has yet been found. Two candidate tetramers from this allelic variant were tested as Qβ-peptides, one holding a possibly analogous position to AGDR within the nonamer unit repeat, and the other based on the four amino acids proximal to the conserved KLKQP region in PvCSP-VK247. The latter tetramer was selected on the hypothesis that AGDR-specific antibodies protect by binding adjacent to this region and by that means sterically interfere with its (unknown) function. Though both PvCSP-VK247 Qβ-tetramers generated antibodies against the peptides displayed on the vaccines, most mice failed to generate antibodies recognising the native PvCSP-VK247 protein or peptides based on the nonamer unit repeat, and so, unsurprisingly, no protective efficacy was seen (§5.2.1). This made it difficult to test either of the hypotheses explaining the mechanism of AGDR-mediated protection. Likewise, PfCSP tetramers alternative to NANP, such as the NVDP tetramer, were shown to be entirely unprotective (§5.2.1). In this latter case it is not known whether the antibodies generated could recognise the native PfCSP sequence. In Chapter 6, however, some further evidence is presented consistent with the hypothesis that AGDR-specific antibodies mediate protection by binding adjacent to the conserved KLKQP motif in the N-terminal domain (§6.1).

The large difference in protective efficacy, of 0% and 100% sterile protection respectively for full-length and truncated (missing the N-terminal domain) forms of PvCSP-VK210 (§5.2.2) has not, to my knowledge, previously been seen nor investigated. This was surprising given that equivalent titres

against full-length PvCSP and $(AGDR)_3$ seen with both the full and truncated forms. The only difference in immunogenicity was in the affinity of the antibodies, with full-length PvCSP-vaccinated mice generating antibodies with significantly greater affinity for the full-length PvCSP. This suggests that there is a conformational difference between the full-length and N-terminal-truncated forms of PvCSP. The N-terminal domain of PfCSP has been shown to be naturally cleaved prior to invasion resulting in an altered conformational state, with the N-terminal domain apparently masking the C-terminal domain when present, and exposing that domain when absent, thus allowing the C-terminal region to perform its hepatocyte-invasion functions (346). The repeat region of PfCSP has been shown to possess multiple conformations (662) and it has been suggested that a constrained version of the NANP repeat, for instance by using a cyclized $(NPNA)_3$ peptide as the immunogen, is required to maintain a β-turn absent in linear forms and to generate antibodies which recognise the native protein (663-666). Thus it is possible that antibodies raised against the repeat region when it is in its full-length conformation do not bind and cannot neutralize the parasite when it displays CSP in its truncated conformation. This is consistent with the preliminary data shown in Chapter 4, where inclusion of the N-terminal domain, on the CSVS-like VLP, seems to decrease immunogenicity and protective efficacy compared to Rv21 (§4.5). It could also explain why VMP001, a full-length chimeric PvCSP vaccine, shows low protective efficacy (453), whereas RTS,S, displaying an N-terminal truncated form of CSP, is highly protective in clinical trials (246), although the latter and not the former is a virus-like particle, almost certainly enhancing immunogenicity. Further work will need done to verify this effect.

If short-peptide VLPs displaying malaria B-cell epitopes are to play some role in the future vaccine development, it would be useful to know how to optimise immune responses against them. Malarial helper T-cell epitopes, or those from unrelated species such as the universal T-cell epitope from tetanus toxin, P2, have been used with most MAPs displaying CSP repeat peptides (417-419, 421, 441-443, 659, 667, 668), because without T-cell help the immune responses are very weak or absent (441, 659). With the Qβ-peptide vaccines used in this thesis, this is evidently not an issue, as high titres were always achieved against the peptide presented on the VLP. Nevertheless, fusion of the P2 epitope to $(NANP)_3$ for presentation on Qβ was tested for improvement in immunogenicity. Titres were enhanced, but only slightly and the improvement was not statistically significant (§5.3.1). The affinity of anti-NANP titres was, however, significantly improved if P2 was present, which could be of value because this chapter also presented data that show that affinity determines challenge outcome when anti-NANP titres are equal (§5.3.1). Further studies could look at the effects on immunogenicity of other T-cell epitopes. This chapter also looked at the possibility of exploiting $CD4^+$ memory T-cell help as a means of boosting anti-NANP titres when encountering the $CD4^+$ epitope only, and not NANP. There is conflicting evidence as to whether this is a theoretical possibility (669-672), and under the conditions of this experiment, does not appear to hold true. A longer prime-boost interval, allowing a greater role for memory $CD4^+$ T-cells in stimulating a secondary response, might be a better experimental test of the hypothesis. If the hypothesis were true, this would potentially enable exploitation of natural infection (say, of pathogens common in sub-Saharan Africa) to boost anti-malarial responses without further vaccinations. Immunity

to non-malarial pathogens has recently been exploited to enhance immunogenicity to a malaria vaccine, with pre-existing OVA or murine CMV memory $CD4^+$ T-cells shown to enhance immune responses to a CSP vaccine which included $CD4^+$ from OVA or CMV (673), but this is not identical to the strategy proposed and tested in this chapter, as in the former case B- and T-cell epitopes are presented simultaneously.

This chapter has also shown an apparently linear relationship between the number of NANP repeats and anti-NANP titres (§5.3.2). It has previously been shown that a PfCSP vaccine with 19 NANP repeats was more immunogenic and protective than one with 5 repeats (658). This was shown again here with short NANP peptides on Qβ with 1, 2, 3 and 6 NANP repeats, which showed increasing immunogenicity and protective efficacy with the number of repeats. The apparently linear relationship has not previously been observed, for no experiment has used more than two alternate NANP repeat numbers. The mathematical model I have presented, relating titre to peptide density, number of unit repeats per peptide, and dose, is apparently novel, and predicts a saturating effect, with extra NANP repeats ultimately failing to significantly increase titres. Increased density of NANP on a VLP has previously been associated with improved immunogenicity (675) and indeed antigen density also appears to dictate immune responses to blood antigens (676) The model accurately fits data from R21 and RTS,S varying dose and density, but it remains to be seen whether it also holds true when the number of unit repeats is increased. It may be an effect particular to NANP, as the effect was not seen when increasing the number of "KLKQP" repeats (data not shown). If the model holds for NANP repeats, then the main benefit of longer NANP sequences presented at

higher densities on VLPs will be dose-sparing, helping reduce the cost of the vaccine, and hence increase its cost-effectiveness. An attempt to couple a construct containing 60 NANP repeats was attempted in this chapter, but was less immunogenic than six NANP repeats, possibly because of inefficient coupling to Qβ. This $(NANP)_{60}$ construct genetically fused to Hepatitis B surface antigen, instead of the 19 NANP repeats used in R21 (189) and RTS,S (188), could enhance immunogenicity and protective efficacy; as could the coupling to VLPs of MAPs displaying 4-8 $(NANP)_6$ repeats, which would increase peptide density 4-8 fold. Further experiments testing the mathematical model by dose variation of VLPs displaying peptides with different numbers of NANP repeats would be interesting as these could shed light on whether the assumptions on which the model is built are valid under these conditions. As the model is based on very simple probabilistic assumptions, verification or falsification of the model would give us insights into the basic biology of B-cell responses to antigens.

Finally, the Qβ-peptide platform was used in this chapter to create a multi-antigen VLP displaying short peptides from the *P. vivax* CSP-VK247, CSP-VK210 and *P. falciparum* CSP repeat regions. Fusion proteins presenting both AGDR and NANP failed to protect against simultaneous challenges with both PvCSP-210 and PfCSP transgenic *P. berghei* sporozoites, despite the single-epitope VLPs conferring partial protective efficacy (§5.4). This was consistent with impaired immunogenicity elicited by the fusion AGDR-NANP constructs: in general, but not always, the epitope proximal to the VLP core generated lower titres than the equivalent single-epitope peptide. A different strategy, coupling short peptides based on the *P. vivax* CSP-210 and PvCSP-247 nonamer unit repeats and the *P. falciparum* NANP repeat to the same Qβ VLP, also saw immune

interference, with anti-PvCSP-210 and especially anti-PvCSP-247 titres decreased substantially in the presence of $(NANP)_6$ (§5.4). This ablation of titres occurred both with and without Matrix M, so unlike the immune interference seen in Chapter 4 between Rv21 and viral-vectored PvTRAP, immunodominance by NANP is not associated with Matrix M adjuvant. The only other study combining *P. vivax* and *P. falciparum* CSP repeats, to my knowledge, is that of Udhayakumar *et al.,* (660). The authors report three multiple antigenic constructs, combining vivax-like with either PvCSP-VK210, PvCSP247 or PfCSP repeats. Although in the absence of single-epitope controls it is difficult to infer immune interference, it does appear at least that the vivax-like epitope suffers some immune interference when presented with PvCSP-VK247 and PfCSP repeat epitopes, compared to when presented with PvCSP-VK210 repeats. No challenge was performed, and so the work in this chapter represents the first such attempt, using transgenic rodent malaria models with replacement of the native PbCSP with human malarial CSPs. Further work will need done optimizing the display of the peptides to avoid immune interference; this is further discussed in Chapter 6.

In summary: the groundwork has been laid for developing a single-component multi-antigen vaccine. A model for examining the protective efficacy of short malarial peptides coupled to the Qβ VLP has been established, and validated by showing that they can confer up to 100% sterile protection in mice against transgenic *P. berghei* challenge. Some peptides, such as the epitope AGDR associated with protection against *P. vivax*, and the PvCSP-VK247 nonamer unit repeat, have been shown for the first time to be capable of conferring sterile protection on vaccinated animals. A novel strategy using ADGR peptides to boost

native PvCSP-primed mice is shown to enhance protection, opening the door to using this strategy in PvCSP-based vaccines. There is scope for optimizing the immunogenicity of these short-peptide Qβ vaccines, and initial steps were taken with use of helper T-cell epitopes and extending the number of unit repeats. A single-component vaccine displaying multiple *P. vivax* and *P. falciparum* CSP repeat epitopes demonstrated the greatest potential obstacle to such a vaccine: immunodominance by one epitope. The following chapter focuses on the search for other linear B-cell epitopes capable of generating neutralising antibodies as the next step on the path towards a multi-epitope single-component malaria vaccine with enhanced protective efficacy.

Chapter 6

Towards a single component multi-epitope vaccine.

Part 2: Alternatives to CSP repeat peptide vaccines

Introduction

In this thesis, enhanced efficacy from combining pre-erythrocytic malaria vaccines has been predicted in theory (Chapter 3) and demonstrated in practice with the combination of Rv21 and viral-vectored PvTRAP (Chapter 4). Although potentially more efficacious, combination vaccines with multiple components are likely to be expensive (654). Chapter 5 set the groundwork for developing a single-component multi-antigen malaria vaccine by establishing that short peptides from the CSP repeat region, displayed on the Qβ virus-like particle, can be highly protective. This chapter reports the search for other linear B-cell epitopes from pre-erythrocytic malaria antigens, capable of generating neutralising antibodies. Ultimately the aim is to combine these with CSP repeat region peptides to produce a single component vaccine of enhanced protective efficacy. Alternative (non-repeat region) epitopes from CSP are first investigated, and then two novel methods of screening linear B-cell epitopes for use as vaccines are described. The first method screens sera from mice vaccinated with a putative antibody-mediated vaccine (PvTRAP) to generate data on linear B-cell epitopes associated with protection; short peptide candidates are then screened as Qβ-peptide vaccines for protective efficacy. The other method exploits conservation in sporozoite invasion proteins to design peptides that may interfere with the function of the proteins, and hence neutralize sporozoites.

Both methods, if validated, could have important implications for vaccinology beyond malaria vaccine development. The rapid identification of potentially neutralising linear B-cell epitopes, including cryptic epitopes, would allow quick and easy screening of their potential protective efficacy, of any enhancement of efficacy in combination, and whether antigenic interference occurs. This would allow rapid pre-clinical development of single-component multi-epitope vaccines of enhanced protective efficacy for any disease model.

The repeat region of CSP has long been known to be a target of neutralising antibodies (362, 363). The first evidence that there were such targets outside of the CSP repeat region came from an experiment where sera from *Saimiri* monkeys immunized with PvCSP-VK210 vaccines were able to inhibit invasion of hepatocytes by *P. vivax* VK247 sporozoites (674). The allelic variants PvCSP-VK210 and PvCSP-VK247 share only the N-terminal- and C-terminal-domains in common; the repeat region is quite different between the two proteins, and therefore the neutralising antibodies cannot have been repeat-region specific. A peptide based on the C-terminal Region II, based around the conserved CSVTCG motif, forming part of the TSR domain implicated in invasion, (343, 345, 594), was later shown to confer protection on C57BL/6 mice challenged with *P. berghei* sporozoites (348). Another study vaccinating with the complete C-terminal domain of *P. falciparum*, however, showed no protective efficacy in mice challenged with PfCSP transgenic *P. berghei* sporozoites (658). In the N-terminal domain, a monoclonal antibody recognising a linear sequence including the conserved Region I KLKQP motif was found to be potently neutralising (349). This region is implicated both as a site of proteolytic cleavage essential for invasion (346, 675) and in hepatocyte binding (344). Vaccinating

with full-length PfCSP, including the N-terminal domain, does nothing to improve protection compared to a truncated PfCSP missing the N-terminal domain, however (658); and peptides representing parts of this region in PfCSP delivered using a virus-like particle are only weakly protective at best, sometimes reducing liver load (676). However, relatively long peptides spanning the Region I and the Region II motifs did induce sterile protection in about half of mice challenged with *P. berghei* (677). In this chapter, peptides based around *P. vivax* and *P. falciparum* Region I or Region II, or CSP-derived peptides showing hepatocyte-binding properties (347) are coupled to Qβ and screened in challenge experiments for protective efficacy.

TRAP vaccine efficacy is known to be mediated by $CD8^+$ T-cells (476, 487, 489, 492) but there is some evidence suggesting a role for antibodies in protection as well. Antibodies to PfTRAP associate with protection from clinical malaria in Kenyan children (144, 678), though it has been argued that natural immune responses to pre-erythrocytic antigens are a marker of exposure rather than mediating protection (146). However, anti-TRAP antibodies inhibit gliding motility in *P. berghei* (498) and inhibit *P. falciparum* hepatocyte invasion *in vitro* (462). Although antibodies raised against synthetic peptides representing PyTRAP epitopes have failed to protect *in vivo* (463), passive transfer of anti-PvTRAP antibodies have been shown to protect mice from malaria challenge (497). In this chapter linear B-cell epitopes from PvTRAP are identified and screened for protective efficacy. Screening sera of animals immunized with a putative malaria vaccine candidate (PfSEA) against short peptides has previously been used to generate information about linear B-cell epitopes associated with protection (679), but in this chapter, for the first time, that technique is extended

to downselect linear B-cell epitopes as vaccine candidates tested for protective efficacy in a challenge experiment, using whole PvTRAP as the original immunogen.

Another novel technique for discovering neutralising linear B-cell epitopes within sporozoite invasion proteins is also pioneered in this chapter. This technique is based on the hypothesis that highly conserved regions of proteins are conserved because they play some functional role (680). Thus if conserved regions in proteins are synthesized as peptides, coupled to a virus-like particle such as Qβ, and used to vaccinate animals to generate antibodies, and if those antibodies raised against the peptides are able to recognise that sequence in the context of the native protein, then those antibodies should have an increased probability of being neutralising by virtue of their sterically interfering with the function of that protein. In this chapter this novel method is applied in an attempt to discover neutralising linear B-cell epitopes from *P. berghei* sporozoite invasion proteins. 12 peptides representing conserved amino acid sequences within the primary structure of ten sporozoite proteins associated with liver-stage invasion are coupled to Qβ VLPs, and challenge with *P. berghei* used to screen those peptides for protective efficacy. The proteins are initially selected using information about sporozoite surface expression (609) since the proteins must at least be surface expressed for antibody neutralisation to occur. Then, if there is further evidence that the proteins are involved in invasion and/or that antibodies against them can inhibit their function, conserved regions shared between malaria species are identified by alignments between sequences from PlasmoDB (plasmodb.org). The conserved peptides, coupled to Qβ, are screened for protective efficacy in mice using *P. berghei* sporozoite challenges.

The proteins used, their initial discovery and the evidence that antibodies against them can be protective are presented in Table 6.1 below.

Table 6.1.1 *P. berghei* proteins used for conservation-based screening of linear B-cell epitopes for protective efficacy

Protein	Accession no.	Initial description	Evidence for role in liver-stage infectivity and as vaccine
PBLP Plasmodium BEM46-like protein	A0A113RBV9	(681)	(681)
SSP3 sporozoite surface protein 3	PBANKA_1425200	(682)	(682)
SIAP 1 sporozoite invasion-associated protein 1	PBANKA_1006200	(683)	(683, 684)
Maebl merozoite adhesive erythrocytic binding protein	PBANKA_0901300.2	(685)	(503, 510, 686, 687)
RON4 rhoptry neck protein 4	PBANKA_0932000	(688)	(689)
P113 surface protein P113	PBANKA_1022500	(690)	(691)
PLP1 sporozoite micronemal protein essential for cell traversal	PBANKA_1006300	(692)	(693-695)
RON3 rhoptry neck protein 3	PBANKA_1464900	(696)	none*
Falstatin	PBANKA_0813000	(697)	(698-700)
TRSP Thrombospondin-related sporozoite protein	A1X5V6-1	(701)	(702)

* Evidence only for RON3 surface expression on sporozoites (609)

Several novel neutralising linear B-cell epitopes are discovered and presented in this thesis. The Region I- and Region-II based CSP peptides, despite generating antibodies that recognise the native protein, show no protective efficacy, either from PvCSP or PfCSP. However, a peptide lying between Region I and the beginning of the repeat region in PfCSP is, for the first time, shown to generate neutralising antibodies which, when used in a combination regime with

an NANP-peptide VLP, results in the enhanced efficacy predicted of combination vaccines in Chapter 3. A screen of seven PvTRAP linear B-cell epitopes coupled to Qβ reveals three conferring partial protection, and the screen of 12 *P. berghei* conserved peptides from pre-erythrocytic invasion proteins produces one peptide, from TRSP, with clear protective ability, and a further two which may be worthy of further investigation.

The methods validated below for discovering neutralising linear B-cell epitopes will be of use not only for the development of a multi-antigen, single-component vaccine for malaria, but for other pathogens as well. The results herein presented are therefore of value for malaria vaccine development and more widely by providing a means of potentially accelerating the development of highly effective and cost-effective vaccines through the pre-clinical stage.

Results

6.1 Non-repeat region CSP peptides as vaccines

There are B-cell epitopes in the N- and C-terminal domains of CSP that can generate neutralising antibodies. The mathematical model presented in chapter 3 suggests that a vaccine eliciting neutralising antibodies to an epitope in addition to the central repeat region of CSP would markedly enhance protective efficacy. This section represents an attempt to elicit such antibodies using candidate linear B-cell epitopes from non-repeat region *P. vivax* and *P. falciparum* CSP administered as Qβ-peptide vaccines.

ELISAs using sera from PvCSP-vaccinated mice against 20-amino acid peptide sequences representing the full length of the protein (Fig. 6.1.1) show that using a PvCSP construct including the N-terminal domain does little better than one missing that domain in eliciting antibodies against linear epitopes in the N-terminal region. Nor does either construct elicit much antibody response against peptides from the C-terminal domain. This, combined with the finding that the full-length construct confers no protective efficacy compared with 100% protection using the truncated version (Fig. 5.2.2) warrants the screening of small peptides from the N- and C-terminal domains as vaccines outside the context of the full CSP protein.

A screen of three candidate linear B-cell epitopes from PvCSP, two from the N-terminal domain ("KLKQP" and "LGEN") and one from the C-terminal domain ("SVTCG") showed no protective efficacy against challenge using transgenic PvCSP-210/PvTRAP *P. berghei* sporozoites (Fig. 6.1.2 A). All three Qβ-peptide vaccines generated antibodies that recognised the native CSP in ELISAs, as well as good responses against the homologous peptide (Fig. 6.1.2 A). KLKQP-

vaccinated mice in particular generated titres and an avidity index comparable to those of the protective "210agdr" and "210qpag" peptides (Fig. 6.1.2 A and Fig. 5.1.2); but this was not sufficient for anti-KLKQP antibodies to be neutralising.

A similar screen using PfCSP linear B-cell epitopes gave similar results (Fig. 6.1.2 B). Two peptides ("Esp short" and "Esp long") were constructed based on the core and expanded linear sequence recognised by a neutralising monoclonal that targets the N-terminal domain of PfCSP in Region I based around the highly conserved KLKQP sequence shared with PvCSP. Despite being immunogenic in homologous and heterologous peptide ELISAs, and giving cross-species reactivity against the vivax-KLKQP peptide and full-length PvCSP-210, these Qβ-peptide vaccines failed to protect against challenge with transgenic PfCSP *P. berghei* sporozoites (Fig. 6.1.2 B).

A third peptide from PfCSP, "ADGN long," with sequence ADGNPDP<u>NANP</u>NVDP, was the only candidate to show protective efficacy against malaria challenge (Fig. 6.1.2 B). Qβ-(ADGN long) contains one NANP tetramer, underlined, and the Qβ-(ADGN long) VLP elicited comparable levels of antibody to Qβ-$(NANP)_6$. However, anti-$(NANP)_6$ antibodies are unlikely to be the mechanism of protection of the Qβ-(ADGN long) vaccine because the avidity index is very low (shown to significantly affect protective efficacy in §5.3.1); furthermore, the Qβ-$(NANP)_6$ vaccine, which normally confers 40% sterile protection, showed none in this challenge, with the challenge in this experiment being more robust than usual, with mice reaching 1% blood-stage parasitaemia approximately 12 hours earlier than average. It is likely that ADGN-long represents a novel non-NANP neutralising epitope in PfCSP.

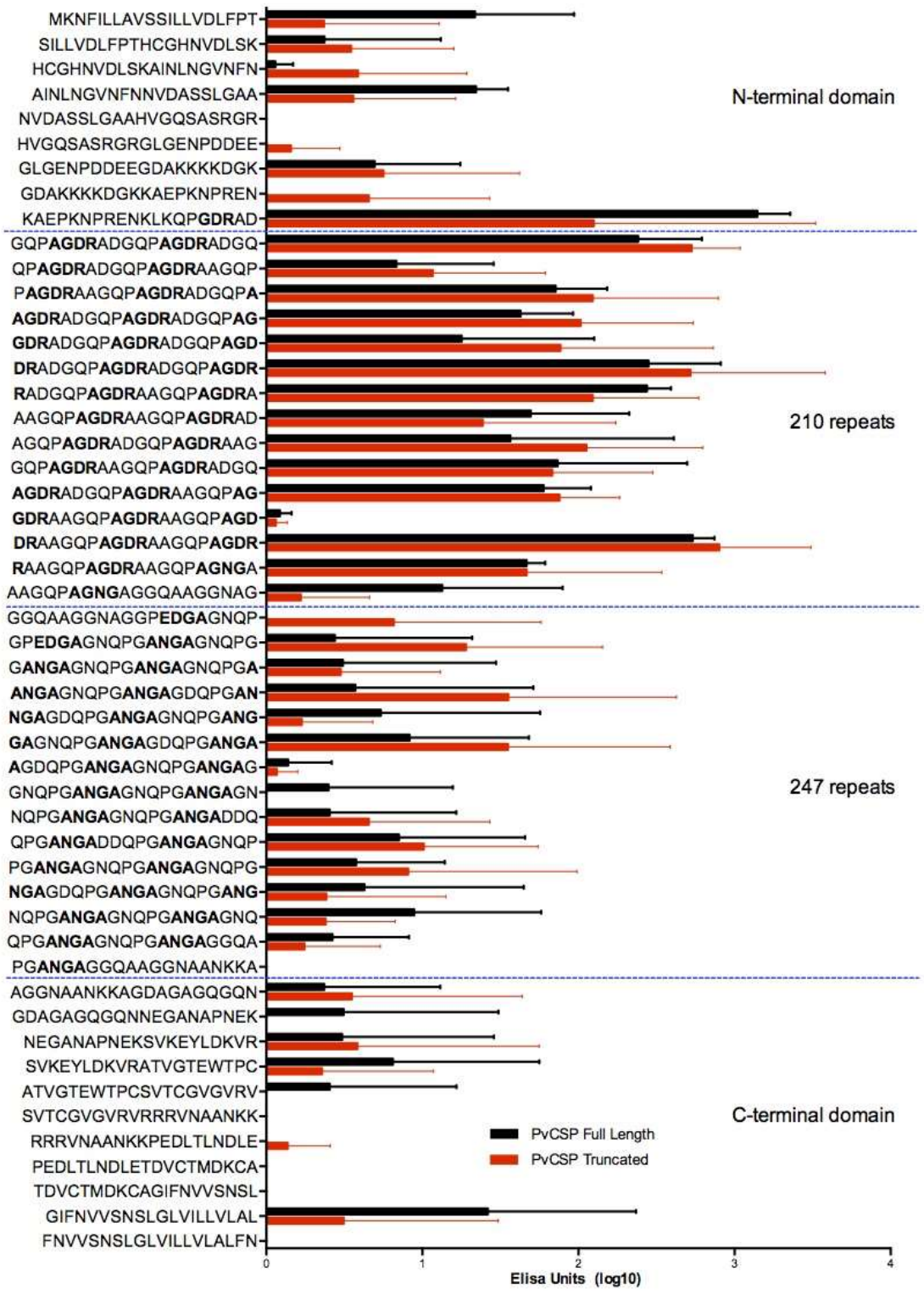


Fig. 6.1.1 Serum responses to overlapping peptides representing the full length of PvCSP from PvCSP-vaccinated mice.

BALB/c mice (n=4 per group) were vaccinated with chimeric versions of PvCSP either possessing (full-length) or missing (truncated) the N-terminal domain, and possessing both PvCSP-210 and PvCSP-247 repeat regions (two doses of 3 μg per dose 3 weeks apart). Sera was taken 2 weeks

post-boost and used in standard curve ELISAs against overlapping 20 amino-acid sequences representing the full primary structure of the chimeric PvCSP.

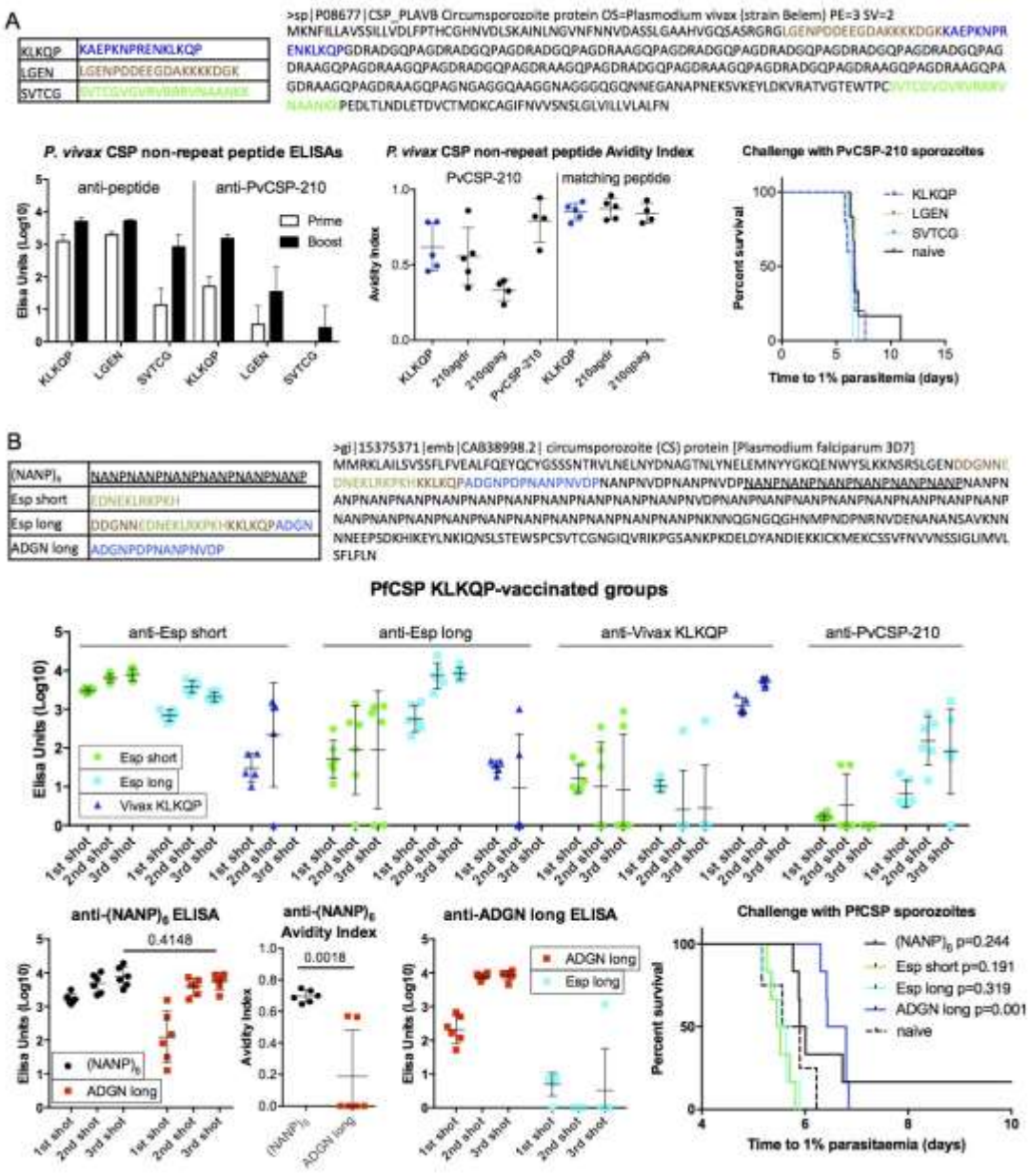


Fig. 6.1.2 Non-repeat region CSP peptides as vaccines.

(A) *P. vivax* CSP and (B) *P. falciparum* CSP peptides used as Qβ-peptide vaccines. BALB/c mice (n=4 to 6 per group) were vaccinated with non-repeat region CSP peptides chemically coupled to Qβ (3 μg per dose, by intramuscular injection), using three-week intervals between shots. The peptides used and positions in the *P. vivax* or *P. falciparum* CSP primary structures are shown. Standard curve ELISAs were performed using sera taken two weeks post-vaccination. Avidity

index represents the ratio of sera treated with 7 M urea to untreated sera in ELISAs. Mice were challenged three weeks after the final shot with 1000 transgenic *P. berghei* sporozoites expressing either PvCSP-210 or PfCSP as shown, and time to reach 1% blood-stage parasitaemia determined by linear regression using daily thin blood smears. Numbers on ELISA graphs represent p-values from t-tests between two groups; those on survival curves are p-values from log-rank tests compared to naïve mice.

To test whether ADGN-long represents a truly novel epitope, rather effects being mediated merely through anti-NANP as with Qβ-$(NANP)_6$, an experiment was carried out combining Qβ-(ADGN long) and Qβ-$(NANP)_6$ vaccines under suboptimal conditions. Chapter 3 predicts, and Chapter 4 shows, that two vaccines generating immune responses against different targets will, if either is weakly neutralising alone, show markedly enhanced protective efficacy when combined. Enhanced protective efficacy was obtained with the combination of Qβ-$(NANP)_6$ and Qβ-(ADGN long) compared to either subunit vaccine alone (Fig. 6.1.3 B). Given that the anti-$(NANP)_6$ and anti-(ADGN long) titres and avidity indices were the same in the single-component and combination groups (Fig. 6.1.3 A), the only remaining explanation for enhanced efficacy is that these vaccines elicit immune responses against different epitopes.

It is possible to use the results shown in Fig. 6.1.3 to test the mathematical model outlined in Chapter 3. From equations **(11)** and **(12)** in that chapter we can obtain the expression

$$\textbf{(26)}\ \frac{L_V}{L_N} = i_{V1} * i_{V2} = g^{Tn-Tv}$$

where L_V and L_N are the numbers of infected hepatocytes in vaccinated and naïve mice respectively; i_{V1} and i_{V2} are the reductions in infectivity caused by two different immune components (in this case, against $(NANP)_6$ and ADGN-long); g is the blood-stage growth rate (calculated in §3.3.1 to be g=3.5); and T_N and T_V are the time-to-1% values of the naïve and vaccinated mice respectively. The reduction in liver load for each group compared to naïve mice can be calculated as $100*(1- i_{V1}*i_{V2})$ and is shown graphically in Fig. 6.1.3 C, where median values are used for the calculations as the distribution of T is theoretically skewed (see Fig. 3.6.1). A predicted value for the reduction in liver load in the combination NANP+ADGN group can be calculated from the actual values of the Qβ-$(NANP)_6$ and Qβ-(ADGN long)-only groups, which have reductions in liver load of 54% and 57% respectively. The predicted reduction in liver load from the combination NANP+ADGN group is 80%, and the actual reduction is 89%. A Wilcoxon signed rank test comparing the predicted and actual reduction confirms the values to be very close, with a p-value for discrepancy of 0.44.

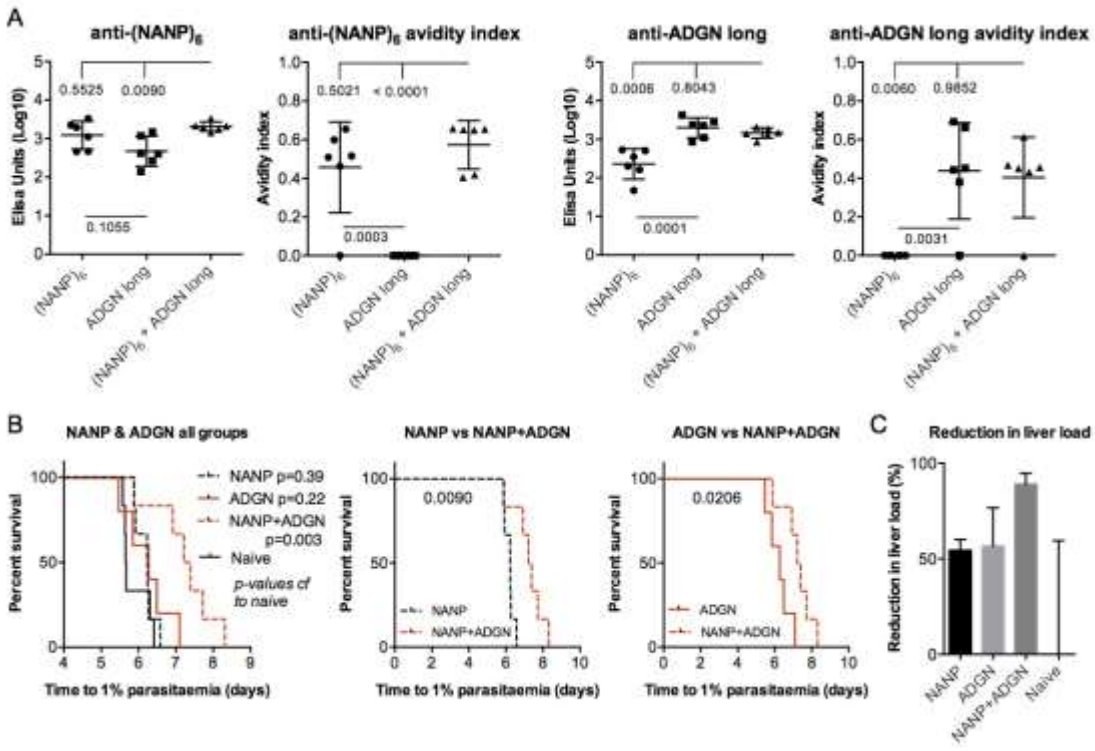


Fig. 6.1.3 Effects on immunogenicity and protective efficacy of combining Qβ-(NANP)$_6$ and Qβ-(ADGN long) vaccines.

BALB/c mice (n=6 per group) were vaccinated with two shots by intramuscular injection of 1 μg of each Qβ-peptide in Matrix M using a three-week prime-boost interval. Qβ-(NANP)$_6$ was delivered into the left leg and Qβ-(ADGN long) into the right leg. (A) Standard curve ELISAs from sera taken two weeks post-boost, with avidity index calculated as the ratio of titres from sera treated to untreated with 7 M urea. Numbers represent p-values from ANOVA with Bonferroni's multiple comparisons test. (B) Mice were challenged three weeks post-boost by intravenous injection of 1000 PfCSP replacement *P. berghei* sporozoites into the tail vein. Time to reach 1% blood stage parasitaemia was calculated by linear regression from thin blood smears taken daily. Numbers represent p-values from log-rank tests between indicated groups. (C) Reduction in liver load, the ratio of infected hepatocytes in vaccinated (L_V) compared to naïve mice (L_N), was calculated using the formula Reduction (%) = (1-i_V)*100, where the vaccine-reduced infectivity i_V = $L_V/L_N = g^{Tn-Tv}$, where g is the blood-stage growth rate, T_N the median time-to1% in naïve mice, and T_V the time-to-1% in vaccinated mice.

In section §5.4 the effects on immunogenicity from combining three CSP epitopes on a single Qβ VLP were reported. In order to further investigate the effects of combining B-cell epitopes, a single-component multi-epitope vaccine ("Multi-VLP") was produced by simultaneously coupling eight epitopes to Qβ using the peptides shown in Fig. 6.1.4. As with the Triple-VLP from §5.4, $(NANP)_6$ presented on the Multi-VLP was immunodominant, with titres unaffected either post-prime or post-boost in comparison to Qβ-$(NANP)_6$ (Fig. 6.1.4 A). This was reflected in a challenge experiment where both the Multi-VLP and Qβ-$(NANP)_6$ conferred similar levels of protective efficacy (Fig. 6.1.4 A). Post-boost, anti-(KLKQP) titres were also undiminished by Multi-VLP vaccination in comparison to Qβ-(KLKQP) vaccination, making $(NANP)_6$ and (KLKQP) co-dominant epitopes. In contrast, antibody responses to the other six epitopes were greatly diminished, by about three orders of magnitude, ($p<0.001$) when the peptides were presented on the Multi-VLP compared to single-peptide Qβ VLPs (Fig 6.1.4 A). The pattern of immunodominance was not identical post-prime and post-boost: post-prime, anti-(KLKQP) titres were slightly but significantly lower using Multi-VLP, whereas anti-$(AEDG)_3$ and anti-$(NADG)_3$ were not abrogated post-prime. This demonstrates that the immune hierarchy post-prime does not necessarily predict the hierarchy of immunodominance we will see post-boost.

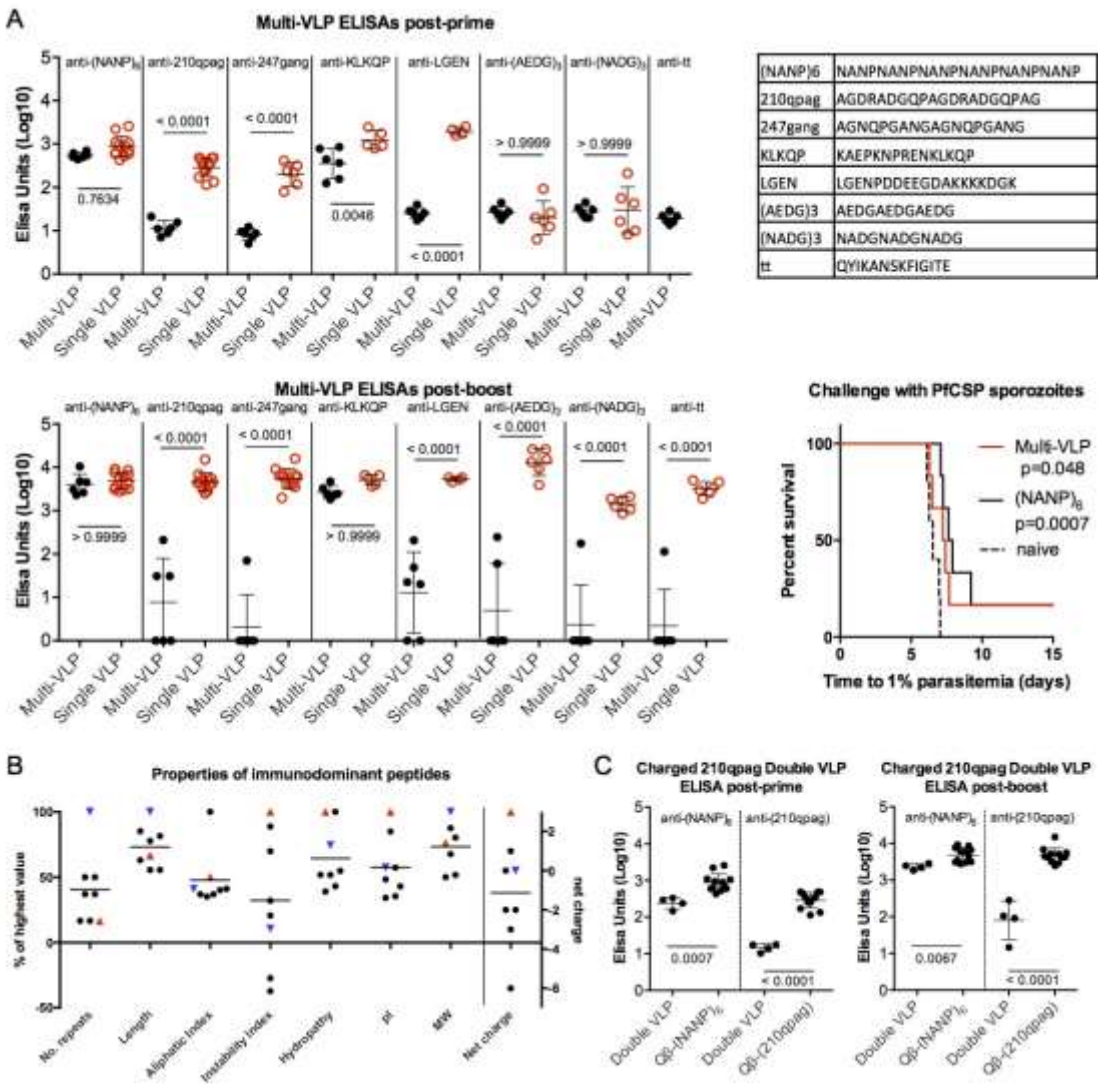


Fig. 6.1.4 Immunodominance on a multi-epitope VLP

A Qβ-peptide vaccine with eight epitopes chemically coupled simultaneously ("Multi-VLP") was produced using the peptides shown in (A). BALB/c mice were vaccinated by intramuscular injection (3 μg per dose, three week prime-boost interval) using either the Multi-VLP or one of eight single-epitope Qβ VLPs displaying one of the peptides. (A) Standard curve ELISAs were performed on sera taken two weeks post-vaccination against the indicated peptides. Numbers on ELISA graphs show p-values from ANOVA with Bonferroni's multiple comparisons test. Mice were challenged three weeks after the final dose with 1000 PfCSP transgenic *P. berghei* sporozoites and thin blood smears taken daily to determine time to reach 1% blood-stage parasitaemia by linear regression. P-values are from log-rank tests compared to naive. (B) The properties of the two immunodominant epitopes, $(NANP)_6$ (blue triangle) and KLKQP (red triangle), were compared to the others. Values of each property are expressed as percent of the

highest value in each case, except for net charge. pI: isoelectric point. MW: molecular weight. (C) Three lysine residues were added to 210qpag to increase the net charge and this was chemically coupled simultaneously with $(NANP)_6$ to Qβ to create a "Double VLP". Mice were vaccinated and ELISAs performed as before. Numbers represent p-values from t-tests.

A survey of the properties of the peptides coupled to Qβ, including the number of repeats, number of amino acids (length), aliphatic index, instability index, hydropathy, pI, molecular weight and net charge, was carried out to identify potential explanations for the immunodominance of $(NANP)_6$ and (KLKQP) (Fig. 6.1.4 B). $(NANP)_6$ has the greatest number of repeats, molecular weight and length. (KLKQP), in contrast, is short and is not repeated. However, (KLKQP) has the highest instability index, hydropathy, pI and net charge. It has yet to be determined which if any of these factors lead to (KLKQP) being co-dominant with $(NANP)_6$ at the expense of the other epitopes.

However, an experiment was carried out to see if increasing the net charge of the 210qpag peptide by addition of three lysine residues would prevent immune interference when this positively charged 210qpag peptide was simultaneously coupled with $(NANP)_6$ to Qβ ("Double VLP"). Fig. 6.1.4 C shows that anti-210qpag titres remain abrogated using the Double VLP post-prime and post-boost ($p<0.0001$, one to two orders of magnitude difference compared to Qβ-210qpag). In this case anti-$(NANP)_6$ titres were also significantly lower when vaccinating with the Double VLP compared to Qβ-$(NANP)_6$ (post-prime, $p=0.0007$, post-boost $p=0.0067$) though the difference in titres was very small. This suggests that increasing peptide charge is not a good strategy for making peptides on a single-component VLP co-dominant.

6.2 High-throughput vaccine screening: from protein to neutralising linear B-cell epitope

There is evidence that the protective efficacy associated with PvTRAP vaccination can be mediated by antibodies as well as by cytotoxic T-cells. Hence PvTRAP was considered a good candidate for application of the strategy shown in Fig. 6.2.1, to obtain peptide vaccine candidates from the sequence of PvTRAP by screening sera from whole PvTRAP-vaccinated mice for responses to linear epitopes, and then associating those responses with protection to downselect candidates for Qβ-peptide vaccines.

Fig. 6.2.1 B shows ELISA responses to PvTRAP 20mer peptides spanning the entire length of PvTRAP, with the most immunogenic linear epitopes located at the C-terminal end. 21 peptides were selected for further ELISAs using sera from 21 PvTRAP viral-vector vaccinated mice (Fig. 6.2.1 C), of which 8 had shown evidence of protective efficacy indicated by a delay in time to reach 1% blood-stage parasitaemia. T-tests failed to significantly associate any given peptide with protection, possibly because of the multi-variate complexity of the protective mechanisms. A cruder method of downselection was therefore employed with peptides ranked according to how many protected mice all had titres specific for a given peptide greater than the next-greatest titre of an unprotected mouse (shown in brackets beside peptide labels in Fig. 6.2.1 C). Seven of the nine peptides showing evidence of protective efficacy by this metric were selected for coupling to Qβ VLPs. The location of two of these peptides on the crystal structure of PvTRAP is shown in Fig. 6.2.1 D.

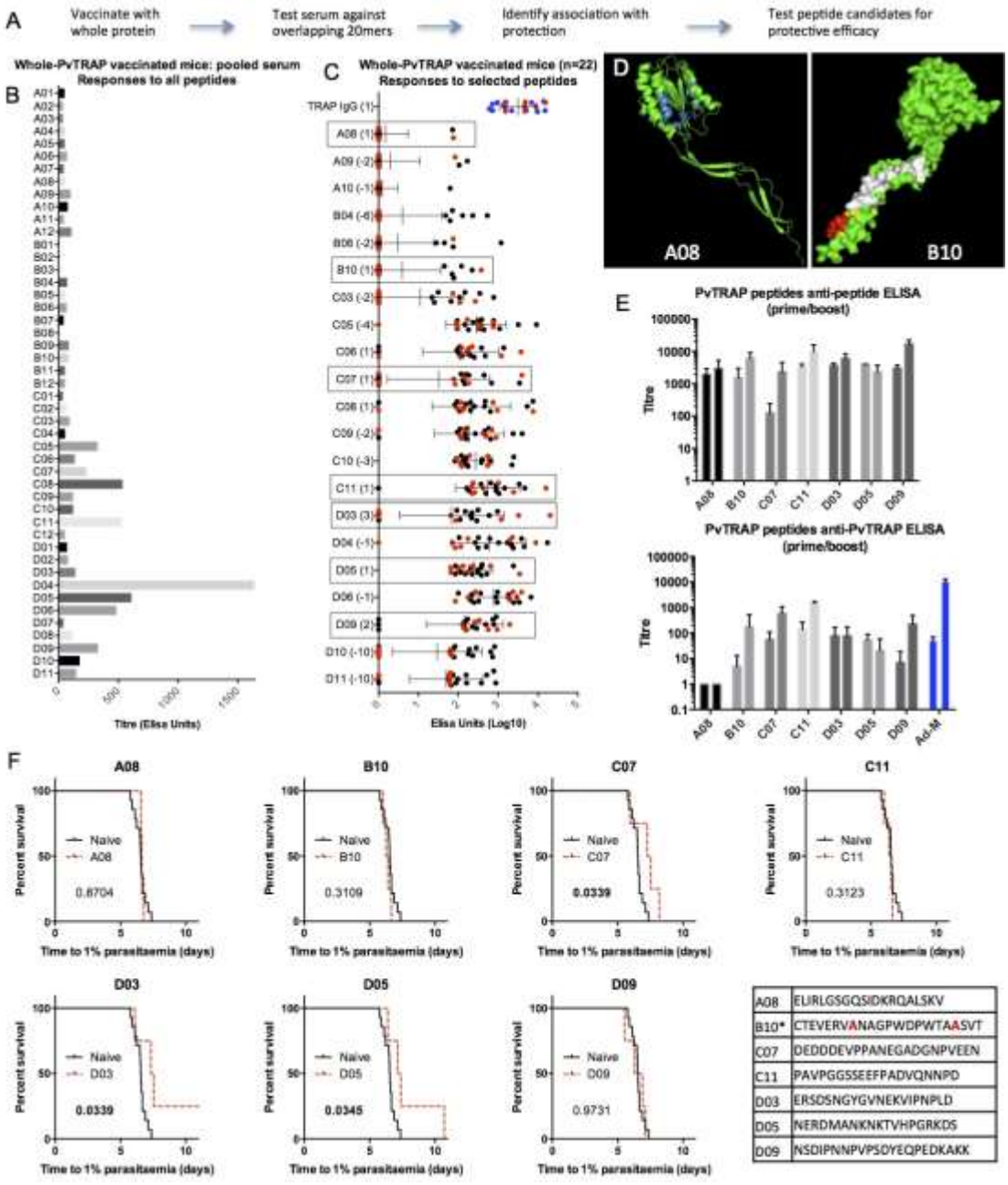


Fig. 6.2.1 Identification of neutralising linear B-cell epitopes in *P. vivax* TRAP

(A) Schematic of screening strategy. (B) Pooled sera from BALB/c mice vaccinated with PvTRAP (viral vectors, adenovirus prime and MVA boost, eight week prime-boost interval) was used to screen responses to overlapping 20-amino acid peptides spanning the length of the protein using standard curve ELISAs. (C) Sera from 21 mice vaccinated as in (B) were used to determine responses to 21 selected PvTRAP peptides by standard curve ELISAs. Also shown ("TRAP IgG") are serum responses to whole PvTRAP. Mice that showed a delay in time to reach 1% blood-stage parasitaemia are coloured red, and those showing no evidence of vaccine effect are coloured

black. Numbers in brackets after the peptide label indicate the number of protected mice showing a titre greater than that of the highest-titre unprotected mouse; or, for negative numbers, the number of unprotected mice showing a greater titre than that of the highest-titre protected mouse. (D) Locations (in red) of the indicated peptides on partial PvTRAP crystal structure. B10 is represented in white apart from the conserved CSVTCG domain, in red, and cysteines yellow (4HQ0, (703)). (E) Selected peptides from (C) were individually coupled to Qβ and used to vaccinate BALB/c mice (1 μg per dose, three shots at three-week intervals, with Matrix M adjuvant). Standard curve ELISAs against homologous peptides and against whole PvTRAP were performed. Also shown (Ad-M) are responses to adenovirus-primed and MVA-boosted viral-vectored PvTRAP, in blue. (F) Mice from (E) were challenged three weeks post-final vaccination by intravenous injection of 1000 PvCSP/PvTRAP transgenic sporozoites, and time to 1% parasitaemia determined by linear regression from thin blood smears taken daily. Numbers indicate p-values from log-rank tests compared to naïve. Also shown are the peptide sequences displayed on Qβ vaccines. For B10, * indicates that cysteines were exchanged for alanines, marked bold red.

All seven Qβ-peptide vaccines were immunogenic according to ELISAs performed against the homologous peptide (Fig. 6.2.1 E). Six of the seven also generated antibodies capable of recognising the native PvTRAP protein in an ELISA (Fig. 6.2.1 E). Interestingly, these six included B10 which contains multiple natural cysteines exchanged in Qβ-B10 for alanines to facilitate chemical coupling (see table, Fig. 6.2.1 F), suggesting that this alanine-exchange did not negatively affect the conformation of the peptide.

Following challenge with 1000 transgenic PvCSP/PvTRAP *P. berghei* sporozoites, three of the seven Qβ-peptides showed evidence of protective efficacy by log-rank test compared to naïve mice: C07 (p=0.034), D03 (p=0.034) and D05 (p=0.035) (Fig. 6.2.1 F). All three peptides lie in the apparently

unstructured region of PvTRAP yet to be successfully crystalised. C07 is upstream of a conserved LDVPDE motif common to *P. vivax, P. falciparum, P. knowlesi, P. cynomolgi,* and *P. reichenowi* TRAP. D03 and D05 are contiguous in the PvTRAP sequence and straddle a conserved LDNER motif common to *P. vivax, P. falciparum* and *P. reichenowi* TRAP.

Further evidence that the disordered region of PvTRAP is a target of neutralising antibodies comes from an experiment with a monoclonal PvTRAP antibody, 2D3, made by the author with the assistance of Gustavo Cabral de Miranda. This monoclonal recognises PvTRAP on transgenic *P. berghei* (Fig. 6.2.2 A) and shows neutralising potency in a challenge trial where PvCSP/PvTRAP sporozoites were incubated with either 2D3 or the PbCSP-specific 3D11 control mAb prior to injection into mice (Fig. 6.2.2 C). Screening of the monoclonal against linear peptides representing selected regions of PvTRAP indicates that 2D3 recognises at least two non-contiguous linear epitopes in the disordered region of PvTRAP, and hence is conformational in nature (Fig. 6.2.2 B).

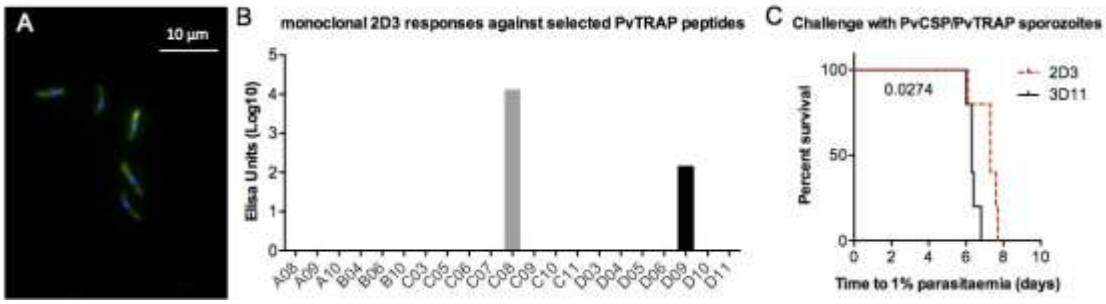


Fig. 6.2.2 2D3 PvTRAP monoclonal antibody specificity and neutralising potency.

The 2D3 monoclonal antibody was obtained by limiting dilutions of hybridomas derived from PvTRAP-vaccinated mice (thanks to Gustavo Cabral de Miranda for assistance). (A) 2D3 recognises PvTRAP-expressing *P. berghei* in an immunofluorescence assay (green: 2D3; blue: Hoechst DNA stain) (thanks to Ahmed Salman for picture). (B) ELISAs using 2D3 were performed

against selected peptides from the PvTRAP sequence. (C) PvCSP/PvTRAP transgenic *P. berghei* sporozoites were incubated at room temperature for 30 minutes with 190 μg/mL of either PbCSP-specific 3D11 mAb or 2D3, then BALB/c mice (n=5 per group) were challenged by intravenous injection of 1000 sporozoites each. Time to reach 1% blood-stage parasitaemia was calculated by linear regression from thin blood smears taken daily. Number represents p-value from log-rank test.

6.3 High-throughput vaccine screening: exploiting conservation to identify neutralising linear B-cell epitopes

One reason for a high degree of conservation in a region of a protein can be because that region plays some important function. One mechanism of neutralisation by antibodies is that they interfere with the function of a protein. This section pursues a strategy of identifying neutralising linear B-cell epitopes by identifying conserved amino acid sequences in *Plasmodium* sporozoite surface proteins involved in invasion, displaying those linear peptides on Qβ to elicit antibodies, and testing those candidates for protective efficacy in a challenge, as shown schematically in Fig. 6.3.1 A.

12 peptides from ten different proteins were selected as candidates (Fig. 6.3.1 B). These were coupled to Qβ and used to vaccinate BALB/c mice. ELISAs against the homologous peptide demonstrates that all candidates are immunogenic, with the exception of the Falstatin peptide, which produced poor anti-Falstatin peptide responses (Fig. 6.3.1 C).

Challenge of vaccinated mice with 1000 sporozoites showed one candidate Qβ-peptide conferring a significant degree of protection on mice, using a peptide derived from TRSP ($p=0.0037$). Two other candidates (P113, $p=0.09$) and PLP1 b ($p=0.056$, with one case of sterile protection) showed borderline efficacy.

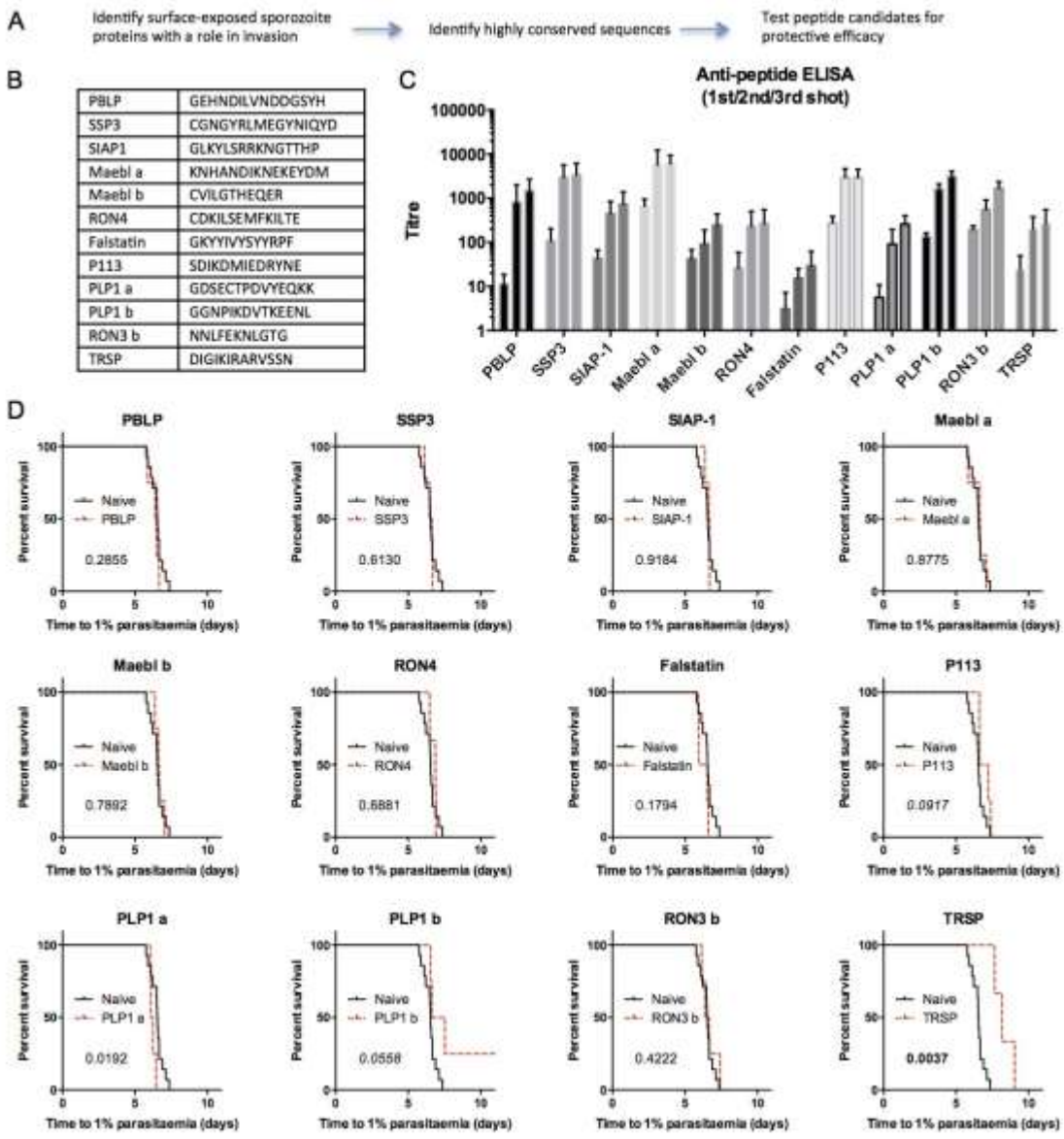


Fig. 6.3.1 Identification of neutralising linear B-cell epitopes by screening conserved peptides in *P. berghei*.

The strategy shown in (A) was used to identify conserved amino acid sequences in the sporozoite surface proteins shown in (B). The peptides were chemically coupled to Qβ and used to vaccinate BALB/c mice (three doses, 1 μg per dose, at three-week intervals, with Matrix M adjuvant). (C) Sera was taken 2 weeks post-vaccination and used in standard curve ELISAs against the homologous protein. (D) Mice were challenged three weeks after the final vaccination by intravenous injection of 1000 PvCSP/PvTRAP transgenic *P. berghei* sporozoites. Time to 1% parasitaemia was calculated by linear regression from daily thin blood smears. Numbers represent p-values from log-rank tests in comparison to naïve.

A further experiment combining Qβ-(PLP1b) and Qβ-(TRSP) was carried out to determine if any enhancement of protective efficacy would be obtained. Qβ-(TRSP) again demonstrated protective efficacy, but Qβ-(PLP1b) did not (Fig. 6.3.2 B, p=0.014 comparing Qβ-(TRSP) to naïve). Interestingly, the combination of Qβ-(TRSP) and Qβ-(PLP1b) did not show evidence of protective efficacy either. This would appear to be because the addition of Qβ-(PLP1b) to Qβ-(TRSP) reduced the avidity index of anti-TRSP peptide antibodies (Fig. 6.3.2 A), and the avidity index, but not the titre, of anti-TRSP peptide antibodies associates with protective efficacy and correlates with time to reach 1% blood-stage parasitaemia (Fig. 6.3.2 C).

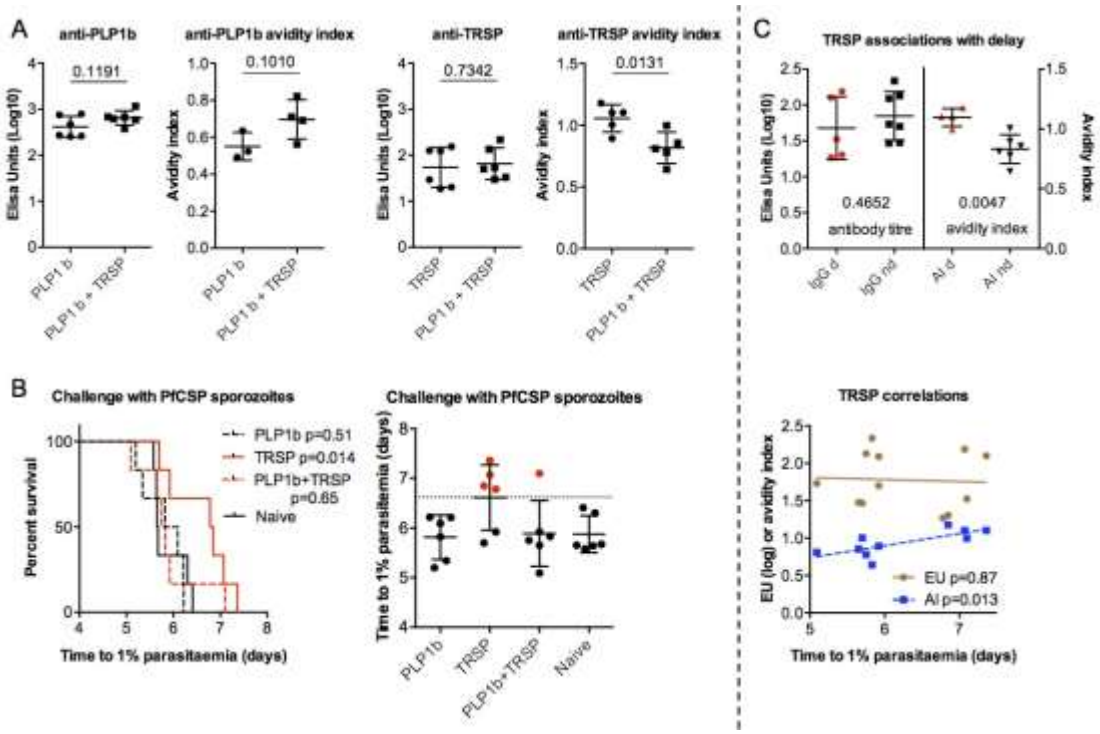


Fig. 6.3.2 Effects on immunogenicity and protective efficacy of combining Qβ-(PLP1b) and Qβ-(TRSP) vaccines.

BALB/c mice (n=6 per group) were vaccinated with two shots by intramuscular injection of 1 μg of each Qβ-peptide in Matrix M using a three-week prime-boost interval. Qβ-(PLP1b) was delivered into the left leg and Qβ-(TRSP) into the right leg. (A) Standard curve ELISAs from sera taken two weeks post-boost, with avidity index calculated as the ratio of titres from sera treated to untreated with 7 M urea. Numbers represent p-values from ANOVA with Bonferroni's multiple comparisons test. (B) Mice were challenged three weeks post-boost by intravenous injection of 1000 PfCSP replacement *P. berghei* sporozoites into the tail vein. Time to reach 1% blood stage parasitaemia was calculated by linear regression from thin blood smears taken daily. Numbers represent p-values from log-rank tests between indicated groups. The column figure indicates which mice show a delay in time-to-1%, coloured red, defined as time-to-1% greater than the mean naïve time-to-1% plus two standard deviations; this is indicated by the hatched line. (C) Mice were divided into two groups, delayed ("d") or no delay ("nd") as shown in (B); p-values shown below groups indicate strengths of association (by t-test) with either titre or avidity index (AI). Correlations between time-to-1% and either titre or avidity index also shown.

Discussion

In this chapter, five novel linear B-cell epitopes were discovered, capable of neutralising *P. berghei* sporozoites when used as Qβ-peptide vaccines. One of these is a novel epitope from PfCSP, ADGNPDPNANPNVDP ("ADGN long"); Qβ-(ADGN long) vaccination conferred partial protection on mice but Region I and Region II peptides from PvCSP and PfCSP failed to do so. Furthermore, a combination of separate Qβ-$(NANP)_6$ and Qβ-(ADGN long) VLPs significantly enhanced protection compared to either component VLP alone, without antigenic interference, suggesting that including the ADGN long epitope in PfCSP-based vaccines should improve protective efficacy as this epitope is not present in the leading malaria vaccine, RTS,S, nor R21. Antigenic interference between eight peptides co-displayed on a single VLP was investigated and it was found that co-dominance existed between two peptides, $(NANP)_6$ and a PvCSP Region I peptide; antibody responses to all other peptides were ablated, reinforcing the conclusion in the previous chapter that immunodominance and antigenic interference will be of prime importance for further research if single-component multi-antigen VLPs are to be taken forward. A screen of seven linear B-cell epitopes from PvTRAP associated with protection validated three new peptides capable of generating neutralising antibodies, and it was also shown that a novel PvTRAP-specific monoclonal antibody, 2D3, has neutralising potency. Finally, a screen of 12 peptides based on conserved regions from ten *P. berghei* sporozoite invasion proteins produced one new candidate peptide, from Thrombospondin Related Sporozoite Protein (TRSP) which as a Qβ-peptide vaccine conferred partial protective efficacy on mice. Taken together, these results represent a step forward in developing a single-component multi-antigen

VLP of enhanced efficacy against malaria. What is more, the techniques used for identifying novel neutralising linear B-cell epitopes are applicable to the development of vaccines against other pathogens.

The failure of the Region I and Region II peptides to generate neutralising antibodies was disappointing, given that PfCSP Region I in particular is the target of a potent neutralising antibody apparently specific to a linear epitope (349), and since in this thesis Region I-peptide-elicited antibodies showed excellent recognition of native full-length PvCSP (Fig. 6.1.2 A). These results were not surprising, however, as attempts to generate vaccines targeting these regions have a chequered history, as detailed in Table 6.2.1. The best results obtained with Region I or II peptide-based vaccines have used longer versions than those used in this thesis, but still only achieved 50-60% protection against a very low dose challenge (100 sporozoite) (677), or reduced liver burden by 18%, low compared to 98% reduction obtained with a repeat-region based vaccine in the same study (676). Such low efficacy would render inclusion of these Region I and II epitopes with CSP repeat region epitopes of little value: as demonstrated in simulations in Chapter 3 (Fig. 3.5.3), only antibodies of similar potency will produce any noticeable enhancement of protective efficacy in combination.

Table 6.2.1 Protective efficacy of CSP Region I and II peptides used as vaccines in this chapter and in previous studies

Region	Species	Sequence	Protective Efficacy/Notes	Ref
II	*P. falciparum*	EWSPCSVTCGNGIQVRIK	None against *P. berghei*	(348)
II	*P. falciparum*	IEQYLKKIKNSISTEWSPCSVTCGNGIQVRIK	80% in 100 sporozoite *P. berghei* challenge	(348)
II	*P. berghei*	GGNNNNKNNNNDDSYIPSAEKILEFVKQIRDSITEEWSQCNVTCGSGIRVRKRKGSNKKAEDLTLEDIDTEICKMDKCS	60% in 100 sporozoite *P. berghei* challenge	(677)

II	*P. falciparum*	KNNQGNGQGHNMPNDPNRNVDENANANSAVKNNNNEEPSDKHIKEYLNKIQNSLSTEWSPCSVTCGNGIQVRIKPGSANKPKDELDYANDIEKKICKMEKCS	No *in vitro* inhibition of HepG2 infection by *P. falciparum* or *P. berghei*	(677)
II	*P. falciparum*	TEWSPCSVTCGNGIQ	No *in vitro* inhibition of HepG2 infection by *P. falciparum*	(362)
II	*P. vivax*	SVTCGVGVRVRRRVNAANKK	None against 1000 PvCSP transgenic *P. berghei*	This thesis
I	*P. berghei*	GYGQNKSIQAQRNLNELCYNEGNDNKLYHVLNSKNGKIYIRNTVNRLLADAPEGKKNEKKNKIERNNKLK	50% in 100 sporozoite *P. berghei* challenge	(677)
I	*P. falciparum*	EYQCYGSSSNTRVLNELNYDNAGTNLYNELEMNYYGKQENWYSLKKNSRSLGENDDGNNEDNEKLRKPKHKKLKQPADGNPDPNANPNV	50% *in vitro* inhibition of HepG2 infection by *P. falciparum*	(677)
I	*P. falciparum*	DGNNEDNEKLRKPKHKKLK	Linear sequence recognised by potently neutralising 5D5 monoclonal antibody	(349)
I	*P. falciparum*	DKRDGNNEDNEKLRKPKHKKL	No reduction in liver burden	(676)
I	*P. falciparum*	KLKQPGDGNPDP	18% reduction in liver burden	(676)
I	*P. falciparum*	CKHKKLKQPGDG	No *in vitro* inhibition of HepG2 infection by *P. falciparum*	(362)
I	*P. vivax*	LGENPDDEEGDAKKKKDGK	None against 1000 PvCSP transgenic *P. berghei*	This thesis
I	*P. vivax*	KAEPKNPRENKLKQP	None against 1000 PvCSP transgenic *P. berghei*	This thesis
I	*P. falciparum*	EDNEKLRKPKH	None against 1000 PfCSP transgenic *P. berghei*	This thesis
I	*P. falciparum*	DDGNNEDNEKLRKPKHKKLKQPADGN	None against 1000 PfCSP transgenic *P. berghei*	This thesis

An effective vaccination strategy to generate antibodies against Region I should remain a priority, however, because a monoclonal antibody (5D5) generated by vaccination with the N-terminal domain is potently neutralising, more so than the 2A10 monoclonal antibody which recognises the NANP repeat region motif (349). The epitope is cryptic, however, not being recognised when presented within the full-length CSP (704). Separate vaccination with the N-terminal region may succeed in eliciting neutralising antibodies, but that strategy would probably increase the expense of the vaccine if combined with, say, RTS,S or R21. A single-component vaccine consisting of the repeat region

and the N-terminal domain only, and missing the C-terminal domain, might allow antibodies to be generated against Region I as then CSP will be in a potentially more immunogenic conformation (346). Evidence this may be a viable strategy comes from this thesis, where a single component vaccine presenting eight different epitopes demonstrated co-dominance between a KLKQP-containing Region I peptide and $(NANP)_6$; thus Region I need not be cryptic in all vaccine formulations. If peptide-based Region I vaccines are to be pursued, extending the length of the peptide may be another good strategy for improving protective efficacy, as it has been found that deleting as few as three amino acids from either end of a 21 residue Region I peptide markedly decreases its ability to inhibit sporozoite invasion (704); however, the potently neutralising monoclonal antibody 5D5 can neutralize without recognising these extra amino acids (349). It is possible that the epitope recognised by 5D5, though apparently linear, is in fact conformational, and that linear epitope mapping cannot detect other residues in the N-terminal domain it might bind to. A crystal structure of 5D5 binding the N-terminal domain would do much to clarify this, and would help inform vaccine design based on this epitope.

More promisingly, this chapter shows that the "ADGN long" epitope, lying just between Region I and the repeat region in PfCSP, demonstrates protective efficacy as a Qβ-peptide vaccine. Its protective efficacy is approximately equal to that of Qβ-$(NANP)_6$. Furthermore, combining the two VLPs, Qβ-(ADGN long) and Qβ-$(NANP)_6$, enhances protective efficacy compared to either VLP alone. This is consistent with the finding that up to one third of neutralising monoclonal antibodies generated from the sera of people naturally exposed to *P. falciparum* recognise this sequence, with the others recognising purely NANP repeats

(Joshua Tan, personal communication from Adrian Hill). There are at least two possible mechanisms for the protection mediated by (ADGN long)-specific antibodies. One was provided as a hypothesis in Chapter 5 for the protective efficacy mediated by AGDR-specific antibodies. GDRA is a tetramer motif lying immediately C-terminal of Region I in *P. vivax* CSP; antibodies recognising this motif may mediate protection by interfering with the function of the conserved Region I, and analogously so could those generated by (ADGN long). Alternatively, the (ADGN long) motif, containing NANP in its sequence (ADGNPDPNANPNVDP), may generate antibodies to NANP of a different conformation to that present in linear $(NANP)_6$; it has been shown that cyclic NANP (663, 664) or conformationally-restricted NPNA (705) generates antibodies which all recognise sporozoites in IFA, whereas not those generated by linear NANP. Whether or not the mechanism is mediated by NANP-recognition, antibodies generated by Qβ-(ADGN long) must recognise a different epitope from those generated by Qβ-$(NANP)_6$ (conformational or otherwise), since combination of these VLPs enhances protection; on the model presented in Chapter 3, this can only happen if neutralising antibodies with different specificities are combined. A single-component VLP presenting both peptides should now be tried; but also, since RTS,S and R21 both present truncated versions of CSP missing the (ADGN long) epitope, extending the repeat sequence to include the (ADGN long) sequence may well generate antibodies specific to that epitope and enhance protective efficacy.

Other sporozoite proteins besides CSP are involved in invasion and can be the target of neutralising antibodies; see Table 6.1 for examples. Thus two novel approaches for identifying and screening linear B-cell epitopes as peptide-based

vaccines were pioneered here. The first strategy used a protein for which there is evidence that antibodies can mediate neutralisation as a mechanism of protection; this protein is PvTRAP (497). Sera from PvTRAP-vaccinated mice was tested in ELISAs for responses against overlapping 20-amino acid linear peptides representing the full length of the protein; peptides eliciting good responses were down-selected for further investigation, and seven of those 21 peptides were preliminarily associated with potential protective efficacy. Six out of the seven peptides, coupled to Qβ, were able to elicit antibodies recognising the native sequence in an ELISA, and three conferred partial protection on mice challenged with PvCSP/PvTRAP double replacement transgenic *P. berghei* sporozoites. It is possible that antibodies don't mediate protection; they may be eliciting cellular responses instead. This is unlikely, however, given that an immunodominant T-cell epitope within PvTRAP has been identified for BALB/c mice (497), and it isn't included in any of the peptides represented here. In addition, VLPs generate low levels of PvTRAP-specific cellular responses (500), whereas very high levels are typically required for protection with pre-erythrocytic vaccines (706). Passive transfer of peptide-elicited antibodies will be the only way to conclusively show that protection is mediated by antibodies, but the evidence given above, together with the protective efficacy associated with a PvTRAP-specific monoclonal antibody, 2D3 (§6.2) suggests this is the likely mechanism of the PvTRAP-peptide vaccines' protective efficacy.

The three protective peptides – C07, D03 and D05 – lie in the apparently disordered region C-terminal of the von Willebrand factor A and TSR domains (703, 707), as apparently do the epitopes recognised by the neutralising monoclonal antibody 2D3. Interestingly, these and other disordered regions in

malaria proteins are predicted to have an abundance of linear B-cell epitopes (707), which was verified here for TRAP (Fig. 6.2.1 B). In this chapter such linear B-cell epitopes have been shown to be targets of neutralising antibodies PvTRAP. It is worth noting that the same authors identify the CSP repeat region as highly disordered; it too is a target of neutralising antibodies. This suggests that the disordered regions of malarial proteins in general may be good candidates for identifying neutralising linear B-cell epitopes by screening Qβ-peptide vaccines in pre-clinical challenge experiments. The exact mechanism of action of the PvTRAP-peptide vaccines here identified is not known, but the identified peptides do either encompass or lie next to conserved motifs in the PvTRAP sequence. C07 lies just C-terminal of an LDVPDE motif common to *P. falciparum*, *P. vivax* and several other species of malaria. D03 and D05, contiguous in the PvTRAP protein sequence, between them straddle an LDNER motif shared by *P. vivax, P. falciparum* and *P. reichenowi*. As conserved regions of proteins often play a functional role (680), it is plausible that the antibodies elicited by these peptides are neutralising by virtue of interfering with some function of PvTRAP in this region. It will be interesting to see if the PvTRAP peptides are able to elicit cross-species immunity, or if the protection is species-specific. A multiple antigenic peptide study has used short peptide sequences (DRYI and TRPHGR) just C-terminal of the equivalent region to D05 in *P. falciparum* TRAP as vaccines (499). This study found that antisera from mice so vaccinated and monoclonal antibodies recognising these peptides could inhibit sporozoite invasion *in vitro*. This underscores the potential of this extended region as a vaccine candidate and should be the focus of further study.

The second screening strategy used in this chapter exploited conservation directly. As stated above, the conserved regions of proteins are often associated with function (680). Therefore antibodies elicited against these regions may be neutralising by virtue of interfering with that function. To my knowledge, this technique has never before been exploited as a means of generating protective vaccines. Of the twelve peptides, generated from the conserved regions of *P. berghei* sporozoite invasion proteins, most were highly immunogenic as Qβ-peptide vaccines, but only one, derived from a conserved TRSP sequence, demonstrated clear evidence of protective efficacy. Though the efficacy was not high, it was as good if not better than that conferred by Qβ-$(NANP)_6$ in the same experiment; in that experiment, the sporozoites showed much higher infectivity than normal, suggesting that under normal circumstances sterile protection would have been seen using Qβ-(TRSP). Given the similarity in their protective efficacy, the three PvTRAP peptides C07, D03 and D05 or their *P. falciparum* counterparts, and the CSP-based $(NANP)_6$ and (ADGN long) epitopes, and the TRSP epitope should now be tested together. In this chapter some initial combination studies were attempted, and a reduction in the affinity of anti-TRSP epitope antibodies when Qβ-(TRSP) was combined with Qβ-(PLP1b) ablated the protective efficacy of that combination vaccine (§6.3). This demonstrates again that the principal challenge facing attempts to make a single-component (or even multi-component) multi-antigen vaccine will be antigenic interference. Interestingly, the co-dominance seen between a KLKQP-epitope and $(NANP)_6$ is not compatible with the only current model of B-cell epitope immunodominance (646), and gives reason for hope that multi-antigen vaccines can be designed to avoid immunodominance by any one B-cell epitope. An attempt to use extra

positive charge to overcome immunodominance was explored in this chapter, but did not demonstrate any improvement. Altering the length or relative density of epitopes may see greater success and could be the first line of attack in dealing with this problem in future studies.

The TRSP epitope here identified as a target of neutralising antibodies lies immediately downstream of the highly conserved EWSQCSKTC motif present (with variations) in the TSR domains present in CSP and TRAP and implicated in binding to hepatocytes and invasion (343, 345, 465, 594). Antibodies elicited by Qβ-(TRSP) do not recognise PvCSP or PvTRAP (data not shown), suggesting they mediate protection by binding to TRSP alone. But what is most interesting is that this epitope represents a short Region II epitope that actually appears to elicit neutralising antibodies, unlike those from CSP presented in this thesis or in other studies (see Table 6.2). A previous study has found that the positively-charged residues downstream of the CSVTCG motif in CSP mediate binding to hepatocytes, probably via negatively charged glycosaminoglycan residues (466). In TRSP, the peptide used in the present chapter contains these basic residues: DIGI**K**I**R**A**R**VSSN. This suggests that peptides based on the positively-charged glycosaminoglycan-binding residues C-terminal of the CSVTCG motifs in CSP and TRAP might also act as good vaccine candidates, especially if they omit the CSVTCG motif altogether, as the cysteines may interfere with the conformation of the peptide, as is the case with some cysteine-containing proteins.

In summary, this chapter focused on the search for linear B-cell epitopes that, as with peptides based on the repeat region of CSP, are able to elicit antibodies capable of neutralising sporozoites. Five new candidate peptide vaccines showed protective efficacy. One of these, (ADGN long), can be exploited

by extending the repeat region of existing CSP vaccines R21 and RTS,S. The three derived from PvTRAP could form part of a multi-peptide vaccine, each presented separately, or as part of a longer polypeptide representing the greater part of the disordered region in PvTRAP or PfTRAP; further experiments will need to be carried out to determine which constructs confer greater protective efficacy. The peptide derived from TRSP may also benefit from further optimization, perhaps by extending its length. The main focus of further work, however, should be combining as many of these novel B-cell epitopes together as possible, as this thesis has shown repeatedly the benefits of so combining effective malaria vaccines. The work presented in this chapter may be of use in creating a highly cost-effective single component multi-antigen malaria vaccine, and that the techniques, screening sera and exploiting conservation, used to identify and test the peptides for protective efficacy, should also be of use in vaccine development against other pathogens.

Chapter 7

Discussion and Future Directions

7.1 Overview

The need for an effective malaria vaccine is pressing, with almost half a million people, mainly children, dying each year (1). Existing interventions, such as drugs and insecticide-treated bednets, though they have halved the incidence of malaria since 2000 (2), are unlikely to prove sufficient in tackling the disease in areas of high transmission (3). An effective vaccine would certainly be a welcome addition to our armoury, and RTS,S, a pre-erythrocytic malaria vaccine, will enter pilot distribution studies in sub-Saharan Africa in 2018 (WHO press release, 24 April 2017). But with under 47% efficacy (28), likely making RTS,S less cost-effective than insecticide-treated bednets (29), this vaccine can only represent a milestone on the road towards the malaria vaccine we need. In addition, RTS,S is specific for *P. falciparum*; vaccine development for the other major species, *P. vivax*, is further behind, with little or no protective efficacy reported in the most advanced clinical trial, of VMP001 (453). This thesis has been an attempt to improve the protective efficacy of malaria vaccines, principally for *P. vivax* but also *P. falciparum*, by means of combination strategies.

The thesis began with a theoretical model of the effects on protective efficacy of combining pre-erythrocytic malaria vaccines. The model, based on simple probabilistic biological assumptions, predicts that combining vaccines will markedly enhance their protective efficacy compared to either component

alone, having typically more than additive effects, as long as there is no antigenic interference.

Chapter Four described the effects of combining two leading pre-erythrocytic vaccines, Rv21 and viral-vectored PvTRAP. Using a murine model of malaria with a novel double-replacement PvCSP/PvTRAP transgenic *P. berghei* parasite, the combination enhanced protection as expected. Antigenic interference was seen, but only with a particular adjuvant, Matrix M, demonstrating for the first time that antigenic interference can be adjuvant dependent and so potentially can be avoided by altering vaccine formulation.

The next chapter, Chapter Five, took the first steps towards a single component multi-antigen vaccine, designed to be both effective and cost-effective, avoiding the costs associated with multiple components (654) without sacrificing enhancement of efficacy. The aim was to discover short linear B-cell epitopes, each individually capable of eliciting neutralising antibodies, in order, ultimately, to array them on a single VLP. Qβ was used as a VLP platform for the ease of coupling peptides and other small moieties to it (192). As proof of principle that short peptides displayed on Qβ could confer protective efficacy, peptides representing 2 – 6 unit repeats from the repeat region of two *P. vivax* allelic variants and from *P. falciparum* CSP were coupled to Qβ. These were protective, in some cases conferring 100% sterile protection.

Chapter Six began the search for other linear B-cell epitopes capable of neutralising sporozoites, with the aim of combining these with the CSP repeat region epitopes tested in Chapter Five. Five new linear B-cell epitopes with neutralising potential were discovered, one from PfCSP, three from PvTRAP, and one from TRSP. The combination of the two PfCSP epitopes, “ADGN long” and the

repeat region peptide $(NANP)_6$, displayed enhancement of protection as predicted by the model presented in Chapter Three, without antigenic interference. Further, two novel methods of discovering linear B-cell epitopes with neutralising capability were described and validated. One method derives epitopes by screening sera of whole protein-vaccinated animals via linear peptide ELISAs, followed by downselection of peptides associated with protection for challenge experiments against Qβ-peptide vaccination. The other method exploits conservation, on the assumption that conservation indicates function, and that antibodies binding functional regions of proteins can by that means neutralise sporozoites. Three new PvTRAP linear B-cell epitopes were discovered by the former method, and one new epitope from TRSP using the latter method. Both methods could be applied in vaccine development against other pathogens.

In short, combining vaccines was shown to be an excellent strategy for enhancing the protective efficacy of pre-erythrocytic malaria vaccines, and the groundwork was laid for producing a single-component, multi-antigen malaria vaccine, using methods with general applicability to vaccine development. Now I will give a brief summary of each chapter with recommendations for further work and some closing remarks.

7.2 A mathematical model of vaccine combination

Chapter Three outlined a novel expression for the probability of protection, and for the time to reach 1% blood-stage parasitaemia, in terms of antibody and cytotoxic T-cell levels, derived, for the first time, from basic biological and probabilistic assumptions. Values for unknown variables such as the blood-stage

growth rate were obtained within the context of the model, and used to simulate various vaccination scenarios in order to predict and inform optimal vaccination strategies. This laid a theoretical foundation for the rest of the thesis. The model shows that more-than-additive improvements in protective efficacy are to be expected from combining pre-erythrocytic malaria vaccines.

The model followed earlier work (611-615) deriving expressions linking protection with antibody levels and/or cellular responses. The novelty of the model from Chapter Three lies in its being derived from simple assumptions about the probabilistic behaviour of antibodies and cytotoxic T-cells, rather than using pre-existing expressions such as the Hill curve or an exponential expression to describe the relationship. One major advantage of this approach is that, should the model be contradicted by data, it will inform us that one of the assumptions is incorrect, and so provide us with an insight into some fundamental mathematical aspects of immune biology or malaria parasitology. Indeed, some evidence exists that one of the assumptions, that the probability of cytotoxic T-cells finding and destroying infected hepatocytes is independent of the number of infected hepatocytes, may be false (630). Should this prove to be the case, the model can easily be altered in a biologically based way to encompass this finding. Further work could be done in developing alternative models that reject some of the assumptions of independence of antibody and cytotoxic T-cell activity and sporozoite dose, and designing experiments to determine which of these alternative models best fits the data. The model could also be adapted to other stages of the malaria life-cycle, including blood- and mosquito-stages, as well as to immune responses against other pathogens. Application of the model to human malaria would necessitate incorporating

population-level variations in immune responses to vaccination, such as is presented in Saul *et al.* and White *et al.* (612, 613).

Estimates of basic biological parameters such as the blood-stage growth rate *g* were also presented, to enable simulations to be performed. The value estimated for *g*, of 3.5 new infected red blood cells per infected red blood cell per day, is lower than that from previously published data (631-635). This may be because the model does not incorporate sequestration (635), or perhaps because of changes in blood-stage growth rate with parasite density (631). The value of *g* obtained must be correct within the context of the model, as it is derived by curve fitting to that model, but it means that estimates of other biological variables derived in the final section of Chapter Three may be unreliable. Nevertheless, the high infectivity of sporozoites to BALB/c mice implied by the model, and in contradiction to the low infectivity reported in previous literature (637-639), may be accurate, given that as few as 150 sporozoites are shown to be 100% infective in 18 mice (§4.5), and improvements in dissection methods avoiding bicarbonate-containing media mean sporozoites survive for longer (642). In addition, another predicted value for the maximum time to reach 1% parasitaemia, occurring when only one infected hepatocyte seeds the blood-stage of infection, is found to be consistent with the maximum such times found in the challenge experiments performed in this thesis. Further work may validate or contradict these predictions and thus shed further light on the biological accuracy of this model.

The model predicts more than additive improvements in protective efficacy from combining pre-erythrocytic malaria vaccines. It suggests that increasing the breadth of antigen targets would reduce the level of each specific

type of antibody or cytotoxic T-cell required to achieve the same level of protection, and since this may be a more biologically achievable scenario than aiming for high responses to a single epitope, it suggests that increasing the breadth of epitope targets is a good vaccination strategy. The simulations also demonstrate, however, that there is little value in combining vaccines unless they are of equivalent potency, as otherwise the additional antigen will add little to the overall protective efficacy, and serve only to increase its cost.

7.3 Combining two *P. vivax* vaccines, Rv21 and viral-vectored TRAP

In Chapter Four the first attempt to combine two of the leading *P. vivax* pre-erythrocytic vaccines, Rv21 (190) and viral-vectored PvTRAP (497), was carried out. The combination of the two vaccines improved protective efficacy from 50% with Rv21 and delayed onset of parasitaemia with PvTRAP to 100% sterile protection in combination. This followed experiments where antigenic interference between the vaccines was seen only when using Matrix M adjuvant, and not other adjuvants. Genetic adjuvants were also shown to enhance the immunogenicity of PvCSP and PvTRAP viral-vectored vaccines. Thus Chapter Four demonstrated that combining pre-erythrocytic vivax malaria vaccines is a good strategy for improving protective efficacy.

The finding that combining Rv21 and viral-vectored PvTRAP enhances protective efficacy adds to a growing body of literature supporting such combinations, with PbCSP and PbTRAP (475, 566) and PfCSP and PbTRAP (189) demonstrating similar enhancements of efficacy in pre-clinical studies. This enhancement should translate to human trials, and some early evidence indicates it does (567) but antigenic interference has also been seen with some

combinations of CSP and TRAP (565, 566) and represents the greatest obstacle to a successful vaccine combination strategy. In Chapter Four antigenic interference was only seen with Matrix M, and not alum, AddaVax, nor when adjuvant was not used. It is encouraging that antigenic interference can at least sometimes be avoided by altering the formulation of the combination vaccine, but further studies on the exact conditions under which antigenic interference occurs, and the mechanisms behind it, should be undertaken as a priority, for as yet no consistent association between antigenic interference and particular conditions of vaccination can be discerned (see Table 4.2).

Rv21 and viral-vectored PvTRAP combination provided support for a strategy of vaccine combination, predicted in Chapter Three to markedly enhance protective efficacy. Rv21 was evidently far more protective than viral-vectored PvTRAP when used optimally, however, and so the addition of PvTRAP to Rv21 under optimal conditions may do little to improve the overall protective efficacy of the vaccine. Furthermore, as the number of components in a vaccine increases, the cost also increases and so the cost-effectiveness potentially goes down (654). For these reasons the rest of the thesis focused on building the foundation for a single component multi-antigen vaccine, and the search for linear B-cell epitopes capable of eliciting equally potent neutralising antibodies.

7.4 Qβ-peptide vaccines: virus-like particles displaying short peptide epitopes from the repeat region of CSP

As a means of combining vaccines without multiplying components, a strategy of displaying multiple linear B-cell epitopes on a single virus-like particle was envisaged. Chapter Five commenced this process by providing proof of principle

that Qβ-peptide vaccines displaying CSP repeat region epitopes, which are known to be the targets of neutralising antibodies (364, 365, 436, 437), could be protect against malaria challenge. Qβ was chosen as a VLP platform on which to display short peptide epitopes as it is relatively straightforward to couple small moieties to it (192), making it relatively straightforward to screen putative epitopes for protective efficacy and examine their interaction with each other.

Short peptides representing two to six unit repeats from the central repeat regions of *P. falciparum*, *P. vivax* VK210 and *P. vivax* VK247 CSP were successfully coupled to Qβ and each conferred protective efficacy on mice against malaria challenge. In the case of peptides derived from the nonamer repeat of PvCSP-VK210, up to 100% protective efficacy was achieved. The potential of short peptide vaccines displayed on Qβ is therefore established. Protective efficacy with similar peptides had previously been established using the NANP unit repeat from PfCSP (365) as well as with the nonamer unit repeat from PvCSP-VK210 (442, 443, 676), but has never before been obtained or tested using the nonamer unit repeat from PvCSP-VK247.

Within the unit repeat nonamer from PvCSP-210 lies the tetramer AGDR. Antibodies capable of recognising AGDR but not other sequences within the nonamer unit repeat are associated with protection (439, 443). In Chapter Five, for the first time, a short peptide epitope consisting of three copies of AGDR coupled to Qβ was shown capable of conferring sterile protection on mice when used as a vaccine. It also enhanced protective efficacy when used to boost mice primed with full-length PvCSP. Further work should be done to see if this can be applied to improve the protective efficacy of existing *P. vivax* CSP-based vaccines. VMP001 shows poor protective efficacy possibly in consequence of eliciting low

or no anti-AGDR responses (453, 455). A search for an equivalent tetramer to AGDR within the PvCSP-VK247 nonamer unit repeat proved fruitless, as did screening of non-NANP PfCSP repeat tetramers NVDP and NADG and PvCSP-VK210 minor unit repeat variant AGNG. Interestingly, the same experiment found a large difference in protective efficacy between full-length and truncated PvCSP-VK210 missing the N-terminal domain, conferring 0% and 100% sterile protection respectively. The difference could be due to conformational differences between the full-length and N terminal-truncated forms of CSP (346, 662) resulting in the generation of non-neutralising antibodies specific for the full-length conformation of PvCSP. An affinity ELISA confirmed that there was a difference in the affinity of the antibodies generated by either construct for the full-length version of the protein. Further work to confirm this finding, and seeing if it extends to PfCSP, should be carried out, as the VMP001 *P. vivax* CSP vaccine is full-length and of low protective efficacy (453), in contrast to that of RTS,S which is missing the N-terminal domain (246), though the latter is a virus-like particle and hence more immunogenic.

Having established that Qβ vaccines displaying short peptides derived from the repeat region of CSP are protective, Chapter Five looked at ways to improve the immunogenicity of Qβ-peptide vaccines. Fusing a helper T-cell epitope, P2 from tetanus toxin, to $(NANP)_3$ did not enhance titres but did improve the avidity index of the antibodies for the epitope. Another experiment showed that a higher avidity index strongly associated with protection when anti-NANP titres were otherwise equal, suggesting that affinity does matter and that adding helper T-cell epitopes to CSP vaccines may be worthwhile. The P2 epitope has been used with peptide-based CSP vaccines before (417-419, 421,

441-443, 659, 667, 668) but it has not, to my knowledge, previously been shown that it enhances the affinity of antibodies to NANP repeats. Other helper T-cell epitopes may prove better, so further research could be carried out in this direction.

An improvement in anti-NANP titres, though not achieved by addition of the P2 epitope, was achieved by increasing the number of NANP unit repeats on each peptide, consistent with at least one previous study (658). An apparently linear relationship was discovered between anti-NANP titre and number of NANP repeats, up to $(NANP)_6$. A novel mathematical model expressing titre as a function of dose, peptide density per VLP and number of repeats per peptide predicted this relationship would eventually saturate. Where exactly saturation occurs can't be predicted from the data obtained in this thesis, but a validation of the model was achieved, showing that it very accurately fits and explains data from Florian Brod comparing anti-NANP titres between R21 with RTS,S, the former VLP displaying four times the density of CSP of the latter.

Finally an attempt was made to combine the CSP repeat region peptides from *P. falciparum*, *P. vivax* VK210 and *P. vivax* VK247 on a single Qβ molecule, thus constructing a cross-species vaccine. One previous attempt has been made at this, but no challenge was performed (660). The PvCSP-VK210 and PvCSP-VK247 responses both suffered antigenic interference from anti-NANP responses, decreasing the protective efficacy compared to that seen with single-epitope vaccines. As stated in the discussion above on Chapter Four, though some work has been done on the topic (570, 645, 646), more research is required to better understand antigenic interference so that multi-epitope

vaccines can be designed to avoid this problem. Only then will the potential of combination vaccines be realised.

Chapter Five demonstrated that short peptides displayed on Qβ can be highly immunogenic and protective. The next step was to identify peptides other than CSP repeat region-based ones capable of conferring protection as vaccines, so that they could ultimately be combined together to create a single component multi-antigen vaccine of enhanced protective efficacy.

7.5 The search for other neutralising linear B-cell epitopes

Chapter Six reported the discovery of five novel linear B-cell epitopes which, as peptides displayed on Qβ, confer partial protective efficacy against challenge on mice. The combination of one of these epitopes, (ADGN long) with $(NANP)_6$ on separate VLPs enhanced the protective efficacy compared to either subunit vaccine alone. The potential of the strategy of combining linear B-cell epitopes displayed on VLPs was thus demonstrated. The chapter also introduced two novel methods for identifying and screening linear B-cell epitopes for protective efficacy, one based on scanning sera from mice vaccinated with a whole protein, and the other exploiting conserved regions of proteins to design peptides with neutralising potential. The final chapter of the thesis therefore represents a significant step towards the development of a single-component multi-antigen vaccine of enhanced protective efficacy using methods with applicability to the development of vaccines against other diseases.

First, B-cell epitopes within CSP other than repeat-region epitopes were screened for potential as peptide vaccines. Vaccines based on Regions I and II of CSP, in the N- and C-terminal domains of the protein respectively, have

previously been investigated for potential protective efficacy, but with no great success (348, 362, 676, 677). That lack of success was repeated in this thesis, for *P. vivax* or *P. falciparum,* using different peptide sequences. However, an epitope lying between Region I and the repeat region in PfCSP, ADGNPDPNANPNVDP or "ADGN long", was found to confer partial protective efficacy at least equal if not greater than that conferred by Qβ-$(NANP)_6$. The combination of Qβ-(ADGN long) with Qβ-$(NANP)_6$ was demonstrated to enhance protective efficacy, as predicted in Chapter Three. Since this epitope is missing in RTS,S and R21, and since no antigenic interference between it and $(NANP)_6$ was found, (ADGN long) should be exploited as a new epitope. It could be displayed either separately from CSP on the Hepatitis B surface antigen, or more simply by extending the repeat region to encompass it. If the results reported in this thesis translate to another VLP and to human vaccine trials, then including the ADGN long epitope should markedly enhance the protective efficacy of RTS,S and R21.

To discover neutralising linear B-cell epitopes in other sporozoite proteins, two methods were employed. The first used vaccination with whole PvTRAP to generate sera subsequently screened against peptides by ELISA to determine which regions of the protein were natural linear B-cell epitopes. A similar method has been used before, associating linear B-cell epitopes in PfSEA with protection (679), but Chapter Six represents the first attempt, to my knowledge, of further screening identified peptides for protective efficacy. Three PvTRAP-derived peptides were found to confer protective efficacy as Qβ-peptide vaccines. All three peptides locate in the disordered region of PvTRAP (703, 707), which may be significant as such regions in malaria proteins are predicted to be rich in linear B-cell epitopes and in CSP is the source of the principal

epitope associated with protection, the repeat region epitope (707). Further work could examine the potential of these disordered regions as sources of neutralising linear B-cell epitopes. The demonstration in Chapter Six of PvTRAP peptide-induced protective efficacy, as well as the neutralising ability of the PvTRAP-specific monoclonal antibody 2D3, adds to the evidence that, as well as $CD8^+$ T-cells (476, 487), anti-TRAP antibodies can mediate protection (144, 462, 497, 498, 678).

The other method employed to find neutralising linear B-cell epitopes exploited conservation. Conserved areas of proteins are sometimes conserved because they play an important role in protein function (680). I therefore developed a strategy for discovering peptides with protective potential by identifying the conserved regions within surface-expressed (609) sporozoite proteins involved in invasion. By performing alignments between proteins from different malaria species, conserved regions were identified and 12 peptides designed from ten sporozoites surface proteins involved in invasion (see Table 6.1). These peptides were synthesised and coupled to Qβ. One peptide, from TRSP, demonstrated protective efficacy, the first time TRSP has shown any potential as a vaccine candidate, though knockout experiments have previously demonstrated it to be important in invasion (702). This demonstrates the potential of this method for identifying linear B-cell epitopes with protective potential, not just for malaria vaccines, but in developing vaccines against other diseases. Further work would undoubtedly optimise the initial selection of candidate peptides to increase the probability of finding effective peptide vaccines, but Chapter Six provides proof of principle that exploiting conservation

can allow effective vaccines to be generated using nothing more than protein primary structures.

In summary, Chapter Six represents a major step towards developing a single component multi-antigen vaccine, by identifying novel linear B-cell epitopes which, as peptide vaccines, show protective efficacy. These can be combined to enhance efficacy, as with $(NANP)_6$ and (ADGN long) and so the next steps will be to test single component vaccines displaying combinations of these epitopes. Antigenic interference occurs between some but not all of them, and so an optimal combination is likely to be found with further work.

7.6 Final remarks

Almost half a million people die each year from malaria. An improved malaria vaccine is urgently needed. This thesis has demonstrated, in theory and practice, that combining subunit vaccines is a good strategy for enhancing protective efficacy. A novel mathematical model was used to demonstrate that enhancements in protective efficacy should be more than additive. The model was also used to explore various strategies for combination. Chapter Four provided the first evidence that Rv21 and viral-vectored PvTRAP could be combined to create a more efficacious *P. vivax* vaccine. Chapters Five and Six built the groundwork for developing a cost-effective, single-component multi-antigen vaccine, using Qβ to display peptides screened for protective efficacy. In this way, nine linear B-cell epitopes, six novel, were shown to confer protective efficacy as Qβ-peptide vaccines. Of wider utility for vaccine development, the methods used to identify those peptides are generally applicable.

The peptides identified in Chapters Five and Six could be displayed on a single Qβ VLP as independent epitopes, as has been the overall vision of this thesis. But this is not the only way to exploit the findings and methods reported in this thesis. Fusion proteins combining linear B-cell epitopes should be tested. Extension of the length of linear B-cell epitopes may further enhance their protective efficacy, as with NANP-repeat based vaccines. An optimal vaccine should also exploit cellular immunity; viral vectors are excellent at eliciting this, and since short malaria epitopes have previously been displayed on the surface of viral vectors (395, 396), the same could be attempted with the peptides identified in Chapter Six. This would allow a viral vector encoding a good $CD8^+$-mediated vaccine candidate like TRAP to be combined with good B-cell epitopes, easy to display on a viral vector surface if they are short and linear. I predict that antigenic interference will be the main obstacle to developing any future combination vaccine, but this thesis has shown that antigenic interference is not inevitable and can be overcome, and that co-dominance of epitopes can occur, so with work a highly cost-effective multi-antigen malaria vaccine should be possible.

References

1. **World Health Organization (WHO)**. World Malaria Report 2016, 2016.
2. **Bhatt S**, **Weiss DJ**, **Cameron E**, **Bisanzio D**, **Mappin B**, **Dalrymple U**, **Battle K**, **Moyes CL**, **Henry A**, **Eckhoff PA**, **Wenger EA**, **Briët O**, **Penny MA**, **Smith TA**, **Bennett A**, **Yukich J**, **Eisele TP**, **Griffin JT**, **Fergus CA**, **Lynch M**, **Lindgren F**, **Cohen JM**, **Murray CLJ**, **Smith DL**, **Hay SI**, **Cibulskis RE**, **Gething PW**. 2015. The effect of malaria control on Plasmodium falciparum in Africa between 2000 and 2015. Nature **526**:207–211.
3. **Griffin JT**, **Bhatt S**, **Sinka ME**, **Gething PW**, **Lynch M**, **Patouillard E**, **Shutes E**, **Newman RD**, **Alonso P**, **Cibulskis RE**, **Ghani AC**. 2016. Potential for reduction of burden and local elimination of malaria by reducing Plasmodium falciparum malaria transmission: a mathematical modelling study. Lancet Infect Dis **16**:465–472.
4. **Martinsen ES**, **Perkins SL**, **Schall JJ**. 2008. A three-genome phylogeny of malaria parasites (Plasmodium and closely related genera): evolution of life-history traits and host switches. Mol. Phylogenet. Evol. **47**:261–273.
5. **Ansari HR**, **Templeton TJ**, **Subudhi AK**, **Ramaprasad A**, **Tang J**, **Lu F**, **Naeem R**, **Hashish Y**, **Oguike MC**, **Benavente ED**, **Clark TG**, **Sutherland CJ**, **Barnwell JW**, **Culleton R**, **Cao J**, **Pain A**. 2016. Genome-scale comparison of expanded gene families in Plasmodium ovale wallikeri and Plasmodium ovale curtisi with Plasmodium malariae and with other Plasmodium species. Int. J. Parasitol. **46**:685–696.
6. **Rutledge GG**, **Böhme U**, **Sanders M**, **Reid AJ**, **Cotton JA**, **Maiga-Ascofare O**, **Djimdé AA**, **Apinjoh TO**, **Amenga-Etego L**, **Manske M**, **Barnwell JW**, **Renaud F**, **Ollomo B**, **Prugnolle F**, **Anstey NM**, **Auburn S**, **Price RN**, **McCarthy JS**, **Kwiatkowski DP**, **Newbold CI**, **Berriman M**, **Otto TD**. 2017. Plasmodium malariae and P. ovale genomes provide insights into malaria parasite evolution. Nature **542**:101–104.
7. **Maguire JD**, **Baird JK**. 2010. The “non-falciparum” malarias: the roles of epidemiology, parasite biology, clinical syndromes, complications and diagnostic rigour in guiding therapeutic strategies. Ann Trop Med Parasitol **104**:283–301.
8. **Price RN**, **Tjitra E**, **Guerra CA**, **Yeung S**, **White NJ**, **Anstey NM**. 2007. Vivax malaria: neglected and not benign. Am. J. Trop. Med. Hyg. **77**:79–87.
9. **Douglas NM**, **Pontororing GJ**, **Lampah DA**, **Yeo TW**, **Kenangalem E**, **Poespoprodjo JR**, **Ralph AP**, **Bangs MJ**, **Sugiarto P**, **Anstey NM**, **Price RN**. 2014. Mortality attributable to Plasmodium vivax malaria: a clinical audit from Papua, Indonesia. BMC Med, 9 ed. **12**:217.
10. **Hay SI**, **Guerra CA**, **Tatem AJ**, **Noor AM**, **Snow RW**. 2004. The global distribution and population at risk of malaria: past, present, and future. Lancet Infect Dis **4**:327–336.
11. **Gething PW**, **Casey DC**, **Weiss DJ**, **Bisanzio D**, **Bhatt S**, **Cameron E**, **Battle KE**, **Dalrymple U**, **Rozier J**, **Rao PC**, **Kutz MJ**, **Barber RM**, **Huynh C**, **Shackelford KA**, **Coates MM**, **Nguyen G**, **Fraser MS**, **Kulikoff R**, **Wang H**, **Naghavi M**, **Smith DL**, **Murray CJL**, **Hay SI**, **Lim SS**. 2016. Mapping Plasmodium falciparum Mortality in Africa between 1990 and 2015. N. Engl. J. Med. **375**:2435–2445.
12. **Gething PW**, **Elyazar IRF**, **Moyes CL**, **Smith DL**, **Battle KE**, **Guerra CA**, **Patil AP**, **Tatem AJ**, **Howes RE**, **Myers MF**, **George DB**, **Horby P**, **Wertheim HFL**, **Price RN**, **Müeller I**, **Baird JK**, **Hay SI**. 2012. A long neglected world malaria map: Plasmodium vivax endemicity in 2010. PLoS Negl Trop Dis **6**:e1814.
13. **Howes RE**, **Battle KE**, **Mendis KN**, **Smith DL**, **Cibulskis RE**, **Baird JK**, **Hay SI**. 2016. Global Epidemiology of Plasmodium vivax. Am. J. Trop. Med. Hyg. **95**:15–34.
14. **Hay SI**, **Sinka ME**, **Okara RM**, **Kabaria CW**, **Mbithi PM**, **Tago CC**, **Benz D**, **Gething PW**, **Howes RE**, **Patil AP**, **Temperley WH**, **Bangs MJ**, **Chareonviriyaphap T**, **Elyazar IRF**, **Harbach RE**, **Hemingway J**, **Manguin S**, **Mbogo CM**, **Rubio-Palis Y**, **Godfray HCJ**. 2010. Developing global maps of the dominant anopheles vectors of human malaria. PLoS Med. **7**:e1000209.

15. **Sinka ME**, **Bangs MJ**, **Manguin S**, **Rubio-Palis Y**, **Chareonviriyaphap T**, **Coetzee M**, **Mbogo CM**, **Hemingway J**, **Patil AP**, **Temperley WH**, **Gething PW**, **Kabaria CW**, **Burkot TR**, **Harbach RE**, **Hay SI**. 2012. A global map of dominant malaria vectors. Parasit Vectors **5**:69.
16. **Massey NC**, **Garrod G**, **Wiebe A**, **Henry AJ**, **Huang Z**, **Moyes CL**, **Sinka ME**. 2016. A global bionomic database for the dominant vectors of human malaria. Sci Data **3**:160014.
17. **Sicuri E**, **Vieta A**, **Lindner L**, **Constenla D**, **Sauboin C**. 2013. The economic costs of malaria in children in three sub-Saharan countries: Ghana, Tanzania and Kenya. Malaria Journal **12**:307.
18. **Sachs J**, **Malaney P**. 2002. The economic and social burden of malaria. Nature **415**:680–685.
19. **Maire N**, **Tediosi F**, **Ross A**, **Smith T**. 2006. Predictions of the epidemiologic impact of introducing a pre-erythrocytic vaccine into the expanded program on immunization in sub-Saharan Africa. Am. J. Trop. Med. Hyg. **75**:111–118.
20. **Penny MA**, **Maire N**, **Studer A**, **Schapira A**, **Smith TA**. 2008. What should vaccine developers ask? Simulation of the effectiveness of malaria vaccines. PLoS ONE **3**:e3193.
21. **Nunes JK**, **Cárdenas V**, **Loucq C**, **Maire N**, **Smith T**, **Shaffer C**, **Måseide K**, **Brooks A**. 2013. Modeling the public health impact of malaria vaccines for developers and policymakers. BMC Infect. Dis. **13**:295.
22. **Centers for Disease Control and Prevention**. 1999. Achievements in Public Health, 1900-1999 Impact of Vaccines Universally Recommended for Children: United States, 1990-1998 MMWR 48 (12) 243-48.
23. **Fenner F**, **Henderson DA**, **Arita I**, **Jezek Z**, **Ladnyi ID**. 1988. Smallpox and its eradication.
24. **Morales M**, **Tangermann RH**, **Wassilak SGF**. 2016. Progress Toward Polio Eradication - Worldwide, 2015-2016. MMWR Morb. Mortal. Wkly. Rep. **65**:470–473.
25. **de Quadros CA**, **Andrus JK**, **Danovaro-Holliday MC**, **Castillo-Solórzano C**. 2008. Feasibility of global measles eradication after interruption of transmission in the Americas. Expert Rev Vaccines **7**:355–362.
26. **Roberts L**, **Enserink M**. 2007. Malaria. Did they really say ... eradication? Science.
27. **Eckhoff P**. 2013. Mathematical models of within-host and transmission dynamics to determine effects of malaria interventions in a variety of transmission settings. Am. J. Trop. Med. Hyg. **88**:817–827.
28. **RTS,S Clinical Trials Partnership**, **Agnandji ST**, **Lell B**, **Fernandes JF**, **Abossolo BP**, **Kabwende AL**, **Adegnika AA**, **Mordmüller B**, **Issifou S**, **Kremsner PG**, **Loembe MM**, **Sacarlal J**, **Aide P**, **Madrid L**, **Lanaspa M**, **Mandjate S**, **Aponte JJ**, **Bulo H**, **Nhama A**, **Macete E**, **Alonso P**, **Abdulla S**, **Salim N**, **Mtoro AT**, **Mutani P**, **Tanner M**, **Mavere C**, **Mwangoka G**, **Lweno O**, **Juma OA**, **Shekalaghe S**, **Tinto H**, **D'Alessandro U**, **Sorgho H**, **Valea I**, **Ouédraogo JB**, **Lompo P**, **Diallo S**, **Traore O**, **Bassole A**, **Dao E**, **Hamel MJ**, **Kariuki S**, **Oneko M**, **Odero C**, **Otieno K**, **Awino N**, **Muturi-Kioi V**, **Omoto J**, **Laserson KF**, **Slutsker L**, **Otieno W**, **Otieno L**, **Otsyula N**, **Gondi S**, **Otieno A**, **Ogutu B**, **Ochola J**, **Onyango I**, **Oyieko J**, **Njuguna P**, **Chilengi R**, **Akoo P**, **Kerubo C**, **Maingi C**, **Olotu A**, **Bejon P**, **Marsh K**, **Mwabingu G**, **Gitaka J**, **Owusu-Agyei S**, **Asante KP**, **Boahen O**, **Dosoo D**, **Adjei G**, **Adeniji E**, **Yawson AK**, **Kayan K**, **Chandramohan D**, **Greenwood B**, **Lusingu J**, **Gesase S**, **Malabeja A**, **Abdul O**, **Mahende C**, **Liheluka E**, **Lemnge M**, **Theander TG**, **Drakeley C**, **Mbwana J**, **Ansong D**, **Agbenyega T**, **Adjei S**, **Boateng HO**, **Rettig T**, **Bawa J**, **Sylverken J**, **Sambian D**, **Sarfo A**, **Agyekum A**, **Martinson F**, **Hoffman I**, **Mvalo T**, **Kamthunzi P**, **Nkomo R**, **Tembo T**, **Tsidya GT**, **Kilembe J**, **Chawinga C**, **Ballou W**, **Cohen J**, **Guerra Y**, **Jongert E**, **Lapierre D**, **Leach A**, **Lievens M**, **Ofori-Anyinam O**, **Olivier A**, **Vekemans J**, **Kaslow D**, **Leboulleux D**, **Savarese B**, **Schellenberg D**. 2014. Efficacy and safety of the RTS,S/AS01 malaria vaccine during 18 months after vaccination: a phase 3 randomized, controlled trial in children and young infants at 11 African sites. PLoS Med. **11**:e1001685.
29. **Penny MA**, **Verity R**, **Bever CA**, **Sauboin C**, **Galactionova K**, **Flasche S**, **White MT**, **Wenger EA**, **Van de Velde N**, **Pemberton-Ross P**, **Griffin JT**, **Smith TA**, **Eckhoff**

PA, **Muhib F**, **Jit M**, **Ghani AC**. 2016. Public health impact and cost-effectiveness of the RTS,S/AS01 malaria vaccine: a systematic comparison of predictions from four mathematical models. The Lancet **387**:367–375.
30. **Rosenberg R**, **Wirtz RA**, **Schneider I**, **Burge R**. 1990. An estimation of the number of malaria sporozoites ejected by a feeding mosquito. Trans. R. Soc. Trop. Med. Hyg. **84**:209–212.
31. **Ponnudurai T**, **Lensen AH**, **van Gemert GJ**, **Bolmer MG**, **Meuwissen JH**. 1991. Feeding behaviour and sporozoite ejection by infected Anopheles stephensi. Trans. R. Soc. Trop. Med. Hyg. **85**:175–180.
32. **Beier JC**, **Davis JR**, **Vaughan JA**, **Noden BH**, **Beier MS**. 1991. Quantitation of Plasmodium falciparum sporozoites transmitted in vitro by experimentally infected Anopheles gambiae and Anopheles stephensi. Am. J. Trop. Med. Hyg. **44**:564–570.
33. **Kebaier C**, **Voza T**, **Vanderberg J**. 2009. Kinetics of mosquito-injected Plasmodium sporozoites in mice: fewer sporozoites are injected into sporozoite-immunized mice. PLoS Pathog. **5**:e1000399.
34. **Sidjanski S**, **Vanderberg JP**. 1997. Delayed migration of Plasmodium sporozoites from the mosquito bite site to the blood. Am. J. Trop. Med. Hyg. **57**:426–429.
35. **Vanderberg JP**, **Frevert U**. 2004. Intravital microscopy demonstrating antibody-mediated immobilisation of Plasmodium berghei sporozoites injected into skin by mosquitoes. Int. J. Parasitol. **34**:991–996.
36. **Yamauchi LM**, **Coppi A**, **Snounou G**, **Sinnis P**. 2007. Plasmodium sporozoites trickle out of the injection site. Cell. Microbiol. **9**:1215–1222.
37. **Shin SC**, **Vanderberg JP**, **Terzakis JA**. 1982. Direct infection of hepatocytes by sporozoites of Plasmodium berghei. J. Protozool. **29**:448–454.
38. **Verhave JP**, **Meuwissen JH**, **Golenser J**. 1980. The dual role of macrophages in the sporozoite-induced malaria infection. A hypothesis. Int J Nucl Med Biol **7**:149–156.
39. **Pinzon-Ortiz C**, **Friedman J**, **Esko J**, **Sinnis P**. 2001. The binding of the circumsporozoite protein to cell surface heparan sulfate proteoglycans is required for plasmodium sporozoite attachment to target cells. J. Biol. Chem. **276**:26784–26791.
40. **Pradel G**, **Garapaty S**, **Frevert U**. 2002. Proteoglycans mediate malaria sporozoite targeting to the liver. Mol. Microbiol. **45**:637–651.
41. **Sihden RE**, **Smith JE**. 1982. The role of the Kupffer cell in the infection of rodents by sporozoites of Plasmodium: uptake of sporozoites by perfused liver and the establishment of infection in vivo. Acta Trop. **39**:11–27.
42. **Tavares J**, **Formaglio P**, **Thiberge S**, **Mordelet E**, **Van Rooijen N**, **Medvinsky A**, **Ménard R**, **Amino R**. 2013. Role of host cell traversal by the malaria sporozoite during liver infection. J. Exp. Med. **210**:905–915.
43. **Mota MM**, **Pradel G**, **Vanderberg JP**, **Hafalla JC**, **Frevert U**, **Nussenzweig RS**, **Nussenzweig V**, **Rodríguez A**. 2001. Migration of Plasmodium sporozoites through cells before infection. Science **291**:141–144.
44. **Mota MM**, **Hafalla JCR**, **Rodriguez A**. 2002. Migration through host cells activates Plasmodium sporozoites for infection. Nat. Med. **8**:1318–1322.
45. **Meis JF**, **Verhave JP**, **Jap PH**, **Sinden RE**, **Meuwissen JH**. 1983. Ultrastructural observations on the infection of rat liver by Plasmodium berghei sporozoites in vivo. J. Protozool. **30**:361–366.
46. **Sastry AS**, **Bhat S**. 2014. **Essentials of Medical Parasitology**.
47. **White NJ**, **Pukrittayakamee S**, **Hien TT**, **Faiz MA**, **Mokuolu OA**, **Dondorp AM**. 2014. Malaria. Lancet **383**:723–735.
48. **Sinden RE**, **Suhrbier A**, **Davies CS**, **Fleck SL**, **Hodivala K**, **Nicholas JC**. 1990. The development and routine application of high-density exoerythrocytic-stage cultures of Plasmodium berghei. Bull. World Health Organ. **68 Suppl**:115–125.
49. **Yoeli M**, **Upmanis RS**, **Vanderberg J**, **Most H**. 1966. Life cycle and patterns of development of Plasmodium berghei in normal and experimental hosts. Mil Med **131**:Suppl:900–14.
50. **Baer K**, **Klotz C**, **Kappe SHI**, **Schnieder T**, **Frevert U**. 2007. Release of hepatic Plasmodium yoelii merozoites into the pulmonary microvasculature. PLoS Pathog. **3**:e171.

51. **Sturm A**, **Amino R**, **van de Sand C**, **Regen T**, **Retzlaff S**, **Rennenberg A**, **Krueger A**, **Pollok J-M**, **Ménard R**, **Heussler VT**. 2006. Manipulation of host hepatocytes by the malaria parasite for delivery into liver sinusoids. Science **313**:1287–1290.
52. **Graewe S**, **Rankin KE**, **Lehmann C**, **Deschermeier C**, **Hecht L**, **Froehlke U**, **Stanway RR**, **Heussler V**. 2011. Hostile takeover by Plasmodium: reorganization of parasite and host cell membranes during liver stage egress. PLoS Pathog. **7**:e1002224.
53. **Burda P-C**, **Caldelari R**, **Heussler VT**. 2017. Manipulation of the Host Cell Membrane during Plasmodium Liver Stage Egress. MBio **8**:e00139–17.
54. **Krotoski WA**, **Collins WE**, **Bray RS**, **Garnham PC**, **Cogswell FB**, **Gwadz RW**, **Killick-Kendrick R**, **Wolf R**, **Sinden R**, **Koontz LC**, **Stanfill PS**. 1982. Demonstration of hypnozoites in sporozoite-transmitted Plasmodium vivax infection. Am. J. Trop. Med. Hyg. **31**:1291–1293.
55. **Richter J**, **Franken G**, **Mehlhorn H**, **Labisch A**, **Häussinger D**. 2010. What is the evidence for the existence of Plasmodium ovale hypnozoites? Parasitol. Res. **107**:1285–1290.
56. **Krotoski WA**, **Krotoski DM**, **Garnham PC**, **Bray RS**, **Killick-Kendrick R**, **Draper CC**, **Targett GA**, **Guy MW**. 1980. Relapses in primate malaria: discovery of two populations of exoerythrocytic stages. Preliminary note. Br Med J **280**:153–154.
57. **Krotoski WA**, **Garnham PC**, **Bray RS**, **Krotoski DM**, **Killick-Kendrick R**, **Draper CC**, **Targett GA**, **Guy MW**. 1982. Observations on early and late post-sporozoite tissue stages in primate malaria. I. Discovery of a new latent form of Plasmodium cynomolgi (the hypnozoite), and failure to detect hepatic forms within the first 24 hours after infection. Am. J. Trop. Med. Hyg. **31**:24–35.
58. **Battle KE**, **Karhunen MS**, **Bhatt S**, **Gething PW**, **Howes RE**, **Golding N**, **Van Boeckel TP**, **Messina JP**, **Shanks GD**, **Smith DL**, **Baird JK**, **Hay SI**. 2014. Geographical variation in Plasmodium vivax relapse. Malaria Journal **13**:144.
59. **Shanks GD**, **White NJ**. 2013. The activation of vivax malaria hypnozoites by infectious diseases. Lancet Infect Dis **13**:900–906.
60. **Clough B**, **Atilola FA**, **Pasvoi G**. 1998. The role of rosetting in the multiplication of Plasmodium falciparum: rosette formation neither enhances nor targets parasite invasion into uninfected red cells. Br. J. Haematol. **100**:99–104.
61. **Liu J**, **Istvan ES**, **Gluzman IY**, **Gross J**, **Goldberg DE**. 2006. Plasmodium falciparum ensures its amino acid supply with multiple acquisition pathways and redundant proteolytic enzyme systems. Proc. Natl. Acad. Sci. U.S.A. **103**:8840–8845.
62. **Gerald N**, **Mahajan B**, **Kumar S**. 2011. Mitosis in the human malaria parasite Plasmodium falciparum. Eukaryotic Cell **10**:474–482.
63. **Craik R**. 1920. A note on the erythrocytes in malaria. The Lancet.
64. **Hegner R**. 1938. Relative frequency of ring-stage plasmodia in reticulocytes and mature erythrocytes in man and monkey. American Journal of Hygiene.
65. **Lim C**, **Pereira L**, **Saliba KS**, **Mascarenhas A**, **Maki JN**, **Chery L**, **Gomes E**, **Rathod PK**, **Duraisingh MT**. 2016. Reticulocyte Preference and Stage Development of Plasmodium vivax Isolates. J. Infect. Dis. **214**:1081–1084.
66. **Cromer D**, **Evans KJ**, **Schofield L**, **Davenport MP**. 2006. Preferential invasion of reticulocytes during late-stage Plasmodium berghei infection accounts for reduced circulating reticulocyte levels. Int. J. Parasitol. **36**:1389–1397.
67. **Simpson JA**, **Silamut K**, **Chotivanich K**, **Pukrittayakamee S**, **White NJ**. 1999. Red cell selectivity in malaria: a study of multiple-infected erythrocytes. Trans. R. Soc. Trop. Med. Hyg. **93**:165–168.
68. **Naing C**, **Whittaker MA**, **Nyunt Wai V**, **Mak JW**. 2014. Is Plasmodium vivax malaria a severe malaria?: a systematic review and meta-analysis. PLoS Negl Trop Dis **8**:e3071.
69. **Pongponratn E**, **Turner GDH**, **Day NPJ**, **Phu NH**, **Simpson JA**, **Stepniewska K**, **Mai NTH**, **Viriyavejakul P**, **Looareesuwan S**, **Hien TT**, **Ferguson DJP**, **White NJ**. 2003. An ultrastructural study of the brain in fatal Plasmodium falciparum malaria. Am. J. Trop. Med. Hyg. **69**:345–359.
70. **Kwiatkowski D**, **Greenwood BM**. 1989. Why is malaria fever periodic? A hypothesis. Parasitol. Today (Regul. Ed.) **5**:264–266.
71. 2014. Severe malaria. Trop. Med. Int. Health, 2nd ed. **19 Suppl 1**:7–131.

72. **White NJ**. 2017. Malaria parasite clearance. Malaria Journal, 3rd ed. **16**:88.
73. **Franke-Fayard B**, **Fonager J**, **Braks A**, **Khan SM**, **Janse CJ**. 2010. Sequestration and tissue accumulation of human malaria parasites: can we learn anything from rodent models of malaria? PLoS Pathog. **6**:e1001032.
74. **Collins WE**, **Jeffery GM**. 1999. A retrospective examination of sporozoite- and trophozoite-induced infections with Plasmodium falciparum: development of parasitologic and clinical immunity during primary infection. Am. J. Trop. Med. Hyg. **61**:4–19.
75. **Bousema T**, **Drakeley C**. 2011. Epidemiology and infectivity of Plasmodium falciparum and Plasmodium vivax gametocytes in relation to malaria control and elimination. Clin. Microbiol. Rev. **24**:377–410.
76. **Janse CJ**, **van der Klooster PF**, **van der Kaay HJ**, **van der Ploeg M**, **Overdulve JP**. 1986. DNA synthesis in Plasmodium berghei during asexual and sexual development. Mol. Biochem. Parasitol. **20**:173–182.
77. **Aly ASI**, **Vaughan AM**, **Kappe SHI**. 2009. Malaria parasite development in the mosquito and infection of the mammalian host. Annu. Rev. Microbiol. **63**:195–221.
78. **Zollner GE**, **Ponsa N**, **Garman GW**, **Poudel S**, **Bell JA**, **Sattabongkot J**, **Coleman RE**, **Vaughan JA**. 2006. Population dynamics of sporogony for Plasmodium vivax parasites from western Thailand developing within three species of colonized Anopheles mosquitoes. Malaria Journal **5**:68.
79. **Rajahram GS**, **Barber BE**, **William T**, **Grigg MJ**, **Menon J**, **Yeo TW**, **Anstey NM**. 2016. Falling Plasmodium knowlesi Malaria Death Rate among Adults despite Rising Incidence, Sabah, Malaysia, 2010-2014. Emerging Infect. Dis. **22**:41–48.
80. **Leech JH**, **Barnwell JW**, **Miller LH**, **Howard RJ**. 1984. Identification of a strain-specific malarial antigen exposed on the surface of Plasmodium falciparum-infected erythrocytes. J. Exp. Med. **159**:1567–1575.
81. **Su XZ**, **Heatwole VM**, **Wertheimer SP**, **Guinet F**, **Herrfeldt JA**, **Peterson DS**, **Ravetch JA**, **Wellems TE**. 1995. The large diverse gene family var encodes proteins involved in cytoadherence and antigenic variation of Plasmodium falciparum-infected erythrocytes. Cell **82**:89–100.
82. **Cheng Q**, **Cloonan N**, **Fischer K**, **Thompson J**, **Waine G**, **Lanzer M**, **Saul A**. 1998. stevor and rif are Plasmodium falciparum multicopy gene families which potentially encode variant antigens. Mol. Biochem. Parasitol. **97**:161–176.
83. **Turner GD**, **Morrison H**, **Jones M**, **Davis TM**, **Looareesuwan S**, **Buley ID**, **Gatter KC**, **Newbold CI**, **Pukritayakamee S**, **Nagachinta B**. 1994. An immunohistochemical study of the pathology of fatal malaria. Evidence for widespread endothelial activation and a potential role for intercellular adhesion molecule-1 in cerebral sequestration. Am. J. Pathol. **145**:1057–1069.
84. **Favre N**, **Da Laperousaz C**, **Ryffel B**, **Weiss NA**, **Imhof BA**, **Rudin W**, **Lucas R**, **Piguet PF**. 1999. Role of ICAM-1 (CD54) in the development of murine cerebral malaria. Microbes Infect. **1**:961–968.
85. **Turner L**, **Lavstsen T**, **Berger SS**, **Wang CW**, **Petersen JEV**, **Avril M**, **Brazier AJ**, **Freeth J**, **Jespersen JS**, **Nielsen MA**, **Magistrado P**, **Lusingu J**, **Smith JD**, **Higgins MK**, **Theander TG**. 2013. Severe malaria is associated with parasite binding to endothelial protein C receptor. Nature **498**:502–505.
86. **Salanti A**, **Dahlbäck M**, **Turner L**, **Nielsen MA**, **Barfod L**, **Magistrado P**, **Jensen ATR**, **Lavstsen T**, **Ofori MF**, **Marsh K**, **Hviid L**, **Theander TG**. 2004. Evidence for the involvement of VAR2CSA in pregnancy-associated malaria. J. Exp. Med. **200**:1197–1203.
87. **Fried M**, **Duffy PE**. 1996. Adherence of Plasmodium falciparum to chondroitin sulfate A in the human placenta. Science **272**:1502–1504.
88. **Kaul DK**, **Roth EF**, **Nagel RL**, **Howard RJ**, **Handunnetti SM**. 1991. Rosetting of Plasmodium falciparum-infected red blood cells with uninfected red blood cells enhances microvascular obstruction under flow conditions. Blood **78**:812–819.
89. **Dondorp AM**, **Ince C**, **Charunwatthana P**, **Hanson J**, **van Kuijen A**, **Faiz MA**, **Rahman MR**, **Hasan M**, **Bin Yunus E**, **Ghose A**, **Ruangveerayut R**, **Limmathurotsakul D**, **Mathura K**, **White NJ**, **Day NPJ**. 2008. Direct in vivo assessment of microcirculatory dysfunction in severe falciparum malaria. J. Infect. Dis. **197**:79–84.

90. **Carlson J**, **Helmby H**, **Hill AV**, **Brewster D**, **Greenwood BM**, **Wahlgren M**. 1990. Human cerebral malaria: association with erythrocyte rosetting and lack of anti-rosetting antibodies. Lancet **336**:1457–1460.
91. **Ringwald P**, **Peyron F**, **Lepers JP**, **Rabarison P**, **Rakotomalala C**, **Razanamparany M**, **Rabodonirina M**, **Roux J**, **Le Bras J**. 1993. Parasite virulence factors during falciparum malaria: rosetting, cytoadherence, and modulation of cytoadherence by cytokines. Infect. Immun. **61**:5198–5204.
92. **Doumbo OK**, **Thera MA**, **Koné AK**, **Raza A**, **Tempest LJ**, **Lyke KE**, **Plowe CV**, **Rowe JA**. 2009. High levels of Plasmodium falciparum rosetting in all clinical forms of severe malaria in African children. Am. J. Trop. Med. Hyg. **81**:987–993.
93. **Rowe JA**, **Moulds JM**, **Newbold CI**, **Miller LH**. 1997. P. falciparum rosetting mediated by a parasite-variant erythrocyte membrane protein and complement-receptor 1. Nature **388**:292–295.
94. **Goel S**, **Palmkvist M**, **Moll K**, **Joannin N**, **Lara P**, **Akhouri RR**, **Moradi N**, **Öjemalm K**, **Westman M**, **Angeletti D**, **Kjellin H**, **Lehtiö J**, **Blixt O**, **Ideström L**, **Gahmberg CG**, **Storry JR**, **Hult AK**, **Olsson ML**, **Heijne von G**, **Nilsson I**, **Wahlgren M**. 2015. RIFINs are adhesins implicated in severe Plasmodium falciparum malaria. Nat. Med. **21**:314–317.
95. **Niang M**, **Bei AK**, **Madnani KG**, **Pelly S**, **Dankwa S**, **Kanjee U**, **Gunalan K**, **Amaladoss A**, **Yeo KP**, **Bob NS**, **Malleret B**, **Duraisingh MT**, **Preiser PR**. 2014. STEVOR is a Plasmodium falciparum erythrocyte binding protein that mediates merozoite invasion and rosetting. Cell Host Microbe **16**:81–93.
96. **Cranston HA**, **Boylan CW**, **Carroll GL**, **Sutera SP**, **Williamson JR**, **Gluzman IY**, **Krogstad DJ**. 1984. Plasmodium falciparum maturation abolishes physiologic red cell deformability. Science **223**:400–403.
97. **Dondorp AM**, **Kager PA**, **Vreeken J**, **White NJ**. 2000. Abnormal blood flow and red blood cell deformability in severe malaria. Parasitol. Today (Regul. Ed.) **16**:228–232.
98. **Wahlgren M**, **Goel S**, **Akhouri RR**. 2017. Variant surface antigens of Plasmodium falciparum and their roles in severe malaria. Nat. Rev. Microbiol. **15**:479–491.
99. **Krishna S**, **Waller DW**, **Kuile ter F**, **Kwiatkowski D**, **Crawley J**, **Craddock CF**, **Nosten F**, **Chapman D**, **Brewster D**, **Holloway PA**. 1994. Lactic acidosis and hypoglycaemia in children with severe malaria: pathophysiological and prognostic significance. Trans. R. Soc. Trop. Med. Hyg. **88**:67–73.
100. **Marsh K**, **English M**, **Crawley J**, **Peshu N**. 1996. The pathogenesis of severe malaria in African children. Ann Trop Med Parasitol **90**:395–402.
101. **Brand NR**, **Opoka RO**, **Hamre KES**, **John CC**. 2016. Differing Causes of Lactic Acidosis and Deep Breathing in Cerebral Malaria and Severe Malarial Anemia May Explain Differences in Acidosis-Related Mortality. PLoS ONE **11**:e0163728.
102. **Dekker E**, **Hellerstein MK**, **Romijn JA**, **Neese RA**, **Peshu N**, **Endert E**, **Marsh K**, **Sauerwein HP**. 1997. Glucose homeostasis in children with falciparum malaria: precursor supply limits gluconeogenesis and glucose production. J. Clin. Endocrinol. Metab. **82**:2514–2521.
103. **White NJ**, **Warrell DA**, **Chanthavanich P**, **Looareesuwan S**, **Warrell MJ**, **Krishna S**, **Williamson DH**, **Turner RC**. 1983. Severe hypoglycemia and hyperinsulinemia in falciparum malaria. N. Engl. J. Med. **309**:61–66.
104. **Madrid L**, **Lanaspa M**, **Maculuve SA**, **Bassat Q**. 2015. Malaria-associated hypoglycaemia in children. Expert Rev Anti Infect Ther, 2nd ed. **13**:267–277.
105. **Willcox ML**, **Forster M**, **Dicko MI**, **Graz B**, **Mayon-White R**, **Barennes H**. 2010. Blood glucose and prognosis in children with presumed severe malaria: is there a threshold for 'hypoglycaemia'? Trop. Med. Int. Health **15**:232–240.
106. **Parroche P**, **Lauw FN**, **Goutagny N**, **Latz E**, **Monks BG**, **Visintin A**, **Halmen KA**, **Lamphier M**, **Olivier M**, **Bartholomeu DC**, **Gazzinelli RT**, **Golenbock DT**. 2007. Malaria hemozoin is immunologically inert but radically enhances innate responses by presenting malaria DNA to Toll-like receptor 9. Proc. Natl. Acad. Sci. U.S.A. **104**:1919–1924.
107. **Gowda NM**, **Wu X**, **Gowda DC**. 2011. The nucleosome (histone-DNA complex) is the TLR9-specific immunostimulatory component of Plasmodium falciparum that activates DCs. PLoS ONE **6**:e20398.

108. **Krishnegowda G**, **Hajjar AM**, **Zhu J**, **Douglass EJ**, **Uematsu S**, **Akira S**, **Woods AS**, **Gowda DC**. 2005. Induction of proinflammatory responses in macrophages by the glycosylphosphatidylinositols of Plasmodium falciparum: cell signaling receptors, glycosylphosphatidylinositol (GPI) structural requirement, and regulation of GPI activity. J. Biol. Chem. **280**:8606–8616.
109. **Dutra FF**, **Alves LS**, **Rodrigues D**, **Fernandez PL**, **de Oliveira RB**, **Golenbock DT**, **Zamboni DS**, **Bozza MT**. 2014. Hemolysis-induced lethality involves inflammasome activation by heme. Proc. Natl. Acad. Sci. U.S.A. **111**:E4110–8.
110. **Finley RW**, **Mackey LJ**, **Lambert PH**. 1982. Virulent P. berghei malaria: prolonged survival and decreased cerebral pathology in cell-dependent nude mice. J. Immunol. **129**:2213–2218.
111. **Haque A**, **Best SE**, **Unosson K**, **Amante FH**, **de Labastida F**, **Anstey NM**, **Karupiah G**, **Smyth MJ**, **Heath WR**, **Engwerda CR**. 2011. Granzyme B expression by CD8+ T cells is required for the development of experimental cerebral malaria. J. Immunol. **186**:6148–6156.
112. **Orengo JM**, **Evans JE**, **Bettiol E**, **Leliwa-Sytek A**, **Day K**, **Rodriguez A**. 2008. Plasmodium-induced inflammation by uric acid. PLoS Pathog. **4**:e1000013.
113. **Couper KN**, **Barnes T**, **Hafalla JCR**, **Combes V**, **Ryffel B**, **Secher T**, **Grau GE**, **Riley EM**, **de Souza JB**. 2010. Parasite-derived plasma microparticles contribute significantly to malaria infection-induced inflammation through potent macrophage stimulation. PLoS Pathog. **6**:e1000744.
114. **Antonelli LRV**, **Leoratti FMS**, **Costa PAC**, **Rocha BC**, **Diniz SQ**, **Tada MS**, **Pereira DB**, **Teixeira-Carvalho A**, **Golenbock DT**, **Gonçalves R**, **Gazzinelli RT**. 2014. The CD14+CD16+ inflammatory monocyte subset displays increased mitochondrial activity and effector function during acute Plasmodium vivax malaria. PLoS Pathog. **10**:e1004393.
115. **Weiser S**, **Miu J**, **Ball HJ**, **Hunt NH**. 2007. Interferon-gamma synergises with tumour necrosis factor and lymphotoxin-alpha to enhance the mRNA and protein expression of adhesion molecules in mouse brain endothelial cells. Cytokine **37**:84–91.
116. **Clark IA**, **Chaudhri G**. 1988. Tumour necrosis factor may contribute to the anaemia of malaria by causing dyserythropoiesis and erythrophagocytosis. Br. J. Haematol. **70**:99–103.
117. **Kurtzhals JA**, **Adabayeri V**, **Goka BQ**, **Akanmori BD**, **Oliver-Commey JO**, **Nkrumah FK**, **Behr C**, **Hviid L**. 1998. Low plasma concentrations of interleukin 10 in severe malarial anaemia compared with cerebral and uncomplicated malaria. Lancet **351**:1768–1772.
118. **Awandare GA**, **Goka B**, **Boeuf P**, **Tetteh JKA**, **Kurtzhals JAL**, **Behr C**, **Akanmori BD**. 2006. Increased levels of inflammatory mediators in children with severe Plasmodium falciparum malaria with respiratory distress. J. Infect. Dis. **194**:1438–1446.
119. **Clark IA**. 1987. Cell-mediated immunity in protection and pathology of malaria. Parasitol. Today (Regul. Ed.) **3**:300–305.
120. **Dodoo D**, **Omer FM**, **Todd J**, **Akanmori BD**, **Koram KA**, **Riley EM**. 2002. Absolute levels and ratios of proinflammatory and anti-inflammatory cytokine production in vitro predict clinical immunity to Plasmodium falciparum malaria. J. Infect. Dis. **185**:971–979.
121. **Marsh K**, **Kinyanjui S**. 2006. Immune effector mechanisms in malaria. Parasite Immunol. **28**:51–60.
122. **Gupta S**, **Snow RW**, **Donnelly CA**, **Marsh K**, **Newbold C**. 1999. Immunity to non-cerebral severe malaria is acquired after one or two infections. Nat. Med. **5**:340–343.
123. **Gupta S**, **Snow RW**, **Donnelly C**, **Newbold C**. 1999. Acquired immunity and postnatal clinical protection in childhood cerebral malaria. Proc. Biol. Sci. **266**:33–38.
124. **Marsh K**, **Snow RW**. 1997. Host-parasite interaction and morbidity in malaria endemic areas. Philos. Trans. R. Soc. Lond., B, Biol. Sci. **352**:1385–1394.
125. **Griffin JT**, **Hollingsworth TD**, **Reyburn H**, **Drakeley CJ**, **Riley EM**, **Ghani AC**. 2015. Gradual acquisition of immunity to severe malaria with increasing exposure.

Proc. Biol. Sci. **282**:20142657–20142657.
126. **Wagner G**, **Koram K**, **McGuinness D**, **Bennett S**, **Nkrumah F**, **Riley E**. 1998. High incidence of asymptomatic malara infections in a birth cohort of children less than one year of age in Ghana, detected by multicopy gene polymerase chain reaction. Am. J. Trop. Med. Hyg. **59**:115–123.
127. **Riley EM**, **Wagner GE**, **Akanmori BD**, **Koram KA**. 2001. Do maternally acquired antibodies protect infants from malaria infection? Parasite Immunol. **23**:51–59.
128. **Dobbs KR**, **Dent AE**. 2016. Plasmodium malaria and antimalarial antibodies in the first year of life. Parasitology **143**:129–138.
129. **Chan J-A**, **Howell KB**, **Reiling L**, **Ataide R**, **Mackintosh CL**, **Fowkes FJI**, **Petter M**, **Chesson JM**, **Langer C**, **Warimwe GM**, **Duffy MF**, **Rogerson SJ**, **Bull PC**, **Cowman AF**, **Marsh K**, **Beeson JG**. 2012. Targets of antibodies against Plasmodium falciparum-infected erythrocytes in malaria immunity. J. Clin. Invest. **122**:3227–3238.
130. **Biggs BA**, **Goozé L**, **Wycherley K**, **Wollish W**, **Southwell B**, **Leech JH**, **Brown GV**. 1991. Antigenic variation in Plasmodium falciparum. Proc. Natl. Acad. Sci. U.S.A. **88**:9171–9174.
131. **Riley EM**, **Allen SJ**, **Wheeler JG**, **Blackman MJ**, **Bennett S**, **Takacs B**, **Schönfeld HJ**, **Holder AA**, **Greenwood BM**. 1992. Naturally acquired cellular and humoral immune responses to the major merozoite surface antigen (PfMSP1) of Plasmodium falciparum are associated with reduced malaria morbidity. Parasite Immunol. **14**:321–337.
132. **Meraldi V**, **Nebié I**, **Tiono AB**, **Diallo D**, **Sanogo E**, **Theisen M**, **Druilhe P**, **Corradin G**, **Moret R**, **Sirima BS**. 2004. Natural antibody response to Plasmodium falciparum Exp-1, MSP-3 and GLURP long synthetic peptides and association with protection. Parasite Immunol. **26**:265–272.
133. **Polley SD**, **Mwangi T**, **Kocken CHM**, **Thomas AW**, **Dutta S**, **Lanar DE**, **Remarque E**, **Ross A**, **Williams TN**, **Mwambingu G**, **Lowe B**, **Conway DJ**, **Marsh K**. 2004. Human antibodies to recombinant protein constructs of Plasmodium falciparum Apical Membrane Antigen 1 (AMA1) and their associations with protection from malaria. Vaccine **23**:718–728.
134. **Dziegiel M**, **Rowe P**, **Bennett S**, **Allen SJ**, **Olerup O**, **Gottschau A**, **Borre M**, **Riley EM**. 1993. Immunoglobulin M and G antibody responses to Plasmodium falciparum glutamate-rich protein: correlation with clinical immunity in Gambian children. Infect. Immun. **61**:103–108.
135. **Douglas AD**, **Williams AR**, **Illingworth JJ**, **Kamuyu G**, **Biswas S**, **Goodman AL**, **Wyllie DH**, **Crosnier C**, **Miura K**, **Wright GJ**, **Long CA**, **Osier FH**, **Marsh K**, **Turner AV**, **Hill AVS**, **Draper SJ**. 2011. The blood-stage malaria antigen PfRH5 is susceptible to vaccine-inducible cross-strain neutralizing antibody. Nat Commun **2**:601.
136. **Richards JS**, **Arumugam TU**, **Reiling L**, **Healer J**, **Hodder AN**, **Fowkes FJI**, **Cross N**, **Langer C**, **Takeo S**, **Uboldi AD**, **Thompson JK**, **Gilson PR**, **Coppel RL**, **Siba PM**, **King CL**, **Torii M**, **Chitnis CE**, **Narum DL**, **Müeller I**, **Crabb BS**, **Cowman AF**, **Tsuboi T**, **Beeson JG**. 2013. Identification and prioritization of merozoite antigens as targets of protective human immunity to Plasmodium falciparum malaria for vaccine and biomarker development. J. Immunol. **191**:795–809.
137. **Barry A**, **Hansen D**. 2016. Naturally acquired immunity to malaria. Parasitology **143**:125–128.
138. **Osier FHA**, **Fegan G**, **Polley SD**, **Murungi L**, **Verra F**, **Tetteh KKA**, **Lowe B**, **Mwangi T**, **Bull PC**, **Thomas AW**, **Cavanagh DR**, **McBride JS**, **Lanar DE**, **Mackinnon MJ**, **Conway DJ**, **Marsh K**. 2008. Breadth and magnitude of antibody responses to multiple Plasmodium falciparum merozoite antigens are associated with protection from clinical malaria. Infect. Immun. **76**:2240–2248.
139. **Moormann AM**, **Sumba PO**, **Chelimo K**, **Fang H**, **Tisch DJ**, **Dent AE**, **John CC**, **Long CA**, **Vulule J**, **Kazura JW**. 2013. Humoral and cellular immunity to Plasmodium falciparum merozoite surface protein 1 and protection from infection with blood-stage parasites. J. Infect. Dis. **208**:149–158.
140. **Taylor-Robinson AW**, **Phillips RS**, **Severn A**, **Moncada S**, **Liew FY**. 1993. The role of TH1 and TH2 cells in a rodent malaria infection. Science **260**:1931–1934.

141. **Lau LS**, **Ruiz DF**, **Davey GM**. 2011. Blood-stage Plasmodium berghei infection generates a potent, specific CD8+ T-cell response despite residence largely in cells lacking MHC I processing machinery. The Journal of ….
142. **Hansen DS**, **Schofield L**. 2010. Natural regulatory T cells in malaria: host or parasite allies? PLoS Pathog. **6**:e1000771.
143. **Esposito F**, **Lombardi S**, **Modiano D**, **Zavala F**, **Reeme J**, **Lamizana L**, **Coluzzi M**, **Nussenzweig RS**. 1988. Prevalence and levels of antibodies to the circumsporozoite protein of Plasmodium falciparum in an endemic area and their relationship to resistance against malaria infection. Trans. R. Soc. Trop. Med. Hyg. **82**:827–832.
144. **John CC**, **Zickafoose JS**, **Sumba PO**, **King CL**, **Kazura JW**. 2003. Antibodies to the Plasmodium falciparum antigens circumsporozoite protein, thrombospondin-related adhesive protein, and liver-stage antigen 1 vary by ages of subjects and by season in a highland area of Kenya. Infect. Immun. **71**:4320–4325.
145. **Fidock DA**, **Pasquetto V**, **Gras H**, **Badell E**, **Eling W**, **Ballou WR**, **Belghiti J**, **Tartar A**, **Druilhe P**. 1997. Plasmodium falciparum sporozoite invasion is inhibited by naturally acquired or experimentally induced polyclonal antibodies to the STARP antigen. Eur. J. Immunol. **27**:2502–2513.
146. **Hoffman SL**, **Oster CN**, **Plowe CV**, **Woollett GR**, **Beier JC**, **Chulay JD**, **Wirtz RA**, **Hollingdale MR**, **Mugambi M**. 1987. Naturally acquired antibodies to sporozoites do not prevent malaria: vaccine development implications. Science **237**:639–642.
147. **John CC**, **Moormann AM**, **Pregibon DC**, **Sumba PO**, **McHugh MM**, **Narum DL**, **Lanar DE**, **Schluchter MD**, **Kazura JW**. 2005. Correlation of high levels of antibodies to multiple pre-erythrocytic Plasmodium falciparum antigens and protection from infection. Am. J. Trop. Med. Hyg. **73**:222–228.
148. **Hill AV**, **Elvin J**, **Willis AC**, **Aidoo M**, **Allsopp CE**, **Gotch FM**, **Gao XM**, **Takiguchi M**, **Greenwood BM**, **Townsend AR**. 1992. Molecular analysis of the association of HLA-B53 and resistance to severe malaria. Nature **360**:434–439.
149. **Gunewardena DM**, **Carter R**, **Mendis KN**. 1994. Patterns of acquired anti-malarial immunity in Sri Lanka. Mem. Inst. Oswaldo Cruz **89 Suppl 2**:63–65.
150. **Müeller I**, **Galinski MR**, **Tsuboi T**, **Arévalo-Herrera M**, **Collins WE**, **King CL**. 2013. Natural acquisition of immunity to Plasmodium vivax: epidemiological observations and potential targets. Adv. Parasitol. **81**:77–131.
151. **Ray P**, **Ansari MA**, **Sharma YD**. 1994. Plasmodium vivax: immune responses in a cross-section of the population in the Delhi area of India. Am. J. Trop. Med. Hyg. **51**:436–443.
152. **Fraser T**, **Michon P**, **Barnwell JW**, **Noe AR**, **Al-Yaman F**, **Kaslow DC**, **Adams JH**. 1997. Expression and serologic activity of a soluble recombinant Plasmodium vivax Duffy binding protein. Infect. Immun. **65**:2772–2777.
153. **Miller LH**, **Mason SJ**, **Clyde DF**, **McGinniss MH**. 1976. The resistance factor to Plasmodium vivax in blacks. The Duffy-blood-group genotype, FyFy. N. Engl. J. Med. **295**:302–304.
154. **Ryan JR**, **Stoute JA**, **Amon J**, **Dunton RF**, **Mtalib R**, **Koros J**, **Owour B**, **Luckhart S**, **Wirtz RA**, **Barnwell JW**, **Rosenberg R**. 2006. Evidence for transmission of Plasmodium vivax among a duffy antigen negative population in Western Kenya. Am. J. Trop. Med. Hyg. **75**:575–581.
155. **Michon P**, **Fraser T**, **Adams JH**. 2000. Naturally acquired and vaccine-elicited antibodies block erythrocyte cytoadherence of the Plasmodium vivax Duffy binding protein. Infect. Immun. **68**:3164–3171.
156. **Nicolete VC**, **Frischmann S**, **Barbosa S**, **King CL**, **Ferreira MU**. 2016. Naturally Acquired Binding-Inhibitory Antibodies to Plasmodium vivax Duffy Binding Protein and Clinical Immunity to Malaria in Rural Amazonians. J. Infect. Dis. **214**:1539–1546.
157. **Nogueira PA**, **Alves FP**, **Fernandez-Becerra C**, **Pein O**, **Santos NR**, **Pereira da Silva LH**, **Camargo EP**, **del Portillo HA**. 2006. A reduced risk of infection with Plasmodium vivax and clinical protection against malaria are associated with antibodies against the N terminus but not the C terminus of merozoite surface protein 1. Infect. Immun. **74**:2726–2733.
158. **Longley RJ**, **Sattabongkot J**, **Müeller I**. 2016. Insights into the naturally acquired

immune response to Plasmodium vivax malaria. Parasitology **143**:154–170.
159. **Lima-Junior JC**, **Jiang J**, **Rodrigues-da-Silva RN**, **Banic DM**, **Tran TM**, **Ribeiro RY**, **Meyer VSE**, **De-Simone SG**, **Santos F**, **Moreno A**, **Barnwell JW**, **Galinski MR**, **Oliveira-Ferreira J**. 2011. B cell epitope mapping and characterization of naturally acquired antibodies to the Plasmodium vivax merozoite surface protein-3α (PvMSP-3α) in malaria exposed individuals from Brazilian Amazon. Vaccine **29**:1801–1811.
160. **Stanisic DI**, **Javati S**, **Kiniboro B**, **Lin E**, **Jiang J**, **Singh B**, **Meyer EVS**, **Siba P**, **Koepfli C**, **Felger I**, **Galinski MR**, **Müeller I**. 2013. Naturally acquired immune responses to P. vivax merozoite surface protein 3α and merozoite surface protein 9 are associated with reduced risk of P. vivax malaria in young Papua New Guinean children. PLoS Negl Trop Dis **7**:e2498.
161. **Alam MT**, **Bora H**, **Mittra P**, **Singh N**, **Sharma YD**. 2008. Cellular immune responses to recombinant Plasmodium vivax tryptophan-rich antigen (PvTRAg) among individuals exposed to vivax malaria. Parasite Immunol. **30**:379–383.
162. **Riccio EKP**, **Totino PRR**, **Pratt-Riccio LR**, **Ennes-Vidal V**, **Soares IS**, **Rodrigues MM**, **de Souza JM**, **Daniel-Ribeiro CT**, **Ferreira-da-Cruz M de F**. 2013. Cellular and humoral immune responses against the Plasmodium vivax MSP-1_{19} malaria vaccine candidate in individuals living in an endemic area in north-eastern Amazon region of Brazil. Malaria Journal **12**:326.
163. **Cheng Y**, **Wang B**, **Changrob S**, **Han J-H**, **Sattabongkot J**, **Ha K-S**, **Chootong P**, **Lu F**, **Cao J**, **Nyunt MH**, **Park WS**, **Hong S-H**, **Lim CS**, **Tsuboi T**, **Han E-T**. 2017. Naturally acquired humoral and cellular immune responses to Plasmodium vivax merozoite surface protein 8 in patients with P. vivax infection. Malaria Journal **16**:211.
164. **Nguyen HV**, **van den Eede P**, **van Overmeir C**, **Thang ND**, **Hung LX**, **D'Alessandro U**, **Erhart A**. 2012. Marked age-dependent prevalence of symptomatic and patent infections and complexity of distribution of human Plasmodium species in central Vietnam. Am. J. Trop. Med. Hyg. **87**:989–995.
165. **Mendis KN**, **Munesinghe YD**, **de Silva YN**, **Keragalla I**, **Carter R**. 1987. Malaria transmission-blocking immunity induced by natural infections of Plasmodium vivax in humans. Infect. Immun. **55**:369–372.
166. **Jones S**, **Grignard L**, **Nébié I**, **Chilongola J**, **Dodoo D**, **Sauerwein R**, **Theisen M**, **Roeffen W**, **Singh SK**, **Singh RK**, **Singh S**, **Kyei-Baafour E**, **Tetteh K**, **Drakeley C**, **Bousema T**. 2015. Naturally acquired antibody responses to recombinant Pfs230 and Pfs48/45 transmission blocking vaccine candidates. J. Infect. **71**:117–127.
167. **Gebru T**, **Ajua A**, **Theisen M**, **Esen M**, **Ngoa UA**, **Issifou S**, **Adegnika AA**, **Kremsner PG**, **Mordmüller B**, **Held J**. 2017. Recognition of Plasmodium falciparum mature gametocyte-infected erythrocytes by antibodies of semi-immune adults and malaria-exposed children from Gabon. Malaria Journal **16**:176.
168. **Stewart AJ**, **Devlin PM**. 2006. The history of the smallpox vaccine. J. Infect. **52**:329–334.
169. **Jenner E**. 1798. An enquiry into the causes and effects of the varriolae vaccinae; a disease discovered in some of the western counties of England, particularly Gloucestershire, and known by the name of the cowpox.
170. **Lock S**. 1995. Research ethics--a brief historical review to 1965.Journal of internal medicine.
171. **Pasteur L**. 1885. Methode pour prevenir la rage apres morsure.
172. **Salmon D**, **Smith T**. 1886. On a new method of producing immunity from contagious diseases.
173. **Roux E**, **Chamberland CE**. 1887. Immunite contre la septicemie conferee par des substances solubles.
174. **Plotkin S**. 2014. History of vaccination. Proc. Natl. Acad. Sci. U.S.A. **111**:12283–12287.
175. **Calmette A**, **Guérin C**, **Boquet A**, **Nègre L**. 1927. La vaccination préventive contre la tuberculose par le“ BCG,.”
176. **Ottenhoff THM**, **Kaufmann SHE**. 2012. Vaccines against tuberculosis: where are we and where do we need to go? PLoS Pathog. **8**:e1002607.
177. **A T Glenny BEH**. 1923. Diphtheria Toxoid as an Immunising Agent. British journal

of experimental pathology **4**:283.
178. **Zöller RE**. 1926. De la valeur antigène de l"ana toxine Aétanique chez l"homme. C. r. Acad. Sci. Paris.
179. **Wolters KL**, **Dehmel H**. 1942. Abschließende Untersuchungen über die Tetanusprophylaxe durch aktive Immunisierung. Zeitschr. f. Hygiene. **124**:326–332.
180. **Institute of Medicine (US) Vaccine Safety Committee**, **Stratton KR**, **Howe CJ**, **Johnston RB**. 1994. Adverse Events Associated with Childhood Vaccines: Evidence Bearing on Causality.
181. **Cate TR**, **Couch RB**, **Kasel JA**, **Six HR**. 1977. Clinical trials of monovalent influenza A/New Jersey/76 virus vaccines in adults: reactogenicity, antibody response, and antibody persistence. J. Infect. Dis. **136 Suppl**:S450–5.
182. **Finland M**, **Ruegsegger JM**. 1935. IMMUNIZATION OF HUMAN SUBJECTS WITH THE SPECIFIC CARBOHYDRATES OF TYPE III AND THE RELATED TYPE VIII PNEUMOCOCCUS. J. Clin. Invest. **14**:829–832.
183. **Gotschlich EC**, **Goldschneider I**, **Artenstein MS**. 1969. Human immunity to the meningococcus. IV. Immunogenicity of group A and group C meningococcal polysaccharides in human volunteers. J. Exp. Med. **129**:1367–1384.
184. **Vipond C**, **Care R**, **Feavers IM**. 2012. History of meningococcal vaccines and their serological correlates of protection. Vaccine **30 Suppl 2**:B10–7.
185. **McAleer WJ**, **Buynak EB**, **Maigetter RZ**, **Wampler DE**, **Miller WJ**, **Hilleman MR**. 1984. Human hepatitis B vaccine from recombinant yeast. Nature **307**:178–180.
186. **Kirnbauer R**, **Booy F**, **Cheng N**, **Lowy DR**, **Schiller JT**. 1992. Papillomavirus L1 major capsid protein self-assembles into virus-like particles that are highly immunogenic. Proc. Natl. Acad. Sci. U.S.A. **89**:12180–12184.
187. **Bachmann MF**, **Jennings GT**. 2010. Vaccine delivery: a matter of size, geometry, kinetics and molecular patterns. Nat. Rev. Immunol. **10**:787–796.
188. **Gordon DM**, **McGovern TW**, **Krzych U**, **Cohen JC**, **Schneider I**, **LaChance R**, **Heppner DG**, **Yuan G**, **Hollingdale M**, **Slaoui M**. 1995. Safety, immunogenicity, and efficacy of a recombinantly produced Plasmodium falciparum circumsporozoite protein-hepatitis B surface antigen subunit vaccine. J. Infect. Dis. **171**:1576–1585.
189. **Collins KA**, **Snaith R**, **Cottingham MG**, **Gilbert SC**, **Hill AVS**. 2017. Enhancing protective immunity to malaria with a highly immunogenic virus-like particle vaccine. Sci Rep **7**:46621.
190. **Salman AM**, **Montoya-Díaz E**, **West H**, **Lall A**, **Erwan Erwan**, **Lopez-Camacho C**, **Ramesar J**, **Bauza K**, **Collins KA**, **Brod F**, **Reis F**, **Pappas L**, **González-Cerón L**, **Janse CJ**, **Hill AVS**, **Khan SM**, **Reyes-Sandoval A**. 2017. Rational development of a protective P. vivax vaccine evaluated with transgenic rodent parasite challenge models. Sci Rep **7**:46482.
191. **Brune KD**, **Leneghan DB**, **Brian IJ**, **Ishizuka AS**, **Bachmann MF**, **Draper SJ**, **Biswas S**, **Howarth M**. 2016. Plug-and-Display: decoration of Virus-Like Particles via isopeptide bonds for modular immunization. Sci Rep **6**:19234.
192. **Maurer P**, **Jennings GT**, **Willers J**, **Rohner F**, **Lindman Y**, **Roubicek K**, **Renner WA**, **Müller P**, **Bachmann MF**. 2005. A therapeutic vaccine for nicotine dependence: preclinical efficacy, and Phase I safety and immunogenicity. Eur. J. Immunol. **35**:2031–2040.
193. **Rutgers T**, **Gordon D**, **Gathoye AM**, **Hollingdale M**, **Hockmeyer W**, **Rosenberg M**, **De Wilde M**. 1988. Hepatitis B Surface Antigen as Carrier Matrix for the Repetitive Epitope of the Circumsporozoite Protein of Plasmodium Falciparum. Nature Biotechnology **6**:1065–1070.
194. **Moss B**, **Smith GL**, **Gerin JL**, **Purcell RH**. 1984. Live recombinant vaccinia virus protects chimpanzees against hepatitis B. Nature **311**:67–69.
195. **World Health Organization (WHO)**. 2013. Summary report on first, second and third generation smallpox vaccines.
196. **Schneider J**, **Gilbert SC**, **Blanchard TJ**, **Hanke T**, **Robson KJ**, **Hannan CM**, **Becker M**, **Sinden R**, **Smith GL**, **Hill AV**. 1998. Enhanced immunogenicity for CD8+ T cell induction and complete protective efficacy of malaria DNA vaccination by boosting with modified vaccinia virus Ankara. Nat. Med. **4**:397–402.
197. **Mwau M**, **Cebere I**, **Sutton J**, **Chikoti P**, **Winstone N**, **Wee EGT**, **Beattie T**, **Chen Y-**

H, **Dorrell L**, **McShane H**, **Schmidt C**, **Brooks M**, **Patel S**, **Roberts J**, **Conlon C**, **Rowland-Jones SL**, **Bwayo JJ**, **McMichael AJ**, **Hanke T**. 2004. A human immunodeficiency virus 1 (HIV-1) clade A vaccine in clinical trials: stimulation of HIV-specific T-cell responses by DNA and recombinant modified vaccinia virus Ankara (MVA) vaccines in humans. Journal of General Virology **85**:911–919.

198. **Nicol MP**, **Grobler LA**. 2010. MVA-85A, a novel candidate booster vaccine for the prevention of tuberculosis in children and adults. Curr. Opin. Mol. Ther. **12**:124–134.

199. **Song G-Y**, **Gibson G**, **Haq W**, **Huang ECC**, **Srivasta T**, **Hollstein M**, **Daftarian P**, **Wang Z**, **Diamond D**, **Ellenhorn JDI**. 2007. An MVA vaccine overcomes tolerance to human p53 in mice and humans. Cancer Immunol. Immunother. **56**:1193–1205.

200. **Berthoud TK**, **Hamill M**, **Lillie PJ**, **Hwenda L**, **Collins KA**, **Ewer KJ**, **Milicic A**, **Poyntz HC**, **Lambe T**, **Fletcher HA**, **Hill AVS**, **Gilbert SC**. 2011. Potent CD8+ T-cell immunogenicity in humans of a novel heterosubtypic influenza A vaccine, MVA-NP+M1. Clin. Infect. Dis. **52**:1–7.

201. **Sedegah M**, **Tamminga C**, **McGrath S**, **House B**, **Ganeshan H**, **Lejano J**, **Abot E**, **Banania GJ**, **Sayo R**, **Farooq F**, **Belmonte M**, **Manohar N**, **Richie NO**, **Wood C**, **Long CA**, **Regis D**, **Williams FT**, **Shi M**, **Chuang I**, **Spring M**, **Epstein JE**, **Mendoza-Silveiras J**, **Limbach K**, **Patterson NB**, **Bruder JT**, **Doolan DL**, **King CR**, **Soisson L**, **Diggs C**, **Carucci D**, **Dutta S**, **Hollingdale MR**, **Ockenhouse CF**, **Richie TL**. 2011. Adenovirus 5-vectored P. falciparum vaccine expressing CSP and AMA1. Part A: safety and immunogenicity in seronegative adults. PLoS ONE **6**:e24586.

202. **Shiver JW**, **Fu T-M**, **Chen L**, **Casimiro DR**, **Davies M-E**, **Evans RK**, **Zhang Z-Q**, **Simon AJ**, **Trigona WL**, **Dubey SA**, **Huang L**, **Harris VA**, **Long RS**, **Liang X**, **Handt L**, **Schleif WA**, **Zhu L**, **Freed DC**, **Persaud NV**, **Guan L**, **Punt KS**, **Tang A**, **Chen M**, **Wilson KA**, **Collins KB**, **Heidecker GJ**, **Fernandez VR**, **Perry HC**, **Joyce JG**, **Grimm KM**, **Cook JC**, **Keller PM**, **Kresock DS**, **Mach H**, **Troutman RD**, **Isopi LA**, **Williams DM**, **Xu Z**, **Bohannon KE**, **Volkin DB**, **Montefiori DC**, **Miura A**, **Krivulka GR**, **Lifton MA**, **Kuroda MJ**, **Schmitz JE**, **Letvin NL**, **Caulfield MJ**, **Bett AJ**, **Youil R**, **Kaslow DC**, **Emini EA**. 2002. Replication-incompetent adenoviral vaccine vector elicits effective anti-immunodeficiency-virus immunity. Nature **415**:331–335.

203. **Jaiswal S**, **Khanna N**, **Swaminathan S**. 2003. Replication-defective adenoviral vaccine vector for the induction of immune responses to dengue virus type 2. J. Virol. **77**:12907–12913.

204. **Tatsis N**, **Ertl HCJ**. 2004. Adenoviruses as vaccine vectors. Mol. Ther. **10**:616–629.

205. **Colloca S**, **Barnes E**, **Folgori A**, **Ammendola V**, **Capone S**, **Cirillo A**, **Siani L**, **Naddeo M**, **Grazioli F**, **Esposito ML**, **Ambrosio M**, **Sparacino A**, **Bartiromo M**, **Meola A**, **Smith K**, **Kurioka A**, **O'Hara GA**, **Ewer KJ**, **Anagnostou N**, **Bliss C**, **Hill AVS**, **Traboni C**, **Klenerman P**, **Cortese R**, **Nicosia A**. 2012. Vaccine vectors derived from a large collection of simian adenoviruses induce potent cellular immunity across multiple species. Sci Transl Med **4**:115ra2–115ra2.

206. **O'Hara GA**, **Duncan CJA**, **Ewer KJ**, **Collins KA**, **Elias SC**, **Halstead FD**, **Goodman AL**, **Edwards NJ**, **Reyes-Sandoval A**, **Bird P**, **Rowland R**, **Sheehy SH**, **Poulton ID**, **Hutchings C**, **Todryk S**, **Andrews L**, **Folgori A**, **Berrie E**, **Moyle S**, **Nicosia A**, **Colloca S**, **Cortese R**, **Siani L**, **Lawrie AM**, **Gilbert SC**, **Hill AVS**. 2012. Clinical assessment of a recombinant simian adenovirus ChAd63: a potent new vaccine vector. J. Infect. Dis. **205**:772–781.

207. **Dicks MDJ**, **Spencer AJ**, **Edwards NJ**, **Wadell G**, **Bojang K**, **Gilbert SC**, **Hill AVS**, **Cottingham MG**. 2012. A novel chimpanzee adenovirus vector with low human seroprevalence: improved systems for vector derivation and comparative immunogenicity. PLoS ONE **7**:e40385.

208. **Limbach K**, **Stefaniak M**, **Chen P**, **Patterson NB**, **Liao G**, **Weng S**, **Krepkiy S**, **Ekberg G**, **Torano H**, **Ettyreddy D**, **Gowda K**, **Sonawane S**, **Belmonte A**, **Abot E**, **Sedegah M**, **Hollingdale MR**, **Moormann A**, **Vulule J**, **Villasante E**, **Richie TL**, **Brough DE**, **Bruder JT**. 2017. New gorilla adenovirus vaccine vectors induce potent immune responses and protection in a mouse malaria model. Malaria Journal **16**:263.

209. **Tine JA**, **Lanar DE**, **Smith DM**, **Wellde BT**, **Schultheiss P**, **Ware LA**, **Kauffman EB**, **Wirtz RA**, **de Taisne C**, **Hui GS**, **Chang SP**, **Church P**, **Hollingdale MR**, **Kaslow DC**,

Hoffman S, **Guito KP**, **Ballou WR**, **Sadoff JC**, **Paoletti E**. 1996. NYVAC-Pf7: a poxvirus-vectored, multiantigen, multistage vaccine candidate for Plasmodium falciparum malaria. Infect. Immun. **64**:3833–3844.

210. **Anderson RJ**, **Hannan CM**, **Gilbert SC**, **Laidlaw SM**, **Sheu EG**, **Korten S**, **Sinden R**, **Butcher GA**, **Skinner MA**, **Hill AVS**. 2004. Enhanced CD8+ T cell immune responses and protection elicited against Plasmodium berghei malaria by prime boost immunization regimens using a novel attenuated fowlpox virus. J. Immunol. **172**:3094–3100.
211. **Odunsi K**, **Matsuzaki J**, **Karbach J**, **Neumann A**, **Mhawech-Fauceglia P**, **Miller A**, **Beck A**, **Morrison CD**, **Ritter G**, **Godoy H**, **Lele S**, **duPont N**, **Edwards R**, **Shrikant P**, **Old LJ**, **Gnjatic S**, **Jäger E**. 2012. Efficacy of vaccination with recombinant vaccinia and fowlpox vectors expressing NY-ESO-1 antigen in ovarian cancer and melanoma patients. Proc. Natl. Acad. Sci. U.S.A. **109**:5797–5802.
212. **Davis NL**, **West A**, **Reap E**, **MacDonald G**, **Collier M**, **Dryga S**, **Maughan M**, **Connell M**, **Walker C**, **McGrath K**, **Cecil C**, **Ping L-H**, **Frelinger J**, **Olmsted R**, **Keith P**, **Swanstrom R**, **Williamson C**, **Johnson P**, **Montefiori D**, **Johnston RE**. 2002. Alphavirus replicon particles as candidate HIV vaccines. IUBMB Life **53**:209–211.
213. **Pan C-H**, **Greer CE**, **Hauer D**, **Legg HS**, **Lee E-Y**, **Bergen MJ**, **Lau B**, **Adams RJ**, **Polo JM**, **Griffin DE**. 2010. A chimeric alphavirus replicon particle vaccine expressing the hemagglutinin and fusion proteins protects juvenile and infant rhesus macaques from measles. J. Virol. **84**:3798–3807.
214. **Tatsis N**, **Fitzgerald JC**, **Reyes-Sandoval A**, **Harris-McCoy KC**, **Hensley SE**, **Zhou D**, **Lin S-W**, **Bian A**, **Xiang ZQ**, **Iparraguirre A**, **Lopez-Camacho C**, **Wherry EJ**, **Ertl HCJ**. 2007. Adenoviral vectors persist in vivo and maintain activated CD8+ T cells: implications for their use as vaccines. Blood **110**:1916–1923.
215. **Bruña-Romero O**, **González-Aseguinolaza G**, **Hafalla JC**, **Tsuji M**, **Nussenzweig RS**. 2001. Complete, long-lasting protection against malaria of mice primed and boosted with two distinct viral vectors expressing the same plasmodial antigen. Proc. Natl. Acad. Sci. U.S.A. **98**:11491–11496.
216. **Reyes-Sandoval A**, **Berthoud T**, **Alder N**, **Siani L**, **Gilbert SC**, **Nicosia A**, **Colloca S**, **Cortese R**, **Hill AVS**. 2010. Prime-boost immunization with adenoviral and modified vaccinia virus Ankara vectors enhances the durability and polyfunctionality of protective malaria CD8+ T-cell responses. Infect. Immun. **78**:145–153.
217. **Draper SJ**, **Moore AC**, **Goodman AL**, **Long CA**, **Holder AA**, **Gilbert SC**, **Hill F**, **Hill AVS**. 2008. Effective induction of high-titer antibodies by viral vector vaccines. Nat. Med. **14**:819–821.
218. **Hansen SG**, **Ford JC**, **Lewis MS**, **Ventura AB**, **Hughes CM**, **Coyne-Johnson L**, **Whizin N**, **Oswald K**, **Shoemaker R**, **Swanson T**, **Legasse AW**, **Chiuchiolo MJ**, **Parks CL**, **Axthelm MK**, **Nelson JA**, **Jarvis MA**, **Piatak M**, **Lifson JD**, **Picker LJ**. 2011. Profound early control of highly pathogenic SIV by an effector memory T-cell vaccine. Nature **473**:523–527.
219. **Hansen SG**, **Sacha JB**, **Hughes CM**, **Ford JC**, **Burwitz BJ**, **Scholz I**, **Gilbride RM**, **Lewis MS**, **Gilliam AN**, **Ventura AB**, **Malouli D**, **Xu G**, **Richards R**, **Whizin N**, **Reed JS**, **Hammond KB**, **Fischer M**, **Turner JM**, **Legasse AW**, **Axthelm MK**, **Edlefsen PT**, **Nelson JA**, **Lifson JD**, **Früh K**, **Picker LJ**. 2013. Cytomegalovirus vectors violate CD8+ T cell epitope recognition paradigms. Science **340**:1237874–1237874.
220. **Ranasinghe S**, **Walker BD**. 2013. Programming CMV for vaccine vector design. Nature Biotechnology **31**:811–812.
221. **Tang DC**, **DeVit M**, **Johnston SA**. 1992. Genetic immunization is a simple method for eliciting an immune response. Nature **356**:152–154.
222. **Ulmer JB**, **Donnelly JJ**, **Parker SE**, **Rhodes GH**, **Felgner PL**, **Dwarki VJ**, **Gromkowski SH**, **Deck RR**, **DeWitt CM**, **Friedman A**. 1993. Heterologous protection against influenza by injection of DNA encoding a viral protein. Science **259**:1745–1749.
223. **MacGregor RR**, **Boyer JD**, **Ugen KE**, **Lacy KE**, **Gluckman SJ**, **Bagarazzi ML**, **Chattergoon MA**, **Baine Y**, **Higgins TJ**, **Ciccarelli RB**, **Coney LR**, **Ginsberg RS**, **Weiner DB**. 1998. First human trial of a DNA-based vaccine for treatment of human immunodeficiency virus type 1 infection: safety and host response. J. Infect.

Dis. **178**:92–100.
224. **Richie TL**, **Charoenvit Y**, **Wang R**, **Epstein JE**, **Hedstrom RC**, **Kumar S**, **Luke TC**, **Freilich DA**, **Aguiar JC**, **Sacci JB**, **Sedegah M**, **Nosek RA**, **la Vega de P**, **Berzins MP**, **Majam VF**, **Abot EN**, **Ganeshan H**, **Richie NO**, **Banania JG**, **Baraceros MFB**, **Geter TG**, **Mere R**, **Bebris L**, **Limbach K**, **Hickey BW**, **Lanar DE**, **Ng J**, **Shi M**, **Hobart PM**, **Norman JA**, **Soisson LA**, **Hollingdale MR**, **Rogers WO**, **Doolan DL**, **Hoffman SL**. 2012. Clinical trial in healthy malaria-naïve adults to evaluate the safety, tolerability, immunogenicity and efficacy of MuStDO5, a five-gene, sporozoite/hepatic stage Plasmodium falciparum DNA vaccine combined with escalating dose human GM-CSF DNA. Hum Vaccin Immunother **8**:1564–1584.
225. **Liu H**, **Moynihan KD**, **Zheng Y**, **Szeto GL**, **Li AV**, **Huang B**, **Van Egeren DS**, **Park C**, **Irvine DJ**. 2014. Structure-based programming of lymph-node targeting in molecular vaccines. Nature **507**:519–522.
226. **Tőke ER**, **Lőrincz O**, **Csiszovszki Z**, **Somogyi E**, **Felföldi G**, **Molnár L**, **Szipőcs R**, **Kolonics A**, **Malissen B**, **Lori F**, **Trocio J**, **Bakare N**, **Horkay F**, **Romani N**, **Tripp CH**, **Stoitzner P**, **Lisziewicz J**. 2014. Exploitation of Langerhans cells for in vivo DNA vaccine delivery into the lymph nodes. Gene Ther. **21**:566–574.
227. **Allen TM**, **Vogel TU**, **Fuller DH**, **Mothé BR**, **Steffen S**, **Boyson JE**, **Shipley T**, **Fuller J**, **Hanke T**, **Sette A**, **Altman JD**, **Moss B**, **McMichael AJ**, **Watkins DI**. 2000. Induction of AIDS virus-specific CTL activity in fresh, unstimulated peripheral blood lymphocytes from rhesus macaques vaccinated with a DNA prime/modified vaccinia virus Ankara boost regimen. J. Immunol. **164**:4968–4978.
228. **McShane H**, **Brookes R**, **Gilbert SC**, **Hill AV**. 2001. Enhanced immunogenicity of CD4(+) t-cell responses and protective efficacy of a DNA-modified vaccinia virus Ankara prime-boost vaccination regimen for murine tuberculosis. Infect. Immun. **69**:681–686.
229. **Masalova OV**, **Lesnova EI**, **Pichugin AV**, **Melnikova TM**, **Grabovetsky VV**, **Petrakova NV**, **Smirnova OA**, **Ivanov AV**, **Zaberezhny AD**, **Ataullakhanov RI**, **Isaguliants MG**, **Kushch AA**. 2010. The successful immune response against hepatitis C nonstructural protein 5A (NS5A) requires heterologous DNA/protein immunization. Vaccine **28**:1987–1996.
230. **Broderick KE**, **Humeau LM**. 2015. Electroporation-enhanced delivery of nucleic acid vaccines. Expert Rev Vaccines **14**:195–204.
231. **Qin Y**, **Tian H**, **Wang G**, **Lin C**, **Li Y**. 2013. A BCR/ABL-hIL-2 DNA vaccine enhances the immune responses in BALB/c mice. Biomed Res Int **2013**:136492–9.
232. **Delves PJ**, **Martin SJ**, **Burton DR**, **Roitt IM**. 2017. Essential immunology.
233. **Petrovsky N**, **Aguilar JC**. 2004. Vaccine adjuvants: current state and future trends. Immunol. Cell Biol. **82**:488–496.
234. **Chauhan N**, **Tiwari S**, **Iype T**, **Jain U**. 2017. An overview of adjuvants utilized in prophylactic vaccine formulation as immunomodulators. Expert Rev Vaccines **16**:491–502.
235. **Lee S**, **Nguyen MT**. 2015. Recent advances of vaccine adjuvants for infectious diseases. Immune Netw **15**:51–57.
236. **Glenny AT**. 1926. The antigenic value of toxoid precipitated by potassium alum. J. Pathol. Bacteriol. **29**:38–45.
237. **Wen Y**, **Shi Y**. 2016. Alum: an old dog with new tricks. Emerg Microbes Infect **5**:e25.
238. **Glenny AT**, **Buttle GAH**, **Stevens MF**. 1931. Rate of disappearance of diphtheria toxoid injected into rabbits and guinea - pigs: Toxoid precipitated with alum. The Journal of Pathology **34**:267–275.
239. **WHITE RG**, **COONS AH**, **CONNOLLY JM**. 1955. Studies on antibody production. III. The alum granuloma. J. Exp. Med. **102**:73–82.
240. **Hutchison S**, **Benson RA**, **Gibson VB**, **Pollock AH**, **Garside P**, **Brewer JM**. 2012. Antigen depot is not required for alum adjuvanticity. FASEB J. **26**:1272–1279.
241. **Eisenbarth SC**, **Colegio OR**, **O'Connor W**, **Sutterwala FS**, **Flavell RA**. 2008. Crucial role for the Nalp3 inflammasome in the immunostimulatory properties of aluminium adjuvants. Nature **453**:1122–1126.
242. **Flach TL**, **Ng G**, **Hari A**, **Desrosiers MD**, **Zhang P**, **Ward SM**, **Seamone ME**, **Vilaysane A**, **Mucsi AD**, **Fong Y**, **Prenner E**, **Ling CC**, **Tschopp J**, **Muruve DA**,

Amrein MW, **Shi Y**. 2011. Alum interaction with dendritic cell membrane lipids is essential for its adjuvanticity. Nat. Med. **17**:479–487.
243. **McKee AS**, **Burchill MA**, **Munks MW**, **Jin L**, **Kappler JW**, **Friedman RS**, **Jacobelli J**, **Marrack P**. 2013. Host DNA released in response to aluminum adjuvant enhances MHC class II-mediated antigen presentation and prolongs CD4 T-cell interactions with dendritic cells. Proc. Natl. Acad. Sci. U.S.A. **110**:E1122–31.
244. **Kool M**, **Soullié T**, **van Nimwegen M**, **Willart MAM**, **Muskens F**, **Jung S**, **Hoogsteden HC**, **Hammad H**, **Lambrecht BN**. 2008. Alum adjuvant boosts adaptive immunity by inducing uric acid and activating inflammatory dendritic cells. J. Exp. Med. **205**:869–882.
245. **Clements CJ**, **Griffiths E**. 2002. The global impact of vaccines containing aluminium adjuvants. Vaccine **20 Suppl 3**:S24–33.
246. **Stoute JA**, **Slaoui M**, **Heppner DG**, **Momin P**, **Kester KE**, **Desmons P**, **Wellde BT**, **Garçon N**, **Krzych U**, **Marchand M**. 1997. A preliminary evaluation of a recombinant circumsporozoite protein vaccine against Plasmodium falciparum malaria. RTS,S Malaria Vaccine Evaluation Group. N. Engl. J. Med. **336**:86–91.
247. **O'Hagan DT**, **Ott GS**, **Nest GV**, **Rappuoli R**, **Giudice GD**. 2013. The history of MF59(®) adjuvant: a phoenix that arose from the ashes. Expert Rev Vaccines **12**:13–30.
248. **Jensen F**, **Savary J**, **Diveley J**, **Chang J**. 1998. Adjuvant activity of incomplete Freund's adjuvant. Adv. Drug Deliv. Rev. **32**:173–186.
249. **Edelman R**. 1980. Vaccine adjuvants. Reviews of infectious diseases.
250. **SALK JE**, **LAURENT AM**, **BAILEY ML**. 1951. Direction of research on vaccination against influenza; new studies with immunologic adjuvants. Am J Public Health Nations Health **41**:669–677.
251. **Calabro S**, **Tortoli M**, **Baudner BC**, **Pacitto A**, **Cortese M**, **O'Hagan DT**, **De Gregorio E**, **Seubert A**, **Wack A**. 2011. Vaccine adjuvants alum and MF59 induce rapid recruitment of neutrophils and monocytes that participate in antigen transport to draining lymph nodes. Vaccine **29**:1812–1823.
252. **Vono M**, **Taccone M**, **Caccin P**, **Gallotta M**, **Donvito G**, **Falzoni S**, **Palmieri E**, **Pallaoro M**, **Rappuoli R**, **Di Virgilio F**, **De Gregorio E**, **Montecucco C**, **Seubert A**. 2013. The adjuvant MF59 induces ATP release from muscle that potentiates response to vaccination. Proc. Natl. Acad. Sci. U.S.A. **110**:21095–21100.
253. **Lofano G**, **Mancini F**, **Salvatore G**, **Cantisani R**, **Monaci E**, **Carrisi C**, **Tavarini S**, **Sammicheli C**, **Rossi Paccani S**, **Soldaini E**, **Laera D**, **Finco O**, **Nuti S**, **Rappuoli R**, **De Gregorio E**, **Bagnoli F**, **Bertholet S**. 2015. Oil-in-Water Emulsion MF59 Increases Germinal Center B Cell Differentiation and Persistence in Response to Vaccination. J. Immunol. **195**:1617–1627.
254. **Nakaya HI**, **Clutterbuck E**, **Kazmin D**, **Wang L**, **Cortese M**, **Bosinger SE**, **Patel NB**, **Zak DE**, **Aderem A**, **Dong T**, **Del Giudice G**, **Rappuoli R**, **Cerundolo V**, **Pollard AJ**, **Pulendran B**, **Siegrist C-A**. 2016. Systems biology of immunity to MF59-adjuvanted versus nonadjuvanted trivalent seasonal influenza vaccines in early childhood. Proc. Natl. Acad. Sci. U.S.A. **113**:1853–1858.
255. **Khurana S**, **Verma N**, **Yewdell JW**, **Hilbert AK**, **Castellino F**, **Lattanzi M**, **Del Giudice G**, **Rappuoli R**, **Golding H**. 2011. MF59 adjuvant enhances diversity and affinity of antibody-mediated immune response to pandemic influenza vaccines. Sci Transl Med **3**:85ra48–85ra48.
256. **Yazdani SS**, **Shakri AR**, **Mukherjee P**, **Baniwal SK**, **Chitnis CE**. 2004. Evaluation of immune responses elicited in mice against a recombinant malaria vaccine based on Plasmodium vivax Duffy binding protein. Vaccine **22**:3727–3737.
257. **Lövgren Bengtsson K**, **Morein B**, **Osterhaus AD**. 2011. ISCOM technology-based Matrix M™ adjuvant: success in future vaccines relies on formulation. Expert Rev Vaccines **10**:401–403.
258. **Lövgren K**, **Morein B**. 1988. The requirement of lipids for the formation of immunostimulating complexes (iscoms). Biotechnol. Appl. Biochem. **10**:161–172.
259. **Madhun AS**, **Haaheim LR**, **Nilsen MV**, **Cox RJ**. 2009. Intramuscular Matrix-M-adjuvanted virosomal H5N1 vaccine induces high frequencies of multifunctional Th1 CD4+ cells and strong antibody responses in mice. Vaccine **27**:7367–7376.
260. **Cox RJ**, **Pedersen G**, **Madhun AS**, **Svindland S**, **Sævik M**, **Breakwell L**, **Hoschler**

K, **Willemsen M**, **Campitelli L**, **Nøstbakken JK**, **Weverling GJ**, **Klap J**, **McCullough KC**, **Zambon M**, **Kompier R**, **Sjursen H**. 2011. Evaluation of a virosomal H5N1 vaccine formulated with Matrix M™ adjuvant in a phase I clinical trial. Vaccine **29**:8049–8059.

261. **Pedersen GK**, **Sjursen H**, **Nøstbakken JK**, **Jul-Larsen Å**, **Hoschler K**, **Cox RJ**. 2014. Matrix M(TM) adjuvanted virosomal H5N1 vaccine induces balanced Th1/Th2 CD4(+) T cell responses in man. Hum Vaccin Immunother **10**:2408–2416.

262. **Reimer JM**, **Karlsson KH**, **Lövgren Bengtsson K**, **Magnusson SE**, **Fuentes A**, **Stertman L**. 2012. Matrix-M™ adjuvant induces local recruitment, activation and maturation of central immune cells in absence of antigen. PLoS ONE **7**:e41451.

263. **Magnusson SE**, **Reimer JM**, **Karlsson KH**, **Lilja L**, **Bengtsson KL**, **Stertman L**. 2013. Immune enhancing properties of the novel Matrix-M™ adjuvant leads to potentiated immune responses to an influenza vaccine in mice. Vaccine **31**:1725–1733.

264. **de Cassan SC**, **Shakri AR**, **Llewellyn D**, **Elias SC**, **Cho JS**, **Goodman AL**, **Jin J**, **Douglas AD**, **Suwanarusk R**, **Nosten FH**, **Renia L**, **Russell B**, **Chitnis CE**, **Draper SJ**. 2015. Preclinical Assessment of Viral Vectored and Protein Vaccines Targeting the Duffy-Binding Protein Region II of Plasmodium Vivax. Front Immunol **6**:348.

265. **Kester KE**, **Cummings JF**, **Ofori-Anyinam O**, **Ockenhouse CF**, **Krzych U**, **Moris P**, **Schwenk R**, **Nielsen RA**, **Debebe Z**, **Pinelis E**, **Juompan L**, **Williams J**, **Dowler M**, **Stewart VA**, **Wirtz RA**, **Dubois M-C**, **Lievens M**, **Cohen J**, **Ballou WR**, **Heppner DG**, **RTS,S Vaccine Evaluation Group**. 2009. Randomized, double-blind, phase 2a trial of falciparum malaria vaccines RTS,S/AS01B and RTS,S/AS02A in malaria-naive adults: safety, efficacy, and immunologic associates of protection. J. Infect. Dis. **200**:337–346.

266. **Ogun SA**, **Dumon-Seignovert L**, **Marchand J-B**, **Holder AA**, **Hill F**. 2008. The oligomerization domain of C4-binding protein (C4bp) acts as an adjuvant, and the fusion protein comprised of the 19-kilodalton merozoite surface protein 1 fused with the murine C4bp domain protects mice against malaria. Infect. Immun. **76**:3817–3823.

267. **Spencer AJ**, **Hill F**, **Honeycutt JD**, **Cottingham MG**, **Bregu M**, **Rollier CS**, **Furze J**, **Draper SJ**, **Søgaard KC**, **Gilbert SC**, **Wyllie DH**, **Hill AVS**. 2012. Fusion of the Mycobacterium tuberculosis antigen 85A to an oligomerization domain enhances its immunogenicity in both mice and non-human primates. PLoS ONE **7**:e33555.

268. **Minhinnick A**, **Satti I**, **Harris S**, **Wilkie M**, **Sheehan S**, **Stockdale L**, **Manjaly Thomas Z-R**, **Lopez-Ramon R**, **Poulton I**, **Lawrie A**, **Vermaak S**, **Le Vert A**, **Del Campo J**, **Hill F**, **Moss P**, **McShane H**. 2016. A first-in-human phase 1 trial to evaluate the safety and immunogenicity of the candidate tuberculosis vaccine MVA85A-IMX313, administered to BCG-vaccinated adults. Vaccine **34**:1412–1421.

269. **Li Y**, **Leneghan DB**, **Miura K**, **Nikolaeva D**, **Brian IJ**, **Dicks MDJ**, **Fyfe AJ**, **Zakutansky SE**, **de Cassan S**, **Long CA**, **Draper SJ**, **Hill AVS**, **Hill F**, **Biswas S**. 2016. Enhancing immunogenicity and transmission-blocking activity of malaria vaccines by fusing Pfs25 to IMX313 multimerization technology. Sci Rep **6**:18848.

270. **Brune KD**, **Buldun CM**, **Li Y**, **Taylor IJ**, **Brod F**, **Biswas S**, **Howarth M**. 2017. Dual Plug-and-Display Synthetic Assembly Using Orthogonal Reactive Proteins for Twin Antigen Immunization. Bioconjug. Chem. **28**:1544–1551.

271. **Sponaas A**, **Carstens C**, **Koch N**. 1999. C-terminal extension of the MHC class II-associated invariant chain by an antigenic sequence triggers activation of naive T cells. Gene Ther. **6**:1826–1834.

272. **Malcherek G**, **Wirblich C**, **Willcox N**, **Rammensee HG**, **Trowsdale J**, **Melms A**. 1998. MHC class II-associated invariant chain peptide replacement by T cell epitopes: engineered invariant chain as a vehicle for directed and enhanced MHC class II antigen processing and presentation. Eur. J. Immunol. **28**:1524–1533.

273. **Rowe HM**, **Lopes L**, **Ikeda Y**, **Bailey R**, **Barde I**, **Zenke M**, **Chain BM**, **Collins MK**. 2006. Immunization with a lentiviral vector stimulates both CD4 and CD8 T cell responses to an ovalbumin transgene. Mol. Ther. **13**:310–319.

274. **Mikkelsen M**, **Holst PJ**, **Bukh J**, **Thomsen AR**, **Christensen JP**. 2011. Enhanced and sustained CD8+ T cell responses with an adenoviral vector-based hepatitis C virus vaccine encoding NS3 linked to the MHC class II chaperone protein invariant

chain. J. Immunol. **186**:2355–2364.
275. **Holst PJ**, **Sorensen MR**, **Mandrup Jensen CM**, **Orskov C**, **Thomsen AR**, **Christensen JP**. 2008. MHC class II-associated invariant chain linkage of antigen dramatically improves cell-mediated immunity induced by adenovirus vaccines. J. Immunol. **180**:3339–3346.
276. **Spencer AJ**, **Cottingham MG**, **Jenks JA**, **Longley RJ**, **Capone S**, **Colloca S**, **Folgori A**, **Cortese R**, **Nicosia A**, **Bregu M**, **Hill AVS**. 2014. Enhanced vaccine-induced CD8+ T cell responses to malaria antigen ME-TRAP by fusion to MHC class ii invariant chain. PLoS ONE **9**:e100538.
277. **Richards WH**. 1966. Active immunization of chicks against Plasmodium gallinaceum by inactivated homologous sporozoites and erythrocytic parasites. Nature **212**:1492–1494.
278. **Nussenzweig RS**, **Vanderberg J**, **Most H**, **Orton C**. 1967. Protective immunity produced by the injection of x-irradiated sporozoites of plasmodium berghei. Nature **216**:160–162.
279. **Sigler CI**, **Leland P**, **Hollingdale MR**. 1984. In vitro infectivity of irradiated Plasmodium berghei sporozoites to cultured hepatoma cells. Am. J. Trop. Med. Hyg. **33**:544–547.
280. **Clyde DF**, **McCarthy VC**, **Miller RM**, **Hornick RB**. 1973. Specificity of protection of man immunized against sporozoite-induced falciparum malaria. Am. J. Med. Sci. **266**:398–403.
281. **Clyde DF**, **Most H**, **McCarthy VC**, **Vanderberg JP**. 1973. Immunization of man against sporozite-induced falciparum malaria. Am. J. Med. Sci. **266**:169–177.
282. **Rieckmann KH**, **Beaudoin RL**, **Cassells JS**, **Sell KW**. 1979. Use of attenuated sporozoites in the immunization of human volunteers against falciparum malaria. Bull. World Health Organ. **57 Suppl 1**:261–265.
283. **Clyde DF**. 1975. Immunization of man against falciparum and vivax malaria by use of attenuated sporozoites. Am. J. Trop. Med. Hyg. **24**:397–401.
284. **Hoffman SL**, **Goh LML**, **Luke TC**, **Schneider I**, **Le TP**, **Doolan DL**, **Sacci J**, **la Vega de P**, **Dowler M**, **Paul C**, **Gordon DM**, **Stoute JA**, **Church LWP**, **Sedegah M**, **Heppner DG**, **Ballou WR**, **Richie TL**. 2002. Protection of humans against malaria by immunization with radiation-attenuated Plasmodium falciparum sporozoites. J. Infect. Dis. **185**:1155–1164.
285. **Hollingdale MR**, **Sedegah M**. 2017. Development of whole sporozoite malaria vaccines. Expert Rev Vaccines **16**:45–54.
286. **Hoffman SL**, **Billingsley PF**, **James E**, **Richman A**, **Loyevsky M**, **Li T**, **Chakravarty S**, **Gunasekera A**, **Chattopadhyay R**, **Li M**, **Stafford R**, **Ahumada A**, **Epstein JE**, **Sedegah M**, **Reyes S**, **Richie TL**, **Lyke KE**, **Edelman R**, **Laurens MB**, **Plowe CV**, **Sim BKL**. 2010. Development of a metabolically active, non-replicating sporozoite vaccine to prevent Plasmodium falciparum malaria. Hum Vaccin **6**:97–106.
287. **Epstein JE**, **Tewari K**, **Lyke KE**, **Sim BKL**, **Billingsley PF**, **Laurens MB**, **Gunasekera A**, **Chakravarty S**, **James ER**, **Sedegah M**, **Richman A**, **Velmurugan S**, **Reyes S**, **Li M**, **Tucker K**, **Ahumada A**, **Ruben AJ**, **Li T**, **Stafford R**, **Eappen AG**, **Tamminga C**, **Bennett JW**, **Ockenhouse CF**, **Murphy JR**, **Komisar J**, **Thomas N**, **Loyevsky M**, **Birkett A**, **Plowe CV**, **Loucq C**, **Edelman R**, **Richie TL**, **Seder RA**, **Hoffman SL**. 2011. Live attenuated malaria vaccine designed to protect through hepatic $CD8^+$ T cell immunity. Science **334**:475–480.
288. **Seder RA**, **Chang L-J**, **Enama ME**, **Zephir KL**, **Sarwar UN**, **Gordon IJ**, **Holman LA**, **James ER**, **Billingsley PF**, **Gunasekera A**, **Richman A**, **Chakravarty S**, **Manoj A**, **Velmurugan S**, **Li M**, **Ruben AJ**, **Li T**, **Eappen AG**, **Stafford RE**, **Plummer SH**, **Hendel CS**, **Novik L**, **Costner PJM**, **Mendoza FH**, **Saunders JG**, **Nason MC**, **Richardson JH**, **Murphy J**, **Davidson SA**, **Richie TL**, **Sedegah M**, **Sutamihardja A**, **Fahle GA**, **Lyke KE**, **Laurens MB**, **Roederer M**, **Tewari K**, **Epstein JE**, **Sim BKL**, **Ledgerwood JE**, **Graham BS**, **Hoffman SL**, **VRC 312 Study Team**. 2013. Protection against malaria by intravenous immunization with a nonreplicating sporozoite vaccine. Science **341**:1359–1365.
289. **Sissoko MS**, **Healy SA**, **Katile A**, **Omaswa F**, **Zaidi I**, **Gabriel EE**, **Kamate B**, **Samake Y**, **Guindo MA**, **Dolo A**, **Niangaly A**, **Niaré K**, **Zeguime A**, **Sissoko K**, **Diallo H**, **Thera I**, **Ding K**, **Fay MP**, **O'Connell EM**, **Nutman TB**, **Wong-Madden S**,

Murshedkar T, **Ruben AJ**, **Li M**, **Abebe Y**, **Manoj A**, **Gunasekera A**, **Chakravarty S**, **Sim BKL**, **Billingsley PF**, **James ER**, **Walther M**, **Richie TL**, **Hoffman SL**, **Doumbo O**, **Duffy PE**. 2017. Safety and efficacy of PfSPZ Vaccine against Plasmodium falciparum via direct venous inoculation in healthy malaria-exposed adults in Mali: a randomised, double-blind phase 1 trial. Lancet Infect Dis **17**:498–509.

290. **Casares S**, **Brumeanu T-D**, **Richie TL**. 2010. The RTS,S malaria vaccine. Vaccine **28**:4880–4894.

291. **Epstein JE**, **Paolino KM**, **Richie TL**, **Sedegah M**, **Singer A**, **Ruben AJ**, **Chakravarty S**, **Stafford A**, **Ruck RC**, **Eappen AG**, **Li T**, **Billingsley PF**, **Manoj A**, **Silva JC**, **Moser K**, **Nielsen R**, **Tosh D**, **Cicatelli S**, **Ganeshan H**, **Case J**, **Padilla D**, **Davidson S**, **Garver L**, **Saverino E**, **Murshedkar T**, **Gunasekera A**, **Twomey PS**, **Reyes S**, **Moon JE**, **James ER**, **Kc N**, **Li M**, **Abot E**, **Belmonte A**, **Hauns K**, **Belmonte M**, **Huang J**, **Vasquez C**, **Remich S**, **Carrington M**, **Abebe Y**, **Tillman A**, **Hickey B**, **Regules J**, **Villasante E**, **Sim BKL**, **Hoffman SL**. 2017. Protection against Plasmodium falciparum malaria by PfSPZ Vaccine. JCI Insight **2**:e89154.

292. **Ishizuka AS**, **Lyke KE**, **DeZure A**, **Berry AA**, **Richie TL**, **Mendoza FH**, **Enama ME**, **Gordon IJ**, **Chang L-J**, **Sarwar UN**, **Zephir KL**, **Holman LA**, **James ER**, **Billingsley PF**, **Gunasekera A**, **Chakravarty S**, **Manoj A**, **Li M**, **Ruben AJ**, **Li T**, **Eappen AG**, **Stafford RE**, **K C N**, **Murshedkar T**, **DeCederfelt H**, **Plummer SH**, **Hendel CS**, **Novik L**, **Costner PJM**, **Saunders JG**, **Laurens MB**, **Plowe CV**, **Flynn B**, **Whalen WR**, **Todd JP**, **Noor J**, **Rao S**, **Sierra-Davidson K**, **Lynn GM**, **Epstein JE**, **Kemp MA**, **Fahle GA**, **Mikolajczak SA**, **Fishbaugher M**, **Sack BK**, **Kappe SHI**, **Davidson SA**, **Garver LS**, **Björkström NK**, **Nason MC**, **Graham BS**, **Roederer M**, **Sim BKL**, **Hoffman SL**, **Ledgerwood JE**, **Seder RA**. 2016. Protection against malaria at 1 year and immune correlates following PfSPZ vaccination. Nat. Med. **22**:614–623.

293. **Doolan DL**, **Hoffman SL**. 2000. The complexity of protective immunity against liver-stage malaria. J. Immunol. **165**:1453–1462.

294. **Vanderberg J**, **Nussenzweig R**, **Most H**. 1969. Protective immunity produced by the injection of x-irradiated sporozoites of Plasmodium berghei. V. In vitro effects of immune serum on sporozoites. Mil Med **134**:1183–1190.

295. **Potocnjak P**, **Yoshida N**, **Nussenzweig RS**, **Nussenzweig V**. 1980. Monovalent fragments (Fab) of monoclonal antibodies to a sporozoite surface antigen (Pb44) protect mice against malarial infection. J. Exp. Med. **151**:1504–1513.

296. **Schofield L**, **Villaquiran J**, **Ferreira A**, **Schellekens H**, **Nussenzweig R**, **Nussenzweig V**. 1987. Gamma interferon, CD8+ T cells and antibodies required for immunity to malaria sporozoites. Nature **330**:664–666.

297. **Weiss WR**, **Sedegah M**, **Beaudoin RL**, **Miller LH**, **Good MF**. 1988. CD8+ T cells (cytotoxic/suppressors) are required for protection in mice immunized with malaria sporozoites. Proc. Natl. Acad. Sci. U.S.A. **85**:573–576.

298. **Tsuji M**, **Romero P**, **Nussenzweig RS**, **Zavala F**. 1990. CD4+ cytolytic T cell clone confers protection against murine malaria. J. Exp. Med. **172**:1353–1357.

299. **Weiss WR**, **Sedegah M**, **Berzofsky JA**, **Hoffman SL**. 1993. The role of CD4+ T cells in immunity to malaria sporozoites. J. Immunol. **151**:2690–2698.

300. **Arévalo-Herrera M**, **Vásquez-Jiménez JM**, **Lopez-Perez M**, **Vallejo AF**, **Amado-Garavito AB**, **Céspedes N**, **Castellanos A**, **Molina K**, **Trejos J**, **Oñate J**, **Epstein JE**, **Richie TL**, **Herrera S**. 2016. Protective Efficacy of Plasmodium vivax Radiation-Attenuated Sporozoites in Colombian Volunteers: A Randomized Controlled Trial. PLoS Negl Trop Dis **10**:e0005070.

301. **Klein SL**, **Flanagan KL**. 2016. Sex differences in immune responses. Nat. Rev. Immunol. **16**:626–638.

302. **Beaudoin RL**, **Strome CP**, **Mitchell F**, **Tubergen TA**. 1977. Plasmodium berghei: immunization of mice against the ANKA strain using the unaltered sporozoite as an antigen. Exp. Parasitol. **42**:1–5.

303. **Roestenberg M**, **McCall M**, **Hopman J**, **Wiersma J**, **Luty AJF**, **van Gemert G-J**, **van de Vegte-Bolmer M**, **van Schaijk B**, **Teelen K**, **Arens T**, **Spaarman L**, **de Mast Q**, **Roeffen W**, **Snounou G**, **Renia L**, **van der Ven A**, **Hermsen CC**, **Sauerwein R**. 2009. Protection against a malaria challenge by sporozoite inoculation. N. Engl. J. Med. **361**:468–477.

304. **Roestenberg M**, **Teirlinck AC**, **McCall MBB**, **Teelen K**, **Makamdop KN**, **Wiersma J**, **Arens T**, **Beckers P**, **van Gemert G**, **van de Vegte-Bolmer M**, **van der Ven AJAM**, **Luty AJF**, **Hermsen CC**, **Sauerwein RW**. 2011. Long-term protection against malaria after experimental sporozoite inoculation: an open-label follow-up study. Lancet **377**:1770–1776.

305. **Bijker EM**, **Bastiaens GJH**, **Teirlinck AC**, **van Gemert G-J**, **Graumans W**, **van de Vegte-Bolmer M**, **Siebelink-Stoter R**, **Arens T**, **Teelen K**, **Nahrendorf W**, **Remarque EJ**, **Roeffen W**, **Jansens A**, **Zimmerman D**, **Vos M**, **van Schaijk BCL**, **Wiersma J**, **van der Ven AJAM**, **de Mast Q**, **van Lieshout L**, **Verweij JJ**, **Hermsen CC**, **Scholzen A**, **Sauerwein RW**. 2013. Protection against malaria after immunization by chloroquine prophylaxis and sporozoites is mediated by preerythrocytic immunity. Proc. Natl. Acad. Sci. U.S.A. **110**:7862–7867.

306. **Bijker EM**, **Teirlinck AC**, **Schats R**, **van Gemert G-J**, **van de Vegte-Bolmer M**, **van Lieshout L**, **IntHout J**, **Hermsen CC**, **Scholzen A**, **Visser LG**, **Sauerwein RW**. 2014. Cytotoxic markers associate with protection against malaria in human volunteers immunized with Plasmodium falciparum sporozoites. J. Infect. Dis. **210**:1605–1615.

307. **Behet MC**, **Foquet L**, **van Gemert G-J**, **Bijker EM**, **Meuleman P**, **Leroux-Roels G**, **Hermsen CC**, **Scholzen A**, **Sauerwein RW**. 2014. Sporozoite immunization of human volunteers under chemoprophylaxis induces functional antibodies against pre-erythrocytic stages of Plasmodium falciparum. Malaria Journal **13**:136.

308. **Mordmüller B**, **Surat G**, **Lagler H**, **Chakravarty S**, **Ishizuka AS**, **Lalremruata A**, **Gmeiner M**, **Campo JJ**, **Esen M**, **Ruben AJ**, **Held J**, **Calle CL**, **Mengue JB**, **Gebru T**, **Ibáñez J**, **Sulyok M**, **James ER**, **Billingsley PF**, **Natasha KC**, **Manoj A**, **Murshedkar T**, **Gunasekera A**, **Eappen AG**, **Li T**, **Stafford RE**, **Li M**, **Felgner PL**, **Seder RA**, **Richie TL**, **Sim BKL**, **Hoffman SL**, **Kremsner PG**. 2017. Sterile protection against human malaria by chemoattenuated PfSPZ vaccine. Nature **542**:445–449.

309. **Bastiaens GJH**, **van Meer MPA**, **Scholzen A**, **Obiero JM**, **Vatanshenassan M**, **van Grinsven T**, **Sim BKL**, **Billingsley PF**, **James ER**, **Gunasekera A**, **Bijker EM**, **van Gemert G-J**, **van de Vegte-Bolmer M**, **Graumans W**, **Hermsen CC**, **de Mast Q**, **van der Ven AJAM**, **Hoffman SL**, **Sauerwein RW**. 2016. Safety, Immunogenicity, and Protective Efficacy of Intradermal Immunization with Aseptic, Purified, Cryopreserved Plasmodium falciparum Sporozoites in Volunteers Under Chloroquine Prophylaxis: A Randomized Controlled Trial. Am. J. Trop. Med. Hyg. **94**:663–673.

310. **Butler NS**, **Schmidt NW**, **Vaughan AM**, **Aly AS**, **Kappe SHI**, **Harty JT**. 2011. Superior antimalarial immunity after vaccination with late liver stage-arresting genetically attenuated parasites. Cell Host Microbe **9**:451–462.

311. **Mueller A-K**, **Camargo N**, **Kaiser K**, **Andorfer C**, **Frevert U**, **Matuschewski K**, **Kappe SHI**. 2005. Plasmodium liver stage developmental arrest by depletion of a protein at the parasite-host interface. Proc. Natl. Acad. Sci. U.S.A. **102**:3022–3027.

312. **Mueller A-K**, **Labaied M**, **Kappe SHI**, **Matuschewski K**. 2005. Genetically modified Plasmodium parasites as a protective experimental malaria vaccine. Nature **433**:164–167.

313. **van Dijk MR**, **Douradinha B**, **Franke-Fayard B**, **Heussler V**, **van Dooren MW**, **van Schaijk B**, **van Gemert G-J**, **Sauerwein RW**, **Mota MM**, **Waters AP**, **Janse CJ**. 2005. Genetically attenuated, P36p-deficient malarial sporozoites induce protective immunity and apoptosis of infected liver cells. Proc. Natl. Acad. Sci. U.S.A. **102**:12194–12199.

314. **VanBuskirk KM**, **O'Neill MT**, **la Vega de P**, **Maier AG**, **Krzych U**, **Williams J**, **Dowler MG**, **Sacci JB**, **Kangwanrangsan N**, **Tsuboi T**, **Kneteman NM**, **Heppner DG**, **Murdock BA**, **Mikolajczak SA**, **Aly ASI**, **Cowman AF**, **Kappe SHI**. 2009. Preerythrocytic, live-attenuated Plasmodium falciparum vaccine candidates by design. Proc. Natl. Acad. Sci. U.S.A. **106**:13004–13009.

315. **Spring M**, **Murphy J**, **Nielsen R**, **Dowler M**, **Bennett JW**, **Zarling S**, **Williams J**, **la Vega de P**, **Ware L**, **Komisar J**, **Polhemus M**, **Richie TL**, **Epstein J**, **Tamminga C**, **Chuang I**, **Richie N**, **O'Neil M**, **Heppner DG**, **Healer J**, **O'Neill M**, **Smithers H**, **Finney OC**, **Mikolajczak SA**, **Wang R**, **Cowman A**, **Ockenhouse C**, **Krzych U**, **Kappe SHI**. 2013. First-in-human evaluation of genetically attenuated Plasmodium

falciparum sporozoites administered by bite of Anopheles mosquitoes to adult volunteers. Vaccine **31**:4975–4983.

316. **Khan SM**, **Janse CJ**, **Kappe SHI**, **Mikolajczak SA**. 2012. Genetic engineering of attenuated malaria parasites for vaccination. Curr. Opin. Biotechnol. **23**:908–916.

317. **Mikolajczak SA**, **Lakshmanan V**, **Fishbaugher M**, **Camargo N**, **Harupa A**, **Kaushansky A**, **Douglass AN**, **Baldwin M**, **Healer J**, **O'Neill M**, **Phuong T**, **Cowman A**, **Kappe SHI**. 2014. A next-generation genetically attenuated Plasmodium falciparum parasite created by triple gene deletion. Mol. Ther. **22**:1707–1715.

318. **Kublin JG**, **Mikolajczak SA**, **Sack BK**, **Fishbaugher ME**, **Seilie A**, **Shelton L**, **VonGoedert T**, **Firat M**, **Magee S**, **Fritzen E**, **Betz W**, **Kain HS**, **Dankwa DA**, **Steel RWJ**, **Vaughan AM**, **Noah Sather D**, **Murphy SC**, **Kappe SHI**. 2017. Complete attenuation of genetically engineered Plasmodium falciparum sporozoites in human subjects. Sci Transl Med **9**:eaad9099.

319. **Aly ASI**, **Mikolajczak SA**, **Rivera HS**, **Camargo N**, **Jacobs-Lorena V**, **Labaied M**, **Coppens I**, **Kappe SHI**. 2008. Targeted deletion of SAP1 abolishes the expression of infectivity factors necessary for successful malaria parasite liver infection. Mol. Microbiol. **69**:152–163.

320. **Vaughan AM**, **O'Neill MT**, **Tarun AS**, **Camargo N**, **Phuong TM**, **Aly ASI**, **Cowman AF**, **Kappe SHI**. 2009. Type II fatty acid synthesis is essential only for malaria parasite late liver stage development. Cell. Microbiol. **11**:506–520.

321. **Yoshida N**, **Nussenzweig RS**, **Potocnjak P**, **Nussenzweig V**, **Aikawa M**. 1980. Hybridoma produces protective antibodies directed against the sporozoite stage of malaria parasite. Science **207**:71–73.

322. **Nardin EH**, **Nussenzweig V**, **Nussenzweig RS**, **Collins WE**, **Harinasuta KT**, **Tapchaisri P**, **Chomcharn Y**. 1982. Circumsporozoite proteins of human malaria parasites Plasmodium falciparum and Plasmodium vivax. J. Exp. Med. **156**:20–30.

323. **Nagasawa H**, **Procell PM**, **Atkinson CT**, **Campbell GH**, **Collins WE**, **Aikawa M**. 1987. Localization of circumsporozoite protein of Plasmodium ovale in midgut oocysts. Infect. Immun. **55**:2928–2932.

324. **Nagasawa H**, **Aikawa M**, **Procell PM**, **Campbell GH**, **Collins WE**, **Campbell CC**. 1988. Plasmodium malariae: distribution of circumsporozoite protein in midgut oocysts and salivary gland sporozoites. Exp. Parasitol. **66**:27–34.

325. **Posthuma G**, **Meis JF**, **Verhave JP**, **Hollingdale MR**, **Ponnudurai T**, **Meuwissen JH**, **Geuze HJ**. 1988. Immunogold localization of circumsporozoite protein of the malaria parasite Plasmodium falciparum during sporogony in Anopheles stephensi midguts. Eur. J. Cell Biol. **46**:18–24.

326. **Hamilton AJ**, **Suhrbier A**, **Nicholas J**, **Sinden RE**. 1988. Immunoelectron microscopic localization of circumsporozoite antigen in the differentiating exoerythrocytic trophozoite of Plasmodium berghei. Cell Biol. Int. Rep. **12**:123–129.

327. **Aikawa M**, **Atkinson CT**, **Beaudoin LM**, **Sedegah M**, **Charoenvit Y**, **Beaudoin R**. 1990. Localization of CS and non-CS antigens in the sporogonic stages of Plasmodium yoelii. Bull. World Health Organ. **68 Suppl**:165–171.

328. **Wang Q**, **Fujioka H**, **Nussenzweig V**. 2005. Exit of Plasmodium sporozoites from oocysts is an active process that involves the circumsporozoite protein. PLoS Pathog. **1**:e9.

329. **Sidjanski SP**, **Vanderberg JP**, **Sinnis P**. 1997. Anopheles stephensi salivary glands bear receptors for region I of the circumsporozoite protein of Plasmodium falciparum. Mol. Biochem. Parasitol. **90**:33–41.

330. **Myung JM**, **Marshall P**, **Sinnis P**. 2004. The Plasmodium circumsporozoite protein is involved in mosquito salivary gland invasion by sporozoites. Mol. Biochem. Parasitol. **133**:53–59.

331. **Hollingdale MR**, **Nardin EH**, **Tharavanij S**, **Schwartz AL**, **Nussenzweig RS**. 1984. Inhibition of entry of Plasmodium falciparum and P. vivax sporozoites into cultured cells; an in vitro assay of protective antibodies. J. Immunol. **132**:909–913.

332. **Lindner SE**, **Swearingen KE**, **Harupa A**, **Vaughan AM**, **Sinnis P**, **Moritz RL**, **Kappe SHI**. 2013. Total and putative surface proteomics of malaria parasite salivary gland sporozoites. Mol. Cell Proteomics **12**:1127–1143.

333. **Kumar KA**, **Sano G-I**, **Boscardin S**, **Nussenzweig RS**, **Nussenzweig MC**, **Zavala F**, **Nussenzweig V**. 2006. The circumsporozoite protein is an immunodominant protective antigen in irradiated sporozoites. Nature **444**:937–940.
334. **Santoro F**, **Cochrane AH**, **Nussenzweig V**, **Nardin EH**, **Nussenzweig RS**, **Gwadz RW**, **Ferreira A**. 1983. Structural similarities among the protective antigens of sporozoites from different species of malaria parasites. J. Biol. Chem. **258**:3341–3345.
335. **Dame JB**, **Williams JL**, **McCutchan TF**, **Weber JL**, **Wirtz RA**, **Hockmeyer WT**, **Maloy WL**, **Haynes JD**, **Schneider I**, **Roberts D**. 1984. Structure of the gene encoding the immunodominant surface antigen on the sporozoite of the human malaria parasite Plasmodium falciparum. Science **225**:593–599.
336. **McCutchan TF**, **Kissinger JC**, **Touray MG**, **Rogers MJ**, **Li J**, **Sullivan M**, **Braga EM**, **Krettli AU**, **Miller LH**. 1996. Comparison of circumsporozoite proteins from avian and mammalian malarias: biological and phylogenetic implications. Proc. Natl. Acad. Sci. U.S.A. **93**:11889–11894.
337. **Wang Q**, **Fujioka H**, **Nussenzweig V**. 2005. Mutational analysis of the GPI-anchor addition sequence from the circumsporozoite protein of Plasmodium. Cell. Microbiol. **7**:1616–1626.
338. **Plassmeyer ML**, **Reiter K**, **Shimp RL**, **Kotova S**, **Smith PD**, **Hurt DE**, **House B**, **Zou X**, **Zhang Y**, **Hickman M**, **Uchime O**, **Herrera R**, **Nguyen V**, **Glen J**, **Lebowitz J**, **Jin AJ**, **Miller LH**, **MacDonald NJ**, **Wu Y**, **Narum DL**. 2009. Structure of the Plasmodium falciparum circumsporozoite protein, a leading malaria vaccine candidate. J. Biol. Chem. **284**:26951–26963.
339. **Amino R**, **Thiberge S**, **Martin B**, **Celli S**, **Shorte S**, **Frischknecht F**, **Ménard R**. 2006. Quantitative imaging of Plasmodium transmission from mosquito to mammal. Nat. Med. **12**:220–224.
340. **Mishra S**, **Nussenzweig RS**, **Nussenzweig V**. 2012. Antibodies to Plasmodium circumsporozoite protein (CSP) inhibit sporozoite's cell traversal activity. J. Immunol. Methods **377**:47–52.
341. **Stewart MJ**, **Nawrot RJ**, **Schulman S**, **Vanderberg JP**. 1986. Plasmodium berghei sporozoite invasion is blocked in vitro by sporozoite-immobilizing antibodies. Infect. Immun. **51**:859–864.
342. **Pancake SJ**, **Holt GD**, **Mellouk S**, **Hoffman SL**. 1992. Malaria sporozoites and circumsporozoite proteins bind specifically to sulfated glycoconjugates. J. Cell Biol. **117**:1351–1357.
343. **Frevert U**, **Sinnis P**, **Cerami C**, **Shreffler W**, **Takacs B**, **Nussenzweig V**. 1993. Malaria circumsporozoite protein binds to heparan sulfate proteoglycans associated with the surface membrane of hepatocytes. J. Exp. Med. **177**:1287–1298.
344. **Robertson RT**, **Baratta JL**, **Haynes SM**, **Longmuir KJ**. 2008. Liposomes incorporating a Plasmodium amino acid sequence target heparan sulfate binding sites in liver. J Pharm Sci **97**:3257–3273.
345. **Cerami C**, **Frevert U**, **Sinnis P**, **Takacs B**, **Clavijo P**, **Santos MJ**, **Nussenzweig V**. 1992. The basolateral domain of the hepatocyte plasma membrane bears receptors for the circumsporozoite protein of Plasmodium falciparum sporozoites. Cell **70**:1021–1033.
346. **Coppi A**, **Natarajan R**, **Pradel G**, **Bennett BL**, **James ER**, **Roggero MA**, **Corradin G**, **Persson C**, **Tewari R**, **Sinnis P**. 2011. The malaria circumsporozoite protein has two functional domains, each with distinct roles as sporozoites journey from mosquito to mammalian host. J. Exp. Med. **208**:341–356.
347. **Suarez JE**, **Urquiza M**, **Puentes A**, **Garcia JE**, **Curtidor H**, **Ocampo M**, **Lopez R**, **Rodriguez LE**, **Vera R**, **Cubillos M**, **Torres MH**, **Patarroyo ME**. 2001. Plasmodium falciparum circumsporozoite (CS) protein peptides specifically bind to HepG2 cells. Vaccine **19**:4487–4495.
348. **Chatterjee S**, **Wery M**, **Sharma P**, **Chauhan VS**. 1995. A conserved peptide sequence of the Plasmodium falciparum circumsporozoite protein and antipeptide antibodies inhibit Plasmodium berghei sporozoite invasion of Hep-G2 cells and protect immunized mice against P. berghei sporozoite challenge. Infect. Immun. **63**:4375–4381.

349. **Espinosa DA**, **Gutierrez GM**, **Rojas-López M**, **Noe AR**, **Shi L**, **Tse S-W**, **Sinnis P**, **Zavala F**. 2015. Proteolytic Cleavage of the Plasmodium falciparum Circumsporozoite Protein Is a Target of Protective Antibodies. J. Infect. Dis. **212**:1111–1119.
350. **Singh AP**, **Buscaglia CA**, **Wang Q**, **Levay A**, **Nussenzweig DR**, **Walker JR**, **Winzeler EA**, **Fujii H**, **Fontoura BMA**, **Nussenzweig V**. 2007. Plasmodium circumsporozoite protein promotes the development of the liver stages of the parasite. Cell **131**:492–504.
351. **Ding Y**, **Huang X**, **Liu T**, **Fu Y**, **Tan Z**, **Zheng H**, **Zhou T**, **Dai J**, **Xu W**. 2012. The Plasmodium circumsporozoite protein, a novel NF-κB inhibitor, suppresses the growth of SW480. Pathol. Oncol. Res. **18**:895–902.
352. **Frevert U**, **Galinski MR**, **Hügel FU**, **Allon N**, **Schreier H**, **Smulevitch S**, **Shakibaei M**, **Clavijo P**. 1998. Malaria circumsporozoite protein inhibits protein synthesis in mammalian cells. EMBO J. **17**:3816–3826.
353. **Hügel FU**, **Pradel G**, **Frevert U**. 1996. Release of malaria circumsporozoite protein into the host cell cytoplasm and interaction with ribosomes. Mol. Biochem. Parasitol. **81**:151–170.
354. **Arnot DE**, **Barnwell JW**, **Tam JP**, **Nussenzweig V**, **Nussenzweig RS**, **Enea V**. 1985. Circumsporozoite protein of Plasmodium vivax: gene cloning and characterization of the immunodominant epitope. Science **230**:815–818.
355. **McCutchan TF**, **Lal AA**, **la Cruz de VF**, **Miller LH**, **Maloy WL**, **Charoenvit Y**, **Beaudoin RL**, **Guerry P**, **Wistar R**, **Hoffman SL**. 1985. Sequence of the immunodominant epitope for the surface protein on sporozoites of Plasmodium vivax. Science **230**:1381–1383.
356. **Rosenberg R**, **Wirtz RA**, **Lanar DE**, **Sattabongkot J**, **Hall T**, **Waters AP**, **Prasittisuk C**. 1989. Circumsporozoite protein heterogeneity in the human malaria parasite Plasmodium vivax. Science **245**:973–976.
357. **Lim CS**, **Tazi L**, **Ayala FJ**. 2005. Plasmodium vivax: recent world expansion and genetic identity to Plasmodium simium. Proc. Natl. Acad. Sci. U.S.A. **102**:15523–15528.
358. **Qari SH**, **Shi YP**, **Goldman IF**, **Udhayakumar V**, **Alpers MP**, **Collins WE**, **Lal AA**. 1993. Identification of Plasmodium vivax-like human malaria parasite. Lancet **341**:780–783.
359. **Lal AA**, **la Cruz de VF**, **Campbell GH**, **Procell PM**, **Collins WE**, **McCutchan TF**. 1988. Structure of the circumsporozoite gene of Plasmodium malariae. Mol. Biochem. Parasitol. **30**:291–294.
360. **Ozaki LS**, **Svec P**, **Nussenzweig RS**, **Nussenzweig V**, **Godson GN**. 1983. Structure of the plasmodium knowlesi gene coding for the circumsporozoite protein. Cell **34**:815–822.
361. **Gwadz RW**, **Cochrane AH**, **Nussenzweig V**, **Nussenzweig RS**. 1979. Preliminary studies on vaccination of rhesus monkeys with irradiated sporozoites of Plasmodium knowlesi and characterization of surface antigens of these parasites. Bull. World Health Organ. **57 Suppl 1**:165–173.
362. **Ballou WR**, **Rothbard J**, **Wirtz RA**, **Gordon DM**, **Williams JS**, **Gore RW**, **Schneider I**, **Hollingdale MR**, **Beaudoin RL**, **Maloy WL**. 1985. Immunogenicity of synthetic peptides from circumsporozoite protein of Plasmodium falciparum. Science **228**:996–999.
363. **Young JF**, **Hockmeyer WT**, **Gross M**, **Ballou WR**, **Wirtz RA**, **Trosper JH**, **Beaudoin RL**, **Hollingdale MR**, **Miller LH**, **Diggs CL**. 1985. Expression of Plasmodium falciparum circumsporozoite proteins in Escherichia coli for potential use in a human malaria vaccine. Science **228**:958–962.
364. **Ballou WR**, **Hoffman SL**, **Sherwood JA**, **Hollingdale MR**, **Neva FA**, **Hockmeyer WT**, **Gordon DM**, **Schneider I**, **Wirtz RA**, **Young JF**. 1987. Safety and efficacy of a recombinant DNA Plasmodium falciparum sporozoite vaccine. Lancet **1**:1277–1281.
365. **Herrington DA**, **Clyde DF**, **Losonsky G**, **Cortesia M**, **Murphy JR**, **Davis J**, **Baqar S**, **Felix AM**, **Heimer EP**, **Gillessen D**. 1987. Safety and immunogenicity in man of a synthetic peptide malaria vaccine against Plasmodium falciparum sporozoites. Nature **328**:257–259.

366. **Egan JE**, **Weber JL**, **Ballou WR**, **Hollingdale MR**, **Majarian WR**, **Gordon DM**, **Maloy WL**, **Hoffman SL**, **Wirtz RA**, **Schneider I**. 1987. Efficacy of murine malaria sporozoite vaccines: implications for human vaccine development. Science **236**:453–456.
367. **Rickman LS**, **Gordon DM**, **Wistar R**, **Krzych U**, **Gross M**, **Hollingdale MR**, **Egan JE**, **Chulay JD**, **Hoffman SL**. 1991. Use of adjuvant containing mycobacterial cell-wall skeleton, monophosphoryl lipid A, and squalane in malaria circumsporozoite protein vaccine. Lancet **337**:998–1001.
368. **Ballou WR**, **Cahill CP**. 2007. Two decades of commitment to malaria vaccine development: GlaxoSmithKline Biologicals. Am. J. Trop. Med. Hyg. **77**:289–295.
369. **Vreden SG**, **Verhave JP**, **Oettinger T**, **Sauerwein RW**, **Meuwissen JH**. 1991. Phase I clinical trial of a recombinant malaria vaccine consisting of the circumsporozoite repeat region of Plasmodium falciparum coupled to hepatitis B surface antigen. Am. J. Trop. Med. Hyg. **45**:533–538.
370. **Kumar S**, **Miller LH**, **Quakyi IA**, **Keister DB**, **Houghten RA**, **Maloy WL**, **Moss B**, **Berzofsky JA**, **Good MF**. 1988. Cytotoxic T cells specific for the circumsporozoite protein of Plasmodium falciparum. Nature **334**:258–260.
371. **Romero P**, **Maryanski JL**, **Corradin G**, **Nussenzweig RS**, **Nussenzweig V**, **Zavala F**. 1989. Cloned cytotoxic T cells recognize an epitope in the circumsporozoite protein and protect against malaria. Nature **341**:323–326.
372. **Malik A**, **Egan JE**, **Houghten RA**, **Sadoff JC**, **Hoffman SL**. 1991. Human cytotoxic T lymphocytes against the Plasmodium falciparum circumsporozoite protein. Proc. Natl. Acad. Sci. U.S.A. **88**:3300–3304.
373. **Stoute JA**, **Kester KE**, **Krzych U**, **Wellde BT**, **Hall T**, **White K**, **Glenn G**, **Ockenhouse CF**, **Garçon N**, **Schwenk R**, **Lanar DE**, **Sun P**, **Momin P**, **Wirtz RA**, **Golenda C**, **Slaoui M**, **Wortmann G**, **Holland C**, **Dowler M**, **Cohen J**, **Ballou WR**. 1998. Long-term efficacy and immune responses following immunization with the RTS,S malaria vaccine. J. Infect. Dis. **178**:1139–1144.
374. **Regules JA**, **Cicatelli SB**, **Bennett JW**, **Paolino KM**, **Twomey PS**, **Moon JE**, **Kathcart AK**, **Hauns KD**, **Komisar JL**, **Qabar AN**, **Davidson SA**, **Dutta S**, **Griffith ME**, **Magee CD**, **Wojnarski M**, **Livezey JR**, **Kress AT**, **Waterman PE**, **Jongert E**, **Wille-Reece U**, **Volkmuth W**, **Emerling D**, **Robinson WH**, **Lievens M**, **Morelle D**, **Lee CK**, **Yassin-Rajkumar B**, **Weltzin R**, **Cohen J**, **Paris RM**, **Waters NC**, **Birkett AJ**, **Kaslow DC**, **Ballou WR**, **Ockenhouse CF**, **Vekemans J**. 2016. Fractional Third and Fourth Dose of RTS,S/AS01 Malaria Candidate Vaccine: A Phase 2a Controlled Human Malaria Parasite Infection and Immunogenicity Study. J. Infect. Dis. **214**:762–771.
375. **Alonso PL**, **Sacarlal J**, **Aponte JJ**, **Leach A**, **Macete E**, **Milman J**, **Mandomando I**, **Spiessens B**, **Guinovart C**, **Espasa M**, **Bassat Q**, **Aide P**, **Ofori-Anyinam O**, **Navia MM**, **Corachan S**, **Ceuppens M**, **Dubois M-C**, **Demoitié M-A**, **Dubovsky F**, **Menéndez C**, **Tornieporth N**, **Ballou WR**, **Thompson R**, **Cohen J**. 2004. Efficacy of the RTS,S/AS02A vaccine against Plasmodium falciparum infection and disease in young African children: randomised controlled trial. Lancet **364**:1411–1420.
376. **Stewart VA**, **McGrath SM**, **Walsh DS**, **Davis S**, **Hess AS**, **Ware LA**, **Kester KE**, **Cummings JF**, **Burge JR**, **Voss G**, **Delchambre M**, **Garçon N**, **Tang DB**, **Cohen JD**, **Heppner DG**. 2006. Pre-clinical evaluation of new adjuvant formulations to improve the immunogenicity of the malaria vaccine RTS,S/AS02A. Vaccine **24**:6483–6492.
377. **Polhemus ME**, **Remich SA**, **Ogutu BR**, **Waitumbi JN**, **Otieno L**, **Apollo S**, **Cummings JF**, **Kester KE**, **Ockenhouse CF**, **Stewart A**, **Ofori-Anyinam O**, **Ramboer I**, **Cahill CP**, **Lievens M**, **Dubois M-C**, **Demoitié M-A**, **Leach A**, **Cohen J**, **Ballou WR**, **Heppner DG**. 2009. Evaluation of RTS,S/AS02A and RTS,S/AS01B in adults in a high malaria transmission area. PLoS ONE **4**:e6465.
378. **Leach A**, **Vekemans J**, **Lievens M**, **Ofori-Anyinam O**, **Cahill C**, **Owusu-Agyei S**, **Abdulla S**, **Macete E**, **Njuguna P**, **Savarese B**, **Loucq C**, **Ballou WR**. 2011. Design of a phase III multicenter trial to evaluate the efficacy of the RTS,S/AS01 malaria vaccine in children across diverse transmission settings in Africa. Malaria Journal **10**:224.
379. **RTS,S Clinical Trials Partnership**, **Agnandji ST**, **Lell B**, **Fernandes JF**, **Abossolo**

BP, **Methogo BGNO**, **Kabwende AL**, **Adegnika AA**, **Mordmüller B**, **Issifou S**, **Kremsner PG**, **Sacarlal J**, **Aide P**, **Lanaspa M**, **Aponte JJ**, **Machevo S**, **Acacio S**, **Bulo H**, **Sigauque B**, **Macete E**, **Alonso P**, **Abdulla S**, **Salim N**, **Minja R**, **Mpina M**, **Ahmed S**, **Ali AM**, **Mtoro AT**, **Hamad AS**, **Mutani P**, **Tanner M**, **Tinto H**, **D'Alessandro U**, **Sorgho H**, **Valea I**, **Bihoun B**, **Guiraud I**, **Kaboré B**, **Sombié O**, **Guiguemdé RT**, **Ouédraogo JB**, **Hamel MJ**, **Kariuki S**, **Oneko M**, **Odero C**, **Otieno K**, **Awino N**, **McMorrow M**, **Muturi-Kioi V**, **Laserson KF**, **Slutsker L**, **Otieno W**, **Otieno L**, **Otsyula N**, **Gondi S**, **Otieno A**, **Owira V**, **Oguk E**, **Odongo G**, **Woods JB**, **Ogutu B**, **Njuguna P**, **Chilengi R**, **Akoo P**, **Kerubo C**, **Maingi C**, **Lang T**, **Olotu A**, **Bejon P**, **Marsh K**, **Mwambingu G**, **Owusu-Agyei S**, **Asante KP**, **Osei-Kwakye K**, **Boahen O**, **Dosoo D**, **Asante I**, **Adjei G**, **Kwara E**, **Chandramohan D**, **Greenwood B**, **Lusingu J**, **Gesase S**, **Malabeja A**, **Abdul O**, **Mahende C**, **Liheluka E**, **Malle L**, **Lemnge M**, **Theander TG**, **Drakeley C**, **Ansong D**, **Agbenyega T**, **Adjei S**, **Boateng HO**, **Rettig T**, **Bawa J**, **Sylverken J**, **Sambian D**, **Sarfo A**, **Agyekum A**, **Martinson F**, **Hoffman I**, **Mvalo T**, **Kamthunzi P**, **Nkomo R**, **Tembo T**, **Tegha G**, **Tsidya M**, **Kilembe J**, **Chawinga C**, **Ballou WR**, **Cohen J**, **Guerra Y**, **Jongert E**, **Lapierre D**, **Leach A**, **Lievens M**, **Ofori-Anyinam O**, **Olivier A**, **Vekemans J**, **Carter T**, **Kaslow D**, **Leboulleux D**, **Loucq C**, **Radford A**, **Savarese B**, **Schellenberg D**, **Sillman M**, **Vansadia P**. 2012. A phase 3 trial of RTS,S/AS01 malaria vaccine in African infants. N. Engl. J. Med. **367**:2284–2295.

380. **Agnandji ST**, **Lell B**, **Soulanoudjingar SS**, **Fernandes JF**, **Abossolo BP**, **Conzelmann C**, **Methogo BGNO**, **Doucka Y**, **Flamen A**, **Mordmüller B**, **Issifou S**, **Kremsner PG**, **Sacarlal J**, **Aide P**, **Lanaspa M**, **Aponte JJ**, **Nhamuave A**, **Quelhas D**, **Bassat Q**, **Mandjate S**, **Macete E**, **Alonso P**, **Abdulla S**, **Salim N**, **Juma O**, **Shomari M**, **Shubis K**, **Machera F**, **Hamad AS**, **Minja R**, **Mtoro A**, **Sykes A**, **Ahmed S**, **Urassa AM**, **Ali AM**, **Mwangoka G**, **Tanner M**, **Tinto H**, **D'Alessandro U**, **Sorgho H**, **Valea I**, **Tahita MC**, **Kaboré W**, **Ouédraogo S**, **Sandrine Y**, **Guiguemdé RT**, **Ouédraogo JB**, **Hamel MJ**, **Kariuki S**, **Odero C**, **Oneko M**, **Otieno K**, **Awino N**, **Omoto J**, **Williamson J**, **Muturi-Kioi V**, **Laserson KF**, **Slutsker L**, **Otieno W**, **Otieno L**, **Nekoye O**, **Gondi S**, **Otieno A**, **Ogutu B**, **Wasuna R**, **Owira V**, **Jones D**, **Onyango AA**, **Njuguna P**, **Chilengi R**, **Akoo P**, **Kerubo C**, **Gitaka J**, **Maingi C**, **Lang T**, **Olotu A**, **Tsofa B**, **Bejon P**, **Peshu N**, **Marsh K**, **Owusu-Agyei S**, **Asante KP**, **Osei-Kwakye K**, **Boahen O**, **Ayamba S**, **Kayan K**, **Owusu-Ofori R**, **Dosoo D**, **Asante I**, **Adjei G**, **Chandramohan D**, **Greenwood B**, **Lusingu J**, **Gesase S**, **Malabeja A**, **Abdul O**, **Kilavo H**, **Mahende C**, **Liheluka E**, **Lemnge M**, **Theander T**, **Drakeley C**, **Ansong D**, **Agbenyega T**, **Adjei S**, **Boateng HO**, **Rettig T**, **Bawa J**, **Sylverken J**, **Sambian D**, **Agyekum A**, **Owusu L**, **Martinson F**, **Hoffman I**, **Mvalo T**, **Kamthunzi P**, **Nkomo R**, **Msika A**, **Jumbe A**, **Chome N**, **Nyakuipa D**, **Chintedza J**, **Ballou WR**, **Bruls M**, **Cohen J**, **Guerra Y**, **Jongert E**, **Lapierre D**, **Leach A**, **Lievens M**, **Ofori-Anyinam O**, **Vekemans J**, **Carter T**, **Leboulleux D**, **Loucq C**, **Radford A**, **Savarese B**, **Schellenberg D**, **Sillman M**, **Vansadia P**, **RTS,S Clinical Trials Partnership**. 2011. First results of phase 3 trial of RTS,S/AS01 malaria vaccine in African children. N. Engl. J. Med. **365**:1863–1875.

381. 2015. Efficacy and safety of RTS,S/AS01 malaria vaccine with or without a booster dose in infants and children in Africa: final results of a phase 3, individually randomised, controlled trial. The Lancet **386**:31–45.

382. **Gessner BD**, **Knobel DL**, **Conan A**, **Finn A**. 2017. Could the RTS,S/AS01 meningitis safety signal really be a protective effect of rabies vaccine? Vaccine **35**:716–721.

383. **Sedegah M**, **Hedstrom R**, **Hobart P**, **Hoffman SL**. 1994. Protection against malaria by immunization with plasmid DNA encoding circumsporozoite protein. Proc. Natl. Acad. Sci. U.S.A. **91**:9866–9870.

384. **Wang R**, **Doolan DL**, **Le TP**, **Hedstrom RC**, **Coonan KM**, **Charoenvit Y**, **Jones TR**, **Hobart P**, **Margalith M**, **Ng J**, **Weiss WR**, **Sedegah M**, **de Taisne C**, **Norman JA**, **Hoffman SL**. 1998. Induction of antigen-specific cytotoxic T lymphocytes in humans by a malaria DNA vaccine. Science **282**:476–480.

385. **Smith GL**, **Godson GN**, **Nussenzweig V**, **Nussenzweig RS**, **Barnwell J**, **Moss B**. 1984. Plasmodium knowlesi sporozoite antigen: expression by infectious recombinant vaccinia virus. Science **224**:397–399.

386. **Sedegah M**, **Beaudoin RL**, **Majarian WR**, **Cochran MD**, **Chiang CH**, **Sadoff J**,

Aggarwal A, **Charoenvit Y**, **Hoffman SL**. 1990. Evaluation of vaccines designed to induce protective cellular immunity against the Plasmodium yoelii circumsporozoite protein: vaccinia, pseudorabies, and Salmonella transformed with circumsporozoite gene. Bull. World Health Organ. **68 Suppl**:109–114.

387. **Li S**, **Rodrigues M**, **Rodriguez D**, **Rodriguez JR**, **Esteban M**, **Palese P**, **Nussenzweig RS**, **Zavala F**. 1993. Priming with recombinant influenza virus followed by administration of recombinant vaccinia virus induces CD8+ T-cell-mediated protective immunity against malaria. Proc. Natl. Acad. Sci. U.S.A. **90**:5214–5218.

388. **Rodrigues EG**, **Zavala F**, **Eichinger D**, **Wilson JM**, **Tsuji M**. 1997. Single immunizing dose of recombinant adenovirus efficiently induces CD8+ T cell-mediated protective immunity against malaria. J. Immunol. **158**:1268–1274.

389. **Ockenhouse CF**, **Sun P-F**, **Lanar DE**, **Wellde BT**, **Hall BT**, **Kester K**, **Stoute JA**, **Magill A**, **Krzych U**, **Farley L**, **Wirtz RA**, **Sadoff JC**, **Kaslow DC**, **Kumar S**, **Church LWP**, **Crutcher JM**, **Wizel B**, **Hoffman S**, **Lalvani A**, **Hill AVS**, **Tine JA**, **Guito KP**, **de Taisne C**, **Anders R**, **Horii T**, **Paoletti E**, **Ballou WR**. 1998. Phase I/IIa Safety, Immunogenicity, and Efficacy Trial of NYVAC-Pf7, a Pox-Vectored, Multiantigen, Multistage Vaccine Candidate for Plasmodium falciparum Malaria. J. Infect. Dis. **177**:1664–1673.

390. **Walther M**, **Thompson FM**, **Dunachie S**, **Keating S**, **Todryk S**, **Berthoud T**, **Andrews L**, **Andersen RF**, **Moore A**, **Gilbert SC**, **Poulton I**, **Dubovsky F**, **Tierney E**, **Correa S**, **Huntcooke A**, **Butcher G**, **Williams J**, **Sinden RE**, **Hill AVS**. 2006. Safety, immunogenicity, and efficacy of prime-boost immunization with recombinant poxvirus FP9 and modified vaccinia virus Ankara encoding the full-length Plasmodium falciparum circumsporozoite protein. Infect. Immun. **74**:2706–2716.

391. **Tamminga C**, **Sedegah M**, **Regis D**, **Chuang I**, **Epstein JE**, **Spring M**, **Mendoza-Silveiras J**, **McGrath S**, **Maiolatesi S**, **Reyes S**, **Steinbeiss V**, **Fedders C**, **Smith K**, **House B**, **Ganeshan H**, **Lejano J**, **Abot E**, **Banania GJ**, **Sayo R**, **Farooq F**, **Belmonte M**, **Murphy J**, **Komisar J**, **Williams J**, **Shi M**, **Brambilla D**, **Manohar N**, **Richie NO**, **Wood C**, **Limbach K**, **Patterson NB**, **Bruder JT**, **Doolan DL**, **King CR**, **Diggs C**, **Soisson L**, **Carucci D**, **Levine G**, **Dutta S**, **Hollingdale MR**, **Ockenhouse CF**, **Richie TL**. 2011. Adenovirus-5-vectored P. falciparum vaccine expressing CSP and AMA1. Part B: safety, immunogenicity and protective efficacy of the CSP component. PLoS ONE **6**:e25868.

392. **Hodgson SH**, **Ewer KJ**, **Bliss CM**, **Edwards NJ**, **Rampling T**, **Anagnostou NA**, **de Barra E**, **Havelock T**, **Bowyer G**, **Poulton ID**, **de Cassan S**, **Longley R**, **Illingworth JJ**, **Douglas AD**, **Mange PB**, **Collins KA**, **Roberts R**, **Gerry S**, **Berrie E**, **Moyle S**, **Colloca S**, **Cortese R**, **Sinden RE**, **Gilbert SC**, **Bejon P**, **Lawrie AM**, **Nicosia A**, **Faust SN**, **Hill AVS**. 2015. Evaluation of the efficacy of ChAd63-MVA vectored vaccines expressing circumsporozoite protein and ME-TRAP against controlled human malaria infection in malaria-naive individuals. J. Infect. Dis. **211**:1076–1086.

393. **Chuang I**, **Sedegah M**, **Cicatelli S**, **Spring M**, **Polhemus M**, **Tamminga C**, **Patterson N**, **Guerrero M**, **Bennett JW**, **McGrath S**, **Ganeshan H**, **Belmonte M**, **Farooq F**, **Abot E**, **Banania JG**, **Huang J**, **Newcomer R**, **Rein L**, **Litilit D**, **Richie NO**, **Wood C**, **Murphy J**, **Sauerwein R**, **Hermsen CC**, **McCoy AJ**, **Kamau E**, **Cummings J**, **Komisar J**, **Sutamihardja A**, **Shi M**, **Epstein JE**, **Maiolatesi S**, **Tosh D**, **Limbach K**, **Angov E**, **Bergmann-Leitner E**, **Bruder JT**, **Doolan DL**, **King CR**, **Carucci D**, **Dutta S**, **Soisson L**, **Diggs C**, **Hollingdale MR**, **Ockenhouse CF**, **Richie TL**. 2013. DNA prime/Adenovirus boost malaria vaccine encoding P. falciparum CSP and AMA1 induces sterile protection associated with cell-mediated immunity. PLoS ONE **8**:e55571.

394. **Sedegah M**, **Hollingdale MR**, **Farooq F**, **Ganeshan H**, **Belmonte M**, **Kim Y**, **Peters B**, **Sette A**, **Huang J**, **McGrath S**, **Abot E**, **Limbach K**, **Shi M**, **Soisson L**, **Diggs C**, **Chuang I**, **Tamminga C**, **Epstein JE**, **Villasante E**, **Richie TL**. 2014. Sterile immunity to malaria after DNA prime/adenovirus boost immunization is associated with effector memory CD8+T cells targeting AMA1 class I epitopes. PLoS ONE **9**:e106241.

395. **Palma C**, **Overstreet MG**, **Guedon J-M**, **Hoiczyk E**, **Ward C**, **Karen KA**, **Zavala F**, **Ketner G**. 2011. Adenovirus particles that display the Plasmodium falciparum circumsporozoite protein NANP repeat induce sporozoite-neutralizing antibodies in mice. Vaccine **29**:1683–1689.
396. **Karen KA**, **Deal C**, **Adams RJ**, **Nielsen C**, **Ward C**, **Espinosa DA**, **Xie J**, **Zavala F**, **Ketner G**. 2015. A replicating adenovirus capsid display recombinant elicits antibodies against Plasmodium falciparum sporozoites in Aotus nancymaae monkeys. Infect. Immun. **83**:268–275.
397. **Deal C**, **Balazs AB**, **Espinosa DA**, **Zavala F**, **Baltimore D**, **Ketner G**. 2014. Vectored antibody gene delivery protects against Plasmodium falciparum sporozoite challenge in mice. Proc. Natl. Acad. Sci. U.S.A. **111**:12528–12532.
398. **Sedegah M**, **Jones TR**, **Kaur M**, **Hedstrom R**, **Hobart P**, **Tine JA**, **Hoffman SL**. 1998. Boosting with recombinant vaccinia increases immunogenicity and protective efficacy of malaria DNA vaccine. Proc. Natl. Acad. Sci. U.S.A. **95**:7648–7653.
399. **Rogers WO**, **Weiss WR**, **Kumar A**, **Aguiar JC**, **Tine JA**, **Gwadz R**, **Harre JG**, **Gowda K**, **Rathore D**, **Kumar S**, **Hoffman SL**. 2002. Protection of rhesus macaques against lethal Plasmodium knowlesi malaria by a heterologous DNA priming and poxvirus boosting immunization regimen. Infect. Immun. **70**:4329–4335.
400. **Dunachie SJ**, **Walther M**, **Epstein JE**, **Keating S**, **Berthoud T**, **Andrews L**, **Andersen RF**, **Bejon P**, **Goonetilleke N**, **Poulton I**, **Webster DP**, **Butcher G**, **Watkins K**, **Sinden RE**, **Levine GL**, **Richie TL**, **Schneider J**, **Kaslow D**, **Gilbert SC**, **Carucci DJ**, **Hill AVS**. 2006. A DNA prime-modified vaccinia virus ankara boost vaccine encoding thrombospondin-related adhesion protein but not circumsporozoite protein partially protects healthy malaria-naive adults against Plasmodium falciparum sporozoite challenge. Infect. Immun. **74**:5933–5942.
401. **Wang R**, **Epstein J**, **Charoenvit Y**, **Baraceros FM**, **Rahardjo N**, **Gay T**, **Banania JG**, **Chattopadhyay R**, **la Vega de P**, **Richie TL**, **Tornieporth N**, **Doolan DL**, **Kester KE**, **Heppner DG**, **Norman J**, **Carucci DJ**, **Cohen JD**, **Hoffman SL**. 2004. Induction in humans of CD8+ and CD4+ T cell and antibody responses by sequential immunization with malaria DNA and recombinant protein. J. Immunol. **172**:5561–5569.
402. **Epstein JE**, **Charoenvit Y**, **Kester KE**, **Wang R**, **Newcomer R**, **Fitzpatrick S**, **Richie TL**, **Tornieporth N**, **Heppner DG**, **Ockenhouse C**, **Majam V**, **Holland C**, **Abot E**, **Ganeshan H**, **Berzins M**, **Jones T**, **Freydberg CN**, **Ng J**, **Norman J**, **Carucci DJ**, **Cohen J**, **Hoffman SL**. 2004. Safety, tolerability, and antibody responses in humans after sequential immunization with a PfCSP DNA vaccine followed by the recombinant protein vaccine RTS,S/AS02A. Vaccine **22**:1592–1603.
403. **Dunachie SJ**, **Walther M**, **Vuola JM**, **Webster DP**, **Keating SM**, **Berthoud T**, **Andrews L**, **Bejon P**, **Poulton I**, **Butcher G**, **Watkins K**, **Sinden RE**, **Leach A**, **Moris P**, **Tornieporth N**, **Schneider J**, **Dubovsky F**, **Tierney E**, **Williams J**, **Heppner DG**, **Gilbert SC**, **Cohen J**, **Hill AVS**. 2006. A clinical trial of prime-boost immunisation with the candidate malaria vaccines RTS,S/AS02A and MVA-CS. Vaccine **24**:2850–2859.
404. **Stewart VA**, **McGrath SM**, **Dubois PM**, **Pau MG**, **Mettens P**, **Shott J**, **Cobb M**, **Burge JR**, **Larson D**, **Ware LA**, **Demoitié M-A**, **Weverling GJ**, **Bayat B**, **Custers JHHV**, **Dubois M-C**, **Cohen J**, **Goudsmit J**, **Heppner DG**. 2007. Priming with an adenovirus 35-circumsporozoite protein (CS) vaccine followed by RTS,S/AS01B boosting significantly improves immunogenicity to Plasmodium falciparum CS compared to that with either malaria vaccine alone. Infect. Immun. **75**:2283–2290.
405. **Ockenhouse CF**, **Regules J**, **Tosh D**, **Cowden J**, **Kathcart A**, **Cummings J**, **Paolino K**, **Moon J**, **Komisar J**, **Kamau E**, **Oliver T**, **Chhoeu A**, **Murphy J**, **Lyke K**, **Laurens M**, **Birkett A**, **Lee C**, **Weltzin R**, **Wille-Reece U**, **Sedegah M**, **Hendriks J**, **Versteege I**, **Pau MG**, **Sadoff J**, **Vanloubbeeck Y**, **Lievens M**, **Heerwegh D**, **Moris P**, **Guerra Mendoza Y**, **Jongert E**, **Cohen J**, **Voss G**, **Ballou WR**, **Vekemans J**. 2015. Ad35.CS.01-RTS,S/AS01 Heterologous Prime Boost Vaccine Efficacy against Sporozoite Challenge in Healthy Malaria-Naïve Adults. PLoS ONE **10**:e0131571.
406. **Gregson AL**, **Oliveira G**, **Othoro C**, **Calvo-Calle JM**, **Thorton GB**, **Nardin E**, **Edelman R**. 2008. Phase I trial of an alhydrogel adjuvanted hepatitis B core virus-

like particle containing epitopes of Plasmodium falciparum circumsporozoite protein. PLoS ONE **3**:e1556.

407. **Phares TW**, **May AD**, **Genito CJ**, **Hoyt NA**, **Khan FA**, **Porter MD**, **DeBot M**, **Waters NC**, **Saudan P**, **Dutta S**. 2017. Rhesus macaque and mouse models for down-selecting circumsporozoite protein based malaria vaccines differ significantly in immunogenicity and functional outcomes. Malaria Journal **16**:115.

408. **Janitzek CM**, **Matondo S**, **Thrane S**, **Nielsen MA**, **Kavishe R**, **Mwakalinga SB**, **Theander TG**, **Salanti A**, **Sander AF**. 2016. Bacterial superglue generates a full-length circumsporozoite protein virus-like particle vaccine capable of inducing high and durable antibody responses. Malaria Journal **15**:545.

409. **Kaba SA**, **McCoy ME**, **Doll TAPF**, **Brando C**, **Guo Q**, **Dasgupta D**, **Yang Y**, **Mittelholzer C**, **Spaccapelo R**, **Crisanti A**, **Burkhard P**, **Lanar DE**. 2012. Protective Antibody and CD8+ T-Cell Responses to the Plasmodium falciparum Circumsporozoite Protein Induced by a Nanoparticle Vaccine. PLoS ONE **7**:e48304.

410. **Seth L**, **Bingham Ferlez KM**, **Kaba SA**, **Musser DM**, **Emadi S**, **Matyas GR**, **Beck Z**, **Alving CR**, **Burkhard P**, **Lanar DE**. 2017. Development of a self-assembling protein nanoparticle vaccine targeting Plasmodium falciparum Circumsporozoite Protein delivered in three Army Liposome Formulation adjuvants. Vaccine.

411. **Rudra JS**, **Mishra S**, **Chong AS**, **Mitchell RA**, **Nardin EH**, **Nussenzweig V**, **Collier JH**. 2012. Self-assembled peptide nanofibers raising durable antibody responses against a malaria epitope. Biomaterials **33**:6476–6484.

412. **Roggero MA**, **Meraldi V**, **López JA**, **Eberl G**, **Romero JC**, **Matile H**, **Betschart B**, **Corradin G**, **Renggli J**. 2000. The synthetic, oxidized C-terminal fragment of the Plasmodium berghei circumsporozoite protein elicits a high protective response. Eur. J. Immunol. **30**:2679–2685.

413. **López JA**, **Weilenman C**, **Audran R**, **Roggero MA**, **Bonelo A**, **Tiercy JM**, **Spertini F**, **Corradin G**. 2001. A synthetic malaria vaccine elicits a potent CD8(+) and CD4(+) T lymphocyte immune response in humans. Implications for vaccination strategies. Eur. J. Immunol. **31**:1989–1998.

414. **Audran R**, **Lurati-Ruiz F**, **Genton B**, **Blythman HE**, **Ofori-Anyinam O**, **Reymond C**, **Corradin G**, **Spertini F**. 2009. The synthetic Plasmodium falciparum circumsporozoite peptide PfCS102 as a malaria vaccine candidate: a randomized controlled phase I trial. PLoS ONE **4**:e7304.

415. **Genton B**, **D'Acremont V**, **Lurati-Ruiz F**, **Verhage D**, **Audran R**, **Hermsen C**, **Wolters L**, **Reymond C**, **Spertini F**, **Sauerwein R**. 2010. Randomized double-blind controlled Phase I/IIa trial to assess the efficacy of malaria vaccine PfCS102 to protect against challenge with P. falciparum. Vaccine **28**:6573–6580.

416. **Tam JP**. 1988. Synthetic peptide vaccine design: synthesis and properties of a high-density multiple antigenic peptide system. Proc. Natl. Acad. Sci. U.S.A. **85**:5409–5413.

417. **Tam JP**, **Clavijo P**, **Lu YA**, **Nussenzweig V**, **Nussenzweig R**, **Zavala F**. 1990. Incorporation of T and B epitopes of the circumsporozoite protein in a chemically defined synthetic vaccine against malaria. J. Exp. Med. **171**:299–306.

418. **Wang R**, **Charoenvit Y**, **Corradin G**, **Porrozzi R**, **Hunter RL**, **Glenn G**, **Alving CR**, **Church P**, **Hoffman SL**. 1995. Induction of protective polyclonal antibodies by immunization with a Plasmodium yoelii circumsporozoite protein multiple antigen peptide vaccine. J. Immunol. **154**:2784–2793.

419. **Nardin EH**, **Oliveira GA**, **Calvo-Calle JM**, **Castro ZR**, **Nussenzweig RS**, **Schmeckpeper B**, **Hall BF**, **Diggs C**, **Bodison S**, **Edelman R**. 2000. Synthetic malaria peptide vaccine elicits high levels of antibodies in vaccinees of defined HLA genotypes. J. Infect. Dis. **182**:1486–1496.

420. **Kumar KA**, **Oliveira GA**, **Edelman R**, **Nardin E**, **Nussenzweig V**. 2004. Quantitative Plasmodium sporozoite neutralization assay (TSNA). J. Immunol. Methods **292**:157–164.

421. **Nardin EH**, **Calvo-Calle JM**, **Oliveira GA**, **Nussenzweig RS**, **Schneider M**, **Tiercy JM**, **Loutan L**, **Hochstrasser D**, **Rose K**. 2001. A totally synthetic polyoxime malaria vaccine containing Plasmodium falciparum B cell and universal T cell epitopes elicits immune responses in volunteers of diverse HLA types. J. Immunol. **166**:481–489.

422. **Sadoff JC**, **Ballou WR**, **Baron LS**, **Majarian WR**, **Brey RN**, **Hockmeyer WT**, **Young JF**, **Cryz SJ**, **Ou J**, **Lowell GH**. 1988. Oral Salmonella typhimurium vaccine expressing circumsporozoite protein protects against malaria. Science **240**:336–338.

423. **Gonzalez C**, **Hone D**, **Noriega FR**, **Tacket CO**, **Davis JR**, **Losonsky G**, **Nataro JP**, **Hoffman S**, **Malik A**, **Nardin E**, **Sztein MB**, **Heppner DG**, **Fouts TR**, **Isibasi A**, **Levine MM**. 1994. Salmonella typhi vaccine strain CVD 908 expressing the circumsporozoite protein of Plasmodium falciparum: strain construction and safety and immunogenicity in humans. J. Infect. Dis. **169**:927–931.

424. **Ruiz-Pérez F**, **León-Kempis R**, **Santiago-Machuca A**, **Ortega-Pierres G**, **Barry E**, **Levine M**, **González-Bonilla C**. 2002. Expression of the Plasmodium falciparum immunodominant epitope (NANP)(4) on the surface of Salmonella enterica using the autotransporter MisL. Infect. Immun. **70**:3611–3620.

425. **Ruiz-Olvera P**, **Ruiz-Pérez F**, **Sepulveda NV**, **Santiago-Machuca A**, **Maldonado-Rodríguez R**, **Garcia-Elorriaga G**, **González-Bonilla C**. 2003. Display and release of the Plasmodium falciparum circumsporozoite protein using the autotransporter MisL of Salmonella enterica. Plasmid **50**:12–27.

426. **Tartz S**, **Rüssmann H**, **Kamanova J**, **Sebo P**, **Sturm A**, **Heussler V**, **Fleischer B**, **Jacobs T**. 2008. Complete protection against P. berghei malaria upon heterologous prime/boost immunization against circumsporozoite protein employing Salmonella type III secretion system and Bordetella adenylate cyclase toxoid. Vaccine **26**:5935–5943.

427. **Chinchilla M**, **Pasetti MF**, **Medina-Moreno S**, **Wang JY**, **Gomez-Duarte OG**, **Stout R**, **Levine MM**, **Galen JE**. 2007. Enhanced immunity to Plasmodium falciparum circumsporozoite protein (PfCSP) by using Salmonella enterica serovar Typhi expressing PfCSP and a PfCSP-encoding DNA vaccine in a heterologous prime-boost strategy. Infect. Immun. **75**:3769–3779.

428. **Matsumoto S**, **Yanagi T**, **Ohara N**, **Wada N**, **Kanbara H**, **Yamada T**. 1996. Stable expression and secretion of the B-cell epitope of rodent malaria from Mycobacterium bovis BCG and induction of long-lasting humoral response in mouse. Vaccine **14**:54–60.

429. **Zheng C**, **Xie P**, **Chen Y**. 2002. Recombinant Mycobacterium bovis BCG producing the circumsporozoite protein of Plasmodium falciparum FCC-1/HN strain induces strong immune responses in BALB/c mice. Parasitol. Int. **51**:1–7.

430. **Rapeah S**, **Norazmi MN**. 2006. Immunogenicity of a recombinant Mycobacterium bovis bacille Calmette-Guèrin expressing malarial and tuberculosis epitopes. Vaccine **24**:3646–3653.

431. **Arama C**, **Waseem S**, **Fernández C**, **Assefaw-Redda Y**, **You L**, **Rodriguez A**, **Radošević K**, **Goudsmit J**, **Kaufmann SHE**, **Reece ST**, **Troye-Blomberg M**. 2012. A recombinant Bacille Calmette-Guérin construct expressing the Plasmodium falciparum circumsporozoite protein enhances dendritic cell activation and primes for circumsporozoite-specific memory cells in BALB/c mice. Vaccine **30**:5578–5584.

432. **Bergmann-Leitner ES**, **Hosie H**, **Trichilo J**, **Deriso E**, **Ranallo RT**, **Alefantis T**, **Savranskaya T**, **Grewal P**, **Ockenhouse CF**, **Venkatesan MM**, **Delvecchio VG**, **Angov E**. 2013. Self-adjuvanting bacterial vectors expressing pre-erythrocytic antigens induce sterile protection against malaria. Front Immunol **4**:176.

433. **Wang HH**, **Rogers WO**, **Kang YH**, **Sedegah M**, **Hoffman SL**. 1995. Partial protection against malaria by immunization with Leishmania enriettii expressing the Plasmodium yoelii circumsporozoite protein. Mol. Biochem. Parasitol. **69**:139–148.

434. **Charest H**, **Sedegah M**, **Yap GS**, **Gazzinelli RT**, **Caspar P**, **Hoffman SL**, **Sher A**. 2000. Recombinant attenuated Toxoplasma gondii expressing the Plasmodium yoelii circumsporozoite protein provides highly effective priming for CD8+ T cell-dependent protective immunity against malaria. J. Immunol. **165**:2084–2092.

435. **Reyes-Sandoval A**, **Bachmann MF**. 2013. Plasmodium vivax malaria vaccines: why are we where we are? Hum Vaccin Immunother **9**:2558–2565.

436. **Barr PJ**, **Gibson HL**, **Enea V**, **Arnot DE**, **Hollingdale MR**, **Nussenzweig V**. 1987. Expression in yeast of a Plasmodium vivax antigen of potential use in a human

malaria vaccine. J. Exp. Med. **165**:1160–1171.
437. **Collins WE**, **Nussenzweig RS**, **Ballou WR**, **Ruebush TK**, **Nardin EH**, **Chulay JD**, **Majarian WR**, **Young JF**, **Wasserman GF**, **Bathurst I**. 1989. Immunization of Saimiri sciureus boliviensis with recombinant vaccines based on the circumsporozoite protein of Plasmodium vivax. Am. J. Trop. Med. Hyg. **40**:455–464.
438. **Gordon DM**, **Cosgriff TM**, **Schneider I**, **Wasserman GF**, **Majarian WR**, **Hollingdale MR**, **Chulay JD**. 1990. Safety and immunogenicity of a Plasmodium vivax sporozoite vaccine. Am. J. Trop. Med. Hyg. **42**:527–531.
439. **Charoenvit Y**, **Collins WE**, **Jones TR**, **Millet P**, **Yuan L**, **Campbell GH**, **Beaudoin RL**, **Broderson JR**, **Hoffman SL**. 1991. Inability of malaria vaccine to induce antibodies to a protective epitope within its sequence. Science **251**:668–671.
440. **Jones TR**, **Yuan LF**, **Marwoto HA**, **Gordon DM**, **Wirtz RA**, **Hoffman SL**. 1992. Low immunogenicity of a Plasmodium vivax circumsporozoite protein epitope bound by a protective monoclonal antibody. Am. J. Trop. Med. Hyg. **47**:837–843.
441. **Herrera MA**, **de Plata C**, **González JM**, **Corradin G**, **Herrera S**. 1994. Immunogenicity of multiple antigen peptides containing Plasmodium vivax CS epitopes in BALB/c mice. Mem. Inst. Oswaldo Cruz **89 Suppl 2**:71–76.
442. **Collins WE**, **Sullivan JS**, **Morris CL**, **Galland GG**, **Jue DL**, **Fang S**, **Wohlhueter R**, **Reed RC**, **Yang C**, **Hunter RL**, **Lal AA**. 1997. Protective immunity induced in squirrel monkeys with a multiple antigen construct against the circumsporozoite protein of Plasmodium vivax. Am. J. Trop. Med. Hyg. **56**:200–210.
443. **Yang C**, **Collins WE**, **Xiao L**, **Saekhou AM**, **Reed RC**, **Nelson CO**, **Hunter RL**, **Jue DL**, **Fang S**, **Wohlhueter RM**, **Udhayakumar V**, **Lal AA**. 1997. Induction of protective antibodies in Saimiri monkeys by immunization with a multiple antigen construct (MAC) containing the Plasmodium vivax circumsporozoite protein repeat region and a universal T helper epitope of tetanus toxin. Vaccine **15**:377–386.
444. **Rogers WO**, **Gowda K**, **Hoffman SL**. 1999. Construction and immunogenicity of DNA vaccine plasmids encoding four Plasmodium vivax candidate vaccine antigens. Vaccine **17**:3136–3144.
445. **Mizutani M**, **Iyori M**, **Blagborough AM**, **Fukumoto S**, **Funatsu T**, **Sinden RE**, **Yoshida S**. 2014. Baculovirus-vectored multistage Plasmodium vivax vaccine induces both protective and transmission-blocking immunities against transgenic rodent malaria parasites. Infect. Immun. **82**:4348–4357.
446. **Herrera S**, **Bonelo A**, **Perlaza BL**, **Valencia AZ**, **Cifuentes C**, **Hurtado S**, **Quintero G**, **López JA**, **Corradin G**, **Arévalo-Herrera M**. 2004. Use of long synthetic peptides to study the antigenicity and immunogenicity of the Plasmodium vivax circumsporozoite protein. Int. J. Parasitol. **34**:1535–1546.
447. **Herrera S**, **Bonelo A**, **Perlaza BL**, **Fernández OL**, **Victoria L**, **Lenis AM**, **Soto L**, **Hurtado H**, **Acuña LM**, **Vélez JD**, **Palacios R**, **Chen-Mok M**, **Corradin G**, **Arévalo-Herrera M**. 2005. Safety and elicitation of humoral and cellular responses in colombian malaria-naive volunteers by a Plasmodium vivax circumsporozoite protein-derived synthetic vaccine. Am. J. Trop. Med. Hyg. **73**:3–9.
448. **Arévalo-Herrera M**, **Soto L**, **Perlaza BL**, **Céspedes N**, **Vera O**, **Lenis AM**, **Bonelo A**, **Corradin G**, **Herrera S**. 2011. Antibody-mediated and cellular immune responses induced in naive volunteers by vaccination with long synthetic peptides derived from the Plasmodium vivax circumsporozoite protein. Am. J. Trop. Med. Hyg. **84**:35–42.
449. **Yadava A**, **Sattabongkot J**, **Washington MA**, **Ware LA**, **Majam V**, **Zheng H**, **Kumar S**, **Ockenhouse CF**. 2007. A novel chimeric Plasmodium vivax circumsporozoite protein induces biologically functional antibodies that recognize both VK210 and VK247 sporozoites. Infect. Immun. **75**:1177–1185.
450. **Bell BA**, **Wood JF**, **Bansal R**, **Ragab H**, **Cargo J**, **Washington MA**, **Wood CL**, **Ware LA**, **Ockenhouse CF**, **Yadava A**. 2009. Process development for the production of an E. coli produced clinical grade recombinant malaria vaccine for Plasmodium vivax. Vaccine **27**:1448–1453.
451. **Lumsden JM**, **Pichyangkul S**, **Srichairatanakul U**, **Yongvanitchit K**, **Limsalakpetch A**, **Nurmukhambetova S**, **Klein J**, **Bertholet S**, **Vedvick TS**, **Reed SG**, **Sattabongkot J**, **Bennett JW**, **Polhemus ME**, **Ockenhouse CF**, **Howard RF**,

Yadava A. 2011. Evaluation of the safety and immunogenicity in rhesus monkeys of a recombinant malaria vaccine for Plasmodium vivax with a synthetic Toll-like receptor 4 agonist formulated in an emulsion. Infect. Immun. **79**:3492–3500.

452. **Yadava A**, **Nurmukhambetova S**, **Pichugin AV**, **Lumsden JM**. 2012. Cross-species immunity following immunization with a circumsporozoite protein-based vaccine for malaria. J. Infect. Dis. **205**:1456–1463.

453. **Bennett JW**, **Yadava A**, **Tosh D**, **Sattabongkot J**, **Komisar J**, **Ware LA**, **McCarthy WF**, **Cowden JJ**, **Regules J**, **Spring MD**, **Paolino K**, **Hartzell JD**, **Cummings JF**, **Richie TL**, **Lumsden J**, **Kamau E**, **Murphy J**, **Lee C**, **Parekh F**, **Birkett A**, **Cohen J**, **Ballou WR**, **Polhemus ME**, **Vanloubbeeck YF**, **Vekemans J**, **Ockenhouse CF**. 2016. Phase 1/2a Trial of Plasmodium vivax Malaria Vaccine Candidate VMP001/AS01B in Malaria-Naive Adults: Safety, Immunogenicity, and Efficacy. PLoS Negl Trop Dis **10**:e0004423.

454. **Yadava A**, **Hall CE**, **Sullivan JS**, **Nace D**, **Williams T**, **Collins WE**, **Ockenhouse CF**, **Barnwell JW**. 2014. Protective efficacy of a Plasmodium vivax circumsporozoite protein-based vaccine in Aotus nancymaae is associated with antibodies to the repeat region. PLoS Negl Trop Dis **8**:e3268.

455. **Vanloubbeeck Y**, **Pichyangkul S**, **Bayat B**, **Yongvanitchit K**, **Bennett JW**, **Sattabongkot J**, **Schaecher K**, **Ockenhouse CF**, **Cohen J**, **Yadava A**, **P. vivax vaccine study group**. 2013. Comparison of the immune responses induced by soluble and particulate Plasmodium vivax circumsporozoite vaccine candidates formulated in AS01 in rhesus macaques. Vaccine **31**:6216–6224.

456. **Charoenvit Y**, **Leef MF**, **Yuan LF**, **Sedegah M**, **Beaudoin RL**. 1987. Characterization of Plasmodium yoelii monoclonal antibodies directed against stage-specific sporozoite antigens. Infect. Immun. **55**:604–608.

457. **Wortman A**, **Rogers P**, **Charoenvit Y**, **McDermott A**, **Leef M**, **Sedegah M**, **Beaudoin RL**. 1989. Cloning of Plasmodium yoelii genes expressing three different sporozoite-specific antigens. Microb. Pathog. **6**:227–231.

458. **Hedstrom RC**, **Campbell JR**, **Leef ML**, **Charoenvit Y**, **Carter M**, **Sedegah M**, **Beaudoin RL**, **Hoffman SL**. 1990. A malaria sporozoite surface antigen distinct from the circumsporozoite protein. Bull. World Health Organ. **68 Suppl**:152–157.

459. **Robson KJ**, **Hall JR**, **Jennings MW**, **Harris TJ**, **Marsh K**, **Newbold CI**, **Tate VE**, **Weatherall DJ**. 1988. A highly conserved amino-acid sequence in thrombospondin, properdin and in proteins from sporozoites and blood stages of a human malaria parasite. Nature **335**:79–82.

460. **Cowan G**, **Krishna S**, **Crisanti A**, **Robson K**. 1992. Expression of thrombospondin-related anonymous protein in Plasmodium falciparum sporozoites. Lancet **339**:1412–1413.

461. **Rogers WO**, **Rogers MD**, **Hedstrom RC**, **Hoffman SL**. 1992. Characterization of the gene encoding sporozoite surface protein 2, a protective Plasmodium yoelii sporozoite antigen. Mol. Biochem. Parasitol. **53**:45–51.

462. **Rogers WO**, **Malik A**, **Mellouk S**, **Nakamura K**, **Rogers MD**, **Szarfman A**, **Gordon DM**, **Nussler AK**, **Aikawa M**, **Hoffman SL**. 1992. Characterization of Plasmodium falciparum sporozoite surface protein 2. Proc. Natl. Acad. Sci. U.S.A. **89**:9176–9180.

463. **Gantt S**, **Persson C**, **Rose K**, **Birkett AJ**, **Abagyan R**, **Nussenzweig V**. 2000. Antibodies against thrombospondin-related anonymous protein do not inhibit Plasmodium sporozoite infectivity in vivo. Infect. Immun. **68**:3667–3673.

464. **Ghosh AK**, **Devenport M**, **Jethwaney D**, **Kalume DE**, **Pandey A**, **Anderson VE**, **Sultan AA**, **Kumar N**, **Jacobs-Lorena M**. 2009. Malaria parasite invasion of the mosquito salivary gland requires interaction between the Plasmodium TRAP and the Anopheles saglin proteins. PLoS Pathog. **5**:e1000265.

465. **Müller HM**, **Reckmann I**, **Hollingdale MR**, **Bujard H**, **Robson KJ**, **Crisanti A**. 1993. Thrombospondin related anonymous protein (TRAP) of Plasmodium falciparum binds specifically to sulfated glycoconjugates and to HepG2 hepatoma cells suggesting a role for this molecule in sporozoite invasion of hepatocytes. EMBO J. **12**:2881–2889.

466. **Gantt SM**, **Clavijo P**, **Bai X**, **Esko JD**, **Sinnis P**. 1997. Cell adhesion to a motif shared by the malaria circumsporozoite protein and thrombospondin is mediated by its glycosaminoglycan-binding region and not by CSVTCG. J. Biol. Chem. **272**:19205–

19213.
467. **Matuschewski K**, **Nunes AC**, **Nussenzweig V**, **Ménard R**. 2002. Plasmodium sporozoite invasion into insect and mammalian cells is directed by the same dual binding system. EMBO J. **21**:1597–1606.
468. **Sultan AA**, **Thathy V**, **Frevert U**, **Robson KJ**, **Crisanti A**, **Nussenzweig V**, **Nussenzweig RS**, **Ménard R**. 1997. TRAP is necessary for gliding motility and infectivity of plasmodium sporozoites. Cell **90**:511–522.
469. **Kappe S**, **Bruderer T**, **Gantt S**, **Fujioka H**, **Nussenzweig V**, **Ménard R**. 1999. Conservation of a gliding motility and cell invasion machinery in Apicomplexan parasites. J. Cell Biol. **147**:937–944.
470. **Bosch J**, **Buscaglia CA**, **Krumm B**, **Ingason BP**, **Lucas R**, **Roach C**, **Cardozo T**, **Nussenzweig V**, **Hol WGJ**. 2007. Aldolase provides an unusual binding site for thrombospondin-related anonymous protein in the invasion machinery of the malaria parasite. Proc. Natl. Acad. Sci. U.S.A. **104**:7015–7020.
471. **Diaz SA**, **Martin SR**, **Howell SA**, **Grainger M**, **Moon RW**, **Green JL**, **Holder AA**. 2016. The Binding of Plasmodium falciparum Adhesins and Erythrocyte Invasion Proteins to Aldolase Is Enhanced by Phosphorylation. PLoS ONE **11**:e0161850.
472. **Baker RP**, **Wijetilaka R**, **Urban S**. 2006. Two Plasmodium rhomboid proteases preferentially cleave different adhesins implicated in all invasive stages of malaria. PLoS Pathog. **2**:e113.
473. **Ejigiri I**, **Ragheb DRT**, **Pino P**, **Coppi A**, **Bennett BL**, **Soldati-Favre D**, **Sinnis P**. 2012. Shedding of TRAP by a rhomboid protease from the malaria sporozoite surface is essential for gliding motility and sporozoite infectivity. PLoS Pathog. **8**:e1002725.
474. **Nemetski SM**, **Cardozo TJ**, **Bosch G**, **Weltzer R**, **O'Malley K**, **Ejigiri I**, **Kumar KA**, **Buscaglia CA**, **Nussenzweig V**, **Sinnis P**, **Levitskaya J**, **Bosch J**. 2015. Inhibition by stabilization: targeting the Plasmodium falciparum aldolase-TRAP complex. Malaria Journal **14**:324.
475. **Khusmith S**, **Charoenvit Y**, **Kumar S**, **Sedegah M**, **Beaudoin RL**, **Hoffman SL**. 1991. Protection against malaria by vaccination with sporozoite surface protein 2 plus CS protein. Science **252**:715–718.
476. **Khusmith S**, **Sedegah M**, **Hoffman SL**. 1994. Complete protection against Plasmodium yoelii by adoptive transfer of a CD8+ cytotoxic T-cell clone recognizing sporozoite surface protein 2. Infect. Immun. **62**:2979–2983.
477. **Wang R**, **Charoenvit Y**, **Corradin G**, **La Vega De P**, **Franke ED**, **Hoffman SL**. 1996. Protection against malaria by Plasmodium yoelii sporozoite surface protein 2 linear peptide induction of CD4+ T cell- and IFN-gamma-dependent elimination of infected hepatocytes. J. Immunol. **157**:4061–4067.
478. **Wizel B**, **Houghten R**, **Church P**, **Tine JA**, **Lanar DE**, **Gordon DM**, **Ballou WR**, **Sette A**, **Hoffman SL**. 1995. HLA-A2-restricted cytotoxic T lymphocyte responses to multiple Plasmodium falciparum sporozoite surface protein 2 epitopes in sporozoite-immunized volunteers. J. Immunol. **155**:766–775.
479. **Wizel B**, **Houghten RA**, **Parker KC**, **Coligan JE**, **Church P**, **Gordon DM**, **Ballou WR**, **Hoffman SL**. 1995. Irradiated sporozoite vaccine induces HLA-B8-restricted cytotoxic T lymphocyte responses against two overlapping epitopes of the Plasmodium falciparum sporozoite surface protein 2. J. Exp. Med. **182**:1435–1445.
480. **Doolan DL**, **Hoffman SL**. 1997. Multi-gene vaccination against malaria: A multistage, multi-immune response approach. Parasitol. Today (Regul. Ed.) **13**:171–178.
481. **McConkey SJ**, **Reece WHH**, **Moorthy VS**, **Webster D**, **Dunachie S**, **Butcher G**, **Vuola JM**, **Blanchard TJ**, **Gothard P**, **Watkins K**, **Hannan CM**, **Everaere S**, **Brown K**, **Kester KE**, **Cummings J**, **Williams J**, **Heppner DG**, **Pathan A**, **Flanagan K**, **Arulanantham N**, **Roberts MTM**, **Roy M**, **Smith GL**, **Schneider J**, **Peto T**, **Sinden RE**, **Gilbert SC**, **Hill AVS**. 2003. Enhanced T-cell immunogenicity of plasmid DNA vaccines boosted by recombinant modified vaccinia virus Ankara in humans. Nat. Med. **9**:729–735.
482. **Moorthy VS**, **Imoukhuede EB**, **Milligan P**, **Bojang K**, **Keating S**, **Kaye P**, **Pinder M**, **Gilbert SC**, **Walraven G**, **Greenwood BM**, **Hill ASV**. 2004. A randomised, double-blind, controlled vaccine efficacy trial of DNA/MVA ME-TRAP against

malaria infection in Gambian adults. PLoS Med. **1**:e33.

483. **Bodescot M**, **Silvie O**, **Siau A**, **Refour P**, **Pino P**, **Franetich J-F**, **Hannoun L**, **Sauerwein R**, **Mazier D**. 2004. Transcription status of vaccine candidate genes of Plasmodium falciparum during the hepatic phase of its life cycle. Parasitol. Res. **92**:449–452.

484. **Webster DP**, **Dunachie S**, **Vuola JM**, **Berthoud T**, **Keating S**, **Laidlaw SM**, **McConkey SJ**, **Poulton I**, **Andrews L**, **Andersen RF**, **Bejon P**, **Butcher G**, **Sinden R**, **Skinner MA**, **Gilbert SC**, **Hill AVS**. 2005. Enhanced T cell-mediated protection against malaria in human challenges by using the recombinant poxviruses FP9 and modified vaccinia virus Ankara. Proc. Natl. Acad. Sci. U.S.A. **102**:4836–4841.

485. **Vuola JM**, **Keating S**, **Webster DP**, **Berthoud T**, **Dunachie S**, **Gilbert SC**, **Hill AVS**. 2005. Differential immunogenicity of various heterologous prime-boost vaccine regimens using DNA and viral vectors in healthy volunteers. J. Immunol. **174**:449–455.

486. **Reyes-Sandoval A**, **Sridhar S**, **Berthoud T**, **Moore AC**, **Harty JT**, **Gilbert SC**, **Gao G**, **Ertl HCJ**, **Wilson JC**, **Hill AVS**. 2008. Single-dose immunogenicity and protective efficacy of simian adenoviral vectors against Plasmodium berghei. Eur. J. Immunol. **38**:732–741.

487. **Reyes-Sandoval A**, **Wyllie DH**, **Bauza K**, **Milicic A**, **Forbes EK**, **Rollier CS**, **Hill AVS**. 2011. CD8+ T effector memory cells protect against liver-stage malaria. J. Immunol. **187**:1347–1357.

488. **Hill AVS**, **Reyes-Sandoval A**, **O'Hara G**, **Ewer K**, **Lawrie A**, **Goodman A**, **Nicosia A**, **Folgori A**, **Colloca S**, **Cortese R**, **Gilbert SC**, **Draper SJ**. 2010. Prime-boost vectored malaria vaccines: progress and prospects. Hum Vaccin **6**:78–83.

489. **Ewer KJ**, **O'Hara GA**, **Duncan CJA**, **Collins KA**, **Sheehy SH**, **Reyes-Sandoval A**, **Goodman AL**, **Edwards NJ**, **Elias SC**, **Halstead FD**, **Longley RJ**, **Rowland R**, **Poulton ID**, **Draper SJ**, **Blagborough AM**, **Berrie E**, **Moyle S**, **Williams N**, **Siani L**, **Folgori A**, **Colloca S**, **Sinden RE**, **Lawrie AM**, **Cortese R**, **Gilbert SC**, **Nicosia A**, **Hill AVS**. 2013. Protective CD8+ T-cell immunity to human malaria induced by chimpanzee adenovirus-MVA immunisation. Nat Commun **4**:2836.

490. **Ogwang C**, **Afolabi M**, **Kimani D**, **Jagne YJ**, **Sheehy SH**, **Bliss CM**, **Duncan CJA**, **Collins KA**, **Garcia Knight MA**, **Kimani E**, **Anagnostou NA**, **Berrie E**, **Moyle S**, **Gilbert SC**, **Spencer AJ**, **Soipei P**, **Mueller J**, **Okebe J**, **Colloca S**, **Cortese R**, **Viebig NK**, **Roberts R**, **Gantlett K**, **Lawrie AM**, **Nicosia A**, **Imoukhuede EB**, **Bejon P**, **Urban BC**, **Flanagan KL**, **Ewer KJ**, **Chilengi R**, **Hill AVS**, **Bojang K**. 2013. Safety and immunogenicity of heterologous prime-boost immunisation with Plasmodium falciparum malaria candidate vaccines, ChAd63 ME-TRAP and MVA ME-TRAP, in healthy Gambian and Kenyan adults. PLoS ONE **8**:e57726.

491. **Kimani D**, **Jagne YJ**, **Cox M**, **Kimani E**, **Bliss CM**, **Gitau E**, **Ogwang C**, **Afolabi MO**, **Bowyer G**, **Collins KA**, **Edwards N**, **Hodgson SH**, **Duncan CJA**, **Spencer AJ**, **Knight MG**, **Drammeh A**, **Anagnostou NA**, **Berrie E**, **Moyle S**, **Gilbert SC**, **Soipei P**, **Okebe J**, **Colloca S**, **Cortese R**, **Viebig NK**, **Roberts R**, **Lawrie AM**, **Nicosia A**, **Imoukhuede EB**, **Bejon P**, **Chilengi R**, **Bojang K**, **Flanagan KL**, **Hill AVS**, **Urban BC**, **Ewer KJ**. 2014. Translating the immunogenicity of prime-boost immunization with ChAd63 and MVA ME-TRAP from malaria naive to malaria-endemic populations. Mol. Ther. **22**:1992–2003.

492. **Ogwang C**, **Kimani D**, **Edwards NJ**, **Roberts R**, **Mwacharo J**, **Bowyer G**, **Bliss C**, **Hodgson SH**, **Njuguna P**, **Viebig NK**, **Nicosia A**, **Gitau E**, **Douglas S**, **Illingworth J**, **Marsh K**, **Lawrie A**, **Imoukhuede EB**, **Ewer K**, **Urban BC**, **Hill AVS**, **Bejon P**, **MVVC group**. 2015. Prime-boost vaccination with chimpanzee adenovirus and modified vaccinia Ankara encoding TRAP provides partial protection against Plasmodium falciparum infection in Kenyan adults. Sci Transl Med **7**:286re5–286re5.

493. **Mensah VA**, **Gueye A**, **Ndiaye M**, **Edwards NJ**, **Wright D**, **Anagnostou NA**, **Syll M**, **Ndaw A**, **Abiola A**, **Bliss C**, **Gomis J-F**, **Petersen I**, **Ogwang C**, **Dieye T**, **Viebig NK**, **Lawrie AM**, **Roberts R**, **Nicosia A**, **Faye B**, **Gaye O**, **Leroy O**, **Imoukhuede EB**, **Ewer KJ**, **Bejon P**, **Hill AVS**, **Cisse B**, **MVVC group**. 2016. Safety, Immunogenicity and Efficacy of Prime-Boost Vaccination with ChAd63 and MVA Encoding ME-TRAP against Plasmodium falciparum Infection in Adults in Senegal. PLoS ONE

11:e0167951.

494. **Afolabi MO**, **Tiono AB**, **Adetifa UJ**, **Yaro JB**, **Drammeh A**, **Nébié I**, **Bliss C**, **Hodgson SH**, **Anagnostou NA**, **Sanou GS**, **Jagne YJ**, **Ouedraogo O**, **Tamara C**, **Ouedraogo N**, **Ouedraogo M**, **Njie-Jobe J**, **Diarra A**, **Duncan CJ**, **Cortese R**, **Nicosia A**, **Roberts R**, **Viebig NK**, **Leroy O**, **Lawrie AM**, **Flanagan KL**, **Kampman B**, **Bejon P**, **Imoukhuede EB**, **Ewer KJ**, **Hill AV**, **Bojang K**, **Sirima SB**. 2016. Safety and Immunogenicity of ChAd63 and MVA ME-TRAP in West African Children and Infants. Mol. Ther. **24**:1470–1477.

495. **Bliss CM**, **Drammeh A**, **Bowyer G**, **Sanou GS**, **Jagne YJ**, **Ouedraogo O**, **Edwards NJ**, **Tarama C**, **Ouedraogo N**, **Ouedraogo M**, **Njie-Jobe J**, **Diarra A**, **Afolabi MO**, **Tiono AB**, **Yaro JB**, **Adetifa UJ**, **Hodgson SH**, **Anagnostou NA**, **Roberts R**, **Duncan CJA**, **Cortese R**, **Viebig NK**, **Leroy O**, **Lawrie AM**, **Flanagan KL**, **Kampmann B**, **Imoukhuede EB**, **Sirima SB**, **Bojang K**, **Hill AVS**, **Nébié I**, **Ewer KJ**. 2017. Viral Vector Malaria Vaccines Induce High-Level T Cell and Antibody Responses in West African Children and Infants. Mol. Ther. **25**:547–559.

496. **Castellanos A**, **Arévalo-Herrera M**, **Restrepo N**, **Gulloso L**, **Corradin G**, **Herrera S**. 2007. Plasmodium vivax thrombospondin related adhesion protein: immunogenicity and protective efficacy in rodents and Aotus monkeys. Mem. Inst. Oswaldo Cruz **102**:411–416.

497. **Bauza K**, **Malinauskas T**, **Pfander C**, **Anar B**, **Jones EY**, **Billker O**, **Hill AVS**, **Reyes-Sandoval A**. 2014. Efficacy of a Plasmodium vivax malaria vaccine using ChAd63 and modified vaccinia Ankara expressing thrombospondin-related anonymous protein as assessed with transgenic Plasmodium berghei parasites. Infect. Immun. **82**:1277–1286.

498. **Spaccapelo R**, **Naitza S**, **Robson KJ**, **Crisanti A**. 1997. Thrombospondin-related adhesive protein (TRAP) of Plasmodium berghei and parasite motility. Lancet **350**:335.

499. **Charoenvit Y**, **Fallarme V**, **Rogers WO**, **Sacci JB**, **Kaur M**, **Aguiar JC**, **Yuan LF**, **Corradin G**, **Andersen E**, **Wizel B**, **Houghten RA**, **Oloo A**, **La Vega De P**, **Hoffman SL**. 1997. Development of two monoclonal antibodies against Plasmodium falciparum sporozoite surface protein 2 and mapping of B-cell epitopes. Infect. Immun. **65**:3430–3437.

500. **Cabral-Miranda G**, **Heath MD**, **Mohsen MO**, **Gomes AC**, **Engeroff P**, **Flaxman A**, **Leoratti FMS**, **El-Turabi A**, **Reyes-Sandoval A**, **Skinner MA**, **Kramer MF**, **Bachmann MF**. 2017. Virus-Like Particle (VLP) Plus Microcrystalline Tyrosine (MCT) Adjuvants Enhance Vaccine Efficacy Improving T and B Cell Immunogenicity and Protection against Plasmodium berghei/vivax. Vaccines (Basel) **5**:10.

501. **Sack B**, **Kappe SHI**, **Sather DN**. 2017. Towards functional antibody-based vaccines to prevent pre-erythrocytic malaria infection. Expert Rev Vaccines **16**:403–414.

502. **Aguiar JC**, **Bolton J**, **Wanga J**, **Sacci JB**, **Iriko H**, **Mazeika JK**, **Han E-T**, **Limbach K**, **Patterson NB**, **Sedegah M**, **Cruz A-M**, **Tsuboi T**, **Hoffman SL**, **Carucci D**, **Hollingdale MR**, **Villasante ED**, **Richie TL**. 2015. Discovery of Novel Plasmodium falciparum Pre-Erythrocytic Antigens for Vaccine Development. PLoS ONE **10**:e0136109.

503. **Peng K**, **Goh YS**, **Siau A**, **Franetich J-F**, **Chia WN**, **Ong ASM**, **Malleret B**, **Wu YY**, **Snounou G**, **Hermsen CC**, **Adams JH**, **Mazier D**, **Preiser PR**, **Sauerwein RW**, **Gruner AC**, **Renia L**. 2016. Breadth of humoral response and antigenic targets of sporozoite-inhibitory antibodies associated with sterile protection induced by controlled human malaria infection. Cell. Microbiol. **18**:1739–1750.

504. **Speake C**, **Pichugin A**, **Sahu T**, **Malkov V**, **Morrison R**, **Pei Y**, **Juompan L**, **Milman N**, **Zarling S**, **Anderson C**, **Wong-Madden S**, **Wendler J**, **Ishizuka A**, **MacMillen ZW**, **Garcia V**, **Kappe SHI**, **Krzych U**, **Duffy PE**. 2016. Identification of Novel Pre-Erythrocytic Malaria Antigen Candidates for Combination Vaccines with Circumsporozoite Protein. PLoS ONE **11**:e0159449.

505. **Longley RJ**, **Salman AM**, **Cottingham MG**, **Ewer K**, **Janse CJ**, **Khan SM**, **Spencer AJ**, **Hill AVS**. 2015. Comparative assessment of vaccine vectors encoding ten malaria antigens identifies two protective liver-stage candidates. Sci Rep **5**:11820.

506. **Limbach K**, **Aguiar J**, **Gowda K**, **Patterson N**, **Abot E**, **Sedegah M**, **Sacci J**, **Richie T**. 2011. Identification of two new protective pre-erythrocytic malaria vaccine

antigen candidates. Malaria Journal **10**:65.
507. **Cha S-J**, **Kim M-S**, **Pandey A**, **Jacobs-Lorena M**. 2016. Identification of GAPDH on the surface of Plasmodium sporozoites as a new candidate for targeting malaria liver invasion. J. Exp. Med. **213**:2099–2112.
508. **Yilmaz B**, **Portugal S**, **Tran TM**, **Gozzelino R**, **Ramos S**, **Gomes J**, **Regalado A**, **Cowan PJ**, **d'Apice AJF**, **Chong AS**, **Doumbo OK**, **Traore B**, **Crompton PD**, **Silveira H**, **Soares MP**. 2014. Gut microbiota elicits a protective immune response against malaria transmission. Cell **159**:1277–1289.
509. **Kariu T**, **Yuda M**, **Yano K**, **Chinzei Y**. 2002. MAEBL is essential for malarial sporozoite infection of the mosquito salivary gland. J. Exp. Med. **195**:1317–1323.
510. **Yang ASP**, **Lopaticki S**, **O'Neill MT**, **Erickson SM**, **Douglas DN**, **Kneteman NM**, **Boddey JA**. 2017. AMA1 and MAEBL are important for Plasmodium falciparum sporozoite infection of the liver. Cell. Microbiol. **19**:e12745.
511. **Leite JA**, **Bargieri DY**, **Carvalho BO**, **Albrecht L**, **Lopes SCP**, **Kayano ACAV**, **Farias AS**, **Chia WN**, **Claser C**, **Malleret B**, **Russell B**, **Castiñeiras C**, **Santos LMB**, **Brocchi M**, **Wunderlich G**, **Soares IS**, **Rodrigues MM**, **Renia L**, **Costa FTM**. 2015. Immunization with the MAEBL M2 Domain Protects against Lethal Plasmodium yoelii Infection. Infect. Immun. **83**:3781–3792.
512. **Kariu T**, **Ishino T**, **Yano K**, **Chinzei Y**, **Yuda M**. 2006. CelTOS, a novel malarial protein that mediates transmission to mosquito and vertebrate hosts. Mol. Microbiol. **59**:1369–1379.
513. **Bergmann-Leitner ES**, **Mease RM**, **la Vega de P**, **Savranskaya T**, **Polhemus M**, **Ockenhouse C**, **Angov E**. 2010. Immunization with pre-erythrocytic antigen CelTOS from Plasmodium falciparum elicits cross-species protection against heterologous challenge with Plasmodium berghei. PLoS ONE **5**:e12294.
514. **Alves E**, **Salman AM**, **Leoratti F**, **Lopez-Camacho C**, **Viveros-Sandoval ME**, **Lall A**, **El-Turabi A**, **Bachmann MF**, **Hill AVS**, **Janse CJ**, **Khan SM**, **Reyes-Sandoval A**. 2017. Evaluation of Plasmodium vivax Cell-Traversal Protein for Ookinetes and Sporozoites as a Preerythrocytic P. vivax Vaccine. Clin. Vaccine Immunol. **24**:e00501–16.
515. **Cummings JF**, **Spring MD**, **Schwenk RJ**, **Ockenhouse CF**, **Kester KE**, **Polhemus ME**, **Walsh DS**, **Yoon I-K**, **Prosperi C**, **Juompan LY**, **Lanar DE**, **Krzych U**, **Hall BT**, **Ware LA**, **Stewart VA**, **Williams J**, **Dowler M**, **Nielsen RK**, **Hillier CJ**, **Giersing BK**, **Dubovsky F**, **Malkin E**, **Tucker K**, **Dubois M-C**, **Cohen JD**, **Ballou WR**, **Heppner DG**. 2010. Recombinant Liver Stage Antigen-1 (LSA-1) formulated with AS01 or AS02 is safe, elicits high titer antibody and induces IFN-gamma/IL-2 CD4+ T cells but does not protect against experimental Plasmodium falciparum infection. Vaccine **28**:5135–5144.
516. **COHEN S**, **McGREGOR IA**, **CARRINGTON S**. 1961. Gamma-globulin and acquired immunity to human malaria. Nature **192**:733–737.
517. **Barnwell JW**, **Asch AS**, **Nachman RL**, **Yamaya M**, **Aikawa M**, **Ingravallo P**. 1989. A human 88-kD membrane glycoprotein (CD36) functions in vitro as a receptor for a cytoadherence ligand on Plasmodium falciparum-infected erythrocytes. J. Clin. Invest. **84**:765–772.
518. **Baruch DI**, **Gamain B**, **Barnwell JW**, **Sullivan JS**, **Stowers A**, **Galland GG**, **Miller LH**, **Collins WE**. 2002. Immunization of Aotus monkeys with a functional domain of the Plasmodium falciparum variant antigen induces protection against a lethal parasite line. Proc. Natl. Acad. Sci. U.S.A. **99**:3860–3865.
519. **Gratepanche S**, **Gamain B**, **Smith JD**, **Robinson BA**, **Saul A**, **Miller LH**. 2003. Induction of crossreactive antibodies against the Plasmodium falciparum variant protein. Proc. Natl. Acad. Sci. U.S.A. **100**:13007–13012.
520. **Patarroyo ME**, **Alba MP**, **Curtidor H**, **Vanegas M**, **Almonacid H**, **Patarroyo MA**. 2014. Using the PfEMP1 head structure binding motif to deal a blow at severe malaria. PLoS ONE **9**:e88420.
521. **Gbédandé K**, **Fievet N**, **Viwami F**, **Ezinmegnon S**, **Issifou S**, **Chippaux J-P**, **Dossou Y**, **Moutairou K**, **Massougbodji A**, **Ndam N**, **de Jongh WA**, **Søgaard TMM**, **Salanti A**, **Nielsen MA**, **Esen M**, **Mordmüller B**, **Deloron P**, **Luty AJF**, **Multi-centre research paper**. 2017. Clinical development of a VAR2CSA-based placental malaria vaccine PAMVAC: Quantifying vaccine antigen-specific memory B & T cell

activity in Beninese primigravidae. Vaccine **35**:3474–3481.
522. **Olugbile S**, **Kulangara C**, **Bang G**, **Bertholet S**, **Suzarte E**, **Villard V**, **Frank G**, **Audran R**, **Razaname A**, **Nebié I**, **Awobusuyi O**, **Spertini F**, **Kajava AV**, **Felger I**, **Druilhe P**, **Corradin G**. 2009. Vaccine potentials of an intrinsically unstructured fragment derived from the blood stage-associated Plasmodium falciparum protein PFF0165c. Infect. Immun. **77**:5701–5709.
523. **Stowers AW**, **Chen Lh L-H**, **Zhang Y**, **Kennedy MC**, **Zou L**, **Lambert L**, **Rice TJ**, **Kaslow DC**, **Saul A**, **Long CA**, **Meade H**, **Miller LH**. 2002. A recombinant vaccine expressed in the milk of transgenic mice protects Aotus monkeys from a lethal challenge with Plasmodium falciparum. Proc. Natl. Acad. Sci. U.S.A. **99**:339–344.
524. **Singh S**, **Miura K**, **Zhou H**, **Muratova O**, **Keegan B**, **Miles A**, **Martin LB**, **Saul AJ**, **Miller LH**, **Long CA**. 2006. Immunity to recombinant plasmodium falciparum merozoite surface protein 1 (MSP1): protection in Aotus nancymai monkeys strongly correlates with anti-MSP1 antibody titer and in vitro parasite-inhibitory activity. Infect. Immun. **74**:4573–4580.
525. **Ogutu BR**, **Apollo OJ**, **McKinney D**, **Okoth W**, **Siangla J**, **Dubovsky F**, **Tucker K**, **Waitumbi JN**, **Diggs C**, **Wittes J**, **Malkin E**, **Leach A**, **Soisson LA**, **Milman JB**, **Otieno L**, **Holland CA**, **Polhemus M**, **Remich SA**, **Ockenhouse CF**, **Cohen J**, **Ballou WR**, **Martin SK**, **Angov E**, **Stewart VA**, **Lyon JA**, **Heppner DG**, **Withers MR**, **MSP-1 Malaria Vaccine Working Group**. 2009. Blood stage malaria vaccine eliciting high antigen-specific antibody concentrations confers no protection to young children in Western Kenya. PLoS ONE **4**:e4708.
526. **Esen M**, **Kremsner PG**, **Schleucher R**, **Gässler M**, **Imoukhuede EB**, **Imbault N**, **Leroy O**, **Jepsen S**, **Knudsen BW**, **Schumm M**, **Knobloch J**, **Theisen M**, **Mordmüller B**. 2009. Safety and immunogenicity of GMZ2 - a MSP3-GLURP fusion protein malaria vaccine candidate. Vaccine **27**:6862–6868.
527. **Sirima SB**, **Tiono AB**, **Ouédraogo A**, **Diarra A**, **Ouédraogo AL**, **Yaro JB**, **Ouédraogo E**, **Gansané A**, **Bougouma EC**, **Konaté AT**, **Kaboré Y**, **Traoré A**, **Chilengi R**, **Roma C**, **Soulama I**, **Luty AJF**, **Druilhe P**, **Cousens S**, **Nébié I**. 2009. Safety and immunogenicity of the malaria vaccine candidate MSP3 long synthetic peptide in 12-24 months-old Burkinabe children. PLoS ONE **4**:e7549.
528. **Sirima SB**, **Cousens S**, **Druilhe P**. 2011. Protection against malaria by MSP3 candidate vaccine. N. Engl. J. Med. **365**:1062–1064.
529. **Sirima SB**, **Mordmüller B**, **Milligan P**, **Ngoa UA**, **Kironde F**, **Atuguba F**, **Tiono AB**, **Issifou S**, **Kaddumukasa M**, **Bangre O**, **Flach C**, **Christiansen M**, **Bang P**, **Chilengi R**, **Jepsen S**, **Kremsner PG**, **Theisen M**, **GMZ2 Trial Study Group**. 2016. A phase 2b randomized, controlled trial of the efficacy of the GMZ2 malaria vaccine in African children. Vaccine **34**:4536–4542.
530. **Thera MA**, **Doumbo OK**, **Coulibaly D**, **Laurens MB**, **Ouattara A**, **Koné AK**, **Guindo AB**, **Traore K**, **Traore I**, **Kouriba B**, **Diallo DA**, **Diarra I**, **Daou M**, **Dolo A**, **Tolo Y**, **Sissoko MS**, **Niangaly A**, **Sissoko M**, **Takala-Harrison S**, **Lyke KE**, **Wu Y**, **Blackwelder WC**, **Godeaux O**, **Vekemans J**, **Dubois M-C**, **Ballou WR**, **Cohen J**, **Thompson D**, **Dube T**, **Soisson L**, **Diggs CL**, **House B**, **Lanar DE**, **Dutta S**, **Heppner DG**, **Plowe CV**. 2011. A field trial to assess a blood-stage malaria vaccine. N. Engl. J. Med. **365**:1004–1013.
531. **Remarque EJ**, **Faber BW**, **Kocken CHM**, **Thomas AW**. 2008. A diversity-covering approach to immunization with Plasmodium falciparum apical membrane antigen 1 induces broader allelic recognition and growth inhibition responses in rabbits. Infect. Immun. **76**:2660–2670.
532. **Kusi KA**, **Remarque EJ**, **Riasat V**, **Walraven V**, **Thomas AW**, **Faber BW**, **Kocken CHM**. 2011. Safety and immunogenicity of multi-antigen AMA1-based vaccines formulated with CoVaccine HT™ and Montanide ISA 51 in rhesus macaques. Malaria Journal **10**:182.
533. **Horii T**, **Shirai H**, **Jie L**, **Ishii KJ**, **Palacpac NQ**, **Tougan T**, **Hato M**, **Ohta N**, **Bobogare A**, **Arakaki N**, **Matsumoto Y**, **Namazue J**, **Ishikawa T**, **Ueda S**, **Takahashi M**. 2010. Evidences of protection against blood-stage infection of Plasmodium falciparum by the novel protein vaccine SE36. Parasitol. Int. **59**:380–386.
534. **Palacpac NMQ**, **Ntege E**, **Yeka A**, **Balikagala B**, **Suzuki N**, **Shirai H**, **Yagi M**, **Ito K**,

Fukushima W, **Hirota Y**, **Nsereko C**, **Okada T**, **Kanoi BN**, **Tetsutani K**, **Arisue N**, **Itagaki S**, **Tougan T**, **Ishii KJ**, **Ueda S**, **Egwang TG**, **Horii T**. 2013. Phase 1b randomized trial and follow-up study in Uganda of the blood-stage malaria vaccine candidate BK-SE36. PLoS ONE **8**:e64073.

535. **Sahly El HM**, **Patel SM**, **Atmar RL**, **Lanford TA**, **Dube T**, **Thompson D**, **Sim BKL**, **Long C**, **Keitel WA**. 2010. Safety and immunogenicity of a recombinant nonglycosylated erythrocyte binding antigen 175 Region II malaria vaccine in healthy adults living in an area where malaria is not endemic. Clin. Vaccine Immunol. **17**:1552–1559.

536. **Koram KA**, **Adu B**, **Ocran J**, **Karikari YS**, **Adu-Amankwah S**, **Ntiri M**, **Abuaku B**, **Dodoo D**, **Gyan B**, **Kronmann KC**, **Nkrumah F**. 2016. Safety and Immunogenicity of EBA-175 RII-NG Malaria Vaccine Administered Intramuscularly in Semi-Immune Adults: A Phase 1, Double-Blinded Placebo Controlled Dosage Escalation Study. PLoS ONE **11**:e0163066.

537. **Grimberg BT**, **Udomsangpetch R**, **Xainli J**, **McHenry A**, **Panichakul T**, **Sattabongkot J**, **Cui L**, **Bockarie M**, **Chitnis C**, **Adams J**, **Zimmerman PA**, **King CL**. 2007. Plasmodium vivax invasion of human erythrocytes inhibited by antibodies directed against the Duffy binding protein. PLoS Med. **4**:e337.

538. **Singh AP**, **Puri SK**, **Chitnis CE**. 2002. Antibodies raised against receptor-binding domain of Plasmodium knowlesi Duffy binding protein inhibit erythrocyte invasion. Mol. Biochem. Parasitol. **121**:21–31.

539. **Payne RO**, **Silk SE**, **Elias SC**, **Milne KH**, **Rawlinson TA**, **Llewellyn D**, **Shakri AR**, **Jin J**, **Labbé GM**, **Edwards NJ**, **Poulton ID**, **Roberts R**, **Farid R**, **Jørgensen T**, **Alanine DG**, **de Cassan SC**, **Higgins MK**, **Otto TD**, **McCarthy JS**, **de Jongh WA**, **Nicosia A**, **Moyle S**, **Hill AV**, **Berrie E**, **Chitnis CE**, **Lawrie AM**, **Draper SJ**. 2017. Human vaccination against Plasmodium vivax Duffy-binding protein induces strain-transcending antibodies. JCI Insight **2**.

540. **Fonseca JA**, **Cabrera-Mora M**, **Singh B**, **Oliveira-Ferreira J**, **da Costa Lima-Junior J**, **Calvo-Calle JM**, **Lozano JM**, **Moreno A**. 2016. A chimeric protein-based malaria vaccine candidate induces robust T cell responses against Plasmodium vivax MSP119. Sci Rep **6**:34527.

541. **Nunes JK**, **Woods C**, **Carter T**, **Raphael T**, **Morin MJ**, **Diallo D**, **Leboulleux D**, **Jain S**, **Loucq C**, **Kaslow DC**, **Birkett AJ**. 2014. Development of a transmission-blocking malaria vaccine: progress, challenges, and the path forward. Vaccine **32**:5531–5539.

542. **Chaturvedi N**, **Bharti PK**, **Tiwari A**, **Singh N**. 2016. Strategies & recent development of transmission-blocking vaccines against Plasmodium falciparum. Indian J. Med. Res. **143**:696–711.

543. **Paul NH**, **Vengesai A**, **Mduluza T**, **Chipeta J**, **Midzi N**, **Bansal GP**, **Kumar N**. 2016. Prevalence of Plasmodium falciparum transmission reducing immunity among primary school children in a malaria moderate transmission region in Zimbabwe. Acta Trop. **163**:103–108.

544. **Theisen M**, **Jore MM**, **Sauerwein R**. 2017. Towards clinical development of a Pfs48/45-based transmission blocking malaria vaccine. Expert Rev Vaccines **16**:329–336.

545. **Outchkourov NS**, **Roeffen W**, **Kaan A**, **Jansen J**, **Luty A**, **Schuiffel D**, **van Gemert G-J**, **van de Vegte-Bolmer M**, **Sauerwein RW**, **Stunnenberg HG**. 2008. Correctly folded Pfs48/45 protein of Plasmodium falciparum elicits malaria transmission-blocking immunity in mice. Proc. Natl. Acad. Sci. U.S.A. **105**:4301–4305.

546. **Chowdhury DR**, **Angov E**, **Kariuki T**, **Kumar N**. 2009. A potent malaria transmission blocking vaccine based on codon harmonized full length Pfs48/45 expressed in Escherichia coli. PLoS ONE **4**:e6352.

547. **Singh SK**, **Thrane S**, **Janitzek CM**, **Nielsen MA**, **Theander TG**, **Theisen M**, **Salanti A**, **Sander AF**. 2017. Improving the malaria transmission-blocking activity of a Plasmodium falciparum 48/45 based vaccine antigen by SpyTag/SpyCatcher mediated virus-like display. Vaccine **35**:3726–3732.

548. **Cao Y**, **Bansal GP**, **Merino K**, **Kumar N**. 2016. Immunological Cross-Reactivity between Malaria Vaccine Target Antigen P48/45 in Plasmodium vivax and P. falciparum and Cross-Boosting of Immune Responses. PLoS ONE **11**:e0158212.

549. **Kumar N**. 1987. Target antigens of malaria transmission blocking immunity exist as a stable membrane bound complex. Parasite Immunol. **9**:321–335.
550. **Williamson KC**, **Keister DB**, **Muratova O**, **Kaslow DC**. 1995. Recombinant Pfs230, a Plasmodium falciparum gametocyte protein, induces antisera that reduce the infectivity of Plasmodium falciparum to mosquitoes. Mol. Biochem. Parasitol. **75**:33–42.
551. **Farrance CE**, **Rhee A**, **Jones RM**, **Musiychuk K**, **Shamloul M**, **Sharma S**, **Mett V**, **Chichester JA**, **Streatfield SJ**, **Roeffen W**, **van de Vegte-Bolmer M**, **Sauerwein RW**, **Tsuboi T**, **Muratova OV**, **Wu Y**, **Yusibov V**. 2011. A plant-produced Pfs230 vaccine candidate blocks transmission of Plasmodium falciparum. Clin. Vaccine Immunol. **18**:1351–1357.
552. **Nikolaeva D**, **Draper SJ**, **Biswas S**. 2015. Toward the development of effective transmission-blocking vaccines for malaria. Expert Rev Vaccines **14**:653–680.
553. **Tomas AM**, **Margos G**, **Dimopoulos G**, **van Lin LH**, **de Koning-Ward TF**, **Sinha R**, **Lupetti P**, **Beetsma AL**, **Rodriguez MC**, **Karras M**, **Hager A**, **Mendoza J**, **Butcher GA**, **Kafatos F**, **Janse CJ**, **Waters AP**, **Sinden RE**. 2001. P25 and P28 proteins of the malaria ookinete surface have multiple and partially redundant functions. EMBO J. **20**:3975–3983.
554. **Kaslow DC**, **Isaacs SN**, **Quakyi IA**, **Gwadz RW**, **Moss B**, **Keister DB**. 1991. Induction of Plasmodium falciparum transmission-blocking antibodies by recombinant vaccinia virus. Science **252**:1310–1313.
555. **Malkin EM**, **Durbin AP**, **Diemert DJ**, **Sattabongkot J**, **Wu Y**, **Miura K**, **Long CA**, **Lambert L**, **Miles AP**, **Wang J**, **Stowers A**, **Miller LH**, **Saul A**. 2005. Phase 1 vaccine trial of Pvs25H: a transmission blocking vaccine for Plasmodium vivax malaria. Vaccine **23**:3131–3138.
556. **Wu Y**, **Ellis RD**, **Shaffer D**, **Fontes E**, **Malkin EM**, **Mahanty S**, **Fay MP**, **Narum D**, **Rausch K**, **Miles AP**, **Aebig J**, **Orcutt A**, **Muratova O**, **Song G**, **Lambert L**, **Zhu D**, **Miura K**, **Long C**, **Saul A**, **Miller LH**, **Durbin AP**. 2008. Phase 1 trial of malaria transmission blocking vaccine candidates Pfs25 and Pvs25 formulated with montanide ISA 51. PLoS ONE **3**:e2636.
557. **Talaat KR**, **Ellis RD**, **Hurd J**, **Hentrich A**, **Gabriel E**, **Hynes NA**, **Rausch KM**, **Zhu D**, **Muratova O**, **Herrera R**, **Anderson C**, **Jones D**, **Aebig J**, **Brockley S**, **MacDonald NJ**, **Wang X**, **Fay MP**, **Healy SA**, **Durbin AP**, **Narum DL**, **Wu Y**, **Duffy PE**. 2016. Safety and Immunogenicity of Pfs25-EPA/Alhydrogel®, a Transmission Blocking Vaccine against Plasmodium falciparum: An Open Label Study in Malaria Naïve Adults. PLoS ONE **11**:e0163144.
558. **McGuire KA**, **Miura K**, **Wiethoff CM**, **Williamson KC**. 2017. New adenovirus-based vaccine vectors targeting Pfs25 elicit antibodies that inhibit Plasmodium falciparum transmission. Malaria Journal **16**:254.
559. **Dinglasan RR**, **Kalume DE**, **Kanzok SM**, **Ghosh AK**, **Muratova O**, **Pandey A**, **Jacobs-Lorena M**. 2007. Disruption of Plasmodium falciparum development by antibodies against a conserved mosquito midgut antigen. Proc. Natl. Acad. Sci. U.S.A. **104**:13461–13466.
560. **Armistead JS**, **Morlais I**, **Mathias DK**, **Jardim JG**, **Joy J**, **Fridman A**, **Finnefrock AC**, **Bagchi A**, **Plebanski M**, **Scorpio DG**, **Churcher TS**, **Borg NA**, **Sattabongkot J**, **Dinglasan RR**. 2014. Antibodies to a single, conserved epitope in Anopheles APN1 inhibit universal transmission of Plasmodium falciparum and Plasmodium vivax malaria. Infect. Immun. **82**:818–829.
561. **Rogers WO**, **Baird JK**, **Kumar A**, **Tine JA**, **Weiss W**, **Aguiar JC**, **Gowda K**, **Gwadz R**, **Kumar S**, **Gold M**, **Hoffman SL**. 2001. Multistage multiantigen heterologous prime boost vaccine for Plasmodium knowlesi malaria provides partial protection in rhesus macaques. Infect. Immun. **69**:5565–5572.
562. **Jiang G**, **Charoenvit Y**, **Moreno A**, **Baraceros MF**, **Banania G**, **Richie N**, **Abot S**, **Ganeshan H**, **Fallarme V**, **Patterson NB**, **Geall A**, **Weiss WR**, **Strobert E**, **Caro-Aquilar I**, **Lanar DE**, **Saul A**, **Martin LB**, **Gowda K**, **Morrissette CR**, **Kaslow DC**, **Carucci DJ**, **Galinski MR**, **Doolan DL**. 2007. Induction of multi-antigen multi-stage immune responses against Plasmodium falciparum in rhesus monkeys, in the absence of antigen interference, with heterologous DNA prime/poxvirus boost immunization. Malaria Journal **6**:135.

563. **Sedegah M**, **Rogers WO**, **Belmonte M**, **Belmonte A**, **Banania G**, **Patterson NB**, **Rusalov D**, **Ferrari M**, **Richie TL**, **Doolan DL**. 2010. Vaxfectin enhances both antibody and in vitro T cell responses to each component of a 5-gene Plasmodium falciparum plasmid DNA vaccine mixture administered at low doses. Vaccine **28**:3055–3065.

564. **Ferraro B**, **Talbott KT**, **Balakrishnan A**, **Cisper N**, **Morrow MP**, **Hutnick NA**, **Myles DJ**, **Shedlock DJ**, **Obeng-Adjei N**, **Yan J**, **Kayatani AKK**, **Richie N**, **Cabrera W**, **Shiver R**, **Khan AS**, **Brown AS**, **Yang M**, **Wille-Reece U**, **Birkett AJ**, **Sardesai NY**, **Weiner DB**. 2013. Inducing humoral and cellular responses to multiple sporozoite and liver-stage malaria antigens using exogenous plasmid DNA. Infect. Immun. **81**:3709–3720.

565. **Kester KE**, **Gray Heppner D**, **Moris P**, **Ofori-Anyinam O**, **Krzych U**, **Tornieporth N**, **McKinney D**, **Delchambre M**, **Ockenhouse CF**, **Voss G**, **Holland C**, **Beckey JP**, **Ballou WR**, **Cohen J**, **RTS,S/TRAP Group**. 2014. Sequential Phase 1 and Phase 2 randomized, controlled trials of the safety, immunogenicity and efficacy of combined pre-erythrocytic vaccine antigens RTS,S and TRAP formulated with AS02 Adjuvant System in healthy, malaria naïve adults. Vaccine **32**:6683–6691.

566. **Bauza K**, **Erwan Erwan**, **Malinauskas T**, **Blagborough AM**, **Reyes-Sandoval A**. 2016. Tailoring a Combination Preerythrocytic Malaria Vaccine. Infect. Immun. **84**:622–634.

567. **Rampling T**, **Ewer KJ**, **Bowyer G**, **Bliss CM**, **Edwards NJ**, **Wright D**, **Payne R**, **Venkatraman N**, **de Barra E**, **Snudden CM**, **Poulton ID**, **de Graaf H**, **Sukhtankar P**, **Roberts R**, **Ivinson K**, **Weltzin R**, **Rajkumar B-Y**, **Wille-Reece U**, **Lee C**, **Ockenhouse C**, **Sinden RE**, **Gerry S**, **Lawrie AM**, **Vekemans J**, **Morelle D**, **Lievens M**, **Ballou RW**, **Cooke GS**, **Faust SN**, **Gilbert S**, **Hill AVS**. 2016. Safety and High Level Efficacy of the Combination Malaria Vaccine Regimen of RTS,S/AS01B with ChAd-MVA Vectored Vaccines Expressing ME-TRAP. J. Infect. Dis. jiw244.

568. **Pichyangkul S**, **Tongtawe P**, **Kum-Arb U**, **Yongvanitchit K**, **Gettayacamin M**, **Hollingdale MR**, **Limsalakpetch A**, **Stewart VA**, **Lanar DE**, **Dutta S**, **Angov E**, **Ware LA**, **Bergmann-Leitner ES**, **House B**, **Voss G**, **Dubois MC**, **Cohen JD**, **Fukuda MM**, **Heppner DG**, **Miller RS**. 2009. Evaluation of the safety and immunogenicity of Plasmodium falciparum apical membrane antigen 1, merozoite surface protein 1 or RTS,S vaccines with adjuvant system AS02A administered alone or concurrently in rhesus monkeys. Vaccine **28**:452–462.

569. **Porter DW**, **Thompson FM**, **Berthoud TK**, **Hutchings CL**, **Andrews L**, **Biswas S**, **Poulton I**, **Prieur E**, **Correa S**, **Rowland R**, **Lang T**, **Williams J**, **Gilbert SC**, **Sinden RE**, **Todryk S**, **Hill AVS**. 2011. A human Phase I/IIa malaria challenge trial of a polyprotein malaria vaccine. Vaccine **29**:7514–7522.

570. **Forbes EK**, **Biswas S**, **Collins KA**, **Gilbert SC**, **Hill AVS**, **Draper SJ**. 2011. Combining liver- and blood-stage malaria viral-vectored vaccines: investigating mechanisms of CD8+ T cell interference. J. Immunol. **187**:3738–3750.

571. **Kedzierski L**, **Black CG**, **Goschnick MW**, **Stowers AW**, **Coppel RL**. 2002. Immunization with a combination of merozoite surface proteins 4/5 and 1 enhances protection against lethal challenge with Plasmodium yoelii. Infect. Immun. **70**:6606–6613.

572. **Williams AR**, **Douglas AD**, **Miura K**, **Illingworth JJ**, **Choudhary P**, **Murungi LM**, **Furze JM**, **Diouf A**, **Miotto O**, **Crosnier C**, **Wright GJ**, **Kwiatkowski DP**, **Fairhurst RM**, **Long CA**, **Draper SJ**. 2012. Enhancing blockade of Plasmodium falciparum erythrocyte invasion: assessing combinations of antibodies against PfRH5 and other merozoite antigens. PLoS Pathog. **8**:e1002991.

573. **Favuzza P**, **Guffart E**, **Tamborrini M**, **Scherer B**, **Dreyer AM**, **Rufer AC**, **Erny J**, **Hoernschemeyer J**, **Thoma R**, **Schmid G**, **Gsell B**, **Lamelas A**, **Benz J**, **Joseph C**, **Matile H**, **Pluschke G**, **Rudolph MG**. 2017. Structure of the malaria vaccine candidate antigen CyRPA and its complex with a parasite invasion inhibitory antibody. Elife **6**:213.

574. **Pandey AK**, **Reddy KS**, **Sahar T**, **Gupta S**, **Singh H**, **Reddy EJ**, **Asad M**, **Siddiqui FA**, **Gupta P**, **Singh B**, **More KR**, **Mohmmed A**, **Chitnis CE**, **Chauhan VS**, **Gaur D**. 2013. Identification of a potent combination of key Plasmodium falciparum merozoite antigens that elicit strain-transcending parasite-neutralizing antibodies.

Infect. Immun. **81**:441–451.
575. **Reddy KS**, **Pandey AK**, **Singh H**, **Sahar T**, **Emmanuel A**, **Chitnis CE**, **Chauhan VS**, **Gaur D**. 2014. Bacterially expressed full-length recombinant Plasmodium falciparum RH5 protein binds erythrocytes and elicits potent strain-transcending parasite-neutralizing antibodies. Infect. Immun. **82**:152–164.
576. **Mazumdar S**, **Mukherjee P**, **Yazdani SS**, **Jain SK**, **Mohmmed A**, **Chauhan VS**. 2010. Plasmodium falciparum merozoite surface protein 1 (MSP-1)-MSP-3 chimeric protein: immunogenicity determined with human-compatible adjuvants and induction of protective immune response. Infect. Immun. **78**:872–883.
577. **Kalra A**, **Edula JR**, **Gupta PK**, **Pandey AK**, **Chauhan VS**. 2016. Antigenicity of a Bacterially Expressed Triple Chimeric Antigen of Plasmodium falciparum AARP, MSP-311 and MSP-119: PfAMSP-Fu35. PLoS ONE **11**:e0165720.
578. **Malkin E**, **Hu J**, **Li Z**, **Chen Z**, **Bi X**, **Reed Z**, **Dubovsky F**, **Liu J**, **Wang Q**, **Pan X**, **Chen T**, **Giersing B**, **Xu Y**, **Kang X**, **Gu J**, **Shen Q**, **Tucker K**, **Tierney E**, **Pan W**, **Long C**, **Cao Z**. 2008. A phase 1 trial of PfCP2.9: an AMA1/MSP1 chimeric recombinant protein vaccine for Plasmodium falciparum malaria. Vaccine **26**:6864–6873.
579. **Zheng L**, **Pang W**, **Qi Z**, **Luo E**, **Cui L**, **Cao Y**. 2016. Effects of transmission-blocking vaccines simultaneously targeting pre- and post-fertilization antigens in the rodent malaria parasite Plasmodium yoelii. Parasit Vectors **9**:433.
580. **Datta D**, **Bansal GP**, **Gerloff DL**, **Ellefsen B**, **Hannaman D**, **Kumar N**. 2017. Immunogenicity and malaria transmission reducing potency of Pfs48/45 and Pfs25 encoded by DNA vaccines administered by intramuscular electroporation. Vaccine **35**:264–272.
581. **Roeffen W**, **Theisen M**, **van de Vegte-Bolmer M**, **van Gemert G**, **Arens T**, **Andersen G**, **Christiansen M**, **Sevargave L**, **Singh SK**, **Kaviraj S**, **Sauerwein R**. 2015. Transmission-blocking activity of antibodies to Plasmodium falciparum GLURP.10C chimeric protein formulated in different adjuvants. Malaria Journal **14**:443.
582. **Wykes MN**, **Good MF**. 2009. What have we learnt from mouse models for the study of malaria? Eur. J. Immunol. **39**:2004–2007.
583. **Vincke IH**, **Lips M**. 1948. Un nouveau plasmodium d'un rongeur sauvage du Congo: P. berghei. Ann. Soc. Beige Med. Trop.
584. **Yoeli M**, **Most H**. 1965. Studies on Sporozoite-Induced Infections of Rodent Malaria. Am. J. Trop. Med. Hyg. **14**:700–714.
585. **Nussenzweig R**, **Herman R**, **Vanderberg J**, **Yoeli M**, **Most H**. 1966. Studies on sporozoite-induced infections of rodent malaria. 3. The course of sporozoite-induced Plasmodium berghei in different hosts. Am. J. Trop. Med. Hyg. **15**:684–689.
586. **van Dijk MR**, **Waters AP**, **Janse CJ**. 1995. Stable transfection of malaria parasite blood stages. Science **268**:1358–1362.
587. **van Dijk MR**, **Janse CJ**, **Waters AP**. 1996. Expression of a Plasmodium gene introduced into subtelomeric regions of Plasmodium berghei chromosomes. Science **271**:662–665.
588. **Kocken CH**, **van der Wel AM**, **Dubbeld MA**, **Narum DL**, **van de Rijke FM**, **van Gemert GJ**, **van der Linde X**, **Bannister LH**, **Janse C**, **Waters AP**, **Thomas AW**. 1998. Precise timing of expression of a Plasmodium falciparum-derived transgene in Plasmodium berghei is a critical determinant of subsequent subcellular localization. J. Biol. Chem. **273**:15119–15124.
589. **Janse CJ**, **Ramesar J**, **Waters AP**. 2006. High-efficiency transfection and drug selection of genetically transformed blood stages of the rodent malaria parasite Plasmodium berghei. Nat Protoc **1**:346–356.
590. **Persson C**, **Oliveira GA**, **Sultan AA**, **Bhanot P**, **Nussenzweig V**, **Nardin E**. 2002. Cutting edge: a new tool to evaluate human pre-erythrocytic malaria vaccines: rodent parasites bearing a hybrid Plasmodium falciparum circumsporozoite protein. J. Immunol. **169**:6681–6685.
591. **Wengelnik K**, **Spaccapelo R**, **Naitza S**, **Robson KJ**, **Janse CJ**, **Bistoni F**, **Waters AP**, **Crisanti A**. 1999. The A-domain and the thrombospondin-related motif of Plasmodium falciparum TRAP are implicated in the invasion process of mosquito salivary glands. EMBO J. **18**:5195–5204.

592. **Mlambo G**, **Maciel J**, **Kumar N**. 2008. Murine model for assessment of Plasmodium falciparum transmission-blocking vaccine using transgenic Plasmodium berghei parasites expressing the target antigen Pfs25. Infect. Immun. **76**:2018–2024.
593. **Ramjanee S**, **Robertson JS**, **Franke-Fayard B**, **Sinha R**, **Waters AP**, **Janse CJ**, **Wu Y**, **Blagborough AM**, **Saul A**, **Sinden RE**. 2007. The use of transgenic Plasmodium berghei expressing the Plasmodium vivax antigen P25 to determine the transmission-blocking activity of sera from malaria vaccine trials. Vaccine **25**:886–894.
594. **Tewari R**, **Spaccapelo R**, **Bistoni F**, **Holder AA**, **Crisanti A**. 2002. Function of region I and II adhesive motifs of Plasmodium falciparum circumsporozoite protein in sporozoite motility and infectivity. J. Biol. Chem. **277**:47613–47618.
595. **Ploemen IHJ**, **Prudêncio M**, **Douradinha BG**, **Ramesar J**, **Fonager J**, **van Gemert G-J**, **Luty AJF**, **Hermsen CC**, **Sauerwein RW**, **Baptista FG**, **Mota MM**, **Waters AP**, **Que I**, **Lowik CWGM**, **Khan SM**, **Janse CJ**, **Franke-Fayard BMD**. 2009. Visualisation and quantitative analysis of the rodent malaria liver stage by real time imaging. PLoS ONE **4**:e7881.
596. **Gomes-Santos CSS**, **Itoe MA**, **Afonso C**, **Henriques R**, **Gardner R**, **Sepúlveda N**, **Simões PD**, **Raquel H**, **Almeida AP**, **Moita LF**, **Frischknecht F**, **Mota MM**. 2012. Highly dynamic host actin reorganization around developing Plasmodium inside hepatocytes. PLoS ONE **7**:e29408.
597. **Zuzarte-Luis V**, **Sales-Dias J**, **Mota MM**. 2014. Simple, sensitive and quantitative bioluminescence assay for determination of malaria pre-patent period. Malaria Journal **13**:15.
598. **Aldrich C**, **Magini A**, **Emiliani C**, **Dottorini T**, **Bistoni F**, **Crisanti A**, **Spaccapelo R**. 2012. Roles of the amino terminal region and repeat region of the Plasmodium berghei circumsporozoite protein in parasite infectivity. PLoS ONE **7**:e32524.
599. **Mestas J**, **Hughes CCW**. 2004. Of mice and not men: differences between mouse and human immunology. J. Immunol. **172**:2731–2738.
600. **Butler NS**, **Schmidt NW**, **Harty JT**. 2010. Differential effector pathways regulate memory CD8 T cell immunity against Plasmodium berghei versus P. yoelii sporozoites. J. Immunol. **184**:2528–2538.
601. **Zuzarte-Luis V**, **Mota MM**, **Vigário AM**. 2014. Malaria infections: what and how can mice teach us. J. Immunol. Methods **410**:113–122.
602. **Kaushansky A**, **Mikolajczak SA**, **Vignali M**, **Kappe SHI**. 2014. Of men in mice: the success and promise of humanized mouse models for human malaria parasite infections. Cell. Microbiol. **16**:602–611.
603. **Mikolajczak SA**, **Vaughan AM**, **Kangwanrangsan N**, **Roobsoong W**, **Fishbaugher M**, **Yimamnuaychok N**, **Rezakhani N**, **Lakshmanan V**, **Singh N**, **Kaushansky A**, **Camargo N**, **Baldwin M**, **Lindner SE**, **Adams JH**, **Sattabongkot J**, **Prachumsri J**, **Kappe SHI**. 2015. Plasmodium vivax liver stage development and hypnozoite persistence in human liver-chimeric mice. Cell Host Microbe **17**:526–535.
604. **Sack BK**, **Miller JL**, **Vaughan AM**, **Douglass A**, **Kaushansky A**, **Mikolajczak S**, **Coppi A**, **Gonzalez-Aseguinolaza G**, **Tsuji M**, **Zavala F**, **Sinnis P**, **Kappe SHI**. 2014. Model for in vivo assessment of humoral protection against malaria sporozoite challenge by passive transfer of monoclonal antibodies and immune serum. Infect. Immun. **82**:808–817.
605. **Moore AC**, **Gallimore A**, **Draper SJ**, **Watkins KR**, **Gilbert SC**, **Hill AVS**. 2005. Anti-CD25 antibody enhancement of vaccine-induced immunogenicity: increased durable cellular immunity with reduced immunodominance. J. Immunol. **175**:7264–7273.
606. **Grangeot-Keros L**, **Mayaux MJ**, **Lebon P**, **Freymuth F**, **Eugene G**, **Stricker R**, **Dussaix E**. 1997. Value of cytomegalovirus (CMV) IgG avidity index for the diagnosis of primary CMV infection in pregnant women. J. Infect. Dis. **175**:944–946.
607. **RUSSELL ES**, **NEUFELD EF**, **HIGGINS CT**. 1951. Comparison of normal blood picture of young adults from 18 inbred strains of mice. Proc. Soc. Exp. Biol. Med. **78**:761–766.
608. **Aricescu AR**, **Lu W**, **Jones EY**. 2006. A time- and cost-efficient system for high-level protein production in mammalian cells. Acta Crystallogr. D Biol. Crystallogr. **62**:1243–1250.

609. **Swearingen KE**, **Lindner SE**, **Shi L**, **Shears MJ**, **Harupa A**, **Hopp CS**, **Vaughan AM**, **Springer TA**, **Moritz RL**, **Kappe SHI**, **Sinnis P**. 2016. Interrogating the Plasmodium Sporozoite Surface: Identification of Surface-Exposed Proteins and Demonstration of Glycosylation on CSP and TRAP by Mass Spectrometry-Based Proteomics. PLoS Pathog. **12**:e1005606.
610. **Chakraborty AK**. 2017. A Perspective on the Role of Computational Models in Immunology. Annu. Rev. Immunol. **35**:403–439.
611. **Saul A**. 2008. Efficacy model for mosquito stage transmission blocking vaccines for malaria. Parasitology **135**:1497–1506.
612. **Saul A**, **Fay MP**. 2007. Human immunity and the design of multi-component, single target vaccines. PLoS ONE **2**:e850.
613. **White MT**, **Griffin JT**, **Riley EM**, **Drakeley CJ**, **Moorman AM**, **Sumba PO**, **Kazura JW**, **Ghani AC**, **John CC**. 2011. Efficacy model for antibody-mediated pre-erythrocytic malaria vaccines. Proc. Biol. Sci. **278**:1298–1305.
614. **White MT**, **Bejon P**, **Olotu A**, **Griffin JT**, **Riley EM**, **Kester KE**, **Ockenhouse CF**, **Ghani AC**. 2013. The relationship between RTS,S vaccine-induced antibodies, $CD4^+$ T cell responses and protection against Plasmodium falciparum infection. PLoS ONE **8**:e61395.
615. **Walker AS**, **Lourenço J**, **Hill AVS**, **Gupta S**. 2015. Modeling Combinations of Pre-erythrocytic Plasmodium falciparum Malaria Vaccines. Am. J. Trop. Med. Hyg. **93**:1254–1259.
616. **Churcher TS**, **Sinden RE**, **Edwards NJ**, **Poulton ID**, **Rampling TW**, **Brock PM**, **Griffin JT**, **Upton LM**, **Zakutansky SE**, **Sala KA**, **Angrisano F**, **Hill AVS**, **Blagborough AM**. 2017. Probability of Transmission of Malaria from Mosquito to Human Is Regulated by Mosquito Parasite Density in Naïve and Vaccinated Hosts. PLoS Pathog. **13**:e1006108.
617. **Bejon P**, **Andrews L**, **Andersen RF**, **Dunachie S**, **Webster D**, **Walther M**, **Gilbert SC**, **Peto T**, **Hill AVS**. 2005. Calculation of liver-to-blood inocula, parasite growth rates, and preerythrocytic vaccine efficacy, from serial quantitative polymerase chain reaction studies of volunteers challenged with malaria sporozoites. J. Infect. Dis. **191**:619–626.
618. **Douglas AD**, **Edwards NJ**, **Duncan CJA**, **Thompson FM**, **Sheehy SH**, **O'Hara GA**, **Anagnostou N**, **Walther M**, **Webster DP**, **Dunachie SJ**, **Porter DW**, **Andrews L**, **Gilbert SC**, **Draper SJ**, **Hill AVS**, **Bejon P**. 2013. Comparison of modeling methods to determine liver-to-blood inocula and parasite multiplication rates during controlled human malaria infection. J. Infect. Dis. **208**:340–345.
619. **Hoshen MB**, **Heinrich R**, **Stein WD**, **Ginsburg H**. 2000. Mathematical modelling of the within-host dynamics of Plasmodium falciparum. Parasitology **121 (Pt 3)**:227–235.
620. **Simpson JA**, **Aarons L**, **Collins WE**, **Jeffery GM**, **White NJ**. 2002. Population dynamics of untreated Plasmodium falciparum malaria within the adult human host during the expansion phase of the infection. Parasitology **124**:247–263.
621. **Anderson RM**, **May RM**, **Gupta S**. 1989. Non-linear phenomena in host-parasite interactions. Parasitology **99 Suppl**:S59–79.
622. **Pinkevych M**, **Petravic J**, **Chelimo K**, **Vulule J**, **Kazura JW**, **Moormann AM**, **Davenport MP**. 2014. Decreased growth rate of P. falciparum blood stage parasitemia with age in a holoendemic population. J. Infect. Dis. **209**:1136–1143.
623. **Pinkevych M**, **Petravic J**, **Bereczky S**, **Rooth I**, **Färnert A**, **Davenport MP**. 2015. Understanding the relationship between Plasmodium falciparum growth rate and multiplicity of infection. J. Infect. Dis. **211**:1121–1127.
624. **Saul A**. 1998. Models for the in-host dynamics of malaria revisited: errors in some basic models lead to large over-estimates of growth rates. Parasitology **117 (Pt 5)**:405–7– discussion 409–10.
625. **Kwiatkowski D**, **Nowak M**. 1991. Periodic and chaotic host-parasite interactions in human malaria. Proc. Natl. Acad. Sci. U.S.A. **88**:5111–5113.
626. **Gravenor MB**, **van Hensbroek MB**, **Kwiatkowski D**. 1998. Estimating sequestered parasite population dynamics in cerebral malaria. Proc. Natl. Acad. Sci. U.S.A. **95**:7620–7624.
627. **Hermsen CC**, **de Vlas SJ**, **van Gemert GJA**, **Telgt DSC**, **Verhage DF**, **Sauerwein**

RW. 2004. Testing vaccines in human experimental malaria: statistical analysis of parasitemia measured by a quantitative real-time polymerase chain reaction. Am. J. Trop. Med. Hyg. **71**:196–201.
628. **Howell KA**, **Brannan JM**, **Bryan C**, **McNeal A**, **Davidson E**, **Turner HL**, **Vu H**, **Shulenin S**, **He S**, **Kuehne A**, **Herbert AS**, **Qiu X**, **Doranz BJ**, **Holtsberg FW**, **Ward AB**, **Dye JM**, **Aman MJ**. 2017. Cooperativity Enables Non-neutralizing Antibodies to Neutralize Ebolavirus. Cell Rep **19**:413–424.
629. **Janse CJ**, **Waters AP**. 1995. Plasmodium berghei: the application of cultivation and purification techniques to molecular studies of malaria parasites. Parasitol. Today (Regul. Ed.) **11**:138–143.
630. **Spencer AJ**, **Longley RJ**, **Gola A**, **Ulaszewska M**, **Lambe T**, **Hill AVS**. 2017. The Threshold of Protection from Liver-Stage Malaria Relies on a Fine Balance between the Number of Infected Hepatocytes and Effector CD8(+) T Cells Present in the Liver. J. Immunol. **198**:2006–2016.
631. **Matz JM**, **Matuschewski K**, **Kooij TWA**. 2013. Two putative protein export regulators promote Plasmodium blood stage development in vivo. Mol. Biochem. Parasitol. **191**:44–52.
632. **Spaccapelo R**, **Janse CJ**, **Caterbi S**, **Franke-Fayard B**, **Bonilla JA**, **Syphard LM**, **Di Cristina M**, **Dottorini T**, **Savarino A**, **Cassone A**, **Bistoni F**, **Waters AP**, **Dame JB**, **Crisanti A**. 2010. Plasmepsin 4-deficient Plasmodium berghei are virulence attenuated and induce protective immunity against experimental malaria. Am. J. Pathol. **176**:205–217.
633. **Gibbons PL**, **Batty KT**, **Barrett PHR**, **Davis TME**, **Ilett KF**. 2007. Development of a pharmacodynamic model of murine malaria and antimalarial treatment with dihydroartemisinin. Int. J. Parasitol. **37**:1569–1576.
634. **Khoury DS**, **Cromer D**, **Best SE**, **James KR**, **Sebina I**, **Haque A**, **Davenport MP**. 2015. Reduced erythrocyte susceptibility and increased host clearance of young parasites slows Plasmodium growth in a murine model of severe malaria. Sci Rep **5**:9412.
635. **Cromer D**, **Best SE**, **Engwerda C**, **Haque A**, **Davenport M**. 2013. Where have all the parasites gone? Modelling early malaria parasite sequestration dynamics. PLoS ONE **8**:e55961.
636. **Murray L**, **Stewart LB**, **Tarr SJ**, **Ahouidi AD**, **Diakite M**, **Amambua-Ngwa A**, **Conway DJ**. 2017. Multiplication rate variation in the human malaria parasite Plasmodium falciparum. Sci Rep **7**:6436.
637. **Scheller LF**, **Wirtz RA**, **Azad AF**. 1994. Susceptibility of different strains of mice to hepatic infection with Plasmodium berghei. Infect. Immun. **62**:4844–4847.
638. **Vanderberg JP**. 1977. Plasmodium berghei: quantitation of sporozoites injected by mosquitoes feeding on a rodent host. Exp. Parasitol. **42**:169–181.
639. **Chatterjee S**, **Ngonseu E**, **Druilhe P**, **Van Marck E**. 2004. Improved quantification of Plasmodium exoerythrocytic forms in rodents. Parasitol. Res. **92**:459–463.
640. **Verhave JP**, **Meis JF**, **De Boo TM**, **Meuwissen JH**. 1985. The delivery of exoerythrocytic parasites of Plasmodium berghei: a hormone controlled process. Ann Soc Belg Med Trop **65 Suppl 2**:35–44.
641. **Frevert U**. 2004. Sneaking in through the back entrance: the biology of malaria liver stages. Trends Parasitol. **20**:417–424.
642. **Hegge S**, **Kudryashev M**, **Barniol L**, **Frischknecht F**. 2010. Key factors regulating Plasmodium berghei sporozoite survival and transformation revealed by an automated visual assay. FASEB J. **24**:5003–5012.
643. **Ashley EA**, **Recht J**, **White NJ**. 2014. Primaquine: the risks and the benefits. Malaria Journal **13**:418.
644. **Sjölander A**, **Ahlborg N**, **Ståhl S**, **Andersson R**. 1998. Characterization of immune responses to experimental polyvalent subunit vaccines assembled in iscoms. Mol. Immunol. **35**:159–166.
645. **Wang X**, **Mu G**, **Dang R**, **Yang Z**. 2016. Up-regulation of IL-10 upon PRRSV vaccination impacts on the immune response against CSFV. Vet. Microbiol. **197**:68–71.
646. **Rao KV**. 1999. Selection in a T-dependent primary humoral response: new insights from polypeptide models. APMIS **107**:807–818.

647. **Prieur E**, **Gilbert SC**, **Schneider J**, **Moore AC**, **Sheu EG**, **Goonetilleke N**, **Robson KJH**, **Hill AVS**. 2004. A Plasmodium falciparum candidate vaccine based on a six-antigen polyprotein encoded by recombinant poxviruses. Proc. Natl. Acad. Sci. U.S.A. **101**:290–295.
648. **Samuel CE**. 2001. Antiviral actions of interferons. Clin. Microbiol. Rev. **14**:778–809– table of contents.
649. **Snapper CM**, **Paul WE**. 1987. Interferon-gamma and B cell stimulatory factor-1 reciprocally regulate Ig isotype production. Science **236**:944–947.
650. **Finkelman FD**, **Holmes J**, **Katona IM**, **Urban JF**, **Beckmann MP**, **Park LS**, **Schooley KA**, **Coffman RL**, **Mosmann TR**, **Paul WE**. 1990. Lymphokine control of in vivo immunoglobulin isotype selection. Annu. Rev. Immunol. **8**:303–333.
651. **Seguin MC**, **Ballou WR**, **Nacy CA**. 1989. Interactions of Plasmodium berghei sporozoites and murine Kupffer cells in vitro. J. Immunol. **143**:1716–1722.
652. **Schwenk R**, **Asher LV**, **Chalom I**, **Lanar D**, **Sun P**, **White K**, **Keil D**, **Kester KE**, **Stoute J**, **Heppner DG**, **Krzych U**. 2003. Opsonization by antigen-specific antibodies as a mechanism of protective immunity induced by Plasmodium falciparum circumsporozoite protein-based vaccine. Parasite Immunol. **25**:17–25.
653. **Chaudhury S**, **Regules JA**, **Darko CA**, **Dutta S**, **Wallqvist A**, **Waters NC**, **Jongert E**, **Lemiale F**, **Bergmann-Leitner ES**. 2017. Delayed fractional dose regimen of the RTS,S/AS01 malaria vaccine candidate enhances an IgG4 response that inhibits serum opsonophagocytosis. Sci Rep **7**:7998.
654. **Hill AVS**. 2011. Vaccines against malaria. Philos. Trans. R. Soc. Lond., B, Biol. Sci. **366**:2806–2814.
655. **Okitsu SL**, **Silvie O**, **Westerfeld N**, **Curcic M**, **Kammer AR**, **Mueller MS**, **Sauerwein RW**, **Robinson JA**, **Genton B**, **Mazier D**, **Zurbriggen R**, **Pluschke G**. 2007. A virosomal malaria peptide vaccine elicits a long-lasting sporozoite-inhibitory antibody response in a phase 1a clinical trial. PLoS ONE **2**:e1278.
656. **Genton B**, **Pluschke G**, **Degen L**, **Kammer AR**, **Westerfeld N**, **Okitsu SL**, **Schroller S**, **Vounatsou P**, **Mueller MM**, **Tanner M**, **Zurbriggen R**. 2007. A randomized placebo-controlled phase Ia malaria vaccine trial of two virosome-formulated synthetic peptides in healthy adult volunteers. PLoS ONE **2**:e1018.
657. **Parra-López CA**, **Bernal-Estévez D**, **Yin L**, **Vargas LE**, **Pulido-Calixto C**, **Salazar LM**, **Calvo-Calle JM**, **Stern LJ**. 2014. An unstable Th epitope of P. falciparum fosters central memory T cells and anti-CS antibody responses. PLoS ONE **9**:e100639.
658. **Porter MD**, **Nicki J**, **Pool CD**, **DeBot M**, **Illam RM**, **Brando C**, **Bozick B**, **la Vega de P**, **Angra D**, **Spaccapelo R**, **Crisanti A**, **Murphy JR**, **Bennett JW**, **Schwenk RJ**, **Ockenhouse CF**, **Dutta S**. 2013. Transgenic parasites stably expressing full-length Plasmodium falciparum circumsporozoite protein as a model for vaccine down-selection in mice using sterile protection as an endpoint. Clin. Vaccine Immunol. **20**:803–810.
659. **Valmori D**, **Pessi A**, **Bianchi E**, **Corradin G**. 1992. Use of human universally antigenic tetanus toxin T cell epitopes as carriers for human vaccination. J. Immunol. **149**:717–721.
660. **Udhayakumar V**, **Saekhou A**, **Fang S**, **Jue D**, **Wohlhueter RM**, **Lal AA**. 1998. Immunogenicity of Plasmodium falciparum and Plasmodium vivax circumsporozoite protein repeat multiple antigen constructs (MAC). Vaccine **16**:982–988.
661. **Moon JJ**, **Suh H**, **Polhemus ME**, **Ockenhouse CF**, **Yadava A**, **Irvine DJ**. 2012. Antigen-displaying lipid-enveloped PLGA nanoparticles as delivery agents for a Plasmodium vivax malaria vaccine. PLoS ONE **7**:e31472.
662. **Patra AP**, **Sharma S**, **Ainavarapu S**. 2017. Force spectroscopy of the Plasmodium falciparum vaccine candidate circumsporozoite protein suggests a mechanically pliable repeat region. Journal of Biological Chemistry.
663. **Etlinger HM**, **Trzeciak A**. 1993. Towards a synthetic malaria vaccine: cyclization of a peptide eliminates the production of parasite-unreactive antibody. Philos. Trans. R. Soc. Lond., B, Biol. Sci. **340**:69–72.
664. **Christian Bisang**, **Luyong Jiang**, **Ernst Freund**, **Fabienne Emery**, **Christian Bauch**, **Hugues Matile**, **Gerd Pluschke A**, **John A Robinson**. 1998. Synthesis, Conformational Properties, and Immunogenicity of a Cyclic Template-Bound

Peptide Mimetic Containing an NPNA Motif from the Circumsporozoite Protein of Plasmodium falciparumJournal of the American Chemical Society. American Chemical Society.
665. **Monette M**, **Opella SJ**, **Greenwood J**, **Willis AE**, **Perham RN**. 2001. Structure of a malaria parasite antigenic determinant displayed on filamentous bacteriophage determined by NMR spectroscopy: implications for the structure of continuous peptide epitopes of proteins. Protein Sci. **10**:1150–1159.
666. **Ghasparian A**, **Moehle K**, **Linden A**, **Robinson JA**. 2006. Crystal structure of an NPNA-repeat motif from the circumsporozoite protein of the malaria parasite Plasmodium falciparum. Chem. Commun. (Camb.) **365**:174–176.
667. **Moreno CA**, **Rodriguez R**, **Oliveira GA**, **Ferreira V**, **Nussenzweig RS**, **Moya Castro ZR**, **Calvo-Calle JM**, **Nardin E**. 1999. Preclinical evaluation of a synthetic Plasmodium falciparum MAP malaria vaccine in Aotus monkeys and mice. Vaccine **18**:89–99.
668. **Mahajan B**, **Berzofsky JA**, **Boykins RA**, **Majam V**, **Zheng H**, **Chattopadhyay R**, **la Vega de P**, **Moch JK**, **Haynes JD**, **Belyakov IM**, **Nakhasi HL**, **Kumar S**. 2010. Multiple antigen peptide vaccines against Plasmodium falciparum malaria. Infect. Immun. **78**:4613–4624.
669. **Vieira P**, **Rajewsky K**. 1990. Persistence of memory B cells in mice deprived of T cell help. Int. Immunol. **2**:487–494.
670. **Hebeis BJ**, **Klenovsek K**, **Rohwer P**, **Ritter U**, **Schneider A**, **Mach M**, **Winkler TH**. 2004. Activation of virus-specific memory B cells in the absence of T cell help. J. Exp. Med. **199**:593–602.
671. **MacLeod MKL**, **Clambey ET**, **Kappler JW**, **Marrack P**. 2009. CD4 memory T cells: what are they and what can they do? Semin. Immunol. **21**:53–61.
672. **Lanzavecchia A**, **Bernasconi N**, **Traggiai E**, **Ruprecht CR**, **Corti D**, **Sallusto F**. 2006. Understanding and making use of human memory B cells. Immunol. Rev. **211**:303–309.
673. **Hills T**, **Jakeman PG**, **Carlisle RC**, **Klenerman P**, **Seymour LW**, **Cawood R**. 2016. A Rapid-Response Humoral Vaccine Platform Exploiting Pre-Existing Non-Cognate Populations of Anti-Vaccine or Anti-Viral CD4+ T Helper Cells to Confirm B Cell Activation. PLoS ONE **11**:e0166383.
674. **Millet P**, **Chizzolini C**, **Wirtz RA**, **Bathurst I**, **Broderson JR**, **Campbell GH**, **Collins WE**. 1992. Inhibitory activity against sporozoites induced by antibodies directed against nonrepetitive regions of the circumsporozoite protein of Plasmodium vivax. Eur. J. Immunol. **22**:519–524.
675. **Coppi A**, **Pinzon-Ortiz C**, **Hutter C**, **Sinnis P**. 2005. The Plasmodium circumsporozoite protein is proteolytically processed during cell invasion. J. Exp. Med. **201**:27–33.
676. **Whitacre DC**, **Espinosa DA**, **Peters CJ**, **Jones JE**, **Tucker AE**, **Peterson DL**, **Zavala FP**, **Milich DR**. 2015. P. falciparum and P. vivax Epitope-Focused VLPs Elicit Sterile Immunity to Blood Stage Infections. PLoS ONE **10**:e0124856.
677. **Bongfen SE**, **Ntsama PM**, **Offner S**, **Smith T**, **Felger I**, **Tanner M**, **Alonso P**, **Nébié I**, **Romero JF**, **Silvie O**, **Torgler R**, **Corradin G**. 2009. The N-terminal domain of Plasmodium falciparum circumsporozoite protein represents a target of protective immunity. Vaccine **27**:328–335.
678. **John CC**, **Tande AJ**, **Moormann AM**, **Sumba PO**, **Lanar DE**, **Min XM**, **Kazura JW**. 2008. Antibodies to pre-erythrocytic Plasmodium falciparum antigens and risk of clinical malaria in Kenyan children. J. Infect. Dis. **197**:519–526.
679. **Nixon CE**, **Park S**, **Pond-Tor S**, **Raj D**, **Lambert LE**, **Orr-Gonzalez S**, **Barnafo EK**, **Rausch KM**, **Friedman JF**, **Fried M**, **Duffy PE**, **Kurtis JD**. 2017. Identification of Protective B-Cell Epitopes within the Novel Malaria Vaccine Candidate Plasmodium falciparum Schizont Egress Antigen 1. Clin. Vaccine Immunol. **24**:e00068–17.
680. **Lee D**, **Redfern O**, **Orengo C**. 2007. Predicting protein function from sequence and structure. Nat. Rev. Mol. Cell Biol. **8**:995–1005.
681. **Groat-Carmona AM**, **Kain H**, **Brownell J**, **Douglass AN**, **Aly ASI**, **Kappe SHI**. 2015. A Plasmodium α/β-hydrolase modulates the development of invasive stages. Cell. Microbiol. **17**:1848–1867.
682. **Harupa A**, **Sack BK**, **Lakshmanan V**, **Arang N**, **Douglass AN**, **Oliver BG**, **Stuart**

AB, **Sather DN**, **Lindner SE**, **Hybiske K**, **Torii M**, **Kappe SHI**. 2014. SSP3 is a novel Plasmodium yoelii sporozoite surface protein with a role in gliding motility. Infect. Immun. **82**:4643–4653.

683. **Siau A**, **Silvie O**, **Franetich J-F**, **Yalaoui S**, **Marinach C**, **Hannoun L**, **van Gemert G-J**, **Luty AJF**, **Bischoff E**, **David PH**, **Snounou G**, **Vaquero C**, **Froissard P**, **Mazier D**. 2008. Temperature shift and host cell contact up-regulate sporozoite expression of Plasmodium falciparum genes involved in hepatocyte infection. PLoS Pathog. **4**:e1000121.

684. **Engelmann S**, **Silvie O**, **Matuschewski K**. 2009. Disruption of Plasmodium sporozoite transmission by depletion of sporozoite invasion-associated protein 1. Eukaryotic Cell **8**:640–648.

685. **Kappe SH**, **Noe AR**, **Fraser TS**, **Blair PL**, **Adams JH**. 1998. A family of chimeric erythrocyte binding proteins of malaria parasites. Proc. Natl. Acad. Sci. U.S.A. **95**:1230–1235.

686. **Ghai M**, **Dutta S**, **Hall T**, **Freilich D**, **Ockenhouse CF**. 2002. Identification, expression, and functional characterization of MAEBL, a sporozoite and asexual blood stage chimeric erythrocyte-binding protein of Plasmodium falciparum. Mol. Biochem. Parasitol. **123**:35–45.

687. **Preiser P**, **Renia L**, **Singh N**, **Balu B**, **Jarra W**, **Voza T**, **Kaneko O**, **Blair P**, **Torii M**, **Landau I**, **Adams JH**. 2004. Antibodies against MAEBL ligand domains M1 and M2 inhibit sporozoite development in vitro. Infect. Immun. **72**:3604–3608.

688. **Alexander DL**, **Arastu-Kapur S**, **Dubremetz J-F**, **Boothroyd JC**. 2006. Plasmodium falciparum AMA1 binds a rhoptry neck protein homologous to TgRON4, a component of the moving junction in Toxoplasma gondii. Eukaryotic Cell **5**:1169–1173.

689. **Giovannini D**, **Späth S**, **Lacroix C**, **Perazzi A**, **Bargieri D**, **Lagal V**, **Lebugle C**, **Combe A**, **Thiberge S**, **Baldacci P**, **Tardieux I**, **Ménard R**. 2011. Independent roles of apical membrane antigen 1 and rhoptry neck proteins during host cell invasion by apicomplexa. Cell Host Microbe **10**:591–602.

690. **Sanders PR**, **Gilson PR**, **Cantin GT**, **Greenbaum DC**, **Nebl T**, **Carucci DJ**, **McConville MJ**, **Schofield L**, **Hodder AN**, **Yates JR**, **Crabb BS**. 2005. Distinct protein classes including novel merozoite surface antigens in Raft-like membranes of Plasmodium falciparum. J. Biol. Chem. **280**:40169–40176.

691. **Offeddu V**, **Rauch M**, **Silvie O**, **Matuschewski K**. 2014. The Plasmodium protein P113 supports efficient sporozoite to liver stage conversion in vivo. Mol. Biochem. Parasitol. **193**:101–109.

692. **Kaiser K**, **Camargo N**, **Coppens I**, **Morrisey JM**, **Vaidya AB**, **Kappe SHI**. 2004. A member of a conserved Plasmodium protein family with membrane-attack complex/perforin (MACPF)-like domains localizes to the micronemes of sporozoites. Mol. Biochem. Parasitol. **133**:15–26.

693. **Ishino T**, **Chinzei Y**, **Yuda M**. 2005. A Plasmodium sporozoite protein with a membrane attack complex domain is required for breaching the liver sinusoidal cell layer prior to hepatocyte infection. Cell. Microbiol. **7**:199–208.

694. **Yuda M**, **Ishino T**. 2004. Liver invasion by malarial parasites--how do malarial parasites break through the host barrier? Cell. Microbiol. **6**:1119–1125.

695. **Yang ASP**, **O'Neill MT**, **Jennison C**, **Lopaticki S**, **Allison CC**, **Armistead JS**, **Erickson SM**, **Rogers KL**, **Ellisdon AM**, **Whisstock JC**, **Tweedell RE**, **Dinglasan RR**, **Douglas DN**, **Kneteman NM**, **Boddey JA**. 2017. Cell Traversal Activity Is Important for Plasmodium falciparum Liver Infection in Humanized Mice. Cell Rep **18**:3105–3116.

696. **Ito D**, **Han E-T**, **Takeo S**, **Thongkukiatkul A**, **Otsuki H**, **Torii M**, **Tsuboi T**. 2011. Plasmodial ortholog of Toxoplasma gondii rhoptry neck protein 3 is localized to the rhoptry body. Parasitol. Int. **60**:132–138.

697. **Pandey KC**, **Singh N**, **Arastu-Kapur S**, **Bogyo M**, **Rosenthal PJ**. 2006. Falstatin, a cysteine protease inhibitor of Plasmodium falciparum, facilitates erythrocyte invasion. PLoS Pathog. **2**:e117.

698. **Rennenberg A**, **Lehmann C**, **Heitmann A**, **Witt T**, **Hansen G**, **Nagarajan K**, **Deschermeier C**, **Turk V**, **Hilgenfeld R**, **Heussler VT**. 2010. Exoerythrocytic Plasmodium parasites secrete a cysteine protease inhibitor involved in sporozoite

invasion and capable of blocking cell death of host hepatocytes. PLoS Pathog. **6**:e1000825.

699. **Boysen KE**, **Matuschewski K**. 2013. Inhibitor of cysteine proteases is critical for motility and infectivity of Plasmodium sporozoites. MBio **4**:e00874–13.

700. **Lehmann C**, **Heitmann A**, **Mishra S**, **Burda P-C**, **Singer M**, **Prado M**, **Niklaus L**, **Lacroix C**, **Ménard R**, **Frischknecht F**, **Stanway R**, **Sinnis P**, **Heussler V**. 2014. A cysteine protease inhibitor of plasmodium berghei is essential for exo-erythrocytic development. PLoS Pathog. **10**:e1004336.

701. **Kaiser K**, **Matuschewski K**, **Camargo N**, **Ross J**, **Kappe SHI**. 2004. Differential transcriptome profiling identifies Plasmodium genes encoding pre-erythrocytic stage-specific proteins. Mol. Microbiol. **51**:1221–1232.

702. **Labaied M**, **Camargo N**, **Kappe SHI**. 2007. Depletion of the Plasmodium berghei thrombospondin-related sporozoite protein reveals a role in host cell entry by sporozoites. Mol. Biochem. Parasitol. **153**:158–166.

703. **Song G**, **Koksal AC**, **Lu C**, **Springer TA**. 2012. Shape change in the receptor for gliding motility in Plasmodium sporozoites. Proc. Natl. Acad. Sci. U.S.A. **109**:21420–21425.

704. **Rathore D**, **Nagarkatti R**, **Jani D**, **Chattopadhyay R**, **la Vega de P**, **Kumar S**, **McCutchan TF**. 2005. An immunologically cryptic epitope of Plasmodium falciparum circumsporozoite protein facilitates liver cell recognition and induces protective antibodies that block liver cell invasion. J. Biol. Chem. **280**:20524–20529.

705. **Satterthwait AC**, **Arrhenius T**, **Hagopian RA**, **Zavala F**, **Nussenzweig V**, **Lerner RA**. 1989. The conformational restriction of synthetic peptides, including a malaria peptide, for use as immunogens. Philos. Trans. R. Soc. Lond., B, Biol. Sci. **323**:565–572.

706. **Schmidt NW**, **Podyminogin RL**, **Butler NS**, **Badovinac VP**, **Tucker BJ**, **Bahjat KS**, **Lauer P**, **Reyes-Sandoval A**, **Hutchings CL**, **Moore AC**, **Gilbert SC**, **Hill AV**, **Bartholomay LC**, **Harty JT**. 2008. Memory CD8 T cell responses exceeding a large but definable threshold provide long-term immunity to malaria. Proc. Natl. Acad. Sci. U.S.A. **105**:14017–14022.

707. **Guy AJ**, **Irani V**, **MacRaild CA**, **Anders RF**, **Norton RS**, **Beeson JG**, **Richards JS**, **Ramsland PA**. 2015. Insights into the Immunological Properties of Intrinsically Disordered Malaria Proteins Using Proteome Scale Predictions. PLoS ONE **10**:e0141729.